Asymmetric Catalytic Friedel–Crafts Reactions of Unactivated Arenes

Inaugural-Dissertation

zur

Erlangung des Doktorgrades

der Mathematisch-Naturwissenschaftlichen Fakultät

der Universität zu Köln

vorgelegt von

Sebastian Brunen

aus München

Köln 2024

"Time is what keeps the light from reaching us."

—Eckhart von Hochheim

Acknowledgments

Table of Contents

Abstract

Aromatic scaffolds are crucial structural elements in all fields of chemical synthesis. The selective functionalization of simple arenes is therefore of vital importance for the preparation of more complex aromatic structures. The Friedel–Crafts reaction has proven to be a particularly powerful tool for this transformation, its dependence on electron-rich arenes, however, limits its scope significantly. The work reported herein describes the development of novel methods for the asymmetric catalytic Friedel–Crafts reaction of unactivated arenes using strong and confined Brønsted acid organocatalysts. To that end, simple alkylbenzene hydrocarbons but also more reactive alkoxybenzenes and heterocyclic arenes could be transformed with *N,O*-acetals to yield corresponding arylglycine esters with generally excellent regio- and enantiomeric ratios and high yields. Building up on the abovementioned studies and stimulated by the relevance of 3-arylpropanals for fragrance applications, the addition of unactivated arenes to simple enal derivates was studied subsequently. To this end, either preformed acylals or enals in combination with anhydrides as activating agents were used to deliver enantioenriched enol esters via asymmetric Brønsted acid-catalysis.

Kurzzusammenfassung

Aromatische Gerüste sind essenzielle Strukturelemente in allen Bereichen der chemischen Synthese. Die selektive Funktionalisierung einfacher Aromaten ist daher von entscheidender Bedeutung für die Herstellung komplexerer aromatischer Verbindungen. Die Friedel–Crafts-Reaktion hat sich als ein besonders leistungsfähiges Werkzeug für diese Umwandlung erwiesen, die Abhängigkeit von elektronenreichen Aromaten schränkt ihren Anwendungsbereich jedoch ein. Die hier vorgestellte Arbeit beschreibt die Entwicklung neuer Methoden für die asymmetrisch-katalytische Friedel–Crafts-Reaktion unreaktiver Aromaten unter Verwendung starker und sterisch eingeschränkter Brønsted-Säure-Organokatalysatoren. Hierzu konnten Alkylbenzole, aber auch Alkoxybenzole und heterocyclische Aromaten mit *N,O*-Acetalen umgesetzt werden um Arylglycine mit exzellenten Regio- und Enantiomerenverhältnissen und hohen Ausbeuten zu erhalten. Aufbauend auf den oben dargelegten Studien und stimuliert durch die Relevanz von 3-Aryl-Propanalen für Duftstoffanwendungen wurde anschließend die Addition von Aromaten an Enal-Derivate untersucht. Dazu wurden entweder Acylale oder Enale mit Anhydriden als Aktivierungsreagenzien verwendet, um enantiomerenangereicherte Enolester unter asymmetrischer Brønsted-Säure-Katalyse zu erhalten.

List of Abbreviations

Ac	acyl
ACDC	asymmetric counteranion-directed catalysis
Alk	alkyl
Ar	aryl
BINOL	1,1'-bi-2-naphtol
Bn	benzyl
Boc	*tert*-butyloxycarbonyl
Box	bisoxazoline
BSTFA	*N*,*O*-bis(trimethylsilyl)trifluoroacetamide
BTX	benzene, toluene, xylenes
Bu	butyl
Bz	benzoyl
Cat.	catalyst or catalytic
Cbz	benzyloxycarbonyl
CPA	chiral phosphoric acid
Cy	cyclohexyl
Cyp	cyclopentyl
D	Debye
DCM	dichloromethane
DFT	density functional theory
DMAP	4-dimethylaminopyridine
DMF	dimethylformamide
DMSO	dimethyl sulfoxide
DSI	disulfonimide
d	douplet (NMR) or day
e.r.	enantiomeric ratio
EDG	electron donating group
eg	ethylenglycolato
EI	electron impact ionization
equiv.	equivalents
Et	ethyl
Fmoc	fluorenylmethyloxycarbonyl
ESI	electrospray ionization

EWG	electron withdrawing group
GC	gas chromatography
GC-MS	gas chromatography coupled with mass spectrometry
GDP	gross domestic product
GP	general procedure
h	hours
HMDS	hexamethyldisilazane
HOMO	highest occupied molecular orbital
HPLC	high performance liquid chromatography
i	iso
in situ	in this place; on site
IDP	imidodiphosphate
IDPi	imidodiphosphorimidate
*i*IDP	iminoimidodiphosphate
Int	intermediate
IUPAC	International Union of Pure and Applied Chemistry
JINGLE	1,1'-binaphthyl-2,2'-bis(sulfuryl)imides
KIE	kinetic isotope effect
L	ligand
LUMO	lowest unoccupied molecular orbital
m	multiplet (NMR)
m	meta
M	molar
*m*CPBA	*meta*-chloroperoxybenzoic acid
Me	methyl
min	minutes
MOM	methoxymethyl ether
MS	mass spectrometry
MTBE	methyl-*tert*-butylether
n	normal
N	Mayr nucleophilicity parameter
NMR	nuclear magnetic resonance spectroscopy
NRP	non-ribosomal peptide
NTPA	*N*-triflyl phosphoramide
o	ortho
p	para

PET	polyethylene terephtalate
PG	protecting group
Ph	phenyl
pin	pinacol
Piv	pivaloyl
Pr	propyl
q	quartet (NMR)
RT	room temperature
r.r.	regioisomeric ratio
sat.	saturated
S_EAr	electrophilic aromatic substitution
SM	starting material
S_NAr	nucleophilic aromatic substitution
t	tertiary
t	triplet (NMR) or time
T	temperature
TBAF	tetrabutylammonium fluoride
TBS	*tert*-butyldimethylsilyl
TCAA	trichloroacetic acid anhydride
TDI	toluene diisocyanate
Tf	trifluoromethylsulfonyl
TFA	trifluoroacetic acid
TFAA	trifluoroacetic acid anhydride
THF	tetrahydrofuran
TIPS	triisopropylsilyl
TLC	thin layer chromatography
TMB	1,3,5-trimethoxybenzene
TMS	trimethylsilyl
TRIP	3,3'-bis(2,4,6-triisopropylphenyl)-1,1'-binaphthyl-2,2'-diyl hydrogenphosphate
t_R	retention time
Ts	toluenesulfonyl
via	by way of

1. Introduction

The concept of aromaticity is so tightly interwoven with the field of synthetic organic chemistry that it often seems like it represents one of its centerpieces. Not only is it one of the first things students learn about in organic chemistry classes, but it is also visibly represented on a multitude of logos of chemical institutes and companies to emphasize their roots in synthetic chemistry.[1] The elucidation of the scientific background that gives aromatic molecules their extraordinary properties has driven researchers for decades and their findings shaped the way we see and understand the molecular sciences today. The importance of aromatic molecules however significantly exceeds the interest of the academic spheres: aromatic structures are crucial scaffolds in basically all fields of the chemical industry, ranging from petrochemical feedstocks to small molecule drugs for life science-applications. This demand has consequently led to extensive research on the synthesis and the transformation of aromatic structures which resulted in the development of a plethora of creative synthetic tools. Though often different in their mode of action, almost all of these reactions have one thing in common: their dependency on a catalyst.

Catalysis is undoubtedly among the most significant technologies that humanity has developed and its relevance is demonstrated impressively by its massive contribution to the global gross domestic product.[2] Since the term catalysis was coined by Berzelius in 1835 and defined as "*the acceleration of a slow chemical process by the presence of a foreign material*" by Ostwald in 1894, more than a century has passed in which scientists pushed the limits of chemical synthesis with the tools provided by catalysis.[3] Countless breakthrough processes have been discovered since then to advance the progress of mankind, many of those have been awarded a Nobel prize. Catalysis however not only holds the power to accelerate a chemical transformation, it can also direct a reaction to selectively yield only a selected product out of a group of multiple possible ones. This trait was impressively demonstrated by Noyori, Knowles and Sharpless who were awarded the Nobel Prize in chemistry for their seminal work on "*chirally catalysed reactions*" in 2001.

The word "chiral" originates from the Greek word "*cheir*" and means "hand". The analogy to our hands perfectly describes the concept of chirality, which is the relation between two mirror-image objects which cannot be superimposed which each other. While chirality is an important

property for many branches of the natural sciences, it is of special interest within the life sciences as chiral molecules are omnipresent in biological systems. Induced by the chiral environment within these systems, interactions with pharmaceutically active molecules are often dependent on their exact spatial orientation, which creates the demand for methods that allow the selective synthesis of a single out of two possible mirror image isomers (enantiomers).[4] To this end, chiral enantiopure molecules, available from natural sources (the chiral pool), can serve as basic framework or chiral auxiliary for further synthetic steps toward the target structure. Alternatively, chiral racemic compounds can be subjected to the separation of the isomers. However, both approaches often suffer from significant drawbacks such as the limited availability of chiral pool materials or the reduced yields resulting from resolution processes. A way to overcome these problems and to provide efficient access to chiral enantioenriched molecules can be found in the field of asymmetric catalysis.

Asymmetric catalysis describes processes in which a catalytic amount of a chiral enantiopure material is used to prepare a chiral enantioenriched product in higher quantity.[4] As demonstrated by Noyori, Knowles and Sharpless, organometallic catalysts, in addition to biocatalysts, have proven to be powerful tools for this quest. Since seminal discoveries by List and MacMillan in the early 2000s however, a third class of asymmetric catalysts emerged: organocatalysts.

2. Background

2.1 The Origin of Aromaticity

When benzene (**1**), the archetypical arene, was discovered in 1825 by Michael Faradey, little was known about the concept of aromaticity.[5] Before these early findings, aromaticity was solely associated with a certain aromatic smell and a surprisingly high chemical stability, considering the compound's high degree of unsaturation. A plethora of proposals were made for the constitution of this iconic molecule, many of them being of exotic nature. Much known is a structure proposed by Dewar (**2**), that was eventually synthesized a century after it was first mentioned (figure **2.1**).[6,7] It was not until 1865 however, that August Kekulé proposed a structure for benzene which should finally prevail: a highly symmetric hexagonal structure of tetravalent carbon atoms with one hydrogen atom bound to each carbon. If the structure was truly revealed to him in two daydreams of a snake devouring its own tail remains unclear.[8] However, since then, each generation of chemists shaped and developed the term aromaticity and further explored the properties of aromatic compounds. In 1866, Erlenmeyer discovered that aromatic compounds tend to undergo electrophilic aromatic substitution reactions rather than addition reactions, as opposed to non-aromatic unsaturated compounds.[9]
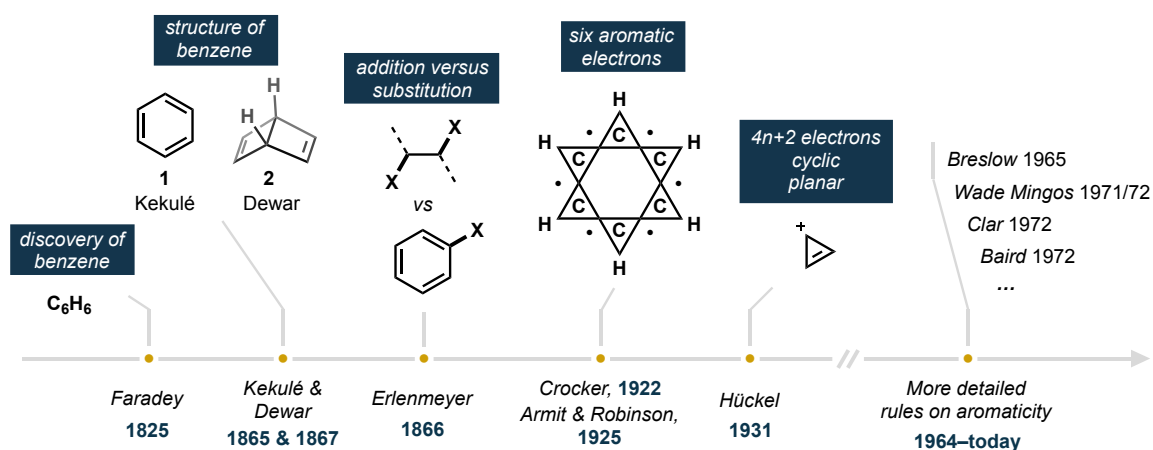
Figure 2.1: Historical development of the term aromaticity over the years.

Even though the structure of benzene was elucidated as early as 1865, it was to take more than 60 years before the quantum chemical theory for its unusual stability was revealed in more detail. In 1922 and 1925, respectively, Crocker, Armit and Robinson proposed an "aromatic

sextet" of electrons as cause for the extraordinary stability of aromatic annulenes; a concept that could even be applied to heteroaromatic systems.[10–12] Fueled by the proceeding of the field of quantum mechanics in the early 20th century, Hückel extended the theories proposed by Crocker, Armit and Robinson by introducing a groundbreaking concept that should later be known as the "Hückel-rule". According to Hückel, a molecule requires a cyclic, planar structure of conjugated atoms (a connected system of *p*-orbitals) and a sum of $4n + 2$ π-electrons (where *n* is a non-negative integer) to display aromatic properties.[13,14] Today, the Hückel-rule still is a powerful tool for the assessment and identification of aromaticity in synthetic organic chemistry. However, plentiful examples for the existence of aromaticity outside of Hückel's rule have been found which led to many more specialized theoretical observations and rules.[15] Especially the criterion of planarity can be widened without the loss of the aromatic character: besides spherical[16] or tubular[17,18] aromaticity, a range of bended or curved aromatic molecules[19–21] could be synthesized (figure **2.2**).

| spheric aromaticity | hyperbolic aromaticity | cylindrical aromaticity |

| buckminsterfullerene | [7]helicene | [9]cycloparaphenylene |
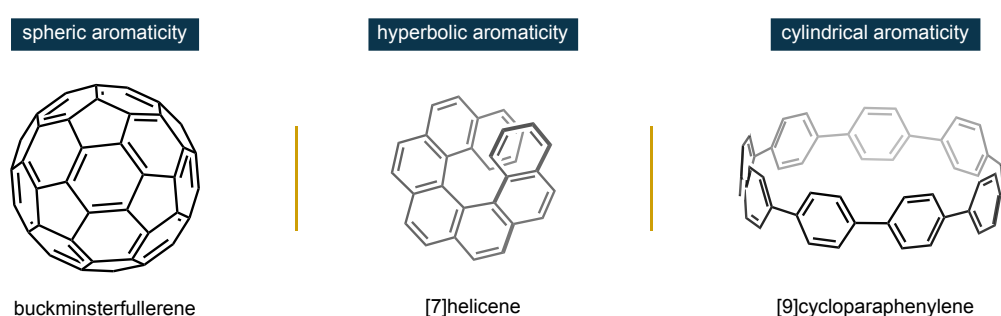
Figure 2.2: Examples for spheric, hyperbolic and cylindrical aromaticity.

In fact, the structural diversity within the family of aromatic compounds has increased so much over the past decades – from simple benzenoids to complex structures bearing multidimensional systems of highly delocalized electrons – that finding a unifying definition of aromaticity has become more and more challenging. The IUPAC (International Union of Pure and Applied Chemistry) provides a definition that bases on the cyclic electron delocalization within aromatic structures which leads to increased thermodynamic stability.[22] Besides that, however, structural and magnetic criteria as well as the nature of the valence shell of the molecule should be considered to evaluate its aromatic character. Existing rules and definitions have become increasingly complex and exceptions to the traditional boundaries of aromaticity are more than just occasional anomalies. An interdisciplinary paradigm shift of our classification and understanding of aromaticity might consequently be due to enable a more precise scientific exchange.[23]

2.1.1 Arenes as Crucial Feedstocks for the Chemical Industry

Classical Hückel arenes are of tremendous relevance in essentially all areas of synthetic chemistry, ranging from the synthesis of small molecule drugs to the multi-ton production of agrochemicals and materials. The importance of simple aromatic feedstocks is impressively underlined by their production volumes: in 2013, the most relevant aromatic commodity chemicals, benzene, toluene (**3**) and the xylenes, reached a combined global production volume of 103 million metric tons and the market has been growing by an expected 3% per year since then.[24,25] The so called "BTX-stream" (benzene, toluene, xylenes) represents one of the core production streams of the petrochemical industries and lays the foundation for a plethora of downstream transformations. The major share of these valuable feedstocks is obtained via catalytic reforming of naphtha and used for the production of polymer materials.[26] Benzene is usually converted to ethylbenzene (**4**) or cumene (**5**) to enable the subsequent production of phenol or styrene while toluene is either transformed into toluenediisocyanate (**TDI**) or disproportionated into benzene and xylenes. The mixture of the xylenes is mostly subjected to isomerization toward the most relevant *para*-isomer **6** which is then oxidized to give rise to terephthalic acid (**7**), a key building block for the production of polyethylene terephthalate (PET, figure **2.3**).[24]
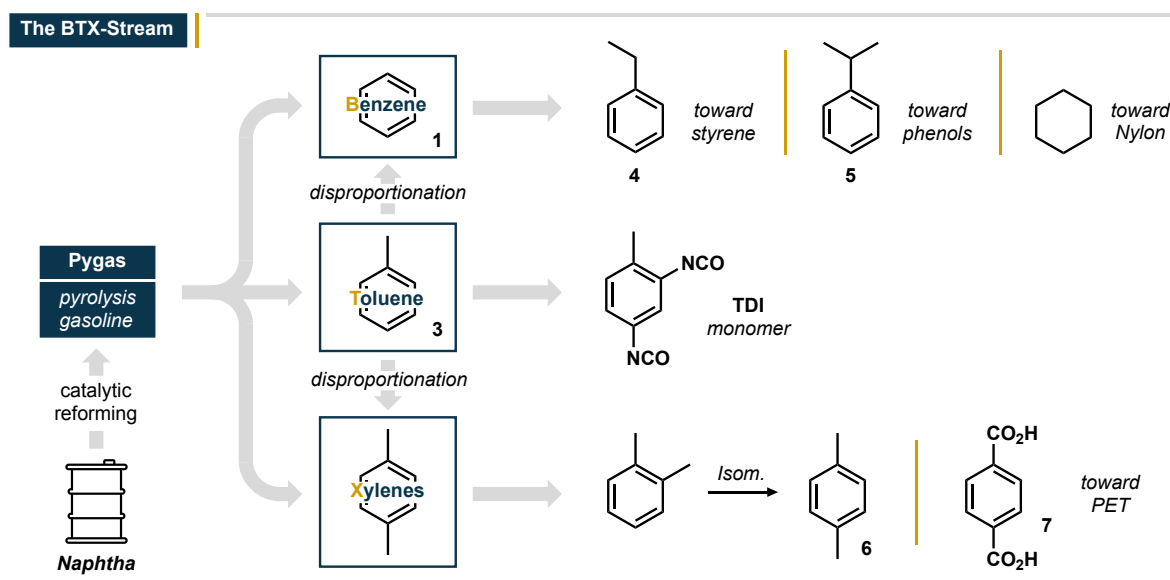
Figure 2.3: The BTX-stream in the petrochemical industries.[24]

The relevance of aromatic scaffolds however goes far beyond their application in the material- and polymer sciences, since especially fine and medicinal chemistry applications rely heavily

on aromatic scaffolds.[27] This great demand for highly functionalized aromatic structures has consequently led to intense research to develop a broad set of methods for the efficient and selective transformation of aromatic molecules. The most powerful tool in the synthetic chemist's toolbox to achieve this goal is catalysis.

2.2 Catalysis as Central Science for Chemical Synthesis

2.2.1 Fundamental Principles of Catalysis

Catalysis is undoubtedly one of the most significant technologies available to mankind. The synthetic power of catalysts often is astonishing: reactions that would take years to reach completion can be carried out in minutes and the proceeding of unwanted side reactions can efficiently be suppressed.[28] An impressive 80% of all chemical products and the major part of liquid fuels are obtained with the help of catalysis, which contributes to more than 35% of the global gross domestic product (GDP).[2] From a strictly economic point of view, catalysis adds value to crude feedstocks through chemical refinement: the goods accessed with the help of catalysts in the petrochemical industry increase the net value of the input raw materials by a factor of 200 to up to 300.[29] In fact, just a few of the most relevant catalytic reactions, such as the Haber-Bosch process for the fixation of nitrogen, have enabled the growth of the human species in the last century as we know it today.[30]

The conscious origin of the science of catalysis dates back to 1835 when Berzelius first introduced the term "catalysis", even though catalytic processes have unconsciously been used by humanity for significantly longer. It was not until 1894 though that Ostwald defined the term catalysis as "the acceleration of a slow chemical process by a foreign material which is not consumed and leaves the equilibrium of the reaction unchanged". In a more modern understanding, catalysts are identified as "substances that increase the rate of a reaction without modifying the overall standard Gibbs energy change in the reaction".[31] Consequently, catalysis is a kinetic phenomenon, in which the energetic ground states of the reactants stay constant but an energetically lower-lying pathway from the reactants to the products can be mediated by a catalyst. In this process, the catalyst interferes with one or more reactants but is not consumed in the overall process. It is consequently both reactant as well as product of the reaction (figure **2.4**).[31]
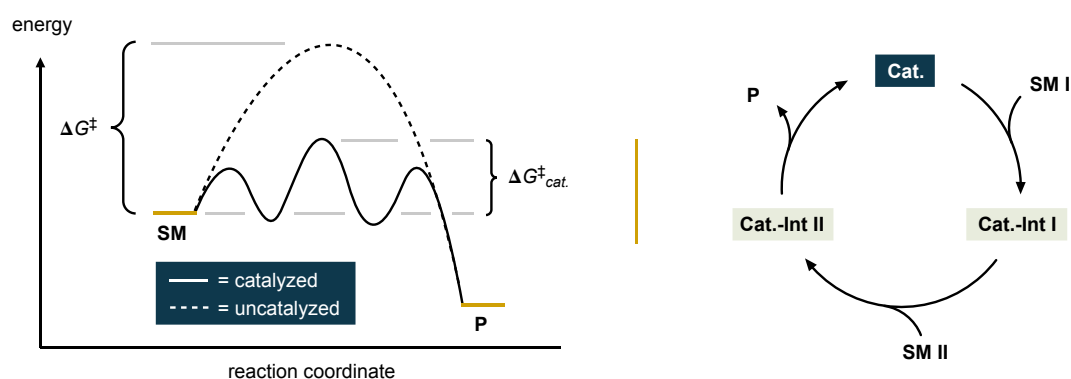
Figure 2.4: Schematic depiction of a catalytic process.

While catalysts are crucial tools for the acceleration of chemical reactions, they can furthermore influence the course of a reaction in a targeted and detailed manner to selectively yield only one out of multiple possible products or even open up paths that lead to completely new reactivity.[32] This can influence different observable parameters like the chemo- or regioselectivity of a reaction. Of particular interest to the chemical community, however, is the art of enantioselective (or asymmetric) catalysis (figure **2.5**).
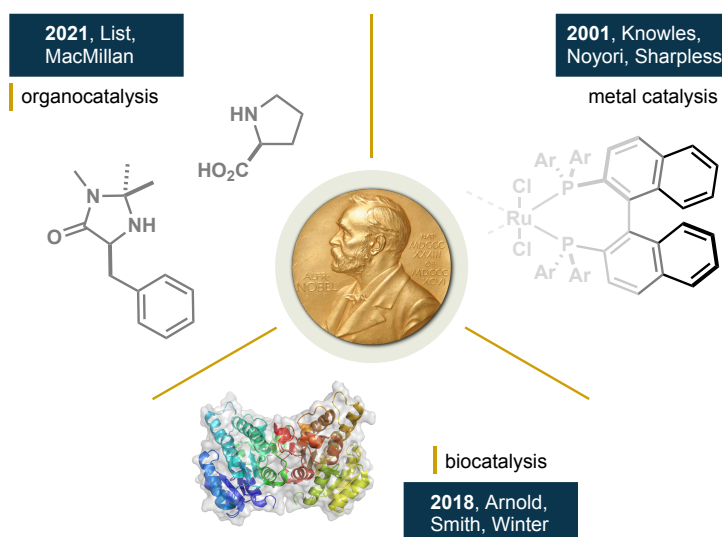
Figure 2.5: Nobel prizes awarded for asymmetric catalysis.

The paramount importance of asymmetric catalysis and the drive of synthetic chemists to understand and design catalytic systems to enable the selective synthesis of one out of two

possible mirror image products is impressively underscored by three Nobel prizes awarded in the last 23 years for work closely related to asymmetric catalysis.[33]

2.2.2 Asymmetric Organocatalysis

Despite the relatively young age of the field of asymmetric catalysis, multiple different branches of the science quickly formed and evolved over the years. All of them however face the same challenge: the selective formation of one out of multiple possible stereoisomers with the aid of a chiral enantiopure catalyst.[34,35] In most cases, asymmetric catalysis refers to the transformation of a non-chiral starting material to a chiral enantioenriched product by means of an enantiopure catalyst that distinguishes between two possible diastereomeric reaction pathways. The difference in activation energy between the two pathways corresponds to the quality of enantioinduction (figure **2.6**).[35] Furthermore, the racemic mixture of a chiral starting material can be subjected to a reaction with a chiral enantioenriched catalyst, in which one isomer is transformed at a significantly higher reaction rate than the other. The converted product and/or the remaining starting material is consequently obtained in enantioenriched form. Such kinetic resolution processes suffer from the intrinsic disadvantage of a maximum theoretical yield of 50%, unless a rapid equilibration of the two starting material isomers is achieved.
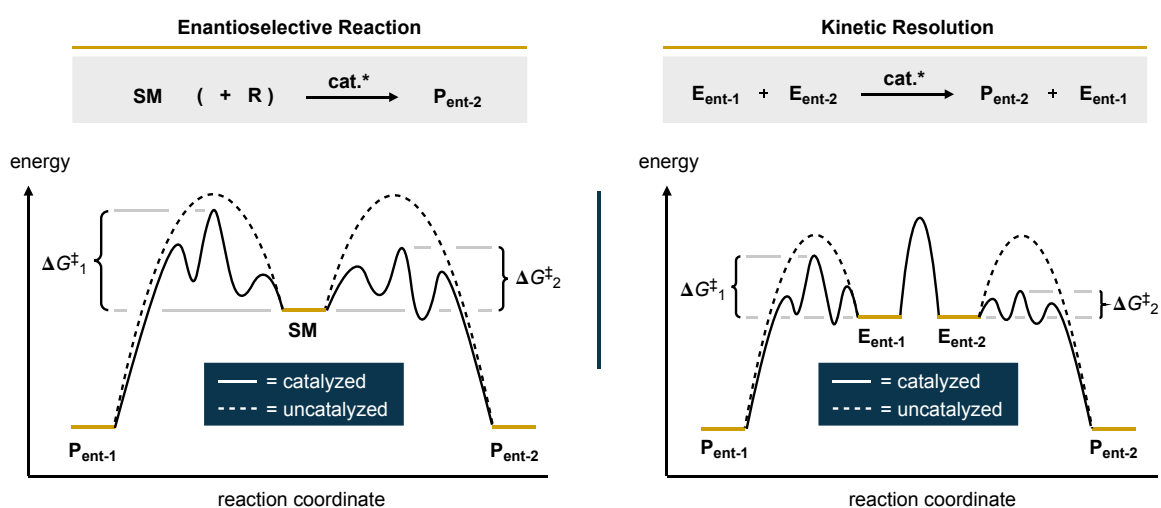
Figure 2.6: Energy diagrams for enantioselective reactions and kinetic resolution processes.

Since the advent of asymmetric catalysis in the 1960s, researchers have mainly focused on the usage of biocatalysts or chiral enantioenriched transition metal complexes. On the other hand,

purely organic small-molecule catalysts have long been overlooked and the existing examples have been regarded as anomalies or curiosities rather than part of a much larger area of the catalytic space.[36] This observation is especially peculiar given the fact that there have been sporadic yet powerful examples for the application of small organic molecules in asymmetric catalysis along with a set of intrinsic benefits these catalysts offer compared to traditional transition metal complexes. Among others, organocatalysts are usually cheap compared to many costly transition metals. They are also generally insensitive toward air or moisture and non-toxic, which makes them predestined catalysts for the synthesis of pharmaceutically active ingredients.[37]

While the application of organic catalysts in achiral synthesis has been known for much longer,[38–40] the first report of a small organic catalyst in asymmetric catalysis dates back to 1912, when Bredig and Fiske investigated the addition of HCN to benzaldehyde in the presence of cinchona alkaloids.[41] Only low enantioenrichment was observed in the corresponding cyanohydrin products, but the usage of cinchona alkaloids in asymmetric transformations was followed up by Pracejus in 1960, who investigated the addition of methanol to ketene **8**. Using similar cinchona alkaloid **9**, the synthesis of the corresponding methyl ester **10** could be achieved with enantiomeric ratios of up to 87:13 (scheme **2.1**).[42]
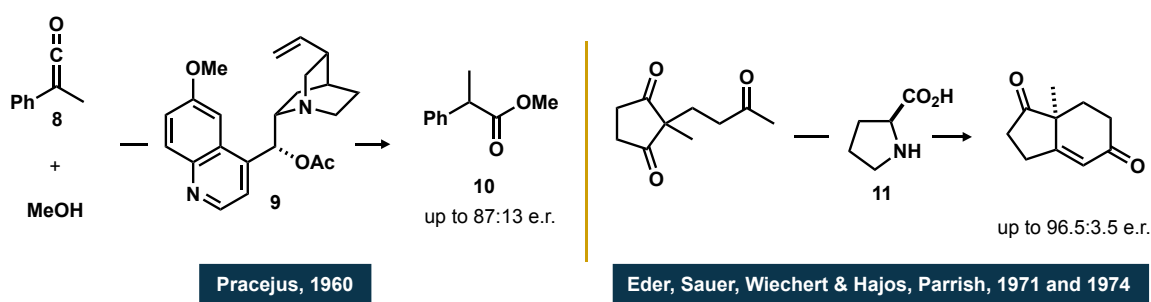
Scheme 2.1: Early reports of asymmetric organocatalytic processes.

Significant progress in the field was achieved by Eder, Sauer and Wiechert in 1971 and Hajos and Parrish in 1974, respectively.[43,44] Both groups independently investigated the asymmetric cyclization of triketones toward the bicyclic products with great success using *L*-proline (**11**) as organocatalyst. Despite these intriguing reports, it was not until the year 2000 that List and MacMillan contributed groundbreaking studies that the full potential of the field was realized and the loose collection of unconnected transformations began to gather under the roof of the freshly coined term of asymmetric organocatalysis (scheme **2.2**).[45,46] Inspired by his earlier

work on antibodies, List investigated the catalytic potential of the elementary building blocks of the parent macromolecular catalyst in similar asymmetric transformations.[47] Using *L*-proline as catalyst for the asymmetric aldol reaction of acetone (**12**) with aromatic- or aliphatic aldehydes **13**, good to excellent enantiomeric ratios and excellent chemoselectivities were observed.[45] Later in that year, MacMillan used the phenylalanine-derived imidazolidinone **14** for asymmetric Diels–Alder reactions to yield enantioenriched bicylco[2.2.2]octanes **15**.[46]
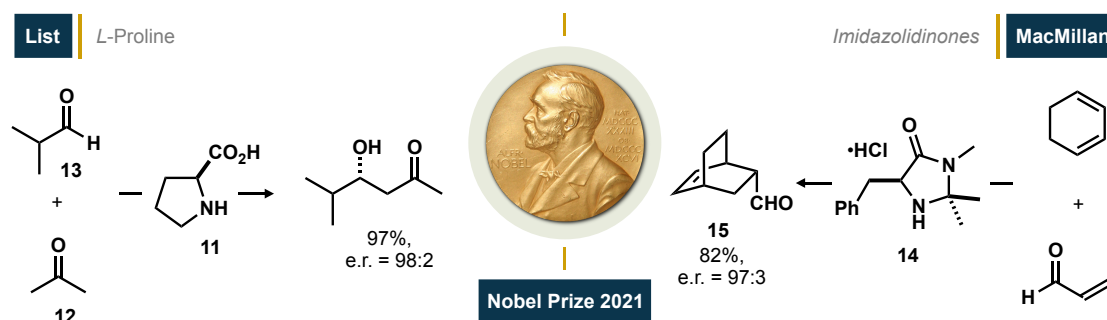
Scheme 2.2: Seminal work by List and MacMillan.

In the years and decades that followed, the discipline grew at such a tremendous rate that the explosion of the field was compared to the "sudden opening of a pressurized bottle of champagne", fueled by the progression of adjacent and supporting fields of research.[48] To bring order to the diverse research field, a number of classification systems have been proposed in the literature. A general approach categorizes the field of asymmetric organocatalysts in four classes: Lewis bases, Lewis acids, Brønsted bases and Brønsted acids.[36]

2.2.3 Asymmetric Brønsted Acid Organocatalysis

Chiral Lewis acid catalysis consists of a Lewis acidic central atom that is associated to a chiral ligand. The central atom usually activates an electrophilic substrate toward the interaction with a nucleophilic reagent by lowering the energy of its lowest unoccupied molecular orbital (**LUMO**). The chiral scaffold then provides an asymmetric environment which enables the subsequent enantioselective transformation.[49] If the central Lewis acidic atom consists of a proton, the simplest Lewis acidic species possible, one speaks of asymmetric Brønsted acid catalysis.[50] One of the most important factors determining the course of asymmetric Brønsted acid catalysis is the acidity of the used catalysts which significantly contributes to whether general or specific Brønsted acid catalysis is the operating mode of activation.[49] While general

Brønsted acid catalysis describes a catalytic process in which the acidic proton is still covalently bound to the catalyst backbone and activation takes place exclusively via hydrogen bonding, specific Brønsted acid catalysis involves protonation of the electrophilic reagent, which consequently requires more acidic catalysts.

Given the rich diversity of Lewis acidic metal ions along with an ever-increasing choice of chiral ligands, it is to no surprise that the field of asymmetric Lewis acid catalysis has been and continues to be one of the most prominent areas for the application of chiral metal complexes. In contrast, the field of asymmetric Brønsted acid catalysis is largely dominated by metal-free catalysts and a broad variety of organocatalysts, covering a wide range of acidity, has been investigated.[51] Among them, the group of chiral phosphoric acids (**CPA**) quickly gained popularity after seminal reports by Akiyama and Terada in 2004.[52,53] Closely associated to the field of chiral phosphoric acid catalysis is its most commonly used chiral backbone, the axially chiral 1,1'-bi-2-naphtol (**BINOL**). The BINOL-structure stands out for its low cost along with an easy functionalization thereof which grants straightforward access to a broad scope of possible catalysts.[54] Inspired by Noyori's breakthrough studies with binaphthyl-based ligands for asymmetric hydrogenation reactions, BINOL-based CPAs were found to possess unique properties. The seven membered ring, created by the phosphorous atom and the BINOL backbone, prevents free rotation and creates a rigid chiral environment (figure **2.7**).[55] The presence of an acidic and a basic site on the phosphoric acid furthermore creates a bifunctional active site which can easily be adjusted via installation of suitable substituents on the BINOL backbone.
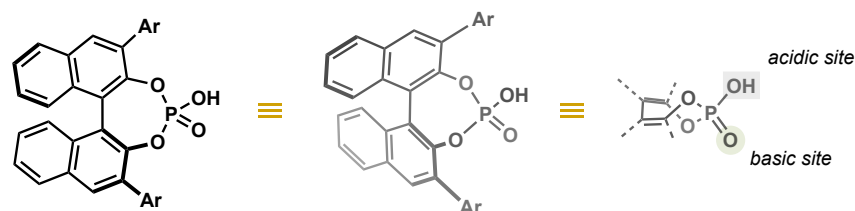
Figure 2.7: Spatial orientation of BINOL-based chiral phosphoric acids.

While BINOL-based chiral phosphoric acids have been known for more than half a century, their application in asymmetric catalysis was initiated only 20 years ago by Akiyama and Terada.[56] Since then, the field has developed significantly, fueled by the commercial access to the catalyst class, and now encompasses a broad variety of applications.

As beautifully illustrated by chiral phosphoric acid organocatalysis, specific Brønsted acid catalysis can be considered extremely general and versatile as the only prerequisite for the activation of a substrate is the presence of electron density – a requirement that all organic molecules fulfill by definition. But this consideration also points toward the limitation of the concept, which is the necessity for the protonation of the substrate. The success of this process depends on two factors, namely the acidity of the catalyst and the basicity of the substrate.[57] While basic substrates like imines can easily be protonated even with moderately acidic catalysts, significantly less reactive substrates such as simple olefins represent a serious challenge as highly acidic catalysts are required to enable proton transfer. This acidity/reactivity correlation has stimulated scientists to design ever more acidic catalysts to selectively functionalize unreactive chemical feedstocks and to pioneer into the realm of more and more inert substrates.[56,58]

2.2.4 Toward Strong and Confined Brønsted Acid Catalysis

While chiral phosphoric acid catalysts (pK_a = ca. 13.0 in MeCN)[59] find broad application in organic synthesis, it was quickly found that their use was strictly limited to basic substrates. The unavailability of less basic substrates for asymmetric Brønsted acid catalysis motivated chemists to design more acidic catalyst motifs which led to the synthesis of novel, highly reactive catalysts (figure **2.8**).
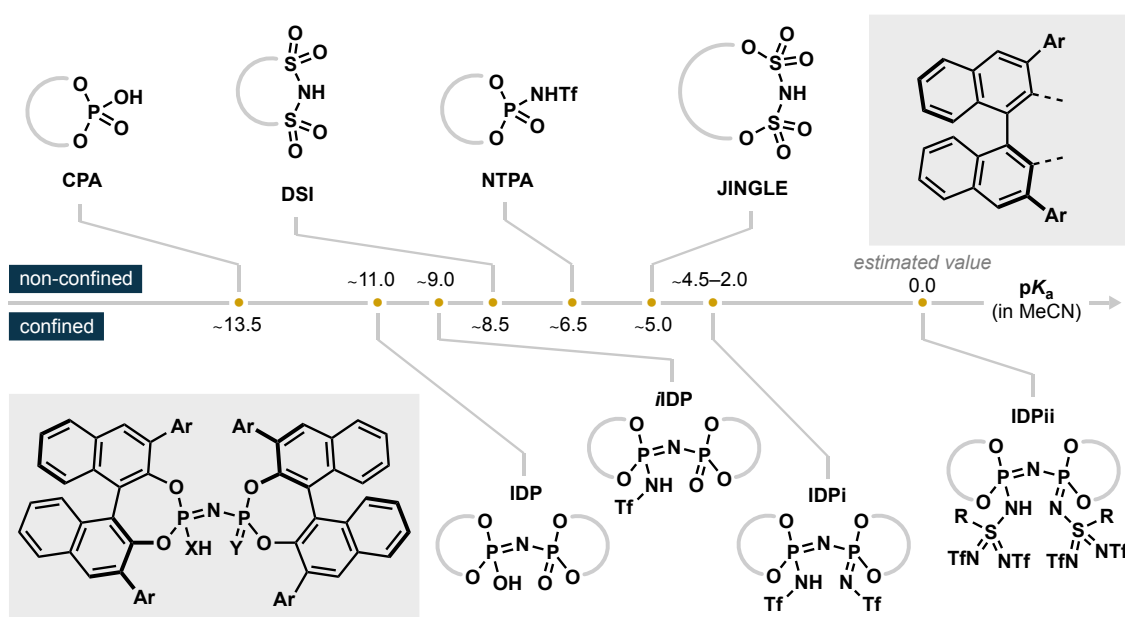
Figure 2.8: Acidity range of chiral Brønsted acid catalysts, given as approximate values.

The exchange of the phosphate moiety of CPAs to a disulfonic acid, a disulfonimide (**DSI**, pK_a = ca. 9.0 in MeCN)[60] or a sulfate unit (1,1-binaphthyl-2,2-bis(sulfuryl)imide, **JINGLE**, pK_a = ca. 5.0 in MeCN)[59] in all cases significantly increased the catalyst's acidity. While the use of these catalysts allowed for the activation of less basic substrates such as ketones or aldehydes, it is worth mentioning that achieving highly enantioselective transformations using disulfonic acid- or JINGLE-based catalysts has proven to be particularly challenging. It has therefore been argued that a too significantly increased acidity on the used acid catalyst, while crucial for the activation of less basic substrates, is detrimental for enantioselectivity.[60] This correlation inevitably raises the question of whether it is even possible to convert very unreactive substrates with high selectivity. With regard to biocatalysis, it is rather obvious that – at least in the realm of enzymatic transformations – this is the case: unactivated C–H bonds can selectively be functionalized using the tools provided by nature.[61,62] A key structural feature of enzymes is their highly confined microenvironment which precisely controls the orientation of a substrate in the active site.[63] Compared to these systems, the active site of the BINOL-based Brønsted acids described above appears rather loose, which complicates the selective transformation of small substrates. When List investigated the asymmetric spiroacetalization of small hydroxyenol ethers, only moderate enantioselectivity was achieved using non-confined catalysts.[64] Inspired by the structure of enzymes, a highly confined system based on two BINOL subunits connected by a bridging imidodiphosphate (**IDP**) linker was therefore designed to yield the spirocyclic products with increased enantioenrichment.

While the imidodiphosphate system developed by List provides a highly confined microenvironment, it lacks the acidity that is required for the activation of less basic substrates (pK_a of **IDPs** = ca. 11 in MeCN).[57] As demonstrated in studies reported by Yagupolskii, a significant acidifying effect can be achieved via replacement of O atoms by NTf groups.[65] When this concept was applied to the IDP scaffold, the resulting imidodiphosphorimidates (**IDPi**, pK_a 4.5 to ≤ 2.0 in MeCN) were found to combine both high confinement and superior acidity in a single catalyst.[57,66] The discovery of this groundbreaking motif enabled the asymmetric transformation of previously inaccessible building blocks such as simple olefins. Even now, almost a decade after its initial discovery, the existing frontiers of asymmetric Lewis and Brønsted acid catalysis continue to be extended using the privileged IDPi system.[67–69]

2.2.5 Asymmetric Counteranion-Directed Catalysis

One mechanistic feature IDPi catalysts share with most Lewis- or Brønsted acid catalysts is the generation of positively (or partially positively) charged intermediates or transition states within the course of a catalytic transformation. The presence of these key cationic species allows to pair them with ions of the opposite, anionic charge. If this anion is of enantiopure nature and furthermore present in a subsequent enantiodetermining step, the transfer of chirality from the anionic to the cationic species becomes possible. This concept has been coined asymmetric counteranion-directed catalysis (ACDC).[70] By definition, the interplay within ion pairs is not limited to Coulomb interactions but also includes further stabilizing interactions such as hydrogen bonds.[70] The distinction between ACDC and the traditional use of chiral anionic ligands in asymmetric transition metal catalysis arises from their role in the selectivity-determining step. If the anion convoys the cationic intermediate in a selectivity determining step, it is referred to as ACDC while anions which are solely bound to a transition metal atom to form a neutral or cationic complex belong to the category of chiral ligands.[70]

The concept of ACDC was illustrated by List, who used catalytical amounts of the salts of a chiral phosphoric acid and an achiral secondary amine for the asymmetric transfer hydrogenation of enals **16** (scheme **2.3**).[71] The strong ion pairing between thus formed iminium ions and BINOL-based phosphate counteranions provides a chiral environment that enables the subsequent asymmetric reduction and therefore differentiates itself from previously reported systems based on the use of chiral secondary amine catalysts.[72]
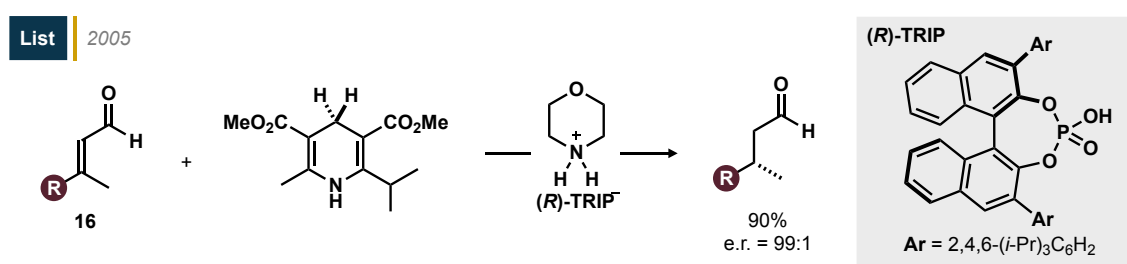
Scheme 2.3: Asymmetric transfer hydrogenation via ACDC reported by List.

Methods for the generation of cationic intermediates are numerous, outnumbered even by an ever-growing range of chiral counteranions known to the synthetic chemist. This has made the field of ACDC not only a powerful tool for the efficient synthesis of enantioenriched products, but also an extremely general and versatile concept that has found broad application in chemical

synthesis. One discipline for which ACDC has become invaluable is the field of electrophilic aromatic substitution reactions towards the functionalization of aromatic structures.

2.3 The Selective Functionalization of Arenes

Aromatic scaffolds are among the most crucial building blocks in synthetic chemistry. Therefore, it is not surprising that the structure and reactivity of arenes are among the first things students embark upon in their organic chemistry classes. The selective functionalization of aromatic structures has occupied scientists for decades and it still is an intensely investigated research area which has led to great innovation.[73] While the origins of the art of the structural modification of arenes date back to electrophilic and nucleophilic aromatic substitution reactions and early metalation approaches in the late 19th century, the field now encompasses a broad variety of methods such as transition metal-catalyzed cross couplings or C–H activation reactions (scheme **2.4**).[74]

Nucleophilic aromatic substitution (S$_N$Ar) reactions describe processes in which an anionic or neutral nucleophile displaces a leaving group on an aromatic substrate. They can therefore be considered orthogonal to the field of electrophilic aromatic substitions.[75] The success of an S$_N$Ar reaction depends mainly on three factors: the nucleophilicity of the nucleophile, the leaving group quality of the leaving group and the electronic nature of the aromatic system.
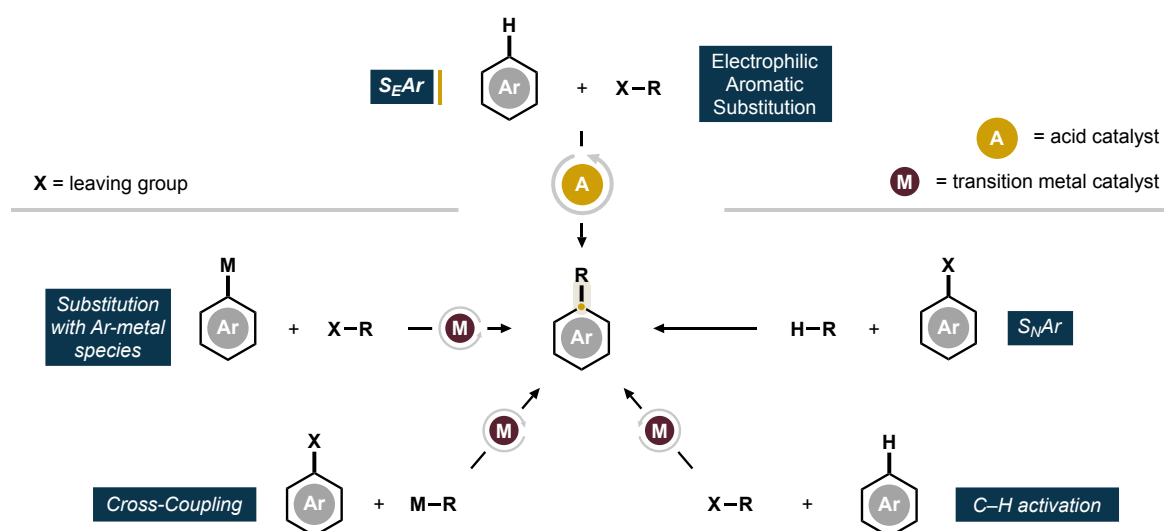
Scheme 2.4: Important methods for the functionalization of arenes.

Today, it is widely recognized that the majority of S$_N$Ar reactions proceed via a bimolecular, stepwise addition-elimination sequence which consequently leads to the highly unfavored

formation of anionic, dearomatized intermediates **I** (also referred to as Meisenheimer complex) (scheme **2.5**).[76]
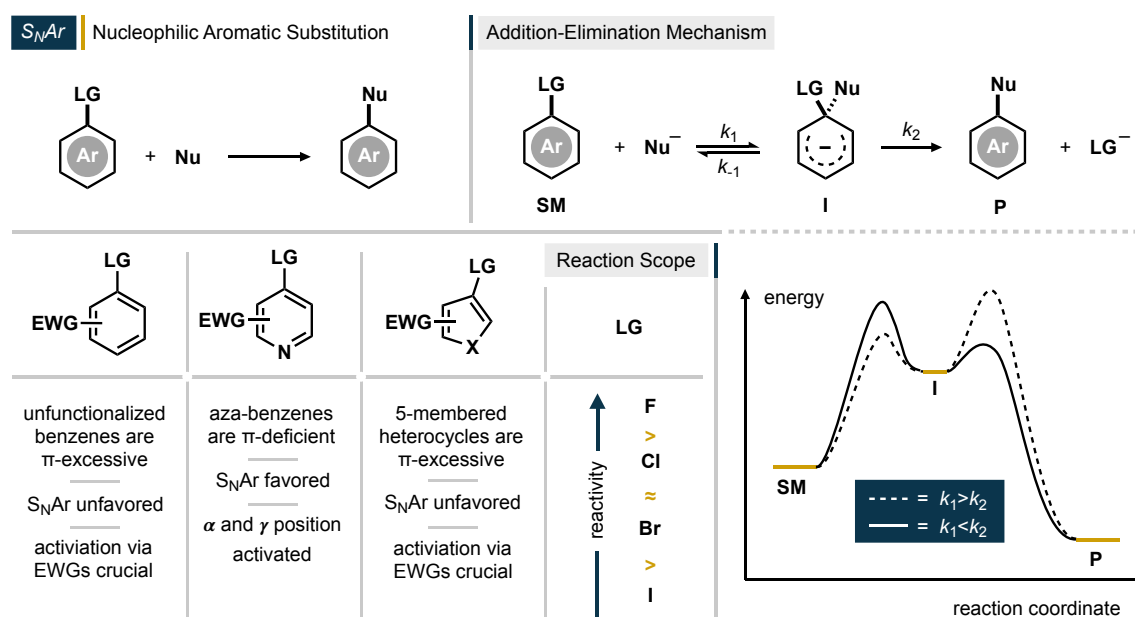
Scheme 2.5: Mechanistic considerations for the nucleophilic aromatic substitution.

Given the high-energy nature of the formed intermediates along with the intrinsic repulsion of an approaching nucleophile with the π-system of the aromatic substrate, it is not surprising that S$_N$Ar reactions are limited to electron deficient arenes and the installation of electron withdrawing substituents is often crucial for the course of the reaction. Despite this limitation, S$_N$Ar reactions have proven to be invaluable tools for the functionalization of electron deficient heterocyclic arenes, which are of particular interest in the field of medicinal chemistry.

A concept that has truly revolutionized arene functionalization chemistry is the field of transition-metal catalyzed cross-coupling reactions. The roots of the field go back to the 19$^{\text{th}}$ century when initial homocoupling reactions of organocopper species were reported by Glaser and Ullmann while Wurtz and Fittig investigated the homocoupling of alkyl and aryl halides in the presence of metallic sodium and potassium.[77–80] While early reports required stoichiometric or even superstoichiometric amounts of the respective metal species, catalytic versions were soon realized by Meerwein and Kharasch and later by Cadiot and Chodkiewicz, who used catalytic amounts of copper, nickel or cobalt salts.[81–84] However, the *cross* coupling, a highly sought-after transformation in synthetic chemistry, remained a challenge even after the report of these seminal methods. A breakthrough in the world of cross coupling reactions was achieved when the transformative power of palladium was recognized (scheme **2.6**).
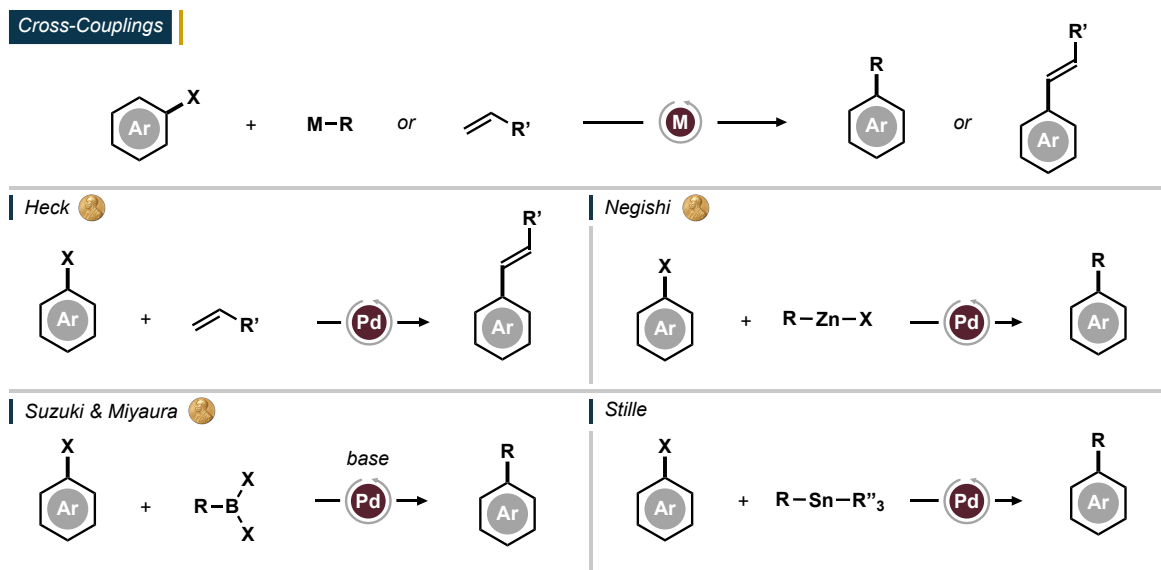
Scheme 2.6: Transition metal catalyzed cross-coupling reactions of arenes.

Inspired by the Wacker process, Heck became interested in the chemistry of aryl palladium complexes.[85] He observed that organomercurial reagents readily undergo coupling with alkenes in the presence of palladium salts. In seven single-author back-to-back publications, he then reported on his groundbreaking work that ignited the burgeoning fire of palladium catalyzed cross coupling reactions and laid the foundation for what should later become known as the Mizoroki-Heck reaction.[86–92] While initially similarly popular in cross-coupling chemistry, palladium soon after prevailed over nickel and copper as the versatile catalyst of choice and the field gave rise to a rich collection of transformations. In 1975, Sonogashira reported the coupling of terminal alkynes with aryl- or vinyl-halides, which was soon followed by Negishi's studies on the implementation of organozinc reagents.[93,94] This prompted chemists to further investigate the range of applicable nucleophiles in related cross coupling reactions. While Stille investigated organotin species, Suzuki and Miyaura introduced boronic acids and boronates to contribute a highly versatile and powerful methodology.[95–97]

The advent of cross-coupling methodologies has revolutionized the way retrosynthesis is conceived and molecules are constructed, a breakthrough that was honored by the 2010 Nobel prize awarded to Heck, Negishi and Suzuki. Despite the great efficiency and diversity that now exists in the world of cross-coupling chemistry, the concept suffers from intrinsic difficulties. Apart from expensive metal catalysts, the used reagents are often sensitive to air and moisture or display toxic properties. Furthermore, the dependency on synthetic handles on both coupling partners is a serious limitation which consequently requires stoichiometric prefunctionalization and/or functional group interconversion of aromatic precursors.[98]

The degree of prefunctionalization can be reduced if the direct activation of ubiquitously present C–H bonds becomes feasible. This has been one of the main motivators for the development of transition metal catalyzed C–H bond functionalization reactions. But while the modification of non-activated C–H bonds enables transformations with higher step and atom efficiencies, their abundance in organic molecules also poses the challenge of achieving selectivity in the bond formation (scheme **2.7**).[99] If a C–H bond can be selectively targeted, a concise modification can occur without preceding transformations which allows a "topologically obvious assembly" where the target has a high similarity to the starting material.[99] This predestines C–H activation methodologies for late stage functionalization reactions which is of particular interest for the field of drug discovery.[100]
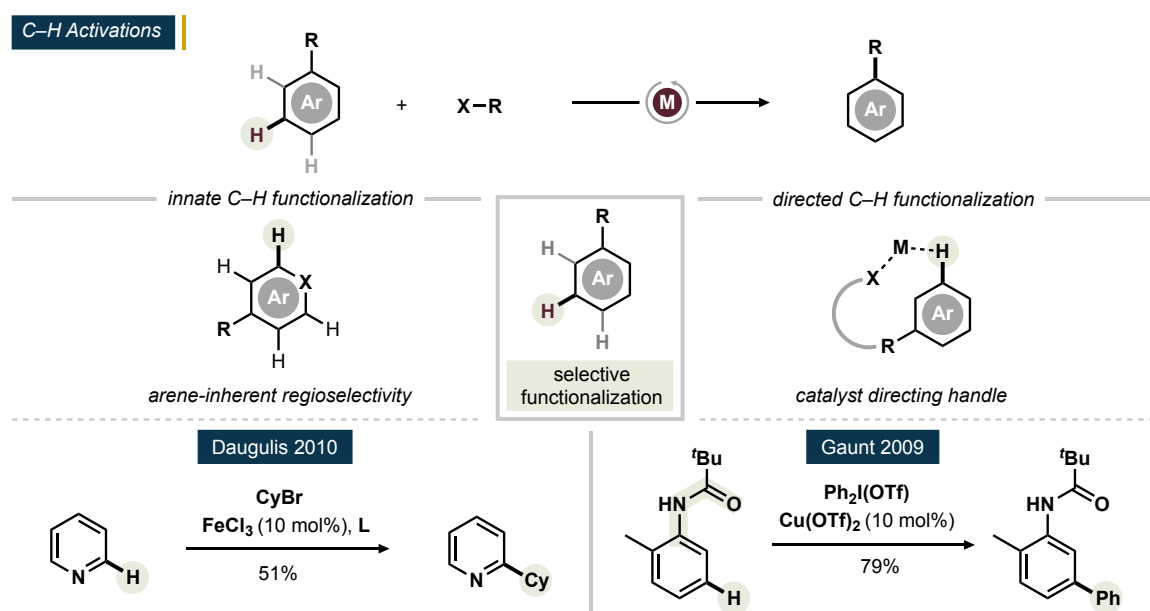
Scheme 2.7: The concept of transition metal catalyzed C–H activation reactions.[101,102]

While enantioselective C–H activation reactions have been studied extensively over the years, the development of methods for the regioselective transformation of aromatic substrates has recently become a particularly coveted goal.[103,104] To this end, the innate reactivity of an aromatic substrate, driven by electronic properties, can be taken advantage of to achieve regioselective C–H activation. In a directed C–H activation reaction, directing groups on the aromatic substrate can, in collaboration with the used catalyst, override intrinsic selectivities to yield unusual connectivities. This is of particular interest if the selectivity thus observed is orthogonal to that of alternative approaches.[101,105] While directed C–H activation reactions can provide unusual regioselectivities, they are by definition dependent on a directing group that,

in most cases, has to be installed and removed which significantly reduces the step, time and atom efficiency of the method.

C–H activation methods enable efficient and elegant transformations in certain cases, but the scope of the concept remains limited and selective versions are mostly dependent on synthetically disadvantageous directing groups.[106] Although modern approaches continue to offer creative alternatives, one of the most efficient and versatile methods for the direct functionalization of aromatic substrates is also one of the oldest: the electrophilic aromatic substitution reaction (S$_E$Ar).

2.3.1 Electrophilic Aromatic Substitution Reactions

One of the most straightforward approaches for the functionalization of many arenes lies in the exploitation of their inherent nucleophilicity, which enables the direct installation of substituents from electrophilic reagents. The electrophilic aromatic substitution (S$_E$Ar), the formal exchange of an aromatic hydrogen atom with a substituent originating from an electrophilic reagent, is consequently among the most crucial tools for the functionalization of arenes. The sheer breadth of possible electrophiles that can be introduced to simple arenes has made the S$_E$Ar particularly suitable for the early-stage functionalization of aromatic molecules: nitration, sulfonation or halogenation are just a few out of many examples for the incorporation of heteroatoms into simple aromatic feedstocks.[107]

Of special relevance is the introduction of organic substituents into aromatic molecules for the construction of more complex scaffolds and the direct diversification of petrochemically available arenes. Among these methods, the electrophilic aromatic alkylation has a particularly rich history, which dates back to two of the most prominent pioneers of the field of S$_E$Ar, Charles Friedel and James M. Crafts. In 1877, Friedel and Crafts treated a solution of amyl chloride (**17**) in benzene with aluminum stripes and shortly after observed the formation of amylbenzenes (**18**) (scheme **2.8**).[108] Soon, *in situ* formed AlCl$_3$ was identified as catalytically active species in the bond-forming event that should later become known as Friedel–Crafts alkylation. Not only did Friedel and Crafts lay the foundation for the field of the electrophilic catalytic alkylation of arenes, their discovery also represents one of the first reports of the usage of a Lewis acid catalyst in organic synthesis.[109]
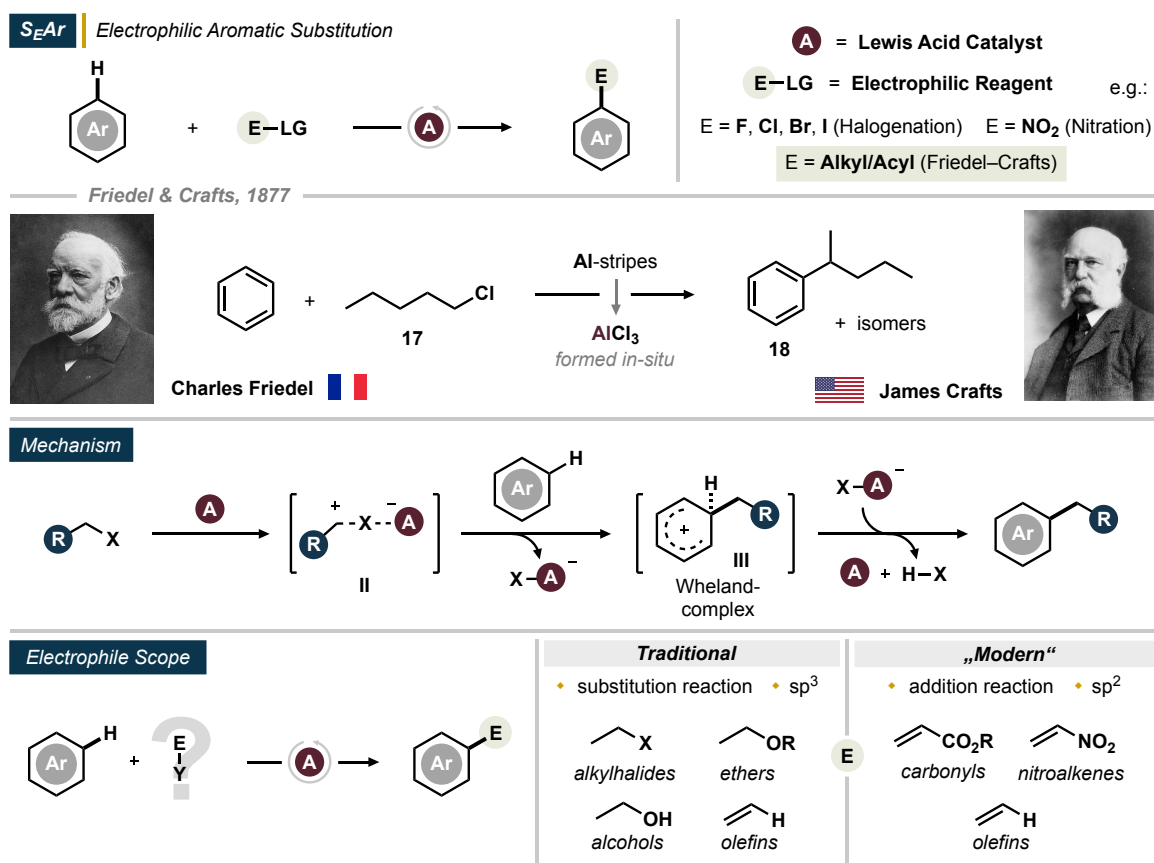
Scheme 2.8: The Friedel–Crafts reaction: origin and reaction scope.

In the more than 140 years since Friedel's and Crafts' groundbreaking discovery, countless scientists have shaped and developed what is known today as the Friedel–Crafts reaction. Simultaneously, the understanding of the chemical community regarding the exact definition of the reaction evolved.

In 1963, Olah and Dear defined Friedel–Crafts reactions as "any isomerization, elimination, cracking, polymerization, or addition reaction taking place under the catalytic effect of Lewis acid type [...] or protic acids", which also includes carbon-heteroatom bond formation.[109,110] A more modern understanding of the reaction however provides a less general definition which limits the scope of the Friedel–Crafts alkylation reaction to the "specific functionalization of arenes with various alkylating agents in the presence of catalytic amounts of a Lewis acid", excluding non-aromatic substrates from the scope of the definition.[111,112] Another aspect that requires further classification is the range of electrophilic alkylating agents which, by definition, fall into the category of the Friedel–Crafts reaction. The traditional Friedel–Crafts reaction involves a substitution reaction on a *sp³*-hybridized electrophilic reagent during the reaction. This stands in contrast to a more modern understanding which includes addition reactions to *sp²*- or *sp*-based reagents to the scope of the Friedel–Crafts reaction. If acyl chlorides or

anhydrides are used under similar conditions, the acylation of arenes can be achieved in what is referred to as Friedel–Crafts acylation.

In addition to the broad diversity of substrates and electrophiles applicable in the Friedel–Crafts reaction, there is a similarly wide range of Lewis and Brønsted acid catalysts that can be applied in the reaction. This enables a plethora of selective transformations which is even further enhanced by the possibility to apply co-catalysts in the reaction. While Friedel and Crafts state that their early studies were performed under anhydrous conditions, their access to a truly anhydrous reaction setup at that time was very limited and it was later found that traces of water, yielding HCl as co-catalyst, promote the reaction. Subsequent studies could even show that completely anhydrous AlCl$_3$ is inactive in many Friedel–Crafts reactions.[113]

Closely linked to the emergence of the Friedel–Crafts reactions is the curiosity of researchers to unravel the mechanistic details of the transformation. In the last century, enormous progress has been made in understanding the mechanism of the reaction, which not only helped to design new electrophilic aromatic substitution reactions but also provided comprehensive insights into the workings of Lewis acid catalysis, the chemistry of carbocationic intermediates and the physical background of aromaticity itself. Today, it is widely acknowledged that the Friedel–Crafts reaction is initiated by the activation of the electrophilic reagent by the Lewis acid catalyst to form an activated complex (**II**) or an ionic species (scheme **2.8**). The activated electrophile then undergoes nucleophilic attack by the aromatic substrate to yield a dearomatized, cationic σ-complex (**III**, also referred to as Wheland complex) from which aromaticity is restored upon deprotonation, releasing the Lewis acid catalyst.[112]

Cationic structures were soon identified as crucial intermediates in the reaction and especially the potential relevance of σ- and π-complexes was intensely researched (figure **2.9**). While the whole aromatic sextet acts as electron donor for the activated electrophile in π-complexes, a σ-bond is formed between the aromatic substrate and the alkylating agent in a σ-complex, leaving a dearomatized conjugated pentadienyl cation.[114]
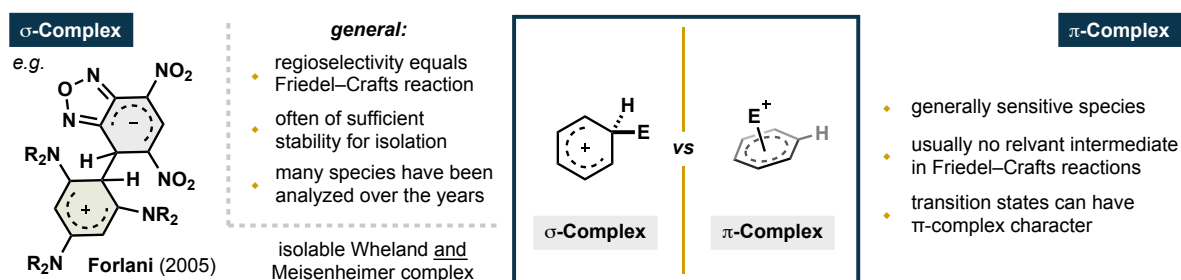
Figure 2.9: σ- and π-complexes as intermediates for electrophilic aromatic substitutions.[115]

Over the years, many σ-complexes could be isolated and analyzed spectroscopically, leaving little doubt about their presence as well as crucial importance in Friedel–Crafts reactions.[115–117] It could also be found that σ-complex-formation follows the general directing patterns of S_EAr and their selective formation is therefore essential for regioselective substitution.[118] π-Complexes are sensitive species that generally are not considered to be intermediates in Friedel–Crafts reactions, the transition states of some reactions however are expected to be of π-complex character.[119–121]

While widely recognized for their efficiency, Friedel–Crafts reactions are often criticized for the harsh reaction conditions that result from the endergonic formation of dearomatized Wheland-type intermediates.[122] In conjunction with this, a number of challenges for the selective functionalization arise.

2.4 The Friedel–Crafts Reaction – Challenges and Potential

2.4.1 Regioselectivity

When multiple aromatic C–H bonds are present in a substrate, distinguishing between them becomes a challenge. Complex mixtures of regioisomeric products can then result from S_EAr which significantly complicates isolation processes. Understanding the guiding principles which favor the achievement of regioselectivity is therefore crucial for the development of systems that allow the selective substitution of a chosen out of a number of possible C–H bonds. The regioselectivity of Friedel–Crafts reactions is mainly determined by the stabilization of the formed Wheland intermediates, which in turn depends on the electronic structure of the aromatic substrate (scheme **2.9**). Electron-donating substituents (EDG) on monosubstituted benzenes have been found to stabilize positive charge in each position of the aromatic ring via conjugation- or hyperconjugation effects, which generally supports the proceeding of the S_EAr. The most significant stabilization however is observed in the 2- and the 4-positions which leads to a *para*- and *ortho*-directing effect of EDGs.[123]
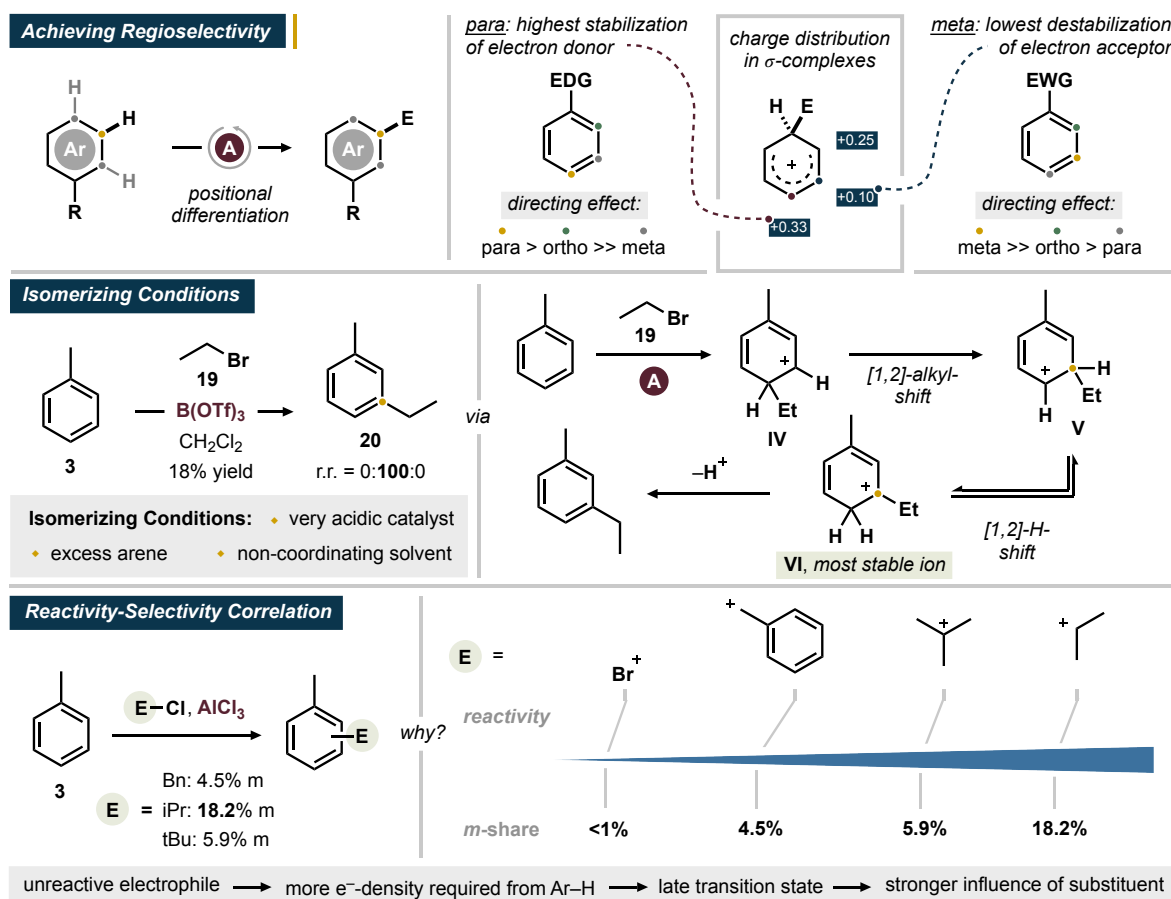
Scheme 2.9: The regioselectivity of the Friedel–Crafts reaction.

Electron-withdrawing substituents (EWG) on the other side destabilize Wheland complexes and therefore disfavor the proceeding of the reaction. Since destabilization is minimized when substitution takes place in the 3-position, EWGs can be found to have a *meta*-directing effect. Intriguingly, very high ratios for the formation of the *meta* isomer can still be observed under certain conditions. When Olah investigated the ethylation of toluene in CH_2Cl_2 using ethyl bromide (**19**) as alkylating agent and $B(OTf)_3$ as Lewis acid catalyst, 3-ethyl toluene (**20**) was even formed as single isomer (scheme **2.9**).[124] As suggested in earlier studies by Brown, this peculiar observation is not due to a direct *meta*-selective bond formation but to a subsequent isomerization from initially formed *ortho-* or *para-σ*-complexes **IV** to the more stable *meta*-complex **VI** under vigorous reaction conditions.[125] Especially high excess of the aromatic substrate in weakly coordinating solvents along with strongly acidic catalysts have shown to favor isomerization to the *meta*-isomer.

However, it was found that variable amounts of the *meta*-isomer could also be found under non-isomerizing conditions. Nelson and Brown became interested in the correlation between the *meta*-share of an S_EAr reaction and the reactivity (which corresponds to the electrophilicity) of

an electrophilic agent.[125] In accordance with later studies by Olah, it was found that the reactivity of an electrophile is directly proportional to the rate of formation of the *meta* isomer in the corresponding S_EAr reaction (scheme **2.9**).[125,126] The authors rationalize this finding with the increased electron density that the aromatic substrate must provide to activate less reactive electrophiles. This consequently leads to the formation of late, product-like transition states in which the influence of the directing group is increased and higher *ortho-* and *para*-selectivities are observed.

The degree of directing strength is illustrated impressively in the bromination of toluene in acetic acid: the relative reaction rate of *ortho*-substitution is more than one hundred times higher than that of *meta*-substitution, which is even surpassed by the rate for *para*-substitution which corresponds to more than a four hundred times higher rate (scheme **2.10**).[127]
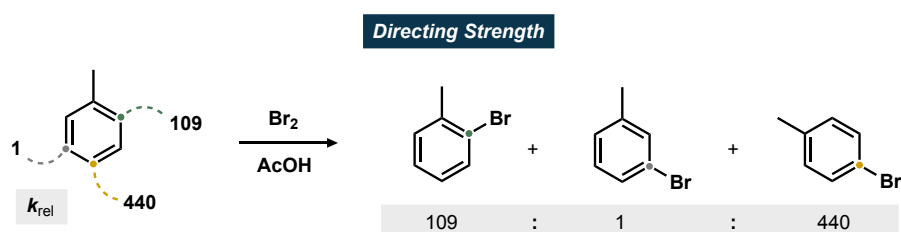
Scheme 2.10: Substituent-directing strength in the bromination of toluene.[127]

Controlling the regioselectivity of the Friedel–Crafts reaction is crucial to ensure selective bond formation and yet, despite decades of research, scientists still have to submit to the intrinsic regioselectivity of arenes that is dictated by directing effects. The development of catalytic systems that allow to intimately guide the regiochemistry of the S_EAr in order to overcome inherent selectivities is therefore a highly desirable and as yet unachieved synthetic goal.

2.4.2 Overalkylation

The potential for undesired overalkylation is another inherent challenge of the Friedel–Crafts reaction. While the phenomenon of overalkylation has long been associated with the electronic activation of alkylated substrates relative to the original starting material, Francis was able to show that the electronic activation of an additional alkyl residue is of limited significance and that a lack of homogeneity in the reaction system could have a stronger influence (scheme **2.11**).[128]
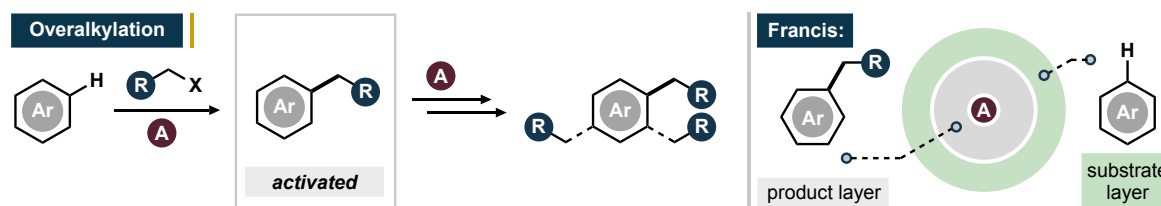
Scheme 2.11: Overalkylation as omnipresent challenge in Friedel–Crafts alkylations.[128]

According to Francis, reactions usually take place in a heterogeneous state of the catalyst-containing layer, which, after initial alkylation, favors polyalkylation over monoalkylation because the alkylated products are statistically more likely to interact with the catalyst. This applies not only to heterogeneous catalysis, but also to initially homogeneous conditions. Harsh reaction conditions can then lead to a fast Friedel–Crafts reaction which creates a local enrichment of alkylated products around the catalyst.[128]

While this problem can potentially be avoided by more efficient stirring methods, the increased steric bulk after the initial alkylation can also be taken advantage of to prevent multiple alkylation by usage of a sterically confined catalyst. Historically, Friedel–Crafts acylation-reduction sequences have often been used as less step- and time-efficient alternative to circumvent the undesired formation of overalkylated side products in Friedel–Crafts alkylation procedures.[112]

2.4.3 Rearrangements and Reversibility

The influence of strong Lewis or Brønsted acids on electrophilic alkylating agents not always leaves them unaffected. Most strikingly, reagents can undergo acid-catalyzed rearrangements to yield a mixture of isomers or form an undesired bond (scheme **2.12**). In the Friedel–Crafts reaction of benzene with 1-propylchloride (**21**) and AlCl$_3$ for example, [1,2]-H shift of *in situ*-formed 1-propyl cation intermediates to the 2-propyl species **VII** leads to the formation of the branched product **22** as predominant isomer. This makes the installation of linear substituents more challenging and often alternative approaches such as Friedel–Crafts acylation-reduction sequences have to be considered.[110]
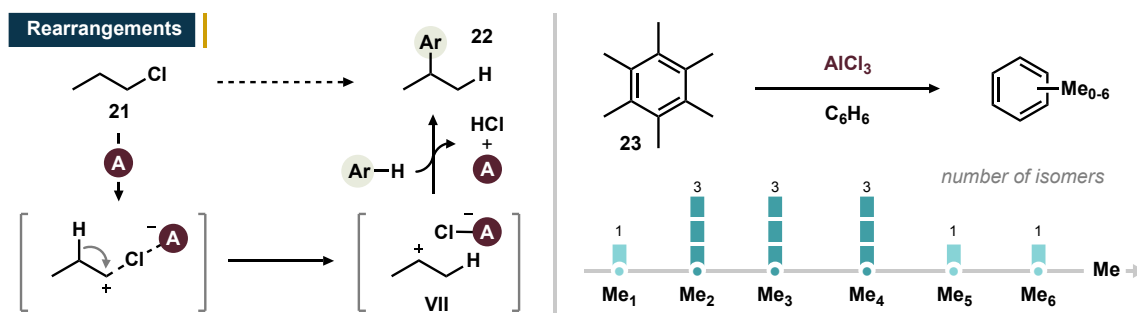
Scheme 2.12: Intra- and intermolecular alkyl-transfer reactions of alkylbenzenes.

Apart from these rearrangements, further skeletal isomerization can take place in the reaction of or toward alkylbenzenes under harsh conditions. In the presence of strong acids, activation of the alkylbenzene scaffold can occur to form σ-complexes that serve as platforms for various further isomerization reactions. Positional shifts of alkyl substituents can then occur to yield products of different regiochemistry and alkyl substituents can even scramble intermolecularly between multiple arene species. If a solution of hexamethylbenzene (**23**) and AlCl$_3$ in benzene is subjected to higher temperatures, a complex mixture of hydrocarbon arenes with zero to six methyl groups is obtained (along with thus formed regioisomers), which gives evidence for the reversible nature of the Friedel–Crafts reaction.[110] This can serve to equilibrate a mixture of alkylbenzenes in order to enrich a desired isomer, but it can also lead to a more complex mixture of product isomers.

2.4.4 Substrate Limitations

Many Friedel–Crafts reactions depend on harsh reaction conditions, including strongly acidic catalysts, elevated temperatures or highly reactive alkylating agents.[129] Because of these conditions, they are often incompatible with substrates that carry sensitive functional groups. Even more restricting is that the Friedel–Crafts reaction (as all S$_E$Ar reactions) is highly dependent on the electronic nature of the aromatic substrate. While electron-rich arenes are well tolerated in many Friedel–Crafts reactions, unactivated arenes require harsh reaction conditions. The activation of arenes bearing electron-withdrawing substituents is particularly challenging and strongly deactivating groups can shut down the S$_E$Ar entirely. Decreased electron density on the aromatic substrate in turn requires harsher reaction conditions to compensate, which generally reduces the selectivity of the reaction. This can be observed for

the regioselectivity of the reaction, but it is particularly apparent for enantioselective versions of the reactions.

2.4.5 Asymmetric Catalytic Friedel–Crafts Reactions

Benzylic stereocenters are ubiquitous motifs in medicinal chemistry, the asymmetric construction of benzylic stereocenters is consequently of great synthetic importance.[130] After Casiraghi reported the first asymmetric Friedel–Crafts alkylation in 1985, Erker contributed the first asymmetric catalytic version of the reaction using a chiral zirconium-based catalyst (scheme **2.13**).[131,132] In the following years, the scientific community gradually discovered the synthetic advantage of the Friedel–Crafts reaction for the selective construction of benzylic stereocenters. Over the following decades, a multitude of highly selective methods has been reported.[133–138] Analysis of the reported procedures however reveals a trend throughout the different approaches: while strongly nucleophilic heteroarenes such as indole (**24**, Mayr nucleophilicity $N = 5.55$)[139] or pyrrole (**25**, $N = 4.63$)[140] are frequently used, less nucleophilic aromatic substrates such as anisole (**26**, $N = -1.18$)[141] find less application and purely hydrocarbon arenes like toluene ($N = -4.36$)[142] have previously been excluded from asymmetric catalytic Friedel–Crafts reactions (scheme **2.13**).
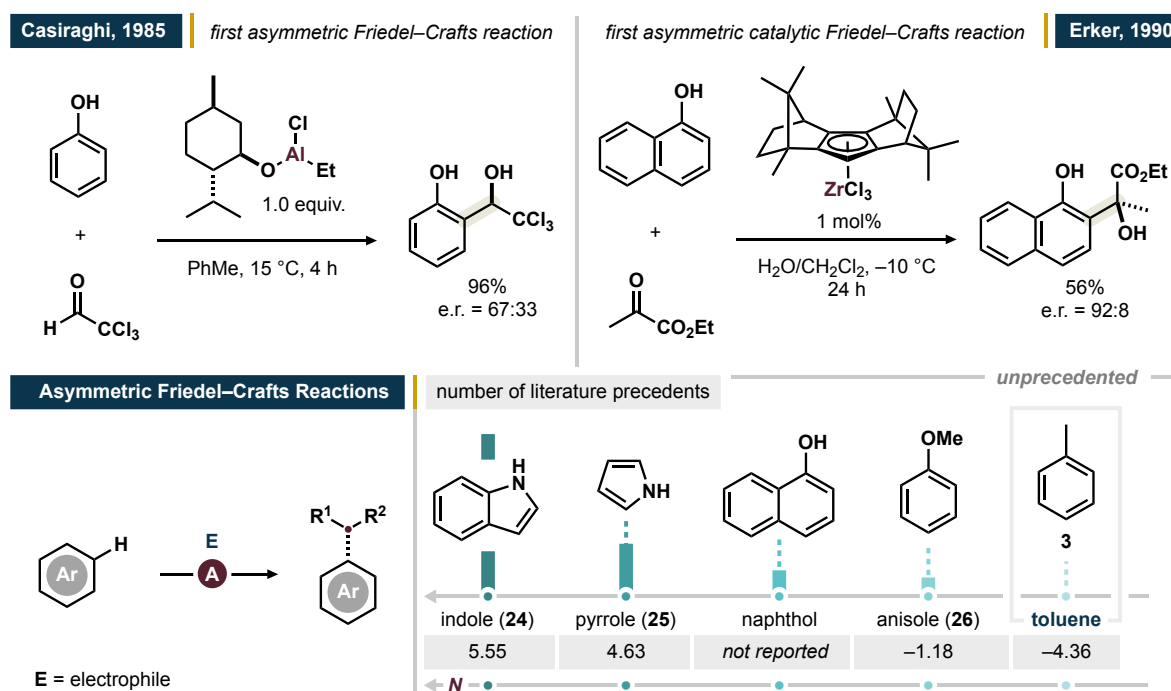
Scheme 2.13: Precedents of the asymmetric catalytic Friedel–Crafts reaction.[139–142]

While the development of an asymmetric catalytic Friedel–Crafts reaction of simple hydrocarbon arenes has been recognized to be a particularly difficult challenge,[133] it would also hold the reward of a streamlined synthesis starting from one of the cheapest available aromatic building blocks, namely alkylbenzenes.

2.5 Friedel–Crafts Alkylation: An Outlook

In three years' time, the year 2027 will mark the 150th anniversary of the groundbreaking discovery made by Friedel and Crafts. Their findings had a lasting impact on the field of synthetic chemistry and in the nearly 15 decades that followed, scientists pushed the limits of the pioneering work to make the Friedel–Crafts reaction a cornerstone in the transformation of arenes. However, as described above, the reaction still faces the same problems as decades ago, which limits it significantly. These limitations have spurred on scientists to explore alternative approaches as a way to overcome the many shortcomings of the Friedel–Crafts reaction – the lack of regioselectivity, the intolerance to functional groups or the poor reactivity of electron-deficient arenes, only to name a few.[129] The synthetic disconnections offered by Friedel–Crafts reactions often are, at least theoretically, unmatched in efficiency by alternative approaches and only avoided due to practical limitations. The investigation of different methods might consequently be one way to overcome these challenges. Further improvement of the time-tested Friedel–Crafts alkylation however undoubtedly holds the potential to not only expand the scope of the iconic reaction, but it might also provide access to previously uncharted chemical space in the constant quest for ever more efficient chemical synthesis. The development of regio- and stereoselective Friedel–Crafts processes of electronically unactivated arenes using strong and confined Brønsted acid catalysts has been investigated in the context of this doctoral thesis and will be described in further detail in chapter 4.

3. Objectives

Friedel-Crafts reactions have been studied extensively to improve the access to modified aromatic structures. However, they are still severely limited by the nucleophilicity of the aromatic substrate which is particularly evident when selective transformations require milder reaction conditions. While nucleophilic heterocyclic arenes have been investigated extensively in the context of enantioselective Friedel–Crafts reactions, the harsher reaction conditions necessary for the activation of unreactive hydrocarbon arenes have so far prevented their use in asymmetric S_EAr reactions.[133] This restricts the accessible chemical space by excluding a group of readily available aromatic feedstocks from the scope of the asymmetric catalytic Friedel–Crafts reaction.

To functionalize unreactive hydrocarbon arenes in Friedel–Crafts pathways, extremely acidic Lewis- or Brønsted acid catalysts and highly reactive electrophilic reagents are required to enable bond formation. Conversely, high regio- and enantioselectivities typically necessitate mild reaction conditions. We consequently envisioned that, if a strong acid catalyst is matched with a suitable confined environment around the catalytic site, the selective Friedel–Crafts reaction of unactivated alkylbenzenes **27** might become possible (scheme **3.1**). To this end, the acid catalyst should be specifically tailored to control the regioselectivity, the stereoselectivity and the degree of alkylation and thus enable the C–C bond formation to proceed with a high general selectivity.
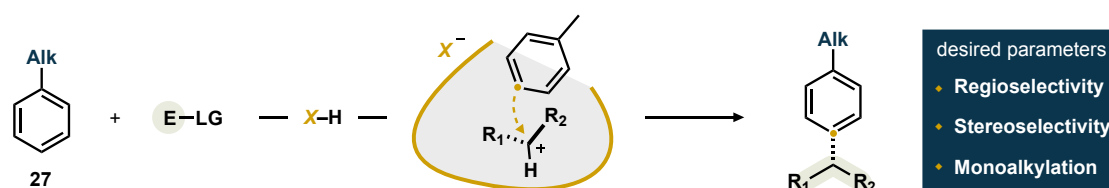
Scheme 3.1: Selective Friedel–Crafts reaction of alkylbenzenes.

Besides strongly acidic catalysts, reactive electrophilic reagents must be used to overcome high energy barriers for the unfavorable formation of Wheland intermediates toward the S_EAr of alkylbenzenes. Therefore, to enable the selective transformation via ACDC, carbocationic intermediates or reagents of exceptional electrophilicity should be used or generated to allow the nucleophilic attack of the alkylbenzene. Stimulated by the relevance of non-canonical amino acids, we envisioned the use of *in situ* generated *N*-acyliminium ions **VIII** as highly reactive

cationic species in the regio- and stereoselective Brønsted acid-catalyzed Friedel–Crafts reaction of alkylbenzenes **27** toward arylglycine products **28** (scheme **3.2**).[143,144]
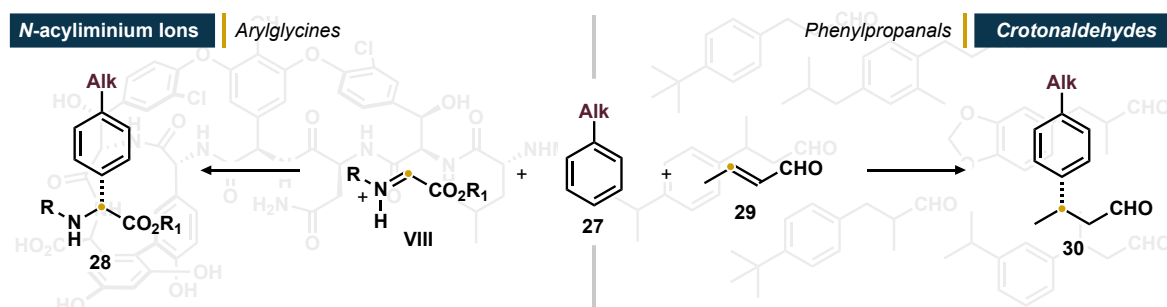
Scheme 3.2: Usage of iminium ions **VIII** and enals **29** in asymmetric Friedel–Crafts reactions.

The selective Friedel–Crafts reaction of unactivated alkylbenzenes **27** is of special interest for the field of fragrance applications as many lily of the valley aroma molecules can potentially be obtained through the reaction of alkylbenzene arenes with simple butenal-derivates **29**. We therefore envisioned the Brønsted acid-catalyzed addition of unactivated hydrocarbon arenes to enal systems toward the synthesis of enantioenriched arylpropanals **30** from inexpensive and readily available feedstocks.

4. Results and Discussion

The research carried out within the scope of this doctoral thesis will be demonstrated in two separate sections. The first part will cover our efforts on the acid-catalyzed transformation of *N*-acyliminium ions, generated from *N,O*-acetals, in the regio- and stereoselective Friedel–Crafts reaction of unactivated arenes toward non-canonical arylglycine esters. The reaction development and the investigation of the scope of the reaction is then followed by mechanistic studies. The second part will cover the development of methods for the chiral Brønsted acid-catalyzed conjugate addition of aromatic substrates to activated enal derivatives toward the synthesis of enantioenriched 3-arylpropanals, important structures for fragrance applications.

4.1 Asymmetric Friedel–Crafts Reaction Toward Arylglycines

4.1.1 Arylglycines as Building Blocks for the Life Sciences

Non-ribosomal peptides (NRPs) are a class of peptides synthesized independently from messenger RNA by nonribosomal peptide synthetases in bacteria and fungi. They are of special interest for medicinal chemistry as their diverse entirety has shown to include a range of molecules with intriguing antibiotic properties.[145,146] Especially, the ever-growing number of multi-resistant germs has consequently spurred on scientists to unravel the secrets that lie beyond the structure of NRPs. One class of amino acid building blocks was found to appear surprisingly often in the peptide structure of NRPs: the class of arylglycines. In nature, arylglycines are usually diversely functionalized representatives of three parent structures: phenylglycine (**31**), 4-hydroxyphenylglycine (**32**) and 3,5-dihydroxyphenylglycine (**33**) (scheme **4.1**). Many prominent biologically active compounds contain arylglycine scaffolds as central structural units: vancomycin (**34**) and teicoplanin, the arylomycins as well as the aminopenicillins **35** are just a few examples out of a vast realm of essential NRPs in the fight against bacterial infections. Arylglycines are also a recurring motif in synthetic medicinal chemistry as recently demonstrated by Neyts and coworkers at Janssen Pharmaceutica who reported the development of arylglycine-derived Dengue-virus inhibitor JNJ-A07 (**36**).[147]

The α-aryl-structure of arylglycines gives these amino acids their unique properties, it however also complicates synthetic transformations as the amino acids are particularly vulnerable toward racemization.[146] Driven by these challenges along with the importance of the arylglycine

4. Results and Discussion
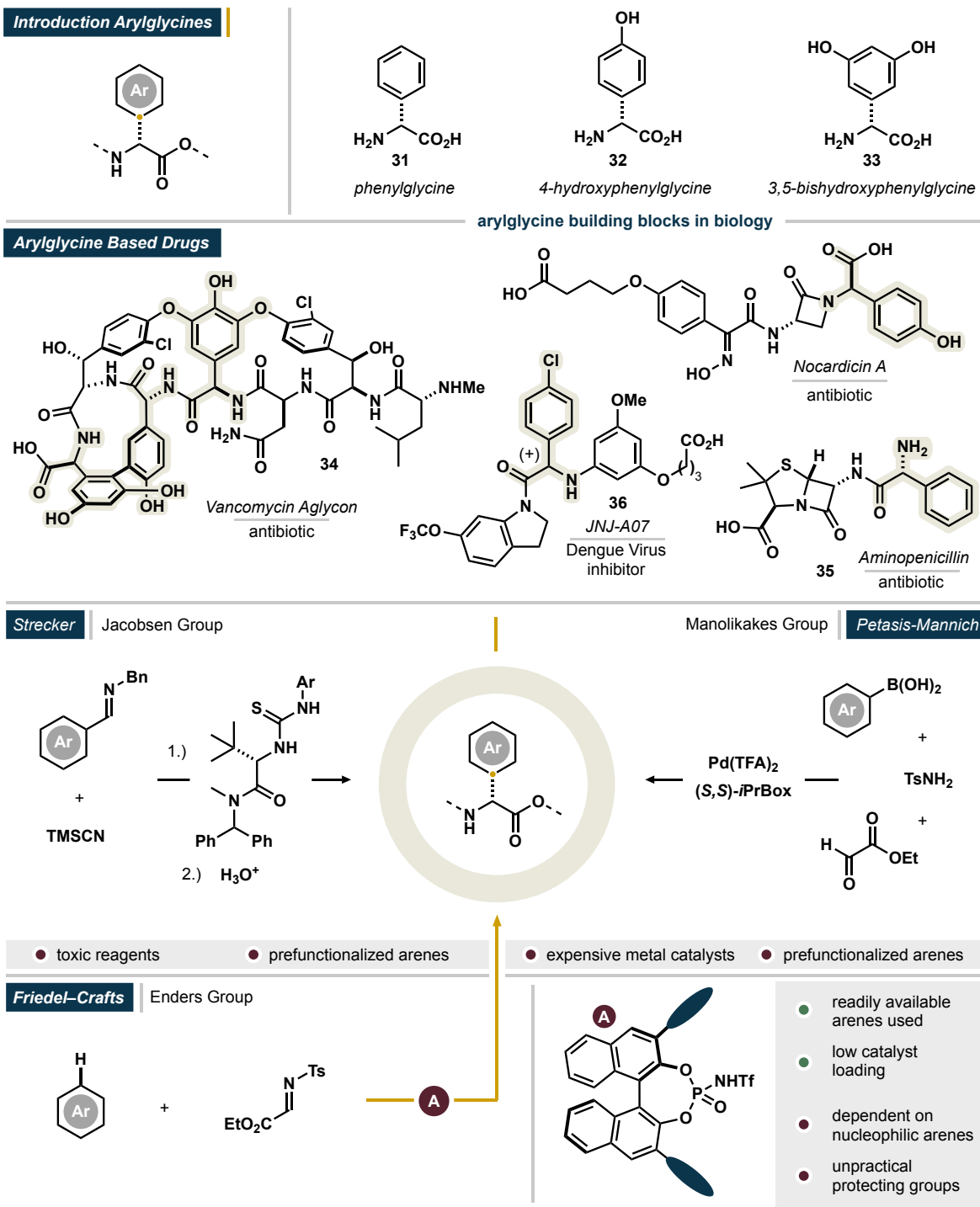
Scheme 4.1: Relevance and synthesis of arylglycines.

motif, many approaches have been developed and constantly improved to enable the efficient synthesis and functionalization of arylglycine structures for total synthesis and medicinal chemistry.[146,148] Stimulated by the relevance of enantioenriched building blocks, asymmetric methods have increasingly been investigated. While Sharpless-aminohydroxylation-oxidation sequences of styrenes have been in the focus of earlier studies by Boger,[149–151] asymmetric

Strecker- or Petasis-Mannich-reactions soon revealed great potential in the selective synthesis of arylglycine motifs as shown by Jacobsen[152] and Manolikakes (scheme **4.1**).[153] The reported methods however often require toxic reagents or rare metal catalysts and, moreover, rely on prefunctionalized aromatic building blocks.

The direct transformation of readily available arenes would allow a more straightforward approach to potentially enable a faster and more economic synthesis. Friedel–Crafts processes toward arylglycines have therefore been investigated over the last decades. Especially contributions by Enders stand out as they provide efficient access to enantioenriched arylglycines.[154] The reported methods however usually suffer from various problems: synthetically disadvantageous protecting groups are required and the scope of applicable arenes is usually limited to substrates of high nucleophilicity. To overcome existing challenges and to contribute an efficient and directly applicable method, we decided to investigate the Friedel–Crafts reaction of unactivated alkylbenzenes to yield enantioenriched arylglycines.

4.1.2 Reaction Design and Initial Studies

Inspired by early work by Ben-Ishai on the Brønsted acid-mediated synthesis of arylglycine derivatives via Friedel–Crafts reaction of hydroxy glycines, we focused our initial investigations on the use of similar hemiaminal reagents (scheme **4.2**).[155,156]
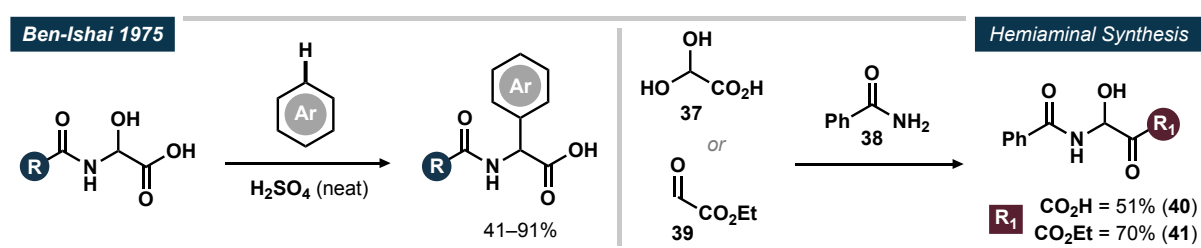
Scheme 4.2: Preceding studies by Ben-Ishai and hemiaminal synthesis.

The required hemiaminal reagents were prepared by condensation of glyoxylic acid monohydrate (**37**) and benzamide (**38**) or the addition thereof to ethyl glyoxylate (**39**). Both reagents **40** and **41** thus acquired were then subjected to the Friedel–Crafts reaction with strong Brønsted acid catalysts (table **4.1**). For a better evaluation of the reactivity of the present system, two aromatic substrates of different nucleophilicity were used as benchmark substrates, namely toluene (**3**) and 1,3,5-trimethoxybenzene (**42**). The general reactivity was evaluated using bis(trifluoromethane)sulfonimide (HNTf$_2$,) and strong and confined imidodisphosphorimidate

organocatalysts in CH$_2$Cl$_2$. Since glyoxylic acid derived hemiaminal **40** was found to be insoluble in most organic solvents, our initial focus was on the transformation of the corresponding ethyl ester **41**.

Using the strong achiral acid HNTf$_2$ together with **42** as highly nucleophilic aromatic substrate, the formation of the desired amino acid ester was observed with an isolated yield of 70% (entry 2). Using strong and confined imidodiphosphorimidate **IDPi-01-a** as chiral Brønsted acid catalyst, the analogous reaction was found to occur, but only with slightly reduced yield and over a significantly prolonged reaction time (entry 3). Transition to the desired class of less

Table 4.1: Initial hemiaminal screening. [a] = crude NMR yield. [b] = isolated yield after flash column chromatography.

entry	R$_1$	acid catalyst	arene substrate	t	T	conc.	additive	yield[a]
1	OH	HNTf$_2$ (10 mol%)	TMB (5 equiv.)	20 h	30 °C	0.1 M	–	<5%
2	OEt	HNTf$_2$ (10 mol%)	TMB (5 equiv.)	12 h	30 °C	0.1 M	–	70%[b]
3	OEt	IDPi-01-a (2.5 mol%)	TMB (5 equiv.)	14 d	30 °C	0.3 M	–	65%
4	OEt	IDPi-01-a (1 mol%)	TMB (5 equiv.)	3 d	40 °C	0.25 M	BSTFA (5.0 equiv.)	<5%
5	OEt	HNTf$_2$ (10 mol%)	PhMe (solvent)	48 h	50 °C	0.1 M	–	14%[b]
6	OEt	IDPi-01-a (2.5 mol%)	PhMe (solvent)	3 d	50 °C	20 h	–	<5%
7	OEt	IDPi-01-a (1 mol%)	PhMe (solvent)	3 d	50 °C	20 h	BSTFA (5.0 equiv.)	<5%

nucleophilic alkylbenzene arenes proved to be more challenging: usage of toluene as substrate and solvent in the reaction with HNTf$_2$ under otherwise analogous reaction conditions yielded significantly reduced amounts of the corresponding product and application of **IDPi-01-a** only gave traces of the target amino acid (entries 5-7). The previously proven addition of *N,O*-bis(trimethylsilyl)trifluoroacetamide (**BSTFA**, **43**) as silylating agent in both cases did not lead to any improvement of the reaction outcome.[157]

4. Results and Discussion

Given the insufficient reactivity of benzamide-derived glycine precursors **40** and **41** with toluene as model substrate for hydrocarbon alkylbenzenes, we focused our attention on different electrophiles and thus chose to investigate the reactivity of carbamate-derived reagents. Not only do the corresponding electrophiles provide different electronic properties, the carbamate protecting group at the amino terminus of thus obtained amino acid products also enables straightforward protecting group manipulations.[158] In preceding studies, Luo disclosed the synthesis of the carbamate-derived hemiaminals via addition of benzyl carbamate (**44**) to ethyl glyoxylate (**39**).[159] To enhance the reactivity of the electrophilic reagents, the hemiaminal **45** was additionally acetylated to yield the corresponding *N,O*-acetal **46** (table **4.2**).

Table 4.2: Synthesis and application of benzylcarbamate derived electrophiles. [a] = crude NMR yield. [b] = isolated yield after flash column chromatography.
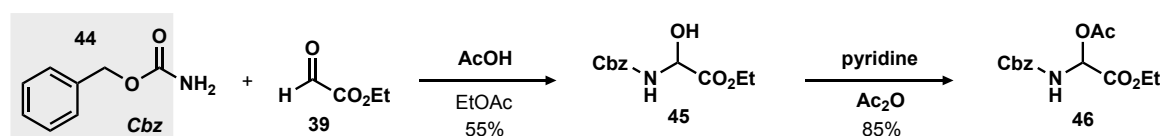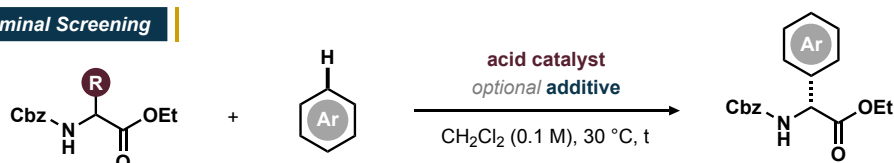
entry	R	acid catalyst	arene substrate	t	additive	yield[a]	r.r. (p/o)	e.r.
1	OH	HNTf$_2$ (10 mol%)	TMB (5 equiv.)	20 h	–	47, 70%[b]	n.d.	–
2	OH	HNTf$_2$ (10 mol%)	TMB (5 equiv.)	20 h	BSTFA (5.0 equiv.)	<5%	–	n.d.
3	OH	IDPi-01-a (1 mol%)	TMB (5 equiv.)	20 h	–	60%	n.d.	n.d.
4	OH	IDPi-01-a (1 mol%)	TMB (5 equiv.)	20 h	BSTFA (5.0 equiv.)	<5%	n.d.	n.d.
5	OH	HNTf$_2$ (10 mol%)	PhMe (solvent)	20 h	–	<5%	n.d.	n.d.
6	OH	IDPi-01-a (1 mol%)	PhMe (solvent)	20 h	–	<5%	n.d.	n.d.
7	OAc	HNTf$_2$ (10 mol%)	TMB (5 equiv.)	16 h	–	47, 82%[b]	–	–
8	OAc	IDPi-01-a (1 mol%)	TMB (5 equiv.)	16 h	–	78%	–	n.d.
9	OAc	HNTf$_2$ (10 mol%)	PhMe (solvent)	16 h	–	36%	7.5:1	–
10	OAc	IDPi-01-a (5 mol%)	PhMe (solvent)	12 h	–	50%	20:1	82:18
11	OAc	IDPi-01-a (1 mol%)	PhMe (solvent)	16 h	48 (3.0 equiv.)	50, >90%	–	n.d.
12	OAc	IDPi-01-a (1 mol%)	PhMe (solvent)	16 h	49 (3.0 equiv.)	51, >90%	–	n.d.
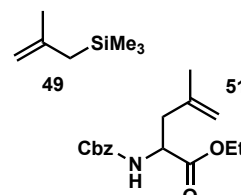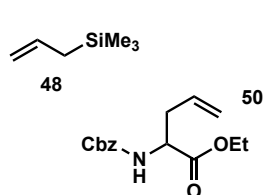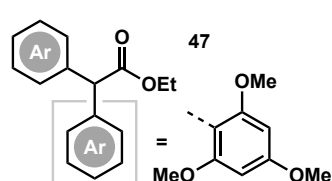
The reactivity of the hemiaminal **45** was initially investigated in the Brønsted acid-catalyzed Friedel–Crafts reaction. In the HNTf$_2$-catalyzed reaction of **45** with **TMB** as aromatic substrate, the double addition of the arene to the hemiaminal was observed, substituting both the hydroxy group as well as the aminocarbamate group. The addition of BSTFA, analogously to previous studies, completely shut down the reaction. While the usage of **IDPi-01-a** in the reaction with **TMB** gave the desired arylglycine product with good yields, both HNTf$_2$ and **IDPi-01-a** were found to be inactive in the Friedel–Crafts reaction of hemiaminal **45** and toluene (entries 5-6). As expected, the acylation of hemiaminal **45** significantly increased the reactivity of the reagent. The reaction of *N,O*-acetal **46** with toluene and HNTf$_2$ as catalyst afforded the desired toluylglycine in moderate yield with a preference for the *para* isomer. Application of 5 mol% of **IDPi-01-a** was furthermore found to yield the Friedel–Crafts adduct with an improved yield of 50%, a *para/ortho* ratio of 20:1 and a promising enantiomeric ratio of 82:18. The use of allyl- (**48**) or methallyl trimethylsilane (**49**) as a catalyst-silylating agent yielded the Hosomi-Sakurai products **50** and **51**, exclusively.

We noticed that in the IDPi-catalyzed reaction of *N,O*-acetal **46** with toluene (see table **4.2**, entry 10), the reaction slows down significantly as the reaction time progresses. TLC-MS analysis of the reaction mixture revealed that multiple catalyst species had formed during the reaction: not only the parent **IDPi-01-a** was detected, also ***i*IDP-01-a** as well as **IDP-01** were found to be present in the reaction mixture (scheme **4.3**). We consequently hypothesized that, induced by the highly electrophilic nature of *in situ* formed *N*-acyliminium ions, stepwise hydrolysis of the catalyst might take place, cleaving the sulfonamide groups and thus yielding Brønsted acid catalysts of reduced, potentially insufficient acidity.[67] Preventing inner core hydrolysis of the used catalyst might therefore be of high relevance to improve the yield of the reaction. More detailed catalyst stability studies are reported later in this thesis (section **4.1.6**).

*TLC of reaction of N,O-acetal **46** with PhMe (see table 4.2 entry 10)*
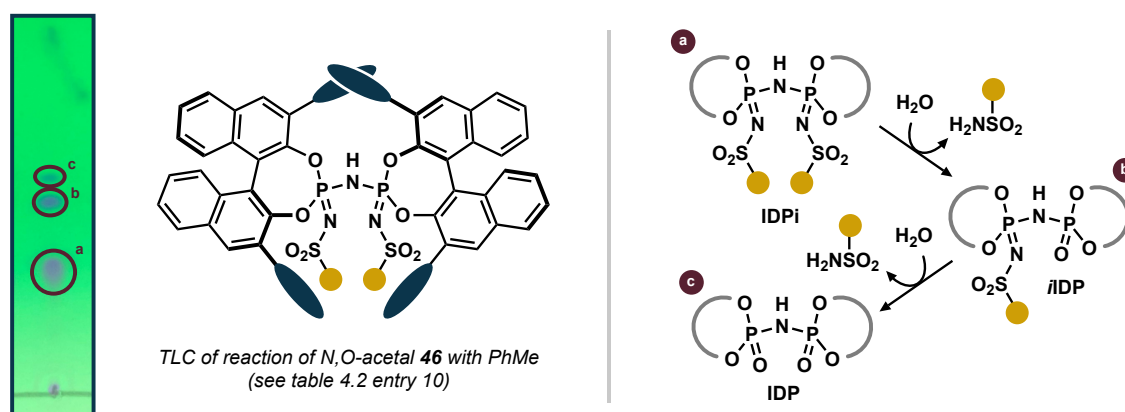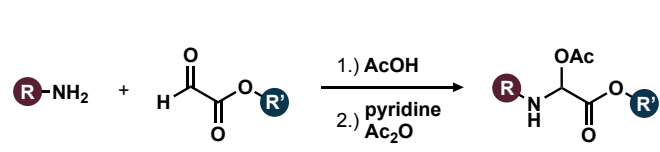
Scheme 4.3: Observed catalyst decomposition and the potential cleavage pathway.
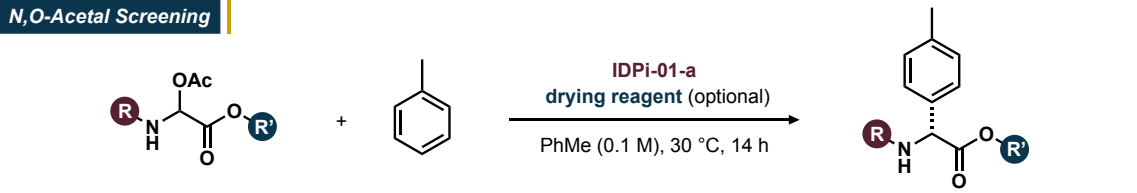
Building up on the initial success of *N,O*-acetal **46** in the investigated Friedel–Crafts reaction, we chose to test similar reagents bearing differing substituents on both the *N*- as well as the *C*-terminus. The synthesis of the required reagents was performed analogously using different carbamates and/or alkyl glyoxylates (table **4.3**). The *tert*-butyloxycarbonyl (Boc) protected *N,O*-acetal **52** was found to be completely unreactive under the aforementioned reaction conditions (presumably due to cleavage of the acid-labile protecting group and subsequent quenching of the catalyst). Installation of a fluorenylmethyloxycarbonyl (Fmoc) protecting group however restored the reactivity and afforded the corresponding arylglycine ester with an improved enantiomeric ratio of 90:10 (entry 2). Modification of the ester on the other hand did not result in a comparable improvement of the selectivity: Et-, Me- and *i*-Pr-substituted *N,O*-acetals **53**-**55** could be transformed with similar regio- and stereoselectivities as well as yields. Therefore, we chose the ethyl-substituted *N,O*-acetal **54** for further studies, since the building blocks for its synthesis are commercially available and superior selectivities were obtained with the Fmoc residue. Furthermore, the Fmoc group is among the most practicable protecting groups in peptide synthesis due to easy and mild installation and deprotection strategies, which additionally supports its application in our studies.[158]

Table 4.3: Initial screening of *N,O*-acetal electrophiles with IDPi catalysts. [a] = crude NMR yield. [b] = isolated yield after flash column chromatography.

entry	R	R'	catalyst loading	drying reagent	yield[a]	r.r. (p/o)	e.r.
1	Boc	Et	5 mol%	–	<5%	n.d.	n.d.
2	Fmoc	Et	5 mol%	–	42%	>20:1	90:10
3	Fmoc	Me	5 mol%	–	38%	>20:1	90:10
4	Fmoc	*i*-Pr	5 mol%	–	44%	>20:1	91:9
5	Cbz	Et	5 mol%	MS 4 Å (1 mg/μmol)	<5%	n.d.	n.d.
6	Cbz	Et	1 mol%	MS 5 Å (1 mg/μmol)	24%	>20:1	84:16
7	Cbz	Et	5 mol%	Na₂SO₄ (1 mg/μmol)	<10%	>20:1	83:17

As described above, stepwise hydrolysis of the imidodiphosphorimidate-core was observed in the reaction of **IDPi-01-a** with *N,O*-acetal **46** in toluene. To prevent the undesired hydrolytic inner-core cleavage, especially anhydrous reaction conditions were expected to support the proceeding of the reaction. As unchanged results were obtained under Schlenk-conditions, we investigated the effect of separately added drying agents to the reaction mixture. The addition of 4 Å molecular sieves resulted in a complete shutdown of the reaction, addition of 5 Å molecular sieves however led to the clean formation of the desired product and while the reaction rate was found to be visibly reduced, slightly increased enantiomeric ratios of the product were observed. Similarly, addition of Na_2SO_4 as drying agent resulted in a significantly reduced reaction rate along with a slight improvement of the enantiomeric ratio. To maintain higher levels of reactivity, we therefore refrained from the addition of drying agents in our subsequent studies.

The catalyst stability, which is expected to correlate to the yield of the reaction, should depend on the nature of the used catalyst. We therefore engaged in a broad catalyst screening to evaluate the most suitable catalyst class (table **4.4**). We quickly identified less acidic catalysts of the general CPA-, DSI-, IDP- and *i*IDP-structure to be completely inactive in the Friedel–Crafts reaction of Fmoc-substituted *N,O*-acetal **54** and toluene. Also at elevated temperatures of up to 90 °C, no significant formation of the desired arylglycine ester **56** was observed (entries 1-6).

Even switching back to one of the most acidic catalyst structures frequently applied in strong and confined Brønsted acid-catalysis, IDPis, initially gave similar results. While **IDPi-01-a** yielded the desired product with moderate yield, only traces of **56** were detected using **IDPi-02-a** bearing a phenyl-residue in the 3,3'-positions of the BINOL. The substituents 03-05, possessing similar electronic properties, followed this initial trend and application of the corresponding IDPi-catalysts did not afford **56** in detectable amounts. Installation of a 4-(pentafluorosulfanyl)-phenyl motif however restored the reactivity to give low amounts of **56**. Usage of **IDPi-06-a** bearing a 3,5-dinitrophenyl group in the 3,3'-positions of the BINOL yielded **56** with significantly improved yield of 53% along with a drastically reduced enantiomeric ratio. Analogously, replacing the CF_3-group of the triflyl-core residue in **IDPi-01-a** with a less electron deficient C_6F_5-moiety (**IDPi-01-b**) led to a significantly reduced reactivity and the desired arylglycine **56** was only detected in trace amounts.

While no improvement in the outcome of the reaction could be achieved in this early catalyst screening, the obtained data revealed a general trend which links the approximate acidity of the catalyst with the detected reactivity of the system (figure **4.1**). Altogether, these results indicate

Table 4.4: Initial catalyst screening in the Friedel–Crafts reaction toward arylglycine **56**. [a] = crude NMR yield.

entry	catalyst	yield[a]	r.r. (p/o)	e.r.	entry	catalyst	yield[a]	r.r. (p/o)	e.r.
1	CPA-01	<5%	n.d.	n.d.	8	IDPi-03-a	<5%	n.d.	n.d.
2	DSI-01	<5%	n.d.	n.d.	9	IDPi-04-a	<5%	n.d.	n.d.
3	IDP-02	<5%	n.d.	n.d.	10	IDPi-05-a	<5%	n.d.	n.d.
4	IDP-08	<5%	n.d.	n.d.	11	IDPi-01-b	<5%	n.d.	n.d.
5	IDP-01	<5%	n.d.	n.d.	12	IDPi-06-a	53%	>20:1	63.5:36.5
6	*i*IDP-01-a	<5%	n.d.	n.d.	13	IDPi-07-a	<10%	>20:1	42:58
7	IDPi-02-a	<5%	n.d.	n.d.	14	IDPi-09-a	<5%	n.d.	n.d.

that highly acidic IDPi-catalysts are required to allow the Friedel–Crafts reaction to proceed while a complete shutdown of the reaction is observed with less acidic specimen of the IDPi family.

We therefore continued our investigations with a diverse scope of highly acidic IDPi-catalysts bearing differing motifs in the 3,3'-positions of the BINOL and in the imidodiphosphorimidate core (table **4.5**). Fueled by the early success using **IDPi-01-a**, we subsequently investigated IDPi-catalysts bearing extended perfluoroalkyl chains in the imidodiphosphorimidate core. Usage of catalysts **IDPi-01-c**, **-e** and **-f** revealed that elongation of the perfluoroalkyl-chain in the core of the catalyst has a profound influence on yield and selectivity, giving a maximum of both for pentafluoroethyl-substituted **IDPi-01-c** (entries 2-4).
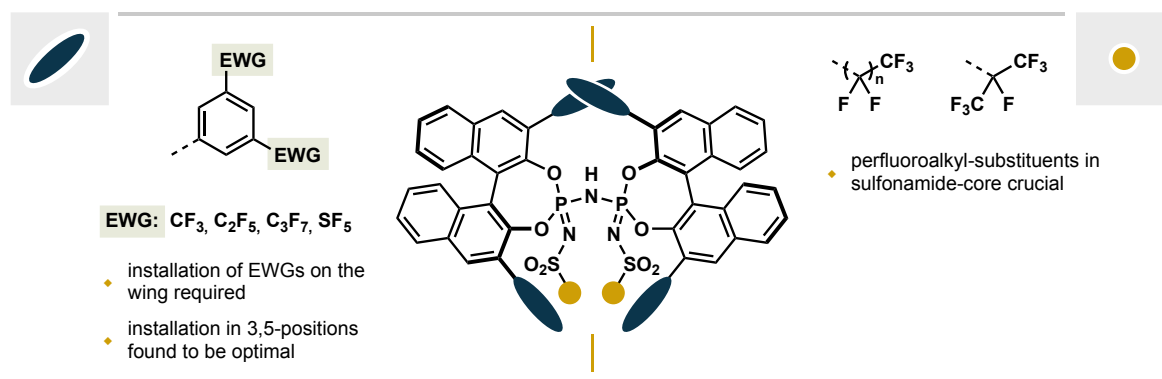
Figure 4.1: Privileged catalyst motifs for the asymmetric Friedel–Crafts reaction.

We then went on to investigate the effect of the installation of different electron withdrawing groups in the 3,5-positions of the aryl residue in the 3,3'-positions of the BINOL. While the

Table 4.5: Screening of highly acidic IDPi-catalysts. [a] = crude NMR yield. [b] = performed at 50 °C. [c] = 86 h reaction time. [d] = 5 d reaction time, performed at 10 °C.

entry	catalyst	yield[a]	r.r. (p/o)	e.r.	entry	catalyst	yield[a]	r.r. (p/o)	e.r.
1	IDPi-01-a	42%	>20:1	90:10	9[b]	IDPi-10-f	65%	>20:1	93:7
2	IDPi-01-c	51%	>20:1	92.5:7.5	10[c]	IDPi-10-d	55%	>20:1	94.5:5.5
3	IDPi-01-e	23%	>20:1	91.5:8.5	11	IDPi-11-a	30%	>20:1	92.5:7.5
4	IDPi-01-f	41%	>20:1	92:8	12	IDPi-11-c	>10%	>20:1	95.5:4.5
5	IDPi-01-g	40%	>20:1	92:8	13	IDPi-12-a	12%	>20:1	80:20
6	IDPi-10-a	29%	>20:1	94:6	14	IDPi-13-c	70%	>20:1	93:7
7	IDPi-10-c	15%	>20:1	95.5:4.5	15	IDPi-13-f	46%	>20:1	93:7
8	IDPi-10-f	30%	>20:1	96:4	16[d]	IDPi-13-c	55%	>20:1	96:4

initially installed trifluoromethyl groups provided moderate reactivity and good enantioselectivity, elongation of the perfluoroalkyl chains to heptafluoropropyl substituents led to reduced reactivity along with a visibly increased enantiomeric ratio on **56**. Exchange of the core substituent to a C_2F_5- or a C_6F_{13}-chain additionally increased the observed enantioselectivity while the yield was found to be reduced (entry 7) or left unchanged (entry 8). Intriguingly, installation of a perfluoroisopropyl substituent as core motif along with the perfluoropropyl-substituted motif in the 3,3'-positions of the BINOL gave high yields on **56** along with a high enantiomeric ratio (entry 10). Further elongation of the perfluoroalkyl chain did not result in any further improvement of yield or enantioselectivity, as illustrated by the usage of catalysts **IDPi-11-a** and **-c**, substituted with a perfluorobutyl chain (entries 11 and 12). As demonstrated in the abovementioned screening entries, elongation of the perfluoroalkyl chains in both the imidodiphosphorimidate core and on the aryl groups in the 3,3'-positions of the BINOL was found to have a profound influence on the enantioselectivity of the reaction, the yield however remained at a low level for the investigated modifications.

We were therefore spurred on to identify electron-withdrawing motifs that could further enhance the acidity of the catalysts without concomitant loss of enantioselectivity. We consequently became interested in the implementation of pentafluorosulfanyl groups, privileged structural motifs within catalysis and chemical synthesis. The SF_5-group is characterized by its unique octahedral structure combined with strong electron withdrawing properties which makes it a predestined motif to enhance acidity and confinement of the acid catalyst.[160] Installation of a single SF_5-group in the meta-position of the 3,3'-phenyl substituent of the parent BINOL scaffold already afforded visible amounts of the desired arylglycine **56** in the reaction of the corresponding **IDPi-07-a**. Usage of the 3,5-bis(pentafluorosulfanyl)phenyl motif along with a C_2F_5-core modification in **IDPi-13-c** finally led to a significant enhancement effect of the yield of the reaction to give **56** with 70% isolated yield and a high enantiomeric ratio of 93:7. Installation of an elongated core modification did not result in any improvement of the reaction, reduction of the reaction temperature to 15 °C however gave the desired product with good yield of 55% along with an excellent enantiomeric ratio of 96:4 (entry 16).

4.1.3 Scope of Unactivated Hydrocarbon Arenes

Having identified **IDPi-13-c** as the optimal catalyst, we were curious about the potential scope of hydrocarbon arenes in the reaction. We therefore tested a range of purely hydrocarbon arenes under neat reaction conditions at 30 °C over a reaction time of 5 days (scheme **4.4**). To our

delight, elongation of the alkyl chain on the alkylbenzene substrate was found to be well tolerated and a maximum on yield and enantiomeric ratio was obtained for ethylbenzene (**4**). Further elongation to a propyl- or a butyl chain led to reduced yields and enantiomeric ratios for the arenes **57** and **58**. The installation of branched alkyl chains led to slightly improved enantiomeric ratios, the yield of the corresponding arylglycines however was found to be visibly reduced. This was particularly evident for the Friedel–Crafts reaction of
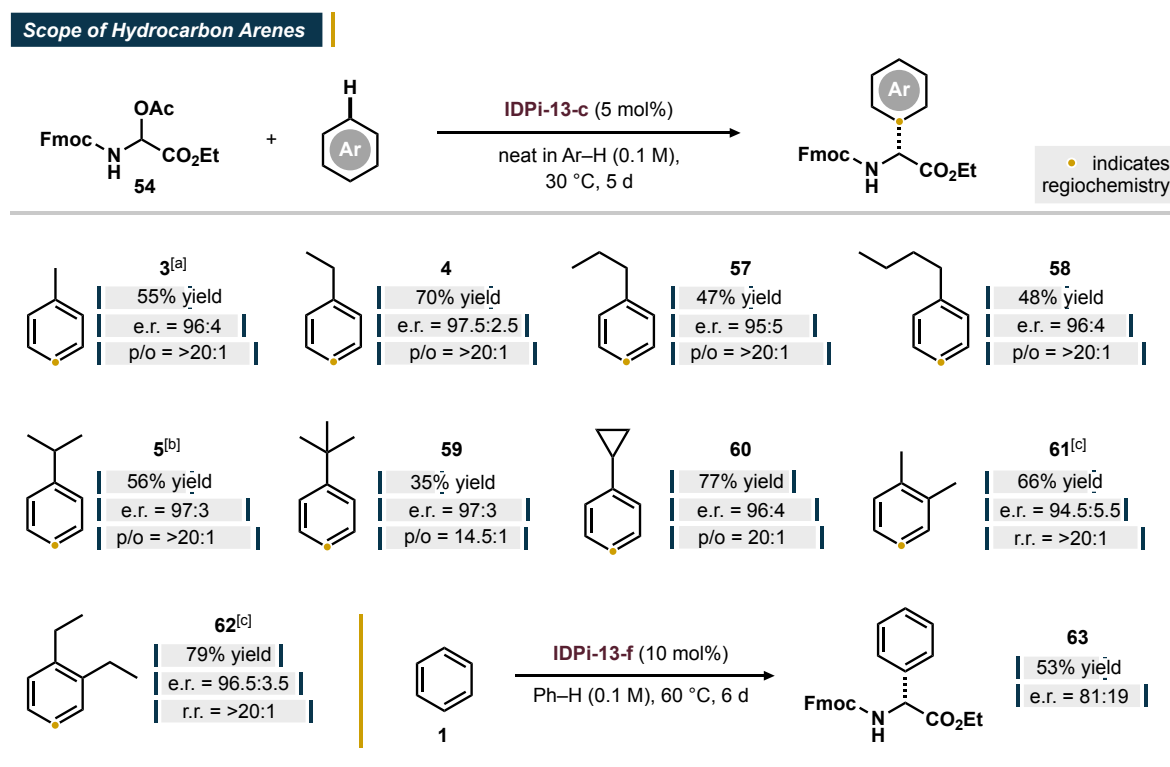
Scheme 4.4: Scope of hydrocarbon arenes in the Friedel–Crafts reaction. [a] = performed at 15 °C. [b] = performed at 20 °C using **IDPi-10-c**. [c] = performed at 0 °C.

tert-butylbenzene (**59**) which only gave 35% yield of the product with a lowered regioisomeric ratio, indicating that the increased steric bulk of the aromatic substrate might exceed the available space in the active site of the catalyst and therefore lead to undesired interactions. Usage of cyclopropylbenzene (**60**) under analogues reaction conditions gave high yield and excellent enantiomeric ratio of the desired product while the cyclopropyl moiety was found to remain intact under the strongly acidic conditions. The reaction of *o*-Xylene (**61**) gave the corresponding arylglycine with high yield but with slightly lower enantioenrichment, even at decreased temperatures. 1,2-Diethylbenzene (**62**) however could be converted with both, high yield and excellent enantioselectivity.

To determine the limitations of the reaction with respect to the nucleophilicity of the aromatic substrate, we subjected benzene (**1**) to the Friedel–Crafts reaction toward phenylglycine **63**. The significantly reduced reactivity of the unsubstituted arene compared to the previously investigated alkylbenzene derivates required both an increased catalyst loading of 10 mol% and higher reaction temperatures of 60 °C to afford **63** with moderate yield and a reduced enantiomeric ratio of 81:19.

Motivated by the results observed for the reaction of benzene, we set out to investigate the reaction of even less reactive arenes and of arenes with alternative substitution patterns (scheme **4.5**). Using *meta*- (**64**) or *para*-xylene (**6**) as substrates, significantly reduced enantiomeric ratios were observed in the formed products. While the yield was found to be additionally reduced using *para*-xylene, the 1,3-dialkyl pattern on *meta*-xylene activates the substrate and thus leads to high yields on the corresponding arylglycine. Similarly, the usage of mesitylene (**65**) gave high yields and even lower enantiomeric ratios. Compared to *ortho*-xylene, which could be converted with excellent enantioselectivity, the presence of a methyl group in adjacency to the reactive center is present in all, *meta*- and *para*-xylene as well as in mesitylene. It therefore seems likely that the substituent adjacent to the reactive center in the arene interferes with desired intermediates or transition states and thus leads to reduced selectivity. The usage of fluorobenzene (**66**) did not result in any visible product formation. We expect that the installation of an additional electron withdrawing fluorine substituent decreased the nucleophilicity to an extent that no bond formation was found to be possible.
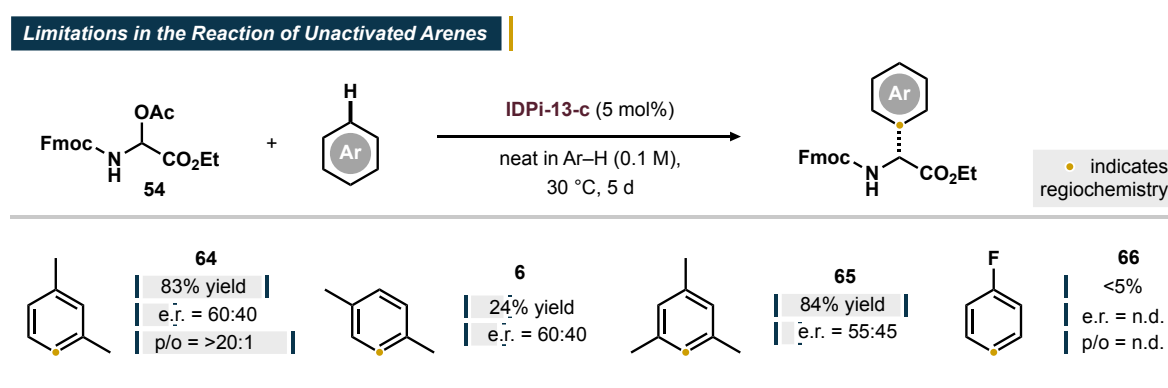
Scheme 4.5: Substrate limitations in the Friedel–Crafts reaction of unactivated arenes.

Having investigated the described reaction scope, we turned our attention to a more specific application of our method. Given its peculiar properties, we were interested in the Friedel–Crafts reaction of azulene (**67**). Azulene, a structural isomer of naphthalene, features

extraordinary properties for a small, purely hydrocarbon arene.[161] The name of the compound is ultimately derived from the Lapis lazuli, a blue rock valued for its intense color. As its name suggests, the compound is deep-blue in color and furthermore possesses fluorescence properties which make it an ideal tool for bioimaging- and photoswitch applications.[162] Azulene exhibits a significant dipole moment of 1.08 D, generated by the electron-rich five-membered ring and the annulated, electron-deficient seven-membered ring. Correspondingly, it shows increased basicity and nucleophilicity in the smaller ring which is expected to be beneficial for S_EAr reactions. As azulene could already be integrated in non-canonical amino acids for bioimaging purposes by the Arnold group,[162] we were interested in the implementation of this intriguing hydrocarbon arene in our Friedel–Crafts reaction (scheme **4.6**). Using **IDPi-01-a** in the
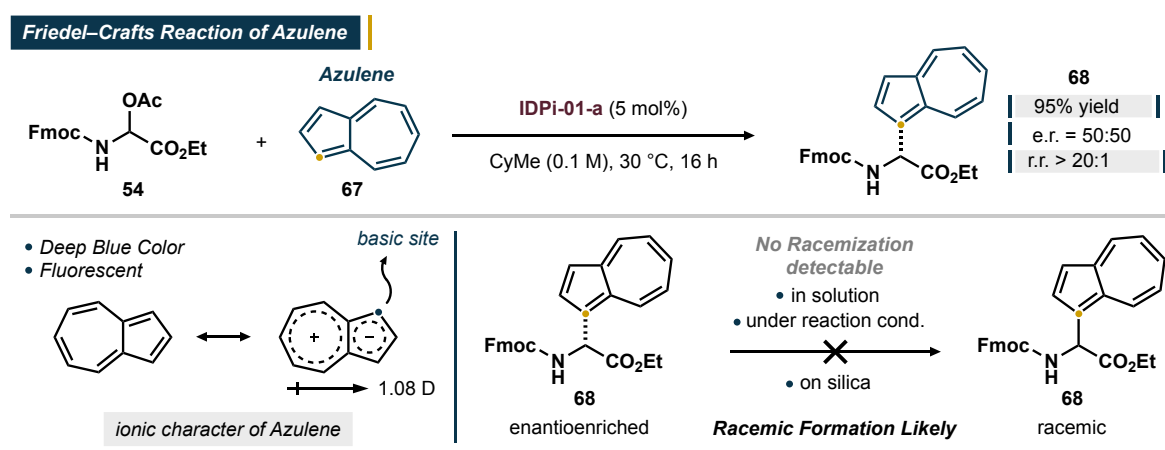
Scheme 4.6: Friedel–Crafts reaction using azulene as aromatic substrate.

reaction of **67** with *N,O*-acetal **54** in CyMe, the formation of the desired deep-blue arylglycine **68** was detected with high yield as a racemic mixture of both enantiomers. Given the discrepancy with the enantiomeric ratios obtained for the reaction of previously studied alkylbenzene arenes, racemization was expected to occur, contributing to the decreased enantiomeric ratio.
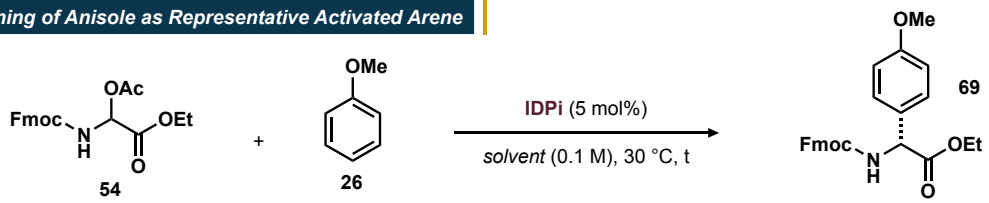
To confirm our hypothesis, we subjected the obtained racemic mixture of arylglycine **68** to the preparative separation of the enantiomers via HPLC. The enantiomerically enriched samples thus obtained were then subjected to various conditions. However, no racemization was observed in solution, under the initial reaction conditions in the presence of **IDPi-01-a** or on silica gel and under irradiation with visible light. We therefore expect racemic formation of the arylglycine **68**, resulting from the highly reactive nature of **67**, to take place. Further investigations are currently ongoing in our laboratory.

4.1.4 Scope of Alkoxybenzenes and Heterocyclic Arenes

After our initial investigation with unactivated, purely hydrocarbon arenes, we turned our attention to a more divers scope of heteroatom-substituted aromatic substrates and heterocyclic arenes. Especially the relevance of alkoxybenzene-derived arylglycine scaffolds in natural products and biologically active compounds motivated us to investigate them further.[163] A significant difference between this class of aromatic substrates and the previously investigated alkylbenzene arenes consists of their differing nucleophilicity, caused by strongly electron donating alkoxy substituents or electron-rich heterocyclic rings. This increased reactivity consequently opens up a myriad of reaction conditions and catalysts that could potentially be applied to the transformation. To determine optimal reaction conditions for these more reactive aromatic substrates, we engaged in an initial screening using anisole (**26**) as representative substrate (table **4.6**).

Table 4.6: Reaction optimization for anisole (**26**) as model substrate. [a] = crude NMR yield.

entry	IDPi	solvent	t	yield[a]	r.r. (p/o)	e.r.
1	IDPi-02-a	PhMe	36 h	13%	n.d.	n.d.
2	IDPi-01-a	PhMe	16 h	83%	>20:1	84:16
3	IDPi-01-a	CHCl$_3$	16 h	>95%	>20:1	67.5:32.5
4	IDPi-01-a	CH$_2$Cl$_2$	16 h	68%	>20:1	58:42
5	IDPi-01-a	CyH	16 h	46%	>20:1	91:9
6	IDPi-01-a	CyMe	16 h	68%	>20:1	87:13
7	IDPi-10-d	CyMe	22 h	90%	>20:1	96:4
8	IDPi-10-c	CyMe	22 h	90%	>20:1	96:4
9	IDPi-10-c	*n*-pentane	22 h	81%	>20:1	98:2
10	IDPi-10-c	*n*-hexane	22 h	94%	>20:1	96:4
11	IDPi-10-c	*n*-heptane	22 h	69%	>20:1	97:3

Initial investigations using **IDPi-02-a** bearing a phenyl residue in the 3,3'-positions of the BINOL showed that, analogous to our previous investigations with toluene, only low amounts of the desired product **69** were formed after prolonged reaction time. Installation of a 3,5-bis(trifluoromethyl)phenyl-residue in the 3,3'-positions of the BINOL led to a significant increase in the yield of the reaction, providing the anisole-derived arylglycine **69** with high yield along with an enantiomeric ratio of 84:16. Switching to chlorinated solvents (entries 3 and 4) visibly reduced the enantiomeric ratio of **69**. However, usage of non-aromatic hydrocarbon solvents led to the inverse effect and the reaction in CyMe finally gave arylglycine **69** with good yield and increased enantioenrichment.

The installation of elongated perfluoroalkyl chains on the used IDPi were found to significantly enhance the performance of the catalyst in the previously investigated reaction of unactivated arenes. Similar catalysts were therefore expected to have promising features for the reaction of anisole (**26**). And indeed, when **IDPi-10-d** was used in the reaction, the desired Friedel–Crafts product **69** was obtained with excellent yield and enantioselectivity. Finally, further optimization revealed *n*-pentane as optimal solvent and using catalyst **IDPi-10-c**, bearing a C_2F_5-modification in the imidodiphosphorimidate core, even further improved yield and enantioenrichment on **69** was obtained (entry 9).

With these optimized conditions for the conversion of more activated arenes in hand, we went on to investigate the scope of applicable substrates in the reaction (scheme **4.7**). To our delight, anisole-d$_3$ (**70**) and thioanisole (**71**) could both be converted to the corresponding arylglycines with excellent enantiomeric ratios and high yields. Installation of a second substituent in the *ortho*-position of the alkoxy residue was found to be well tolerated: usage of *ortho*-methyl (**72**) or *ortho*-iodo anisole (**73**) gave the corresponding products with high yields and excellent enantiomeric ratios. Similarly, the dialkoxylated substrate 1,3-benzodioxole (**74**) could be converted with comparable results. The reaction of *ortho*-trimethylsilyl anisole (**75**) was performed in CyMe as solvent to yield the corresponding arylglycine ester with excellent yield and enantioenrichment. Intriguingly, usage of HNTf$_2$ as strong but non-confined Brønsted acid catalyst led to complete protodesilylation of the aromatic ring as indicated by the exclusive formation of anisole-derived arylglycine **69**. The occurrence of this undesired side reaction might indicate the importance of a confined environment along with the carefully optimized acidity of the used catalyst to allow a chemoselective proceeding of the reaction. Furthermore, alkylbromide-substituents (substrate **76**) as well as alkylazide-substituents (substrate **77**) were found to be well tolerated. When allylphenylether (**78**) and propargylphenylether (**79**) were subjected to analogous reaction conditions, the corresponding products were formed with

excellent yields and enantiomeric ratios. Notably, no Claisen rearrangement or deallylation side-reactions were observed using **IDPi-10-c**, again demonstrating the general chemoselectivity provided by IDPi catalysts in the Friedel–Crafts reaction toward arylglycines.

Scope of Alkoxybenzenes and Heterocyclic Arenes

	26		**70**		**71**		**72**
OMe	92% yield	OCD₃	95% yield	SMe	73% yield	OMe	94% yield
	e.r. = 97.5:2.5		e.r. = 97.5:2.5		e.r. = 97:3		e.r. = 95.5:4.5
	p/o = >20:1		p/o = >20:1		p/o = >20:1		r.r. = >20:1
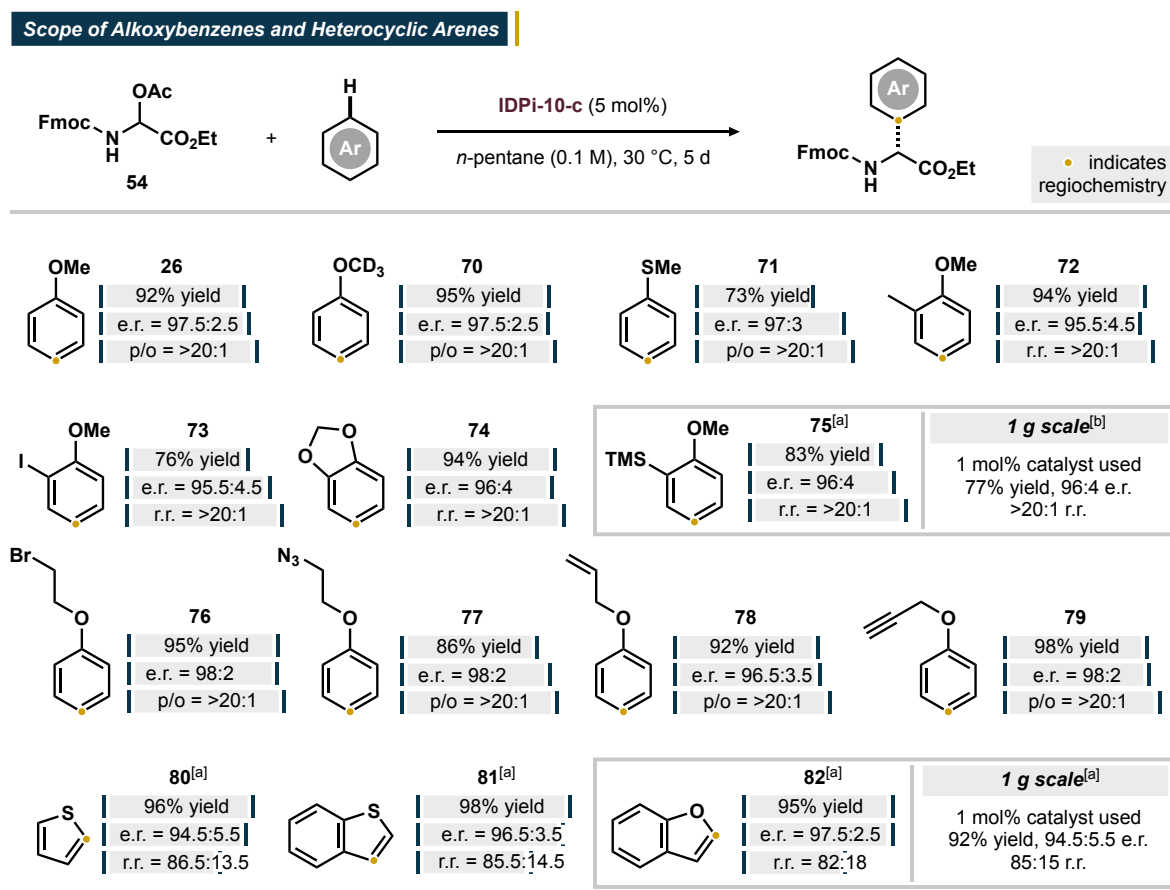
Scheme 4.7: Scope of more activated alkoxybenzenes and heterocyclic arenes. [a] = CyMe was used as solvent, c = 0.1 M. [b] = *n*-hexane was used as solvent, c = 0.1 M.

We then turned our attention to the electrophilic functionalization of small heterocyclic arenes. The reaction of thiophene (**80**), a notoriously challenging substrate for asymmetric Friedel–Crafts reactions, gave excellent yield of the corresponding arylglycine along with high enantiomeric excess.[164] However, the regioisomeric ratio of the formed product mixture was found to be significantly reduced – a trend that was to be continued in the reaction of benzothiophene (**81**) and benzofuran (**82**). Both substrates were converted with high yields and excellent enantiomeric ratios along with reduced regioselectivity.

The scalability of the reaction was investigated for **75** and **82** as representative substrates. The respective reactions were performed on 1 g scales corresponding to *N,O*-acetal **54** using 1 mol% of **IDPi-10-c** as catalyst. While the reaction of **75** gave similar results compared to the

previously performed reaction on a smaller scale, a visibly reduced enantiomeric ratio was observed for the reaction of **82** on larger scale. We speculate that the reaction of **82** as reactive aromatic substrate might lead to temperature inhomogeneity within the reaction vessel at larger scale, decreasing the observed selectivity. Crystallization of the thus obtained arylglycine improved the enantiomeric ratio to 98:2 and the regioisomeric ratio to 90.5:9.5.

A wide range of more activated arenes have been found to be compatible with the developed Friedel–Crafts reaction toward arylglycine esters, but we have encountered some limitations. While thiophene (**80**) could be converted to the corresponding arylglycine with high yields and enantiomeric ratio, the reaction of furan (**83**) was found to be significantly less selective and a plethora of ongoing oligomerization side-reactions additionally diminished the yield of the transformation (scheme **4.8**).

Limitations in the Reaction of Activated Arenes

IDPi-10-a (5 mol%)

n-pentane (0.1 M), 30 °C, 5 d

• indicates regiochemistry

83	**84**	**85**	**86**	**24**
40% yield	OH	NH		
e.r. = 80:20	<5%	<5%	<5%	<5%
r.r. = 84:16	e.r. = n.d.	e.r. = n.d.	e.r. = n.d.	e.r. = n.d.
	p/o = n.d.	p/o = n.d.	p/o = n.d.	p/o = n.d.
	C–X bond formation observed		*messy sidereactions*	*no reaction*
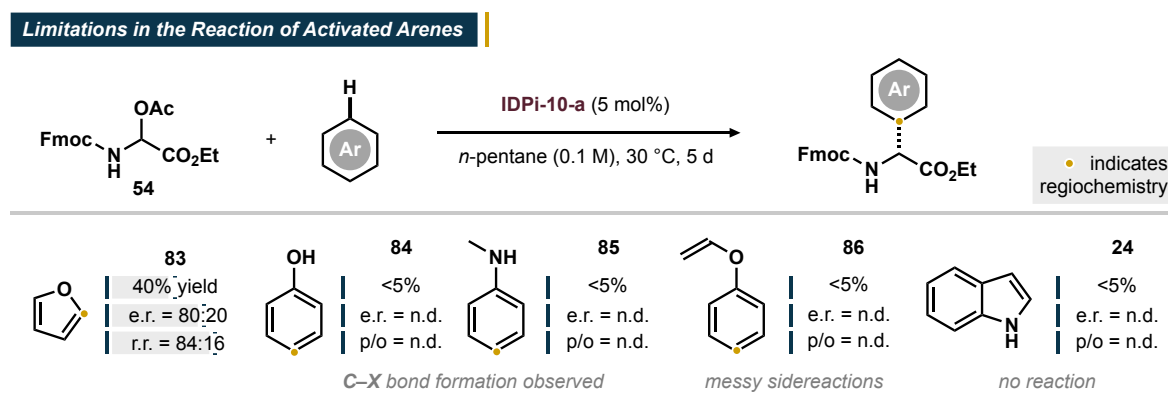
Scheme 4.8: Limitations for the Friedel–Crafts reaction of more activated arenes.

As the heteroatom-bound products were obtained for the reaction of the substrates **84** and **85**, we expect those substrates to exhibit insufficient nucleophilicity in the aromatic ring in competition to the respective X–H bond for the Friedel–Crafts reaction to occur. When vinylphenylether (**86**) was used in the reaction, no formation of the desired product but a complex mixture of side products was observed. Surprisingly, the reaction of indole (**24**), a highly nucleophilic and consequently extensively investigated substrate, did not occur under our reaction conditions.[165] The low conversion of *N,O*-acetal **54** suggests deactivation of the catalyst through the aromatic substrate **24**, potentially via deprotonation.

4.1.5 Toward the Arylglycine Fragments of Vancomycin

Having investigated the scope of applicable substrates, both of unactivated as well as more activated arenes, we were eager to test the reaction in a more applied challenge. A suitable target to evaluate the synthetic utility of our method was found in the assembly of the arylglycine units of the antibiotic agent vancomycin (**34**) (scheme **4.9**).[166–168]
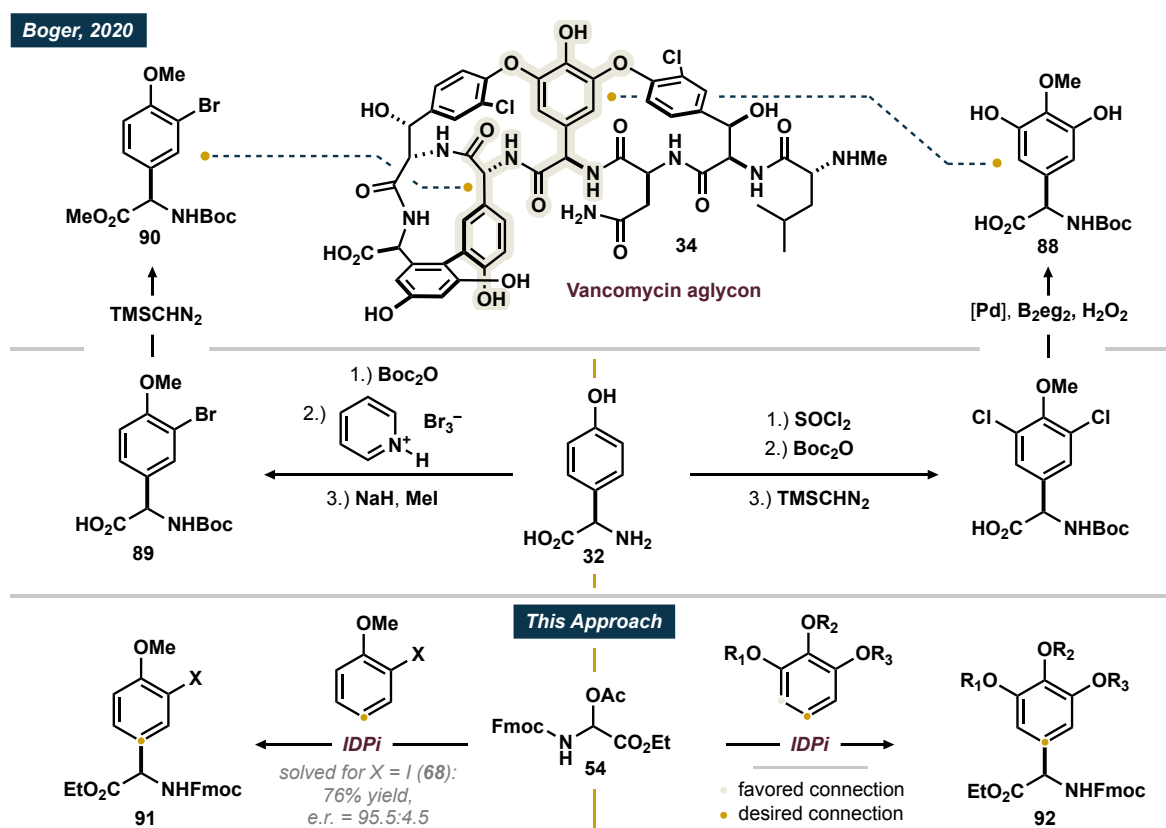
Scheme 4.9: Synthesis of the vancomycin aglycon by Boger and the IDPi-based approach.

As reported in total syntheses by Boger, two of the arylglycine fragments of the parent vancomycin structure **34** can be assembled in multiple steps starting from 4-hydroxyphenylglycine (**32**) as commercially available building block. The central arylglycine linker **88** is obtained starting with a dichlorination in both *ortho*-positions of the phenol moiety of **32**. Subsequent carbamate-protection and methylation enables the final Miyaura borylation-oxidation sequence to yield the desired bishydroxylated structure **88**. The eastern fragment **90** is obtained in four steps from **32**, starting with the Boc-protection of the amino group. *ortho*-Bromination and methylation of the hydroxy group then gives rise to intermediate **89** which is finally methylated to yield the methyl ester building block **90**.

4. Results and Discussion

While the routes reported by Boger provide efficient access to the required chiral building blocks **88** and **90**, they suffer from a reduced step efficiency and depend on the usage of costly metal catalysts. Therefore, we envisioned the application of our newly developed method in the synthesis of the relevant arylglycine building blocks toward the synthesis of the vancomycin aglycon starting from *N,O*-acetal **54** as a synthetic platform.

While *ortho*-brominated building block **89** was used by Boger, we were already able to obtain the *ortho*-iodinated arylglycine starting from 2-iodoanisole (**73**) with high yield and excellent enantio- as well as regioselectivity. We are therefore convinced that our method provides an efficient alternative to the *ortho*-halogenated building block **90** in a straightforward approach. We consequently focused our attention on the synthesis of the central arylglycine fragment **92** of the vancomycin aglycon **34**.

The challenge in the selective formation of the building block **92** following our synthetic approach lies in the regioselective electrophilic functionalization of the preinstalled 1,2,3-trihydroxybenzene (or 1,2,3-trialkoxybenzene) structure which generally directs the electrophilic aromatic substitution in the undesired 4-position instead of the desired 5-position of the aromatic ring (scheme **4.10**). We therefore set out to investigate methods to override the
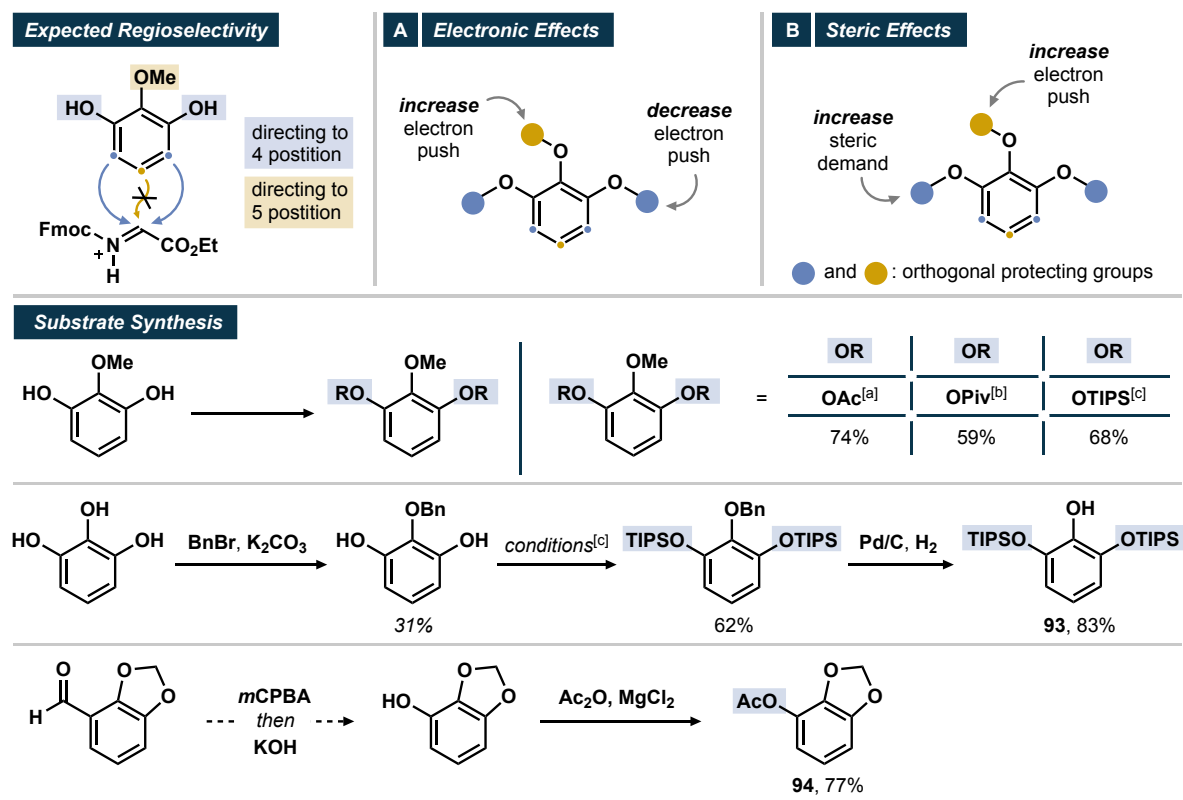
Scheme 4.10: Substrate synthesis toward the vancomycin building block **92**. Reaction conditions: [a] = Ac$_2$O, *p*-TsOH. [b] = PivCl, DMAP, pyridine. [c] = TIPSCl, imidazole.

innate directing effects and to enable selective C–C bond formation in the 5-position of the arene. We identified two general concepts to potentially overcome the formation of the undesired regioisomers in the Friedel–Crafts reaction. Firstly, the two outer phenolic hydroxy groups could be substituted with deactivating groups to reduce their directing effect toward the undesired 4-position. Simultaneously, the central hydroxy group, whose directing effect is desired to promote C–C bond formation in the 5-position, should be left unsubstituted to maintain the strong +M-effect of the free phenol. Alternatively, the outer hydroxy groups of the substrate could be decorated with sterically demanding groups. The adjacent positions are consequently expected to be shielded by the bulky substituents. Especially in cooperation with a confined catalyst, we hypothesized substitution to then occur preferably in the desired, sterically most accessible 5-position of the ring.

To investigate these approaches, we engaged in the synthesis of the required substrates. For our "electronics-driven" approach, deactivating acetate- or pivalate-groups were installed at the outer positions while the central hydroxy group was substituted with an alkyl group. Additionally, 1,3-benzodioxole **94** bearing an acetoxy group in a neighboring position was prepared. For the "sterics-driven" approach, bulky triisopropylsilyl-groups were installed at the outer hydroxy groups of the parent substrate. Finally, both approaches were combined in substrate **93** bearing outer triisopropylsilyl groups and a free phenol unit in the central position between the two silyloxy residues. The enol-character of the free phenol was expected to have a significant electronic directing effect to the desired position, supported further by the bulky groups that shield neighboring positions to prevent electrophilic functionalization in their adjacency.

We initiated our investigations using commercial *ortho*-bishalogenated phenols and anisoles as aromatic substrates in the reaction with *N,O*-acetal **54** under the previously proven reaction conditions (scheme **4.11**). While usage of the phenols **95-97** led to a complex mixture of side reactions, the application of the corresponding anisoles **98** and **99** did not result in the Friedel–Crafts reaction, even at elevated temperatures. Similarly, when the pyrogallol-derived 2-methoxy-1,3-phenylene diacetate (**100**) or its corresponding pivalate **101** was used in the reaction, the Friedel–Crafts product could not be detected in visible amounts. We expect that the combined deactivating effect of both acyloxy groups reduce the nucleophilicity of the arene so drastically that the $S_E Ar$ could not take place. In contrast, the more nucleophilic 1,3-benzodioxole derived substrate **94** was found to yield the Friedel–Crafts adduct with low yield as a mixture of all possible regioisomers with the desired regioisomer being the minor product of the reaction. The lack of selectivity in the reaction to only yield one single regioisomer
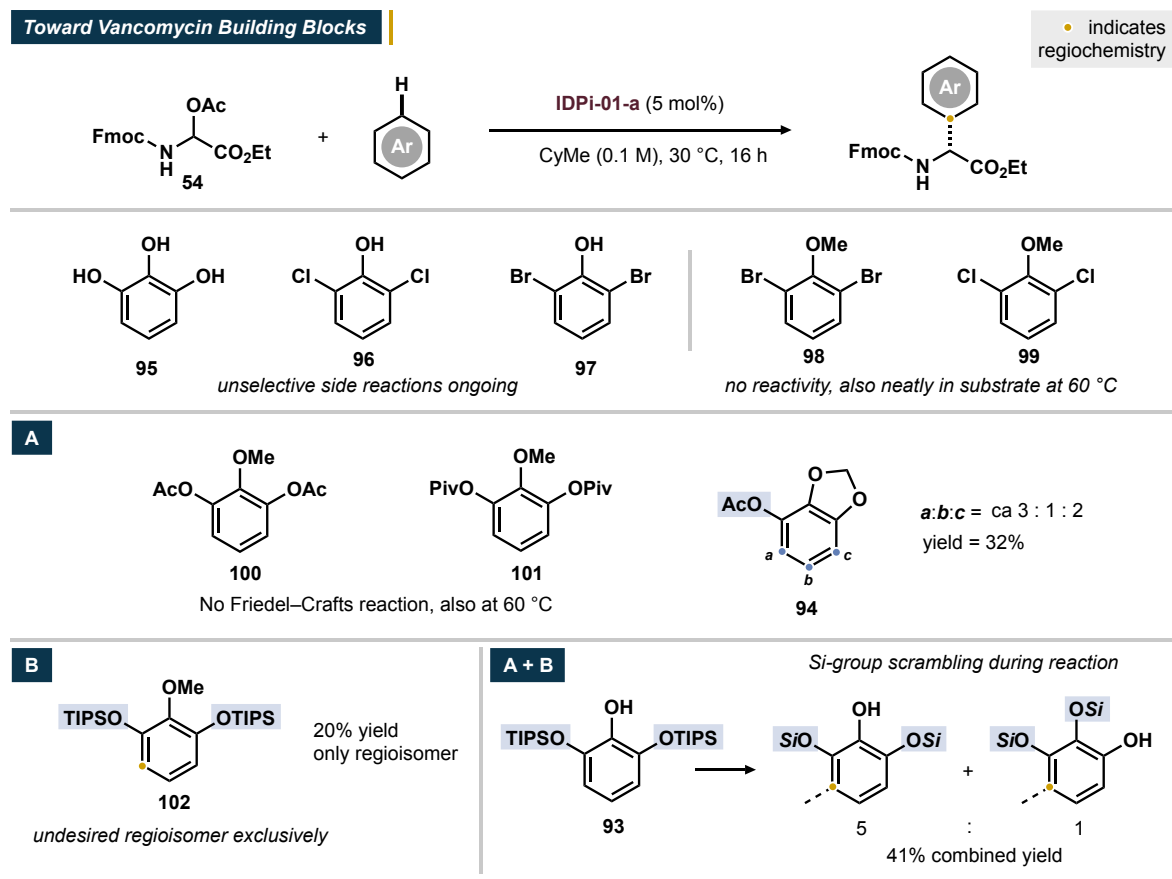
Scheme 4.11: Investigations toward the arylglycin building blocks of vancomycin (**34**).

indicates that the installation of specifically tailored substituents can generally lead to the formation of unexpected regioisomers for the 1,2,3-trioxygenated scaffold present in arylglycine **92**. Encouraged by this result, we turned our attention to the application of substrates with bulky substituents in both adjacent positions. Surprisingly, usage of methoxybenzene **102** bearing two (tris)isopropylsilyloxy-residues in the 1- and 3-positions resulted in the exclusive formation of the undesired regioisomer. This finding indicates that electronic properties are of superior directing strength compared to steric effects, even using highly confined IDPi-catalysts. We therefore went on to test dealkylated phenol **93** under analogues conditions. Our hypothesis that the strongly *para*-directing phenol together with the shielding silyloxy-residues in both adjacent positions might allow to form the desired C–C bond could not be confirmed as the undesired regioisomer was found to be formed exclusively. Intriguingly, partial scrambling of the silyl-group to the inner position was observed in the course of the reaction to yield a mixture of both isomers.

As disclosed above, our efforts to override the regiochemical outcome in the Friedel–Crafts reaction of differently substituted 1,2,3-trihydroxybenzene-derivates have not yet been successful. Further studies are currently ongoing in our laboratory.

4.1.6 Mechanistic Investigations

In the course of the abovementioned studies, we quickly became interested in the mechanistic details to further understand the elementary steps of the transformation. Especially, the observation that only a small group of highly acidic catalysts was able to promote the Friedel–Crafts reactions with *N,O*-acetal **54** while slightly less acidic species failed to do so motivated us to develop experimental tools to allow a more detailed investigation of the reaction.

Leaving Group Scrambling Studies

The following studies were performed in collaboration with Dr. Markus Leutzsch.

Based on preceding studies, the formation of highly reactive *N*-acyliminium ion intermediates from *N,O*-acetal **54** seems likely to proceed in the course of the reaction (scheme **4.12**).[143] The inactivity of many IDPi-catalysts in the reaction can however not be explained trivially following this approach since the high reactivity of the formed *N*-acyliminium ions **IX** should readily enable the subsequent nucleophilic attack of the aromatic substrate.
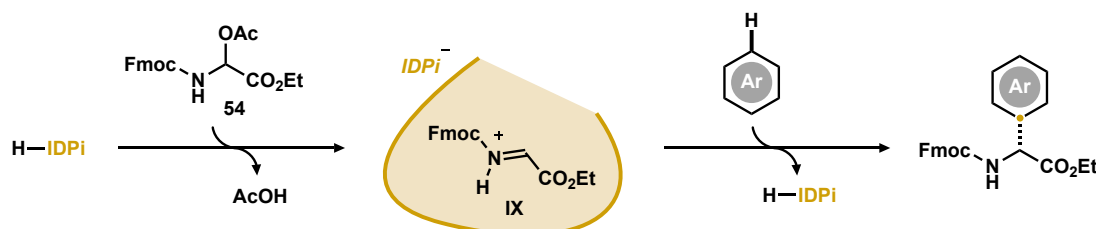
Scheme 4.12: Expected *N*-acyliminium ion intermediate **IX** in the Friedel–Crafts reaction.

To more specifically evaluate the reactivity of previously unreactive catalyst **IDPi-02-a**, it was subjected to the reaction of *N,O*-acetal **54** with a variety of benchmark arenes of differing nucleophilicity (scheme **4.13**). As shown earlier, less reactive arenes such as toluene, *meta*-xylene or anisole were completely unreactive under the described reaction conditions. Surprisingly however, also 3-methylanisole (**103**) was found to be completely unreactive and only low amounts of the desired Friedel–Crafts adduct were observed using significantly more reactive 1,3-dimethoxybenzene (**104**). Only using highly nucleophilic 1,3,5-trimethoxybenzene (**42**), good yields of the corresponding arylglycine ester were observed. The described study in combination with our earlier investigations indicate that the proceeding of the reaction is
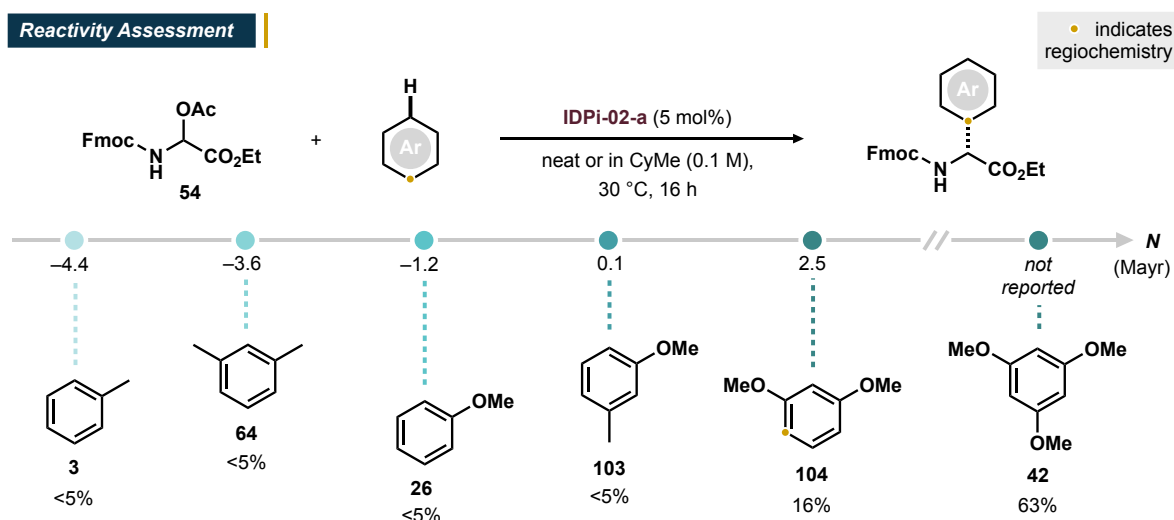
Scheme 4.13: Reactivity assessment of **IDPi-02-a** with various benchmark arenes.

mainly dependent on two factors, namely the acidity of the catalyst and the nucleophilicity of the arene. The successful transformation of unreactive arenes such as toluene consequently requires the application of highly reactive (acidic) catalysts.

The exact reason for the lack of reactivity using catalysts of the type of **IDPi-02-a** could potentially be found in one (or more) elementary steps toward product formation:

1. iminium ion-formation
2. nucleophilic attack of the aromatic substrate (insufficient activation of the iminium ion)
3. rearomatization of the Wheland intermediate

To investigate the relevance of the putative iminium ion formation, we were curious to develop methods that allow the observation and – potentially – quantification of the rate of its formation from *N,O*-acetal **54** with different Brønsted acid catalysts. As we expected iminium ion-formation to be a reversible process, we envisioned a test reaction of sufficient rate so that detection via NMR-spectroscopy might be feasible. The test system should additionally resemble the original reaction conditions as much as possible so direct conclusions regarding the actual reaction process could be drawn.

Against this background, we designed a test system consisting of the *N,O*-acetal **54**, a tested IDPi catalyst <u>and</u> an additional equivalent of deuterium-labeled acetic acid-d4 in deuterated toluene to allow direct tracking via NMR-spectroscopy (scheme **4.14**). Assuming the reversible formation of corresponding iminium ion intermediates **IX** and the presence of deuterated acetic acid, the enrichment of *N,O*-acetal **54** bearing deuterated acetate markers is expected to be

4. Results and Discussion
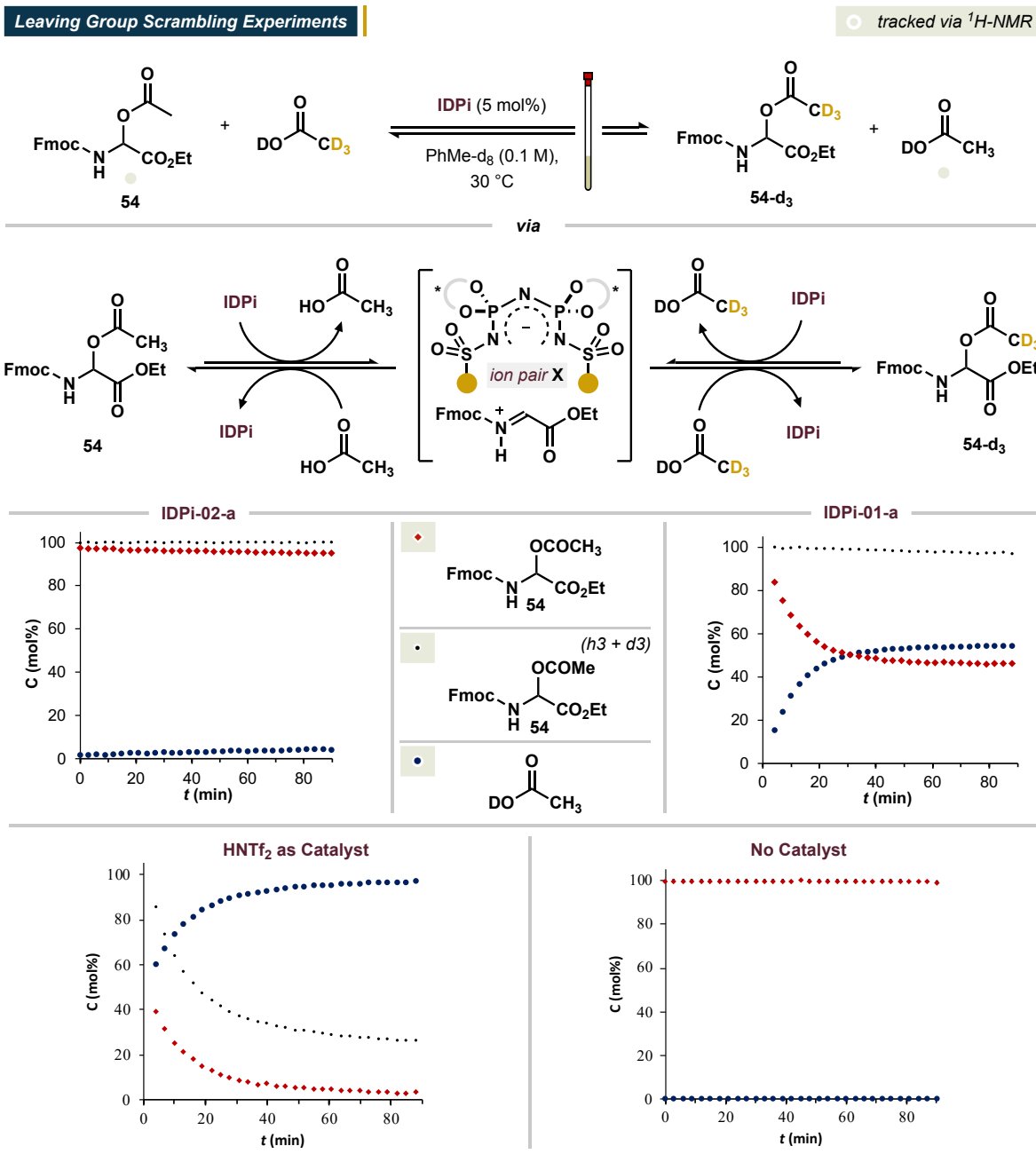
Scheme 4.14: Setup and outcome of the leaving group scrambling experiments.

observable spectroscopically, depending on the capability of the catalyst to form ion pair **X**. We focused our investigations on two simple benchmark catalysts: **IDP-02-a**, inactive in the Friedel–Crafts reaction, and **IDPi-01-a**, active in the Friedel–Crafts reaction. As to be seen in the above diagrams, only very slow exchange of acetate-h_3 with acetate-d_3 (and consequent release of acetic acid-h_3) was observed using catalytically inactive catalyst **IDPi-02-a**. Usage of catalytically active **IDPi-01-a** however led to full equilibration within one hour. Application of HNTf$_2$ as Brønsted acid catalyst led to an even clearer result: full equilibration was reached

before the first spectroscopic measurement was recorded (full equilibration in less than three minutes) and even further consumption of the *N,O*-acetal starting material **54** towards the Friedel–Crafts product with toluene-d$_8$ can rapidly be observed on the investigated timescale. In the absence of a Brønsted acid catalyst, no sign of equilibration can be observed.

The abovementioned results are in agreement with the observed activity (or inactivity) of the respective catalyst in the Friedel–Crafts reaction. The lack of leaving group exchange using catalyst **IDPi-02-a** indicates that it is unable to activate *N,O*-acetal **54** toward further transformations. More specifically, we hypothesize that the catalyst is not acidic (reactive) enough to form or sufficiently stabilize the *in situ*-generated, highly reactive iminium ion intermediates **IX** which seems to be at least partially limiting for its applicability in the reaction. Rapid exchange of the leaving groups is observed using **IDPi-01-a**, iminium ion-formation therefore seems to be a rapid and highly dynamic process. We were furthermore unable to detect iminium ion pair **X** spectroscopically. We consequently conclude that the equilibrium of its formation lies heavily on the side of the *N,O*-acetal **54** starting material and that the catalyst-depended lifetime of this elusive species might influence the overall reaction rate.

The Effect of Additional Acetic Acid on the Reaction Rate

The following studies were performed in collaboration with Dr. Markus Leutzsch.

The proposed formation of iminium ion intermediates **IX** toward the Friedel–Crafts reaction consequently indicates that the state of the equilibrium determines the concentration of the ion pair **X** which, finally, limits or enables the proceeding of the reaction. Shifting this equilibrium to either side should therefore increase or decrease the concentration of ion pair **X** which should then lead to an increase or a decrease of the rate of product formation. According to Le Chatelier's principle, there should be multiple options to investigate this hypothesis.[169] Among the easiest methods to test its validity is the addition of the side product of iminium ion **IX** formation, acetic acid. Increased concentration of the released leaving group should favor the reaction of the ion pair **X** back to *N,O*-acetal **54** under restoration of the catalyst, reducing the active concentration of ion pair **X** and consequently reducing the rate of product formation.

The hypothesis was tested in the reaction of anisole (**26**) with *N,O*-acetal **54** in the presence of **IDPi-01-a** and an optional equivalent of acetic acid. The reaction was tracked via ^{1}H-NMR spectroscopy to follow the rate of product formation and starting material consumption. The corresponding graphic is displayed below (scheme **4.15**).

Indeed, addition of external acetic acid has a visible effect on the reaction rate and significantly slower product formation can be observed. This observation supports our previously suggested hypothesis of the formation of iminium ion pair **X** to be a key step toward product formation. Alternative S_N2-type substitution of the acetate group of *N,O*-acetal **54** would be expected
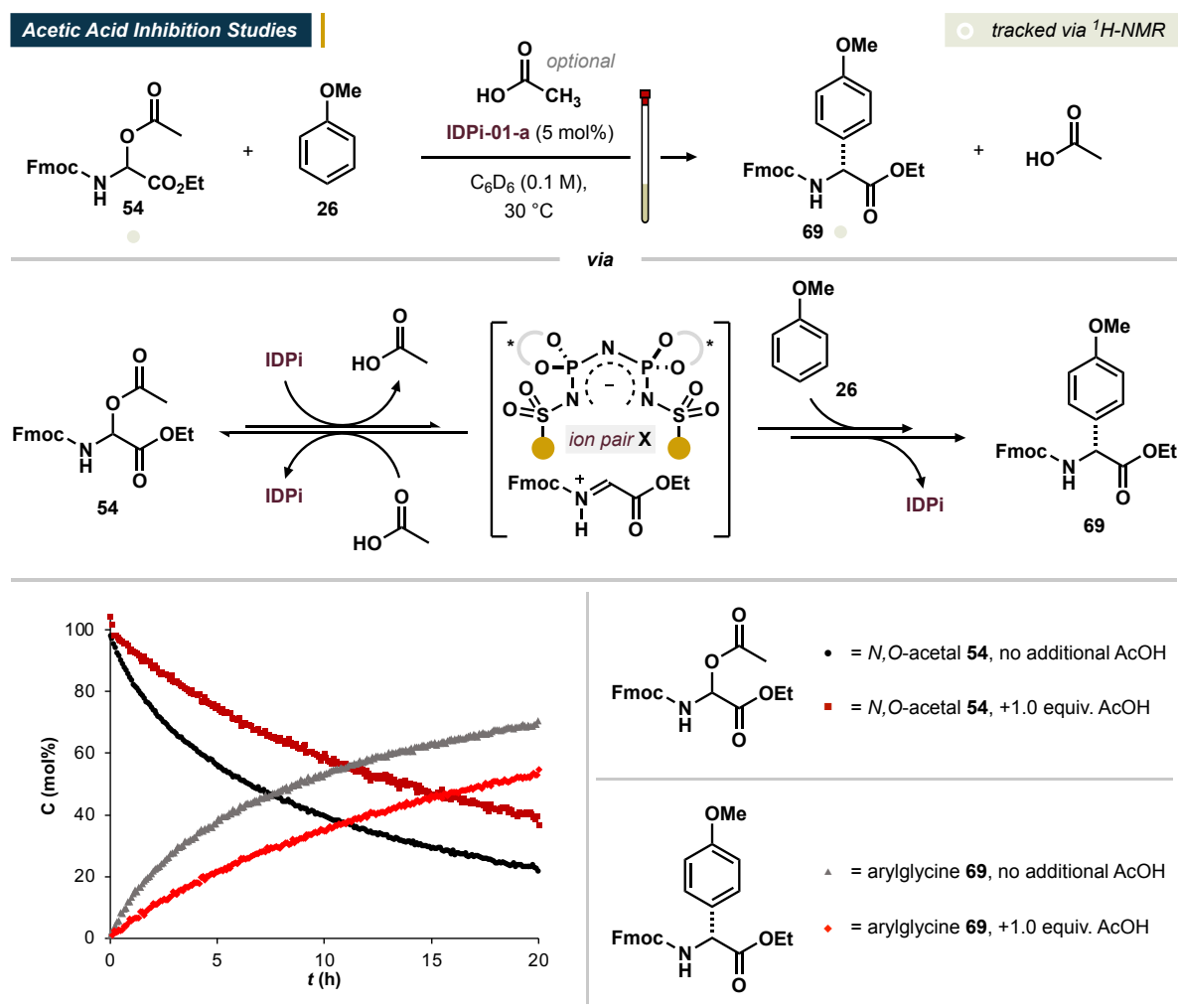
Scheme 4.15: Influence of additional acetic acid to the reaction rates.

to be independent on the concentration of acetic acid. To rule out a potential preceding kinetic resolution process of *N,O*-acetal **54** with *in situ* formed or initially added acetic acid, leading to enantioenrichment of the starting material **54**, we added acetic acid to the reactions of toluene (**3**) and anisole (**26**) to determine a potential influence on the enantioselectivity of the reaction (table **4.7**). While the yield of the reaction with toluene (**3**) was found to be significantly lower than the yield in the reaction of anisole (**26**) (as to be traced back to the higher nucleophilicity of **26**), the enantiomeric ratios of formed products were found to be almost completely unaffected by the presence or absence of additional acetic acid. Both results point

toward the formation of iminium ion-intermediates **IX** as crucial and potentially rate determining species, kinetic resolution processes however do not seem to be relevant and enantiodetermination is consequently expected to occur exclusively on the stage of ion pair **X** via asymmetric counteranion directed catalysis.

Table 4.7: Investigations on potential preceding kinetic resolution processes. [a] = crude NMR yield.

Effect of Acetic Acid on the Selectivity

entry	arene	acetic acid	yield[a]	p/o	e.r.
1	**PhMe (3)** (neat, 0.1 M)	–	55%	>20:1	90:10
2	**PhMe (3)** (neat, 0.1 M)	1.0 equiv.	35%	>20:1	90:10
3	**anisole (26)** in CyMe (2.0 equiv.)	–	67%	>20:1	87:13
4	**anisole (26)** in CyMe (2.0 equiv.)	1.0 equiv.	63%	>20:1	88:12

As disclosed above, progressive formation of acetic acid, released from *N,O*-acetal **54** in the course of the reaction, is expected to slow the Friedel–Crafts reaction or even limit the yield at higher levels of conversion which should be especially visible for less reactive aromatic substrates. According to Le Chatelier's principle, removal of *in situ*-formed acetic acid should consequently shift the underlying equilibrium to increase the active concentration of ion pair **X** and to therefore enable higher levels of conversion and overall reaction rates. Investigations in this regard are part of the ongoing research in our laboratory.

Kinetic Isotope Effect Studies

The following studies were performed in collaboration with Dr. Markus Leutzsch.

As our initial mechanistic studies were directed on the investigation and elucidation of iminium ion-intermediates **X**, we then turned our attention toward the determination of the rate limiting step of the reaction. We therefore chose to investigate the kinetic H/D isotope effect (**KIE**) in the reaction of *N,O*-acetal **54** in a direct competition study between toluene-h_8 and toluene-d_8 (scheme **4.16**). Since the reaction was performed neatly in a homogeneous mixture of toluene-h_8 and toluene-d_8, a large excess of both species is present in the reaction mixture which leaves

their concentration approximately constant. Via spectroscopic analysis of the obtained product mixture, a KIE of 1.55 ± 0.04 could be determined.

The maximum theoretical value for a secondary KIE is expected at around 1.4 and typical values range at around 1.1–1.2. The value observed in this study consequently resembles more the one of a small primary KIE.[170] While secondary KIEs usually indicate a change in hybridization during the rate determining step for the bond that has been labeled isotopically, measurement of primary KIEs indicates that the isotope replacement occurred in a bond that is broken in the rate determining step.[170] In the literature of Friedel–Crafts acylation reactions, primary KIEs are reported frequently as exemplified by Olah and Effenberger in 1964 and 2001, respectively.[171,172] The large KIEs are usually explained to originate from the formation of comparatively stable Wheland complexes that are formed in a reversible manner which makes their deprotonation towards the aromatic product at least partially rate determining.

In Friedel–Crafts alkylation or nitration reactions on the other hand, secondary or inverse KIEs are usually observed as illustrated by Olah in 1961 and Nakane in 1971.[173,174] These lower or even inverse KIE-values are usually traced back to Wheland complex formation and not to the
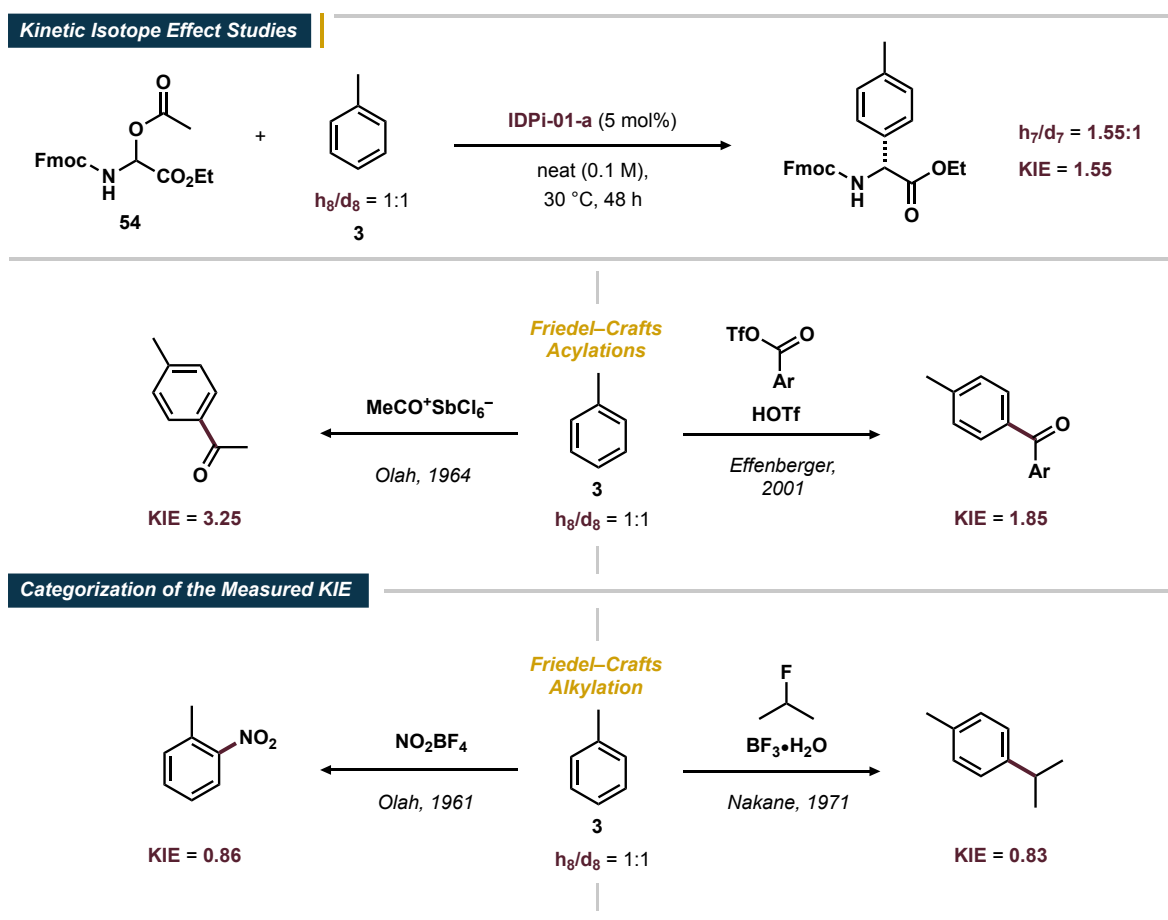
Scheme 4.16: Kinetic isotope effect studies and comparison with literature precedents.[171–174]

rearomatization process to be rate determining. The KIE of 1.55 measured in the context of this work therefore exceeds the theoretical maximum of a secondary KIE. The experiment consequently points toward rearomatization, the breaking of the isotope-labeled bond, to be at least partially rate limiting. With reference to the abovementioned literature precedents, this suggests a comparatively high stability of the thus formed Wheland complex. We hypothesize that the electron-rich carbamate moiety of the Fmoc-protecting group could have a stabilizing influence on the Wheland intermediate, potentially even via formation of a cyclic, six-membered intermediate of type **XI** (see scheme **4.17** for reference). In a direct comparison of the iminium ion derived from *N,O*-acetal **54** with the acylation agents reported by Olah and Effenberger as well as typical alkylhalide-alkylating agents as described by Nakane, a significant degree of similarity regarding structural features and hybridization can be found for the acylating agents. It is therefore not surprising that similar yet slightly smaller KIE values are observed in the investigated reaction.

[13]C-Kinetic Isotope Effect Studies at a Natural Abundance

The studies described in the following were performed in collaboration with Samuel Steinfeld, Dr. Matthew Vetticatt and Dr. Markus Leutzsch.

The determination of kinetic isotope effects can be a helpful tool for the identification of rate determining processes. KIEs are furthermore powerful methods to investigate which bonds undergo rehybridization or even cleavage during critical steps of the reaction mechanism.[170] As the structure of potential Wheland intermediates is generally of outstanding importance for the understanding and the improvement of Friedel–Crafts processes, we were interested in the elucidation of possible σ-complex intermediates. Other techniques which provide in-depth information on the change of bonding and hybridization and, consequently, the nature of fleeting intermediates, are ^{13}C-kinetic isotope effect studies. To avoid challenging and tedious isotope-labeling processes, Singleton reported the measurement of ^{13}C-KIEs at the natural abundance of the isotope to allow the straightforward analysis of suitable reactions.[175,176] To further investigate the structure of possible Wheland intermediates, especially with respect to potential stabilizing interactions with the carbamate backbone, we envisioned ^{13}C-KIE studies at a natural abundance for the herewith investigated system.

We chose 1,3-benzodioxole (**74**) as substrate for the planned studies as it possesses a symmetric plane which undergoes desymmetrization in the course of the reaction. In that way, the direct comparison of the ^{13}C-values of each position in the aromatic ring becomes possible.

Additionally, high yields were observed in the reaction of *N,O*-acetal **54** with **74**. As larger amounts of the analytical substance are usually required to obtain representative results for ^{13}C-KIE studies at a natural abundance, high reaction yields are desirable to obtain sufficient material for the precise spectroscopic analysis.[176]

[13]C-KIEs at a natural abundance are usually small values, especially compared to many H/D-KIEs. The samples therefore have to fulfill requirements which allow the precise spectroscopic analysis. In the herewith investigated reaction however, the carbamate moiety of the Fmoc-protecting group leads to the formation of multiple rotameric species which significantly complicates the analytical process and demands for follow-up manipulations. We therefore chose to prepare arylglycine **105** on larger scale and to then remove the carbamate protecting group (scheme **4.17**).
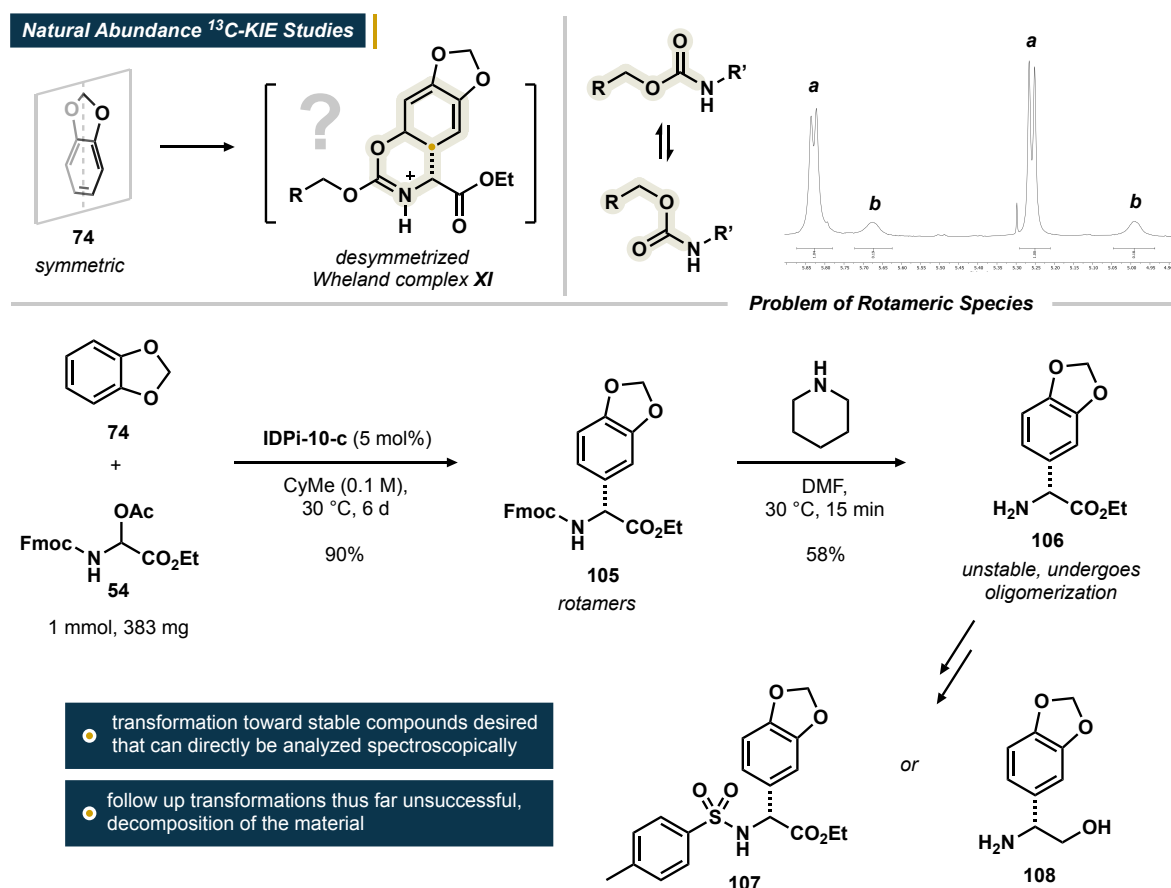
Scheme 4.17: Toward the determination of ^{13}C-KIEs at a natural abundance.

The Friedel–Crafts reaction was performed on a 1 mmol scale (383 mg) corresponding to *N,O*-acetal **54** to yield the arylglycine **105** with excellent yield and unchanged regio- and stereoselectivity (see scheme **4.7** for reference). As described above, a mixture of rotamers was

observed spectroscopically for **105**. The cleavage of the Fmoc-group was therefore performed subsequently to yield the free amino acid ester **106**. While the thus obtained amine **107** shows promising properties for direct spectroscopic analysis, slow oligomerization processes were detected which prevents precise measurements. We therefore set out to transform amino acid ester **106** further to obtain a stable compound without the presence of groups that diminish the quality of the spectroscopic analysis. Further efforts to transforming amine **106** to either its corresponding tosylate **107** or amino alcohol **108** have thus far been unsuccessful and decomposition of amine **106** was observed exclusively. Further studies to transforming arylglycine **105** into a stable analyte are ongoing in our laboratory.

Catalyst Stability Studies

The following studies were performed in collaboration with Dr. Markus Leutzsch.

As described in section **4.1.2**, the stepwise inner-core cleavage of IDPi-based catalysts to initially form the corresponding *i*IDP- and finally the IDP-species was observed in the course of the Friedel–Crafts reaction of *N,O*-acetals with unactivated aromatic substrates (scheme **4.18**). With reference to earlier investigations using *para*-formaldehyde as electrophilic reagent, we expect the highly reactive nature of the *N,O*-acetal-derived iminium ions **IX** to promote a stepwise hydrolysis with finally leads to the degradation of the used catalyst.[67,177] Preceding studies with *i*IDP- and IDP-derived catalysts could already show that these catalyst classes are completely unreactive in the investigated Friedel–Crafts reaction (see table **4.4**). The stepwise inner-core cleavage, which equates to the reduction of the effective catalyst loading of the only catalytically active species, consequently corresponds to a reduction of the reaction rate and, finally, of the obtained yield on the arylglycine product.

To prevent the hydrolytic catalyst degradation, the usage of drying agents has been investigated. While, qualitatively, reduced rates of catalyst degradation could be observed in their presence, the lower rate of catalyst hydrolysis was accompanied by a significant loss of reactivity (see table **4.3**). As described in preceding studies, inner-core cleavage is envisioned to proceed via the formation of covalent intermediates, formed between the core structures of *i*IDP- or IDPi-catalysts and highly electrophilic reagents. The covalent structures then subsequently or in the course of the reaction promote hydrolytic P–N bond cleavage.[177] The tendency of the respective catalysts to form covalent intermediates and thus undergo hydrolytic cleavage should therefore depend on the electronic and steric nature of the respective IDPi which consequently allows for the development of more robust catalysts.
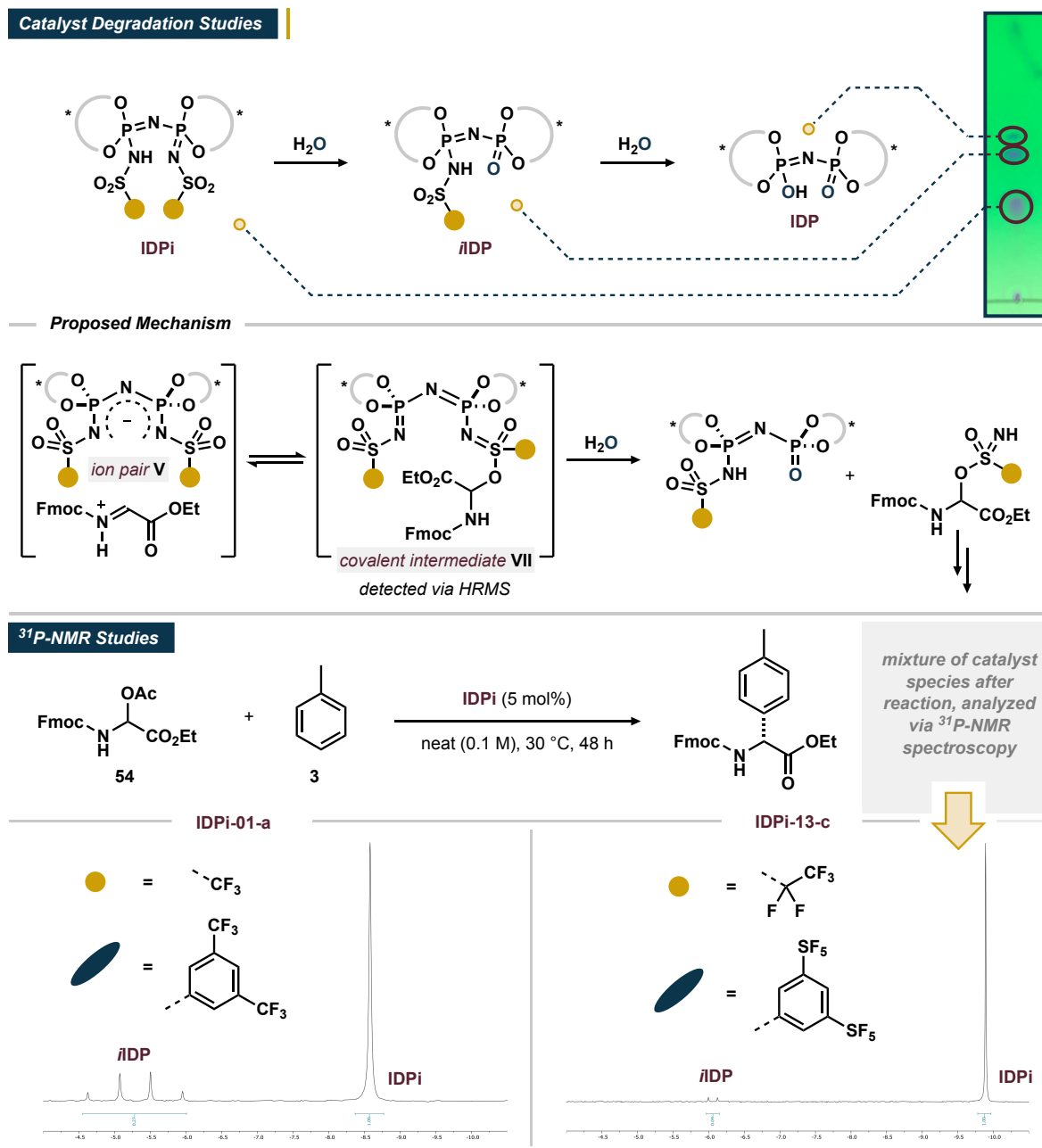
Scheme 4.18: Catalyst stability studies via ^{31}P-NMR spectroscopy.

Installation of more electron-withdrawing substituents on the Brønsted acid should not only increase the rate of the reaction via enhancement of the acidity of the catalyst but also via reduction of the nucleophilicity of the corresponding counteranion. The formation of covalent intermediates might consequently be suppressed to prevent catalyst degradation.

In our catalyst development studies for the Friedel–Crafts reaction between *N,O*-acetal **54** and toluene (**3**) we could already identify significant trends in the reaction yield upon modification of the substituents (see table **4.4**). Transitioning from catalyst **IDPi-01-a** to **IDPi-13-c** led to an increase in the yield from 42% to 70%. To investigate if this improvement corresponds to a

decreased rate of catalyst degradation, we analyzed each respective reaction mixture via ^{31}P-NMR spectroscopy to detect and quantify the rate of catalyst decomposition (scheme **4.18**). As shown in scheme **4.18**, **IDPi-01-a** undergoes significant inner-core cleavage during the Friedel–Crafts reaction of *N,O*-acetal **54** with toluene (**3**). Analysis of the reaction mixture of the optimized catalyst **IDPi-13-c** however indicates that only traces of the corresponding *i*IDP and the IDP, the products of hydrolytic core-cleavage, can be detected spectroscopically. The experiments are therefore in line with the reactivities observed for the respective Friedel–Crafts reactions. It remains unclear whether the increased yield can solely be attributed to improved catalyst stability or if the enhanced acidity plays a major role in a higher reaction rate. However, it seems plausible to expect both factors to contribute to the high reactivity of **IDPi-13-c** and that its increased acidity positively affects both catalyst stability as well as the general reaction rate.

Computational Investigation of Reaction Intermediates

The following studies were performed in collaboration with Benjamin Mitschke.

To further examine the nature of ion pair **X**, which is expected to be of paramount importance for the proceeding of the reaction, we engaged in computational studies to investigate its structure and the existing interactions between the IDPi-catalyst and electrophile **54**. Therefore, the DFT structure of the lowest energy conformer of the iminium ion pair **X** resulting from reaction of *N,O*-acetal **54** with **IDPi-13-c** was calculated. The resulting structures are shown below (figure **4.2**).

The most prominent interaction between iminium ion **IX** and the chiral IDPi-derived counteranion is a tight hydrogen bond of the iminium N–H to the pentafluoroethylsulfonyl core of the catalyst (1.54 Å bond distance). Intriguingly, a second hydrogen bond can be identified between the bis-benzylic proton of the fluorenyl portion of the iminium ion and the imidodiphosphorimidate core of the catalyst which supports in locking and controlling the conformational arrangement of ion pair **X** (2.36 Å). Additional π-π-stacking effects between the fluorenyl moiety with the $3,5\text{-}(SF_5)_2\text{-}C_6H_3$-groups contribute to the stability of **X**. The improved capability of the Fmoc group to form stabilizing π-π-interactions is consistent with the observed improvement of enantioselectivity upon replacement of the Cbz-group with an Fmoc-protecting group on the *N,O*-acetal (table **4.3**). Another noteworthy detail is the protrusion of the alkyl chain of the ester group of iminium ion **IX** from the active pocket of the catalyst. This structural feature of ion pair **X** is in good agreement with the experimentally found independence of the

enantiomeric ratio from the shape and the size of the alkyl residue of the ester group (see table **4.3** for reference).

*calculated structure of iminium ion pair **X** derived from N,O-acetal **54** and **IDPi-13-c***

Calculated H–bond interactions of the iminium ion with the catalyst core

Calculated H–bond interactions of the fluorenyl scaffold with the catalyst core

Isosurface of the electron density, colored by electrostatic potential
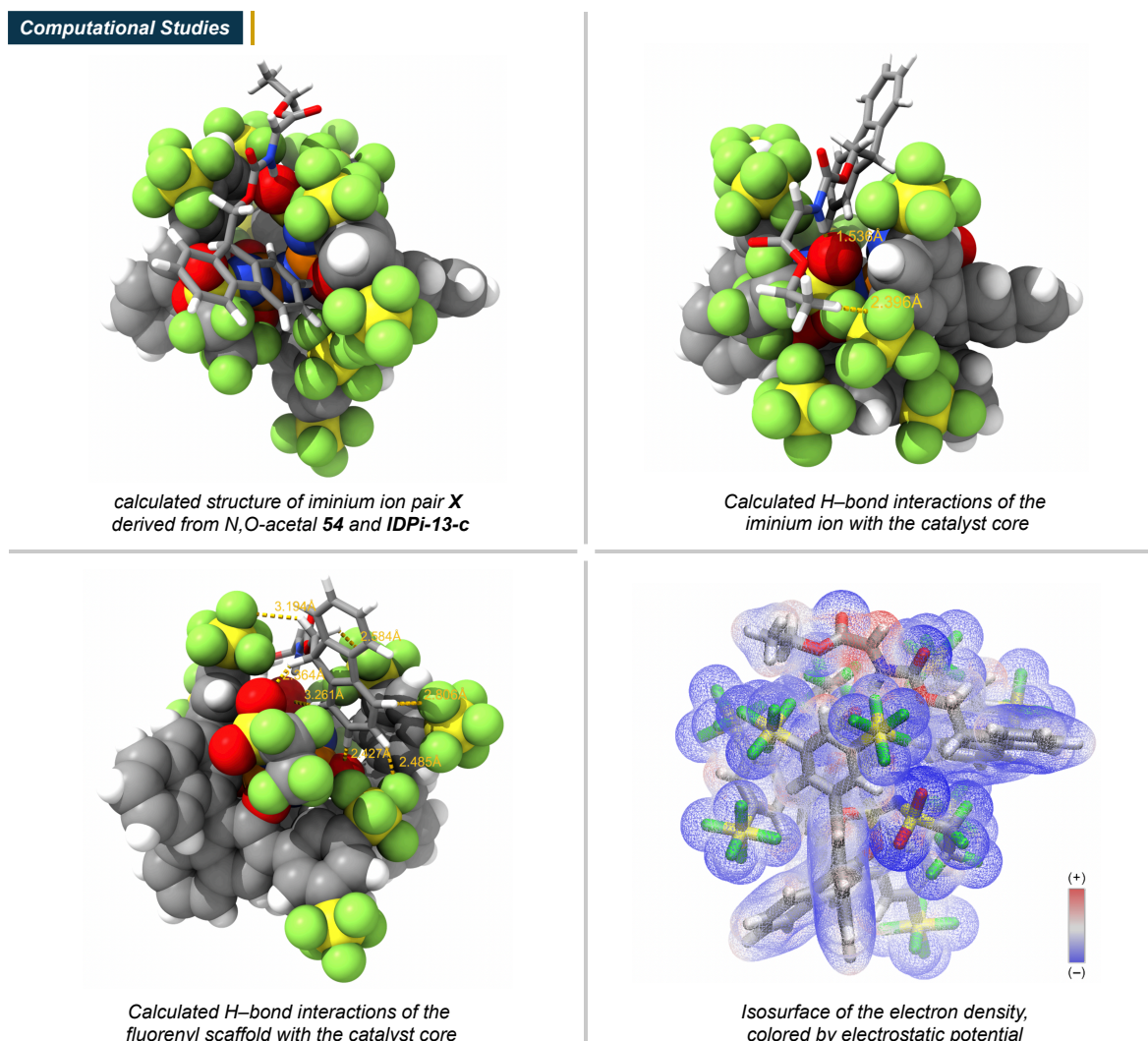
Figure 4.2: DFT-structures, calculated for ion pair **X** (resulting from **54** and **IDPi-13-c**).

To furthermore visualize the charge distribution on iminium ion pair **X** we engaged in the determination of the isosurface of the electron density, which is illustrated in figure **4.2** as electrostatic potential. As indicated in preceding experiments, the major electron deficiency is located around the carbon atom of the iminium ion **IX** which underlines its extraordinary electrophilicity. This highly electrophilic nature is expected to be a crucial feature to allow the nucleophilic attack of unreactive aromatic substrates in the investigated Friedel–Crafts reaction.

4.1.7 Proposed Catalytic Cycle of the Friedel–Crafts Reaction

Based on the preceding mechanistic studies described in the chapters **4.1.6**, we propose the following catalytic cycle to be operating in the IDPi-catalyzed Friedel–Crafts reaction between *N,O*-acetals and (unactivated) aromatic substrates (scheme **4.19**):
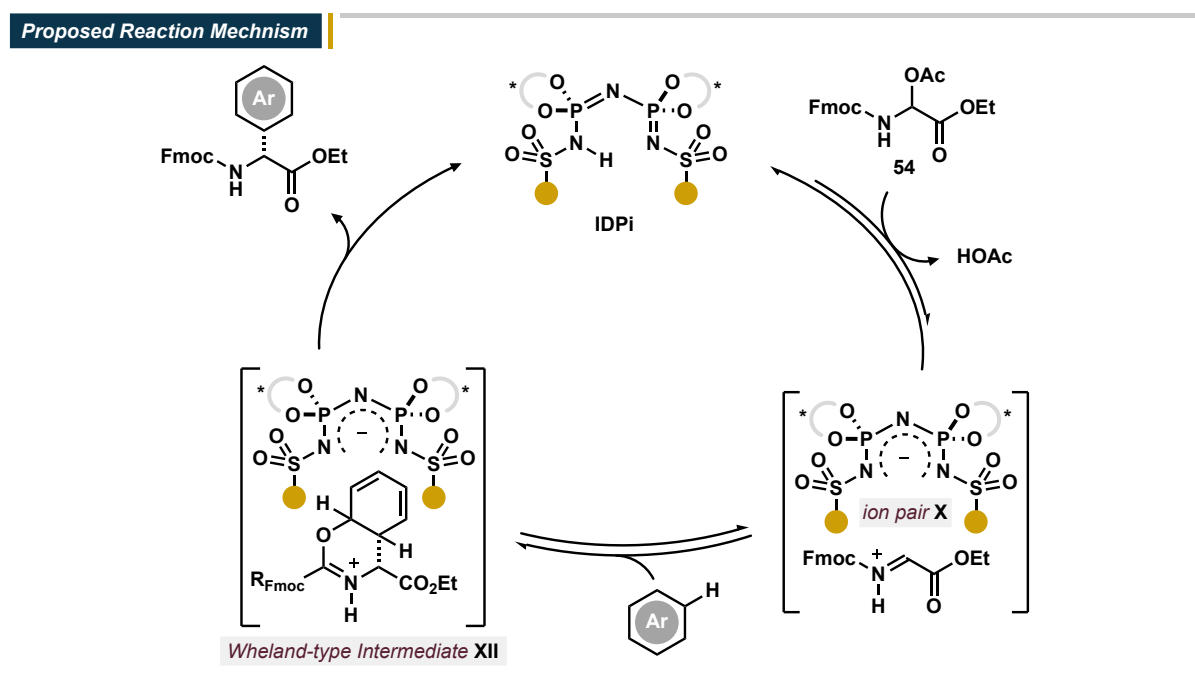
Scheme 4.19: Proposed catalytic cycle.[178]

Based on the abovementioned leaving group scrambling experiments, we envisioned the reaction of *N,O*-acetal **54** with the IDPi-catalyst to form the ion pair **X** via the concomitant release of acetic acid. As a rapid exchange of the leaving groups was observed in the scrambling studies, we expect the formation of ion pair **X** to proceed in a dynamic equilibrium with **54** and the IDPi-catalyst. The highly electrophilic iminium ion pair **X** is then expected to undergo nucleophilic attack by the aromatic substrate to form Wheland complex **XII** as key intermediate. We furthermore propose an interaction of the electron-rich carbamate-moiety of the Fmoc-protecting group of *N,O*-acetal **54** to have an additional stabilizing effect on Wheland-type intermediate **XII** via formation of a cyclic iminium ion. Subsequent deprotonation of **XII** finally releases the arylglycine-product, restores the IDPi catalyst and closes the catalytic cycle.

4.2 The Asymmetric Catalytic Scriabine Reaction

4.2.1 Scriabine Reaction: Origin and Perspective

The iconic scent of the lily of the valley has inspired perfumers for decades in their creative journey to create ever-more pleasing fragrances.[179] Ironically, however, it has not yet been possible to extract an essential oil from the actual flower that possesses its original olfactory properties. Consequently, chemists have tried to mimic the smell of the flower with the tools provided by synthetic organic chemistry. Over the decades, a number of small molecules with a lily of the valley-(also called muguet-) like scent have been discovered and used in a myriad of products, ranging from soaps and detergents to body care products and fine perfumery.[180] Blockbuster fragrance molecules such as Lilial (**109**), Cyclamen aldehyde (**110**), Burgeonal (**111**), Hivernal® or Nympheal™ (**112**) are just a few out of a wide range of lily of the valley-inspired scent molecules of enormous economic significance (scheme **4.20**). Upon comparison of the molecular structure of the muguet-type aroma molecules, a common structural feature can quickly be identified: the parent dihydrocinnamaldehyde scaffold. The presence of this scaffold consequently gives rise to a potential synthetic platform for the synthesis of a broad variety of structurally related scent molecules via conjugate addition of aromatic substrates to enals.

Stimulated by the high demand for the muguet scent molecules, Igor Scriabine, a chemist working at Rhône-Poulenc (A former French chemical and pharmaceutical company) investigated this approach in the 1960s. In this context, Scriabine studied the Lewis acid-catalyzed addition of hydrocarbon arenes to enals to enable the synthesis of Cyclamen aldehyde (**110**). While Scriabine observed low yields in the Friedel–Crafts addition of cumene (**5**) to methacrolein (**113**), a significant improvement in yield was observed upon exchange of **113** with the corresponding acylal **114** to yield enol acetate **115**, which can easily be hydrolyzed to give cyclamen aldehyde.[181–183] The necessity of superstoichiometric amounts of $TiCl_4$ along with catalytic amounts of $BF_3 \cdot OEt_2$ indicates that both acetate groups need to be activated independently to allow the reaction to proceed.[184]

Despite the intriguing findings reported by Scriabine, more than four decades passed until catalytic versions of the reaction were investigated at Firmenich and at the UBE cooperation, both individually tailored for the synthesis of fragrance molecules.[185,186] However, the reported methods were found to be significantly limited in their scope of applicable aromatic substrates as well as electrophilic acceptor reagents. The first general catalytic Scriabine reaction was

reported only in 2018 by Gandon who used gallium-based Lewis acid catalysts to promote the desired bond formation (scheme **4.20**).[184]
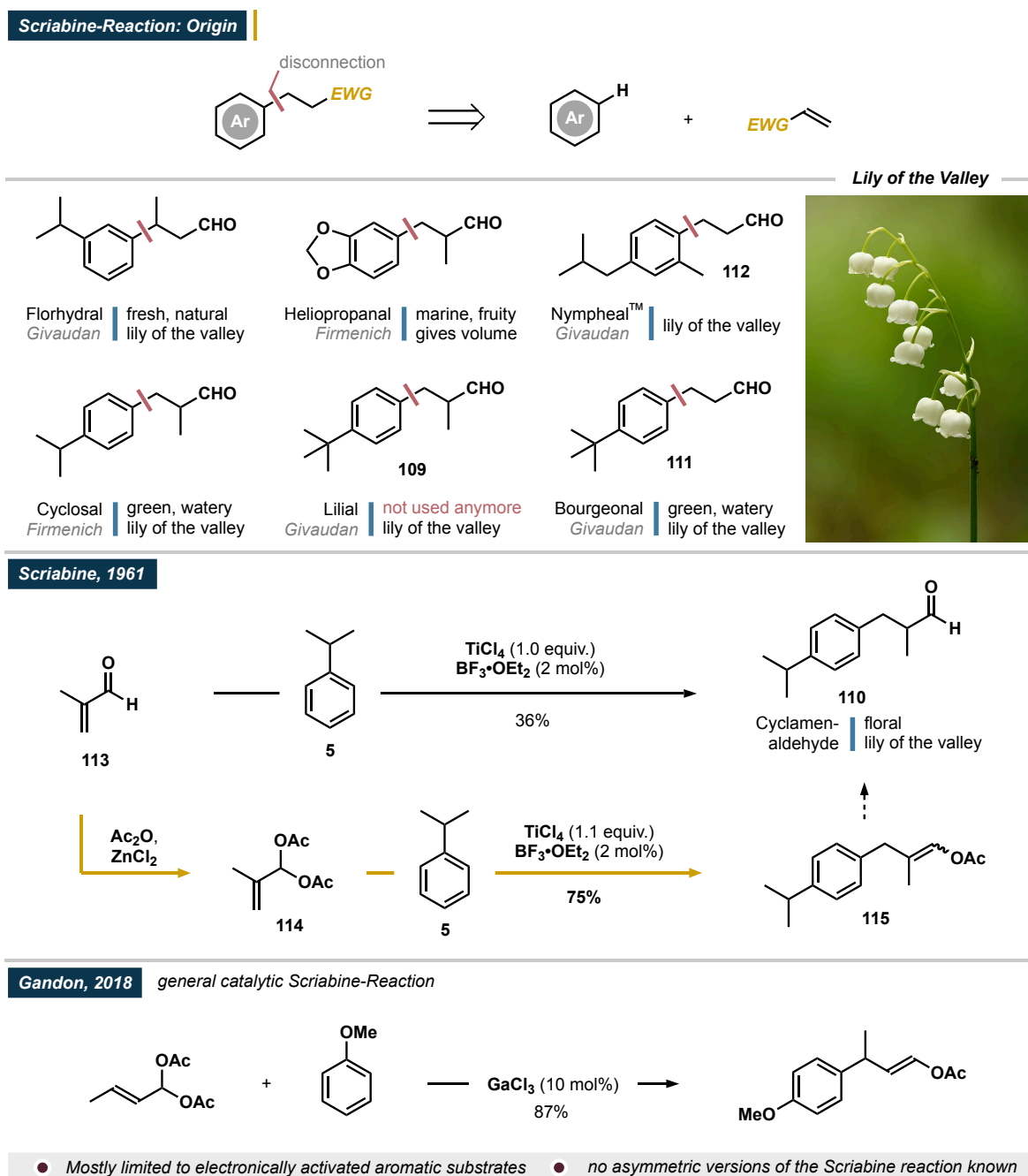
Scheme 4.20: Relevance and concept of the Scriabine reaction.

Even though acylals could already be used in asymmetric catalysis, asymmetric catalytic Scriabine reactions are still unknown until this day.[187] This finding is especially peculiar given the importance of benzylic carbon stereocenters as ubiquitous structural motif in biologically

active molecules. Against this background, we decided to investigate a general method for the asymmetric catalytic Scriabine reaction using strong and confined Brønsted acid catalysts.
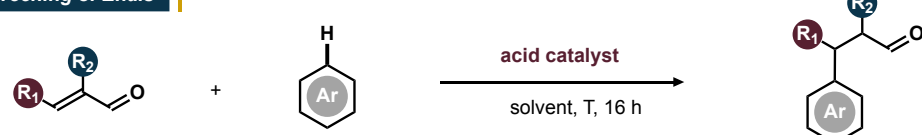
4.2.2 Reaction Design and Initial Studies

The following studies were performed in collaboration with Samuel Steinfeld and Luc Debie.
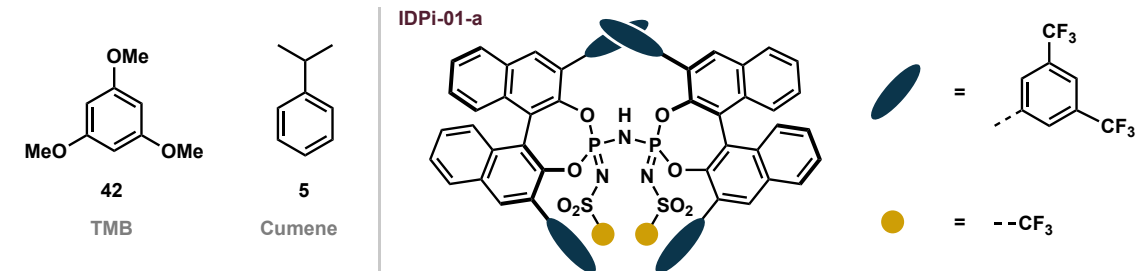
We commenced our studies analogously to the early work carried out by Scriabine more than 60 years ago. To study and evaluate the reactivity of simple hydrocarbon arenes in the chiral Brønsted acid-catalyzed addition to enal acceptor molecules, we investigated their behavior in the presence of strong and confined acid catalysts (table **4.8**).

Table 4.8: Screening of the Brønsted acid-catalyzed addition of arenes to enals. [a] = crude NMR yield.

entry	R$_1$	R$_2$	acid catalyst	arene substrate	T	solvent	yield[a]
1	Me	H	HNTf$_2$ (10 mol%)	PhMe (neat)	40 °C	PhMe (0.1 M)	<5%
2	Me	H	IDPi-01-a (5 mol%)	PhMe (neat)	40 °C	PhMe (0.1 M)	<5%
3	Me	H	HNTf$_2$ (10 mol%)	TMB (5 equiv.)	40 °C	PhMe (0.1 M)	<5%
4	Me	H	IDPi-01-a (5 mol%)	TMB (5 equiv.)	40 °C	PhMe (0.1 M)	<5%
5	H	Me	IDPi-01-a (5 mol%)	cumene (4 equiv.)	30 °C	neat	<5%
6	H	Me	IDPi-01-a (5 mol%)	o-xylene (4 equiv.)	30 °C	neat	<5%
7	Et	H	IDPi-01-a (5 mol%)	cumene (4 equiv.)	30 °C	neat	<5%
8	Et	H	IDPi-01-a (5 mol%)	o-xylene (4 equiv.)	30 °C	neat	<5%

As described above, usage of the strong Brønsted acid catalysts HNTf$_2$ as well as **IDPi-01-a** in the Friedel–Crafts type addition of toluene (**3**) to (*E*)-crotonaldehyde did not result in the formation of the desired dihydrocinnamaldehyde product in detectable amounts. Even transition to the significantly more nucleophilic **TMB** as aromatic substrate proved to be unsuccessful in

the desired transformation while partial decomposition of the enal was observed. Inspired by the studies carried out by Scriabine, we decided to investigate the IDPi-catalyzed addition of cumene and *ortho*-xylene to methacrolein as model system under higher concentrations (entries 5-6). Nonetheless, no product formation was observed in detectable amounts. Similarly, the reaction of (*E*)-2-pentenal under analogous conditions was found to be unsuccessful (entries 7-8).

As reported earlier, stoichiometric amounts of strong Lewis acids are necessary to promote the addition of simple hydrocarbon arenes to enals and despite these harsh reaction conditions, only low yields of the desired products are obtained. We therefore speculate that the catalysts used in our abovementioned studies do not possess the required acidity to form the desired products. Since our studies on the direct addition of simple aromatic substrates to enal-based acceptor molecules did not lead to the proceeding of the desired Friedel–Crafts reaction, we reconsidered this initial approach. As described by Scriabine, a significant increase in reactivity can be observed via transition from enals as acceptor molecules to their corresponding acylals. The higher reactivity of the corresponding acylals can partially be traced back to the increased Lewis basicity of the diacyl-structure which allows for close interactions with Lewis acid catalysts to achieve a strong activating effect of the C–C double bond.[184] Intrigued by these studies, we envisioned a potential way to increase the reactivity of our system while simultaneously provide an efficient platform for the construction of benzylic stereocenters via asymmetric counteranion directed catalysis.

To test the ability of strong and confined acids to catalyze asymmetric Scriabine reactions, we initially engaged in the synthesis of a number of structurally diverse acylal reagents from enals (scheme **4.21**). Following a protocol reported earlier by Trost, anhydrous $FeCl_3$ was used as Lewis acid catalyst under neat reaction conditions.[187] However, we quickly noticed that under these harsh reaction conditions significant amounts of isomerization side products were formed which proved to be particularly hard to remove chromatographically. To enable a more selective acylal synthesis we tested a range of Lewis acid catalysts in the synthesis of the (*E*)-2-pentenal (**116**) derived diacetate. Testing the Lewis acids $FeCl_3$, $Zn(BF_4)_2$, $Bi(OTf)_3$, $Ga(OTf)_3$, and $InCl_3$, we found the most selective reaction profile for $Zn(BF_4)_2$. $Zn(BF_4)_2$ was however found to lack generality in the synthesis of acylals as the usage of isobutyric anhydride as reagent did not yield the desired product with the Zn(II)-based catalyst. For further studies, we therefore chose to use $FeCl_3$ as relatively selective and highly general catalyst for the synthesis of acylals. Following reported procedures, a range of linear or cyclic aliphatic enals or cinnamaldehyde-

4. Results and Discussion
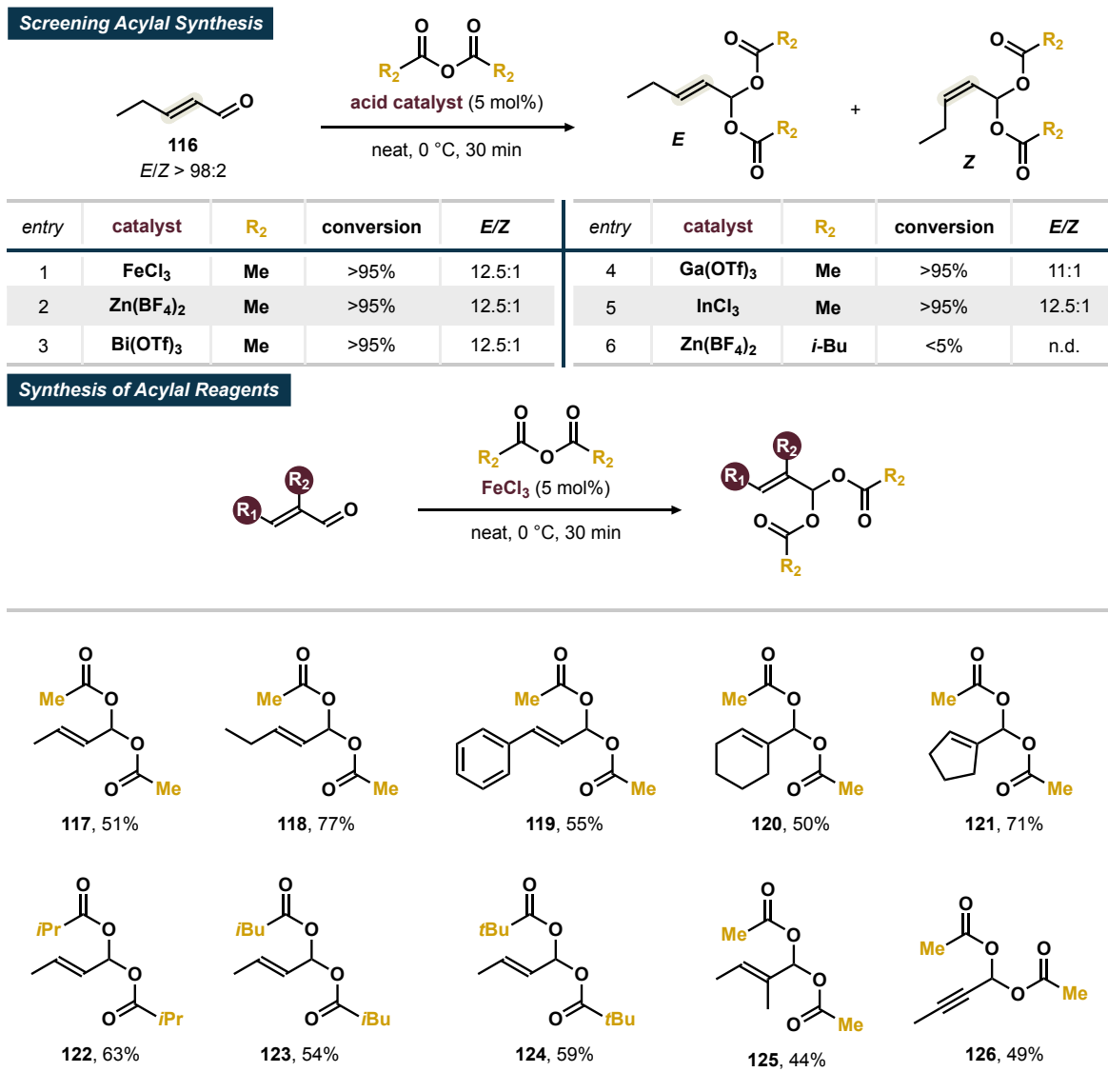
Scheme 4.21: Synthesis of enal-derived acylals.

derived acceptors were transformed with a number of aliphatic anhydrides to yield the corresponding acylals with generally high yields.[187] Having synthesized the required acylal reagents, we were eager to test their reactivity in the chiral Brønsted acid-catalyzed Scriabine reaction. We started our studies using acrolein diacetate in the Scriabine reaction of toluene using HNTf$_2$ and **IDPi-01-a** as acid catalysts (table **4.9**, entries 1-2). Under neat reaction conditions, we observed the formation of corresponding enol acetates with promising yields. Surprisingly, however, transition to the (*E*)-crotonaldehyde derived diacetate **117** under otherwise analogous reaction conditions led to a complete shutdown of the reactivity both using HNTf$_2$ as well as **IDPi-01-a** as acid catalysts. Only upon usage of anisole (**26**) as significantly more reactive aromatic substrate, the reactivity could be restored and the corresponding enol

4. Results and Discussion

acetate was obtained with moderate to high yields, a moderate *E/Z*-ratio and, for the usage of **IDPi-01-a**, a promising enantiomeric ratio of 65:35 (entry 7).

Table 4.9: Initial screening toward the asymmetric Scriabine reaction. [a] = crude NMR yield.

Initial Screening Asymmetric Scriabine Reaction
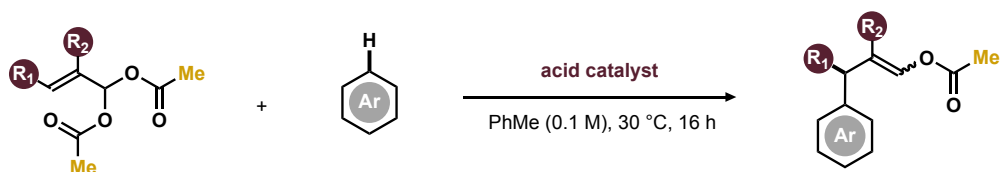
entry	R₁	R₂	acid catalyst	arene substrate	E/Z	e.r.	yield[a]
1	H	H	HNTf₂ (5 mol%)	PhMe (neat)	–	–	42%
2	H	H	IDPi-01-a (2.5 mol%)	PhMe (neat)	–	–	52%
3	H	H	IDPi-01-a (2.5 mol%)	anisole (1 equiv.)	–	–	29%
4	Me	H	HNTf₂ (5 mol%)	PhMe (neat)	n.d.	n.d.	<5%
5	Me	H	IDPi-01-a (2.5 mol%)	PhMe (neat)	n.d.	n.d.	<5%
6	Me	H	HNTf₂ (5 mol%)	anisole (1 equiv.)	4:1	–	72%
7	Me	H	IDPi-01-a (2.5 mol%)	anisole (1 equiv.)	5:1	65:35	29%
8	Et	H	HNTf₂ (5 mol%)	PhMe (neat)	n.d.	n.d.	<5%
9	Et	H	IDPi-01-a (5 mol%)	PhMe (neat)	n.d.	n.d.	<5%
10	Et	H	HNTf₂ (5 mol%)	anisole (1 equiv.)	n.d.	n.d.	<5%
11	Et	H	IDPi-01-a (5 mol%)	anisole (1 equiv.)	n.d.	n.d.	<5%
12	Ph	H	HNTf₂ (5 mol%)	PhMe (neat)	n.d.	n.d.	<5%
13	Ph	H	IDPi-01-a (5 mol%)	PhMe (neat)	n.d.	n.d.	<5%
14	Ph	H	HNTf₂ (5 mol%)	anisole (1 equiv.)	n.d.	n.d.	<5%
15	Ph	H	IDPi-01-a (5 mol%)	anisole (1 equiv.)	n.d.	n.d.	<5%

IDPi-01-a
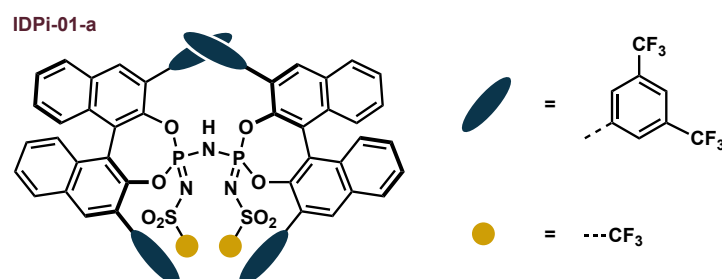
The initially observed correlation between the reactivity and the substitution pattern of the geminal diacetate was found to be even more pronounced for (*E*)-2-pentenal diacetate **118** as well as cinnamic aldehyde diacetate **119**: no product formation could be observed using HNTf₂ or **IDPi-01-a** for both toluene as well as anisole under the reported reaction conditions.
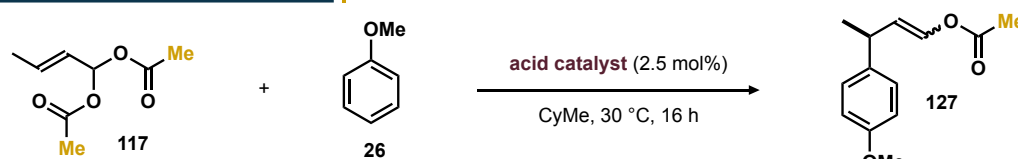
As described above, initial problems in the investigated reaction could quickly be identified: besides the challenge of a selective synthesis of the acylal reagents, the system seems to be very sensitive to substituents situated at the β-position of the acceptor which significantly limits the
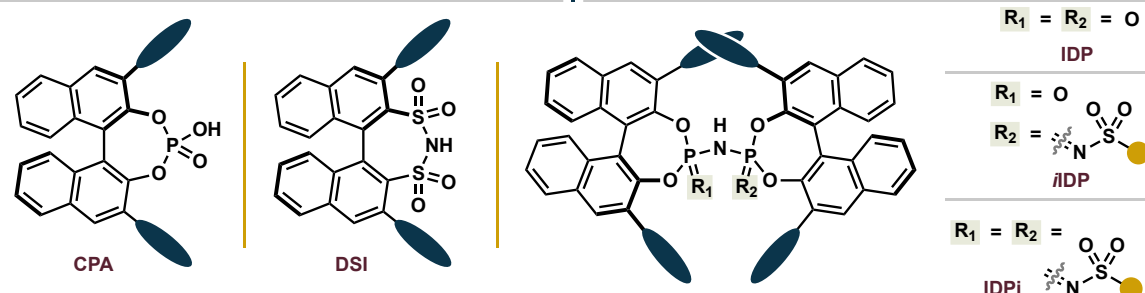
method. As we however observed promising reactivity with (*E*)-crotonaldehyde-derived acylal **117** in the IDPi-catalyzed Scriabine reaction with **26**, we chose to further investigate and improve the reaction system to optimize yield and selectivity of the reaction. We therefore engaged in a broad screening of reaction conditions and catalyst motifs prior to the evaluation of potential scope entries (table **4.10**).

Table 4.10: Catalyst screening for the asymmetric Scriabine reaction. [a] = crude NMR yield.
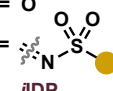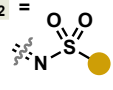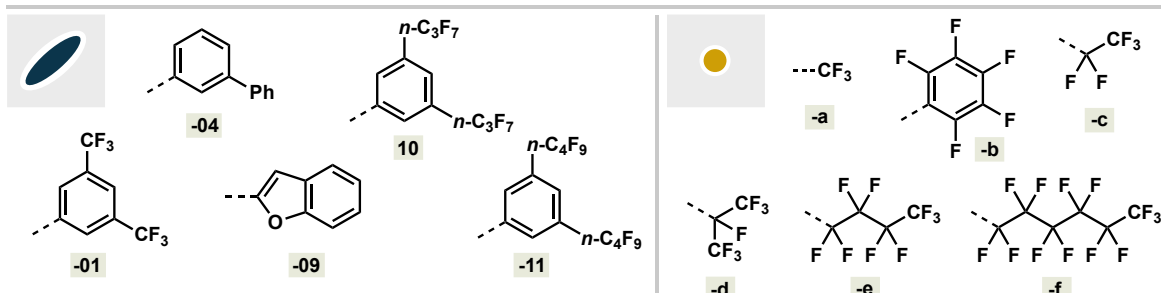
entry	catalyst	yield[a]	E/Z	e.r.	entry	catalyst	yield[a]	E/Z	e.r.
1	CPA-01	<5%	n.d.	n.d.	7	IDPi-01-c	>95%	14:1	72:28
2	DSI-01	<5%	n.d.	n.d.	8	IDPi-04-a	<5%	n.d.	n.d.
3	IDP-01	<5%	n.d.	n.d.	9	IDPi-09-b	<5%	n.d.	n.d.
4	*i*IDP-01-a	<5%	n.d.	n.d.	10	IDPi-10-a	>95%	>20:1	80:20
5	IDPi-01-a	62%	20:1	75:25	11	IDPi-11-a	>95%	20:1	80:20
6	IDPi-01-b	<5%	n.d.	n.d.	12	IDPi-10-f	>95%	16:1	73:27
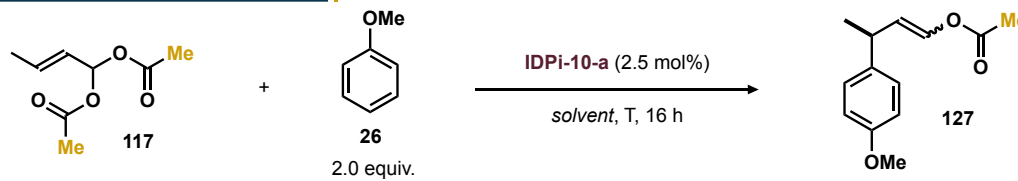
In analogy to our preceding studies, we chose CyMe as solvent. Reminiscent of the catalyst screening we performed earlier for the Friedel–Crafts reaction toward the synthesis of enantioenriched arylglycines (see table **4.4**), we observed that the application of CPA-, DSI-, IDP- or *i*IDP-based catalysts in each case did not result in the formation of detectable amounts

of the desired enol acetate **127**. Furthermore, usage of **IDPi-04-a**, bearing a biphenyl substituent or of **IDPi-01-b**, featuring a C_6F_5-core modification proved to be unsuccessful in the desired transformation. Only upon installation of both, a 3,5-bis(trifluoromethyl)phenyl substituent in the 3,3'-positions of the BINOL as well as a triflyl substituent in the active imidodiphosphorimidate core, the formation of enol acetate **127** was observed with good yields, a high *E/Z* ratio and a promising enantiomeric ratio of 75:25. Unlike to the trend observed in the synthesis of arylglycines, elongation of the perfluoroalkyl chain in the imidodiphosphorimidate core did not lead to an improvement of the reaction outcome and a visibly reduced enantiomeric ratio was obtained. Contrarily, elongation of the CF$_3$-groups in the 3,5-positions of the 3,3'-aryl substituents of the BINOL to perfluoro-*n*-propyl- or -butyl substituents was found to improve the enantiomeric ratio of the product **127** to 80:20 (entry 10). As transition from toluene as solvent to its hexahydrogenated equivalent methylcyclohexane led to a visible improvement of the enantiomeric ratio on enol acetate **127**, we were intrigued if the observed selectivity could be improved even further via choice of different aliphatic solvents. We therefore performed a broader screening of hydrocarbon solvents (table **4.11**).

Table 4.11: Solvent screening studies for the asymmetric Scriabine reaction. [a] = crude NMR yield.

entry	solvent	T	yield[a]	e.r.	entry	solvent	T	yield[a]	e.r.
1	CyMe (0.1 M)	30 °C	>95%	80:20	5	*n*-pentane (0.5 M)	30 °C	>95%	70:30
2	*n*-pentane (0.1 M)	30 °C	>95%	83:17	6	*n*-pentane (0.1 M)	20 °C	>95%	83.5:16.5
3	*n*-hexane (0.1 M)	30 °C	>95%	80:20	7	*n*-pentane (0.1 M)	0 °C	>95%	85.5:14.5
4	*n*-heptane (0.1 M)	30 °C	>95%	81:19					

The observed improvement in enantioselectivity upon transition from toluene to methylcyclohexane was found to be even outperformed by the usage of *n*-pentane as solvent. Finally, the enantiomeric ratio on enol acetate **127** could be improved to 85.5:14.5 at a reduced temperature of 0 °C.

4.2.3 Scope and Limitations for the Asymmetric Scriabine Reaction of Acylals

The following studies were performed in collaboration with Samuel Steinfeld and Luc Debie.

With these improved reaction conditions, we set out to investigate the generality of the reaction and to determine potential limitations of the preliminary reaction system. We therefore tested a range of acylal acceptor molecules along with anisole (**26**) and benzofuran (**82**) as aromatic substrates (scheme **4.22**).
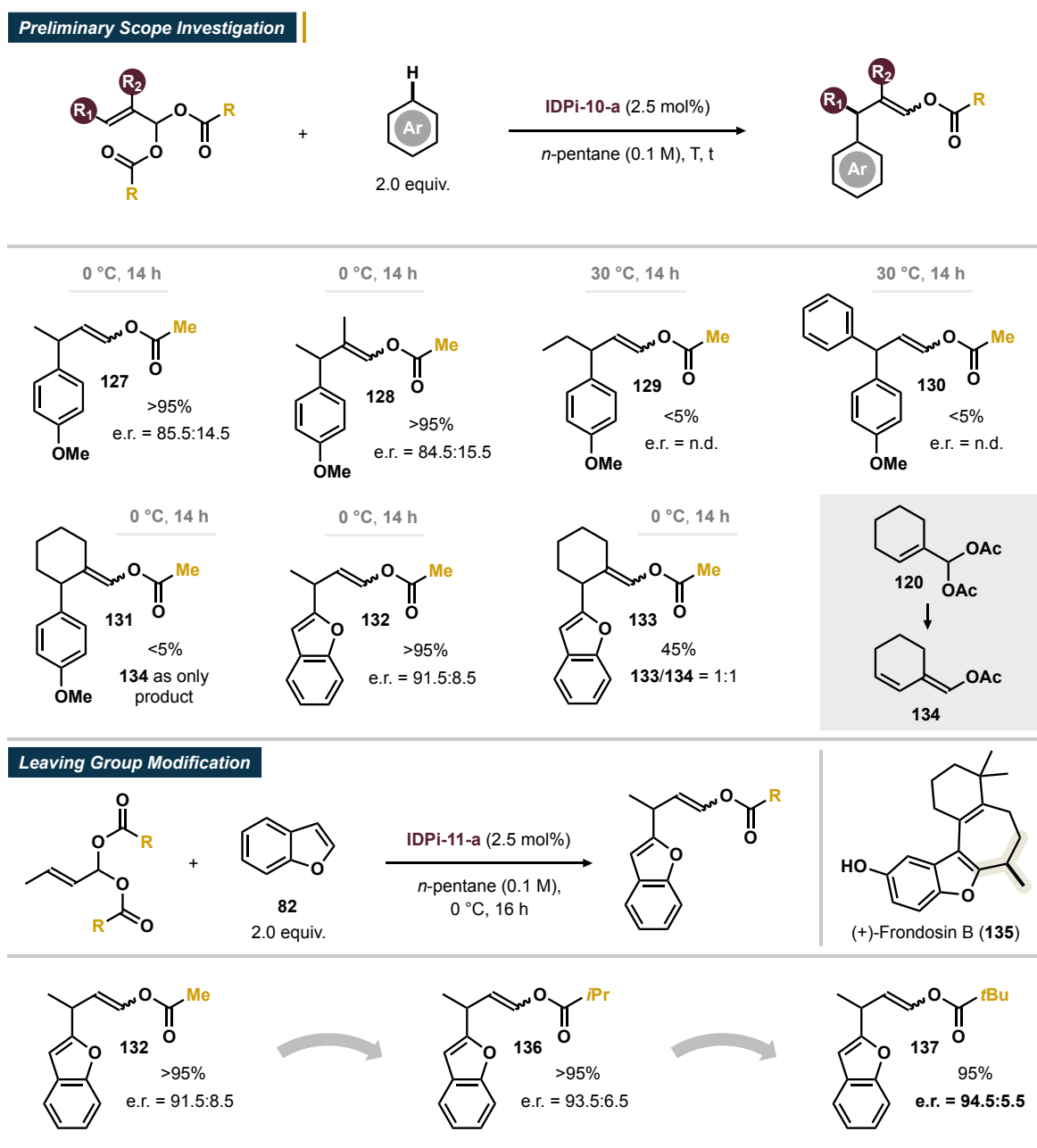
Scheme 4.22: Preliminary substrate scope and leaving group modification studies.

Crotonaldehyde- as well as tiglinaldehyde-derived diacetate **117** and **125** smoothly underwent Scriabine reaction with anisole to give the corresponding enol acetates **127** and **128** with excellent yields and good enantioselectivities. However, the (*E*)-2-pentenal-derived acylal **118** just like the cinnamaldehyde-derived acylal **119** were found to be entirely unreactive under the previously optimized reaction conditions. When cyclohex-1-ene-1-carbaldehyde-derived diacetate **120** was reacted with anisole under analogous reaction conditions, elimination toward dienol acetate **134** was observed as only reaction. To furthermore identify the potential scope of aromatic substrates, we went on to test benzofuran (**82**) in the system described above. In the reaction with crotonaldehyde-derived acylal **117**, excellent yield and high enantiomeric ratio on enol acetate **132** was obtained. The reaction profile was furthermore found to be especially clean with only traces of the *Z*-configured byproduct. Intriguingly, upon reaction with cyclic acylal **120**, the cyclic enol acetate **133** was formed in a 1:1 ratio with the undesired elimination side product **134**. We consequently speculate that the increased nucleophilicity of benzofuran **82** compared to anisole enables the competitive C–C bond formation to take place.

Enantioenriched 2-alkylated benzofuran derivates are relevant building blocks for total synthesis as exemplified in the synthesis of (+)-Frondosin B (**135**), a potent interleukin-8 receptor inhibitor, reported by MacMillan in 2010.[188] Inspired by the importance of benzofuran-derived scaffolds along with the increased selectivity observed for the reaction of **82**, we chose to further optimize the asymmetric Scriabine reaction of **82** with crotonaldehyde-derived acylals (scheme **4.22**).

To our delight, transition from the acetic anhydride derived acylal **117** to the corresponding isobutyric anhydride-derived reagent and, finally, to the pivalic anhydride derived acylal led to a successive improvement of the observed enantiomeric ratio from an initial 85.5:14.5 for **132** over 93.5:6.5 for **136** to finally reach the excellent level of 94.5:5.5 for **137** while simultaneously delivering the corresponding product with nearly quantitative yield. Despite the described improvement in the selectivity of the reaction, achieved through variation of the alkyl substituent of the leaving group, the investigated reaction was still suffering from significant scope limitations, especially regarding modification of the substituent in the β-position of the acylal. To overcome these limitations, we envisioned that installation of electron withdrawing substituents on the acyl groups might lead to improved leaving group properties and consequently increase the electrophilicity of the reagent (scheme **4.23**). We therefore engaged in the synthesis of trifluoroacetic anhydride- (**TFAA**) and trichloroacetic anhydride- (**TCAA**) derived acylals **138** and **139** based on the parent (*E*)-crotonaldehyde (**140**) structure. The obtained acylal reagents were found to be of unstable nature and prone to thermal

rearrangements, especially in the presence of Lewis acids. This behavior led to significant side reactions in the acid-catalyzed Scriabine reaction. When cinnamaldehyde (**141**) was transformed with TCAA, the corresponding acylal **142** was obtained as stable crystalline solid. Upon reaction of **142** with **IDPi-01-a** under the previously optimized conditions for the asymmetric Scriabine reaction, no sign of conversion toward the desired product **143** was observed for aromatic substrates of varying nucleophilicity. Based on preceding studies reported by Gandon, we speculate that the reduced electron density around the trichloro- or trifluoroacetate groups leads to reduced interactions thereof with the used acid catalysts and consequently decreases the degree of acylal activation.[184]
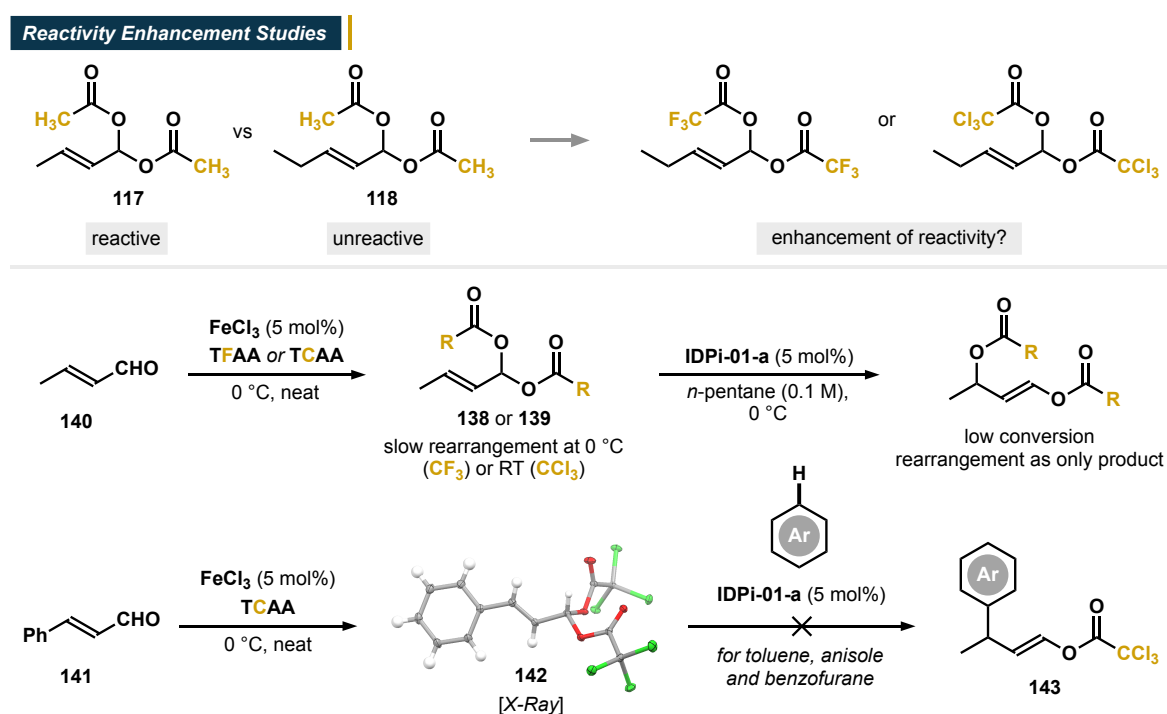
Scheme 4.23: Reactivity enhancement studies via installation of trihalogenated leaving groups.

To efficiently activate acylal reagents, we expect that sufficient Lewis basicity at the leaving groups is essential to enable coordination of the Lewis- or Brønsted acid catalyst and to therefore allow the reaction to proceed.

4.2.4 *in situ* Scriabine Reaction toward Increased Efficiency and Reactivity

The following studies were performed in collaboration with Samuel Steinfeld and Manuel Scharf.

As described above, installation of electron withdrawing substituents on the leaving groups of the acylal did not lead to the initially expected reactivity enhancement-effect and a broad substrate scope could not yet be established. Furthermore, an additional step for the synthesis of the acylal reagents reduces the overall step, time and atom efficiency for the functionalization of the enal substrates. The reaction is even complicated further by isomerization side reactions that occur during the formation of the acylal reagents (scheme **4.24**).

Based on these limitations along with the general capability of Lewis and Brønsted acid catalysts to promote acylal formation, we envisioned the previously unprecedented, direct activation of enal substrates with anhydrides using strong and confined Brønsted acid catalysts. Via activation of anhydrides, the acyl group is expected to be transferred to the enal substrate to form the corresponding *O*-acyloxocarbenium ions **XIII** which can then undergo the direct
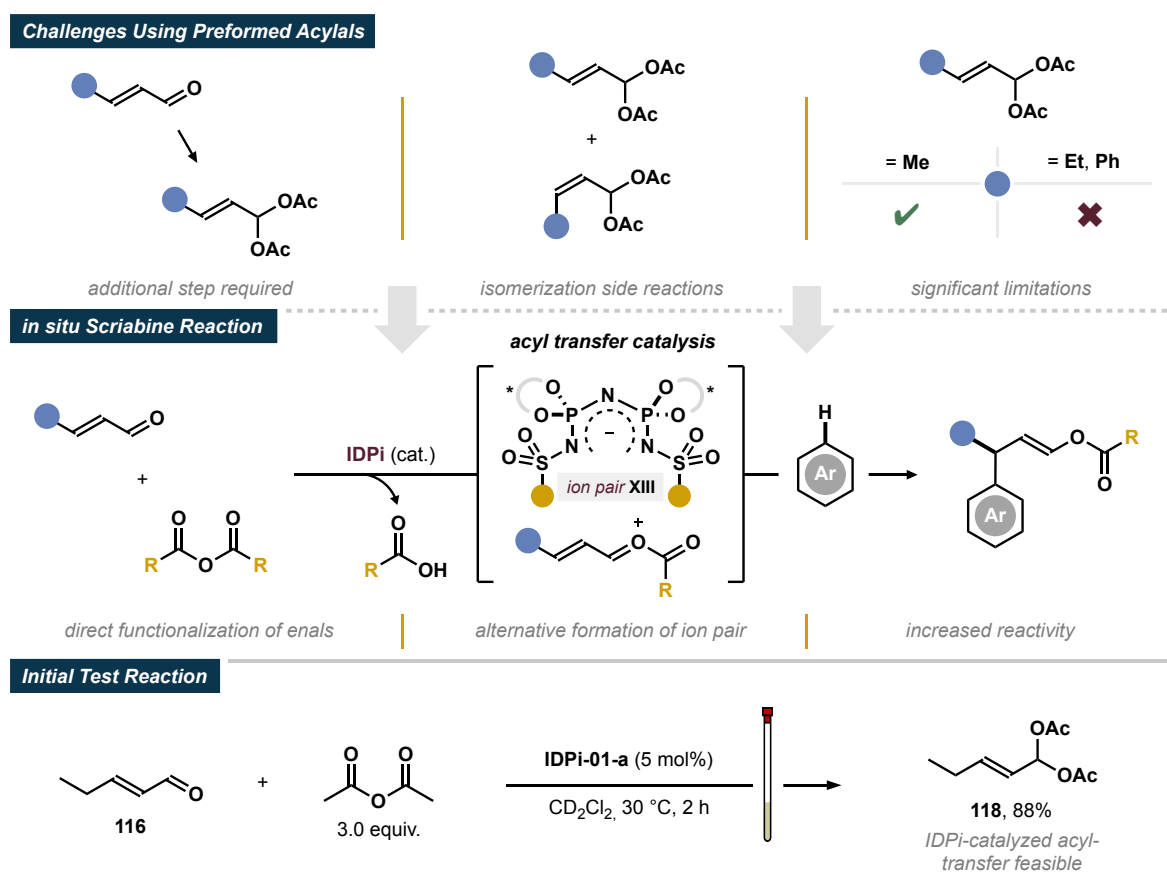
Scheme 4.24: Design and proof-of-concept studies for the *in situ* Scriabine reaction.

asymmetric Scriabine reaction via asymmetric counteranion directed attack of the aromatic substrate. Following this approach, the formation and activation of acylal reagents just like the challenges associated therewith might be circumvented completely to enable a more general as well as time and atom efficient reaction. To investigate the general feasibility of the IDPi-catalyzed anhydride transfer, we observed the reaction of (*E*)-2-pentenal (**116**) with acetic anhydride in the presence of **IDPi-01-a** via ^{1}H-NMR-spectroscopy. To our delight, almost full conversion of the parent enal **116** to its corresponding acylal **118** was observed within 2 hours. This experiment consequently serves as proof-of-concept that IDPi catalysts can indeed catalyze the synthesis of acylal reagents. We furthermore speculate that the formation of the geminal diacetate proceeds via stepwise acyl transfer to form the highly electrophilic ion pair **XIII** which is then attacked by the previously released acetic acid. If the ion pair **XIII** is of sufficient lifetime, the described approach might provide increased reactivity compared to the activation of preformed acylals and thus help to overcome the previously observed limitations of the reaction.

To investigate the potential of an *in situ* Scriabine reaction, we engaged in an initial screening of catalysts and conditions to evaluate the overall reactivity (scheme **4.25**). We could find that the direct activation of enals with anhydrides is generally feasible and the reaction of (*E*)-crotonaldehyde **140** with benzofuran **82** was found to give corresponding enol esters with high yields in the presence of simple alkyl-substituted anhydrides. As already observed in preceding studies (see scheme **4.23**), usage of trifluoroacetic anhydride proved to be unsuccessful in the reaction. The significantly reduced Lewis-basicity of TFAA is expected to hinder activation thereof via the used acid catalyst, which prevents a potential acyl transfer toward the formation of the desired product.

We quickly found that previously challenging substrates or generally problematic substitution patterns in the activation of acylals were now tolerated following the *in situ* Scriabine-approach. Not only could (*E*)-2-pentenal (**116**) be converted efficiently, also intrinsically more challenging substrates like dienal **144** or enones **145** and **146** were found to undergo the *in situ* Scriabine reaction with benzofuran in a regioselective fashion. Intriguingly, cinnamaldehyde (**141**) was still found to be reluctant toward arene addition and no sign of product formation was observed. The scope of applicable arenes was found to be less broad: while the heterocyclic arenes benzofuran (**82**), benzothiophene (**81**) and thiophene (**80**) smoothly underwent reaction toward corresponding enol acetates in the reaction with (*E*)-crotonaldehyde (**140**), phenol (**84**) just like the hydrocarbon arenes toluene (**3**), *o*-xylene (**61**), mesitylene (**65**) and 1,2-diethylbenzene (**62**) were unreactive under the described reaction conditions.
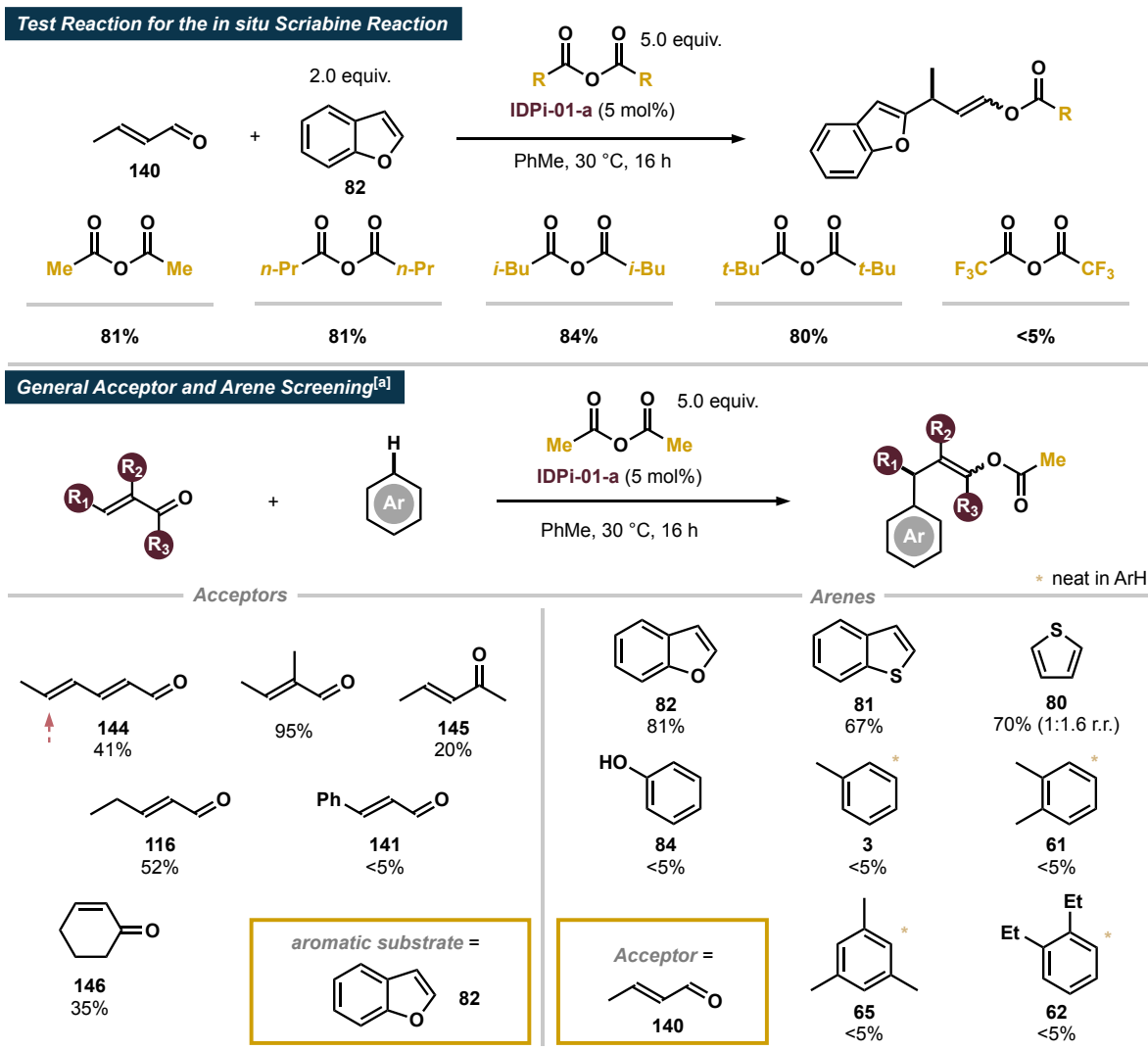
Scheme 4.25: Reactivity assessment for the *in situ* Scriabine reaction. [a] = determined via crude ^{1}H-NMR.

While the reactivity of the *in situ* Scriabine reaction is enhanced compared to the transformation of preformed acylals, we were curious to then compare the enantioselectivity of the novel system to our previous results. We therefore chose to investigate the addition of benzofuran (**82**) to (*E*)-crotonaldehyde (**140**) as benchmark reaction under the newly investigated reaction conditions. To evaluate the general reactivity and the potential breadth of applicable IDPi-catalysts, we initially engaged in a broader catalyst screening (table **4.12**). Similarly to our preceding studies (see table **4.4**), a complete shutdown of the reaction was observed upon installation of perfluorophenyl residues in the imidodiphosphorimidate core. Also catalysts bearing unfunctionalized aryl substituents in the 3,3'-positions of the BINOL backbone proved to be unsuccessful in the investigated transformation (entries 1-4). Usage of **IDPi-10-a**, the optimal catalyst for the activation of acylals, bearing a 3,5-bis(perfluoro-*n*-propyl)phenyl

substituent and a triflyl modification in the imidodiphosphorimidate core, restored the reactivity but the enantiomeric ratio of enol pivalate **147** was found to be significantly reduced.

Table 4.12: Catalyst screening for the *in situ* Scriabine reaction. [a] = crude NMR yield.

entry	catalyst	yield[a]	e.r.	entry	catalyst	yield[a]	e.r.
1	IDPi-02-a	<5%	n.d.	12	IDPi-14-b	38%	82:18
2	IDPi-02-b	<5%	n.d.	13	IDPi-15-b	40%	89:11
3	IDPi-03-b	<5%	n.d.	14	IDPi-16-b	46%	84:16
4	IDPi-05-b	<5%	n.d.	15	IDPi-17-b	<5%	n.d.
5	IDPi-10-a	78%	76:24	16	IDPi-18-b	70%	88:12
6	IDPi-09-b	65%	87:13	17	IDPi-19-b	87%	87:13
7	IDPi-09-c	40%	67:33	18	IDPi-20-b	51%	77:23
8	IDPi-09-e	55%	70:30	19	IDPi-21-b	55%	70:30
9	IDPi-09-h	68%	85:15	20	IDPi-22-b	<5%	n.d.
10	IDPi-09-i	49%	86.5:13.5	21	IDPi-23-a	30%	60:40
11	IDPi-09-j	<5%	n.d.	22	IDPi-24-a	15%	71:29

Intriguingly, installation of a 2-benzofuran substituent in the 3,3'-positions of the BINOL and of a perfluorophenyl group in the catalyst core afforded the desired enol pivalate **147** with high yield and increased enantioenrichment (entry 6).

This datapoint stands out even more considering that **IDPi-09-b** is unreactive in the initially investigated activation of acylal **117** (see table **4.10**). Motivated by this result, we engaged in a more detailed screening of benzofuran-substituted IDPi-catalysts, prepared earlier in our laboratory for investigations on asymmetric Pictet-Spengler reactions.[144] We quickly found that perfluoroaryl core substituents lead to an improvement on the observed enantiomeric ratio while installation of perfluoroalkyl residues reduce both yield and the enantiomeric ratio on enol pivalate **147**. Installation of a methyl group in different positions of the benzofuran backbone led to an intriguing finding: while introduction in the 5- (**IDPi-14-b**) or the 7-position (**IDPi-16-b**) resulted in both decreased yield and enantioselectivity, introduction of the methyl group in the 6-position increased the enantiomeric ratio to 89:11. Introduction of bulkier groups in the 6-position of the benzofuran substituent was found to be detrimental to the selectivity of the reaction (entries 20-21). While installation of a methyl group in the 6-position of the benzofury-substituent of the used catalyst decreased yield and selectivity on **147**, usage of **IDPi-18-b** or **IDPi-19-b**, bearing a trifluoromethyl- or a pentafluorophenyl group in the 6-position, gave slightly increased enantiomeric ratio and visibly increased yield. Furthermore, when a structurally related 5-phenyl furan substituent was installed on the 3,3'-positions of the BINOL, no formation of the product was detected using the corresponding IDPi (entry 20).

4.2.5 Benzofuran-Derived IDPi-Catalysts for *in situ* Scriabine Reactions

The following studies were performed in collaboration with Samuel Steinfeld, Manuel Scharf, Wencke Leinung, Benjamin Mitschke and Lennard Brücher.

Based on the abovementioned studies as well as preceding work in our research group, we could identify the 2-benzofuran motif in the 3,3'-positions of the BINOL along with a pentafluorophenyl core motif to be a privileged catalyst structure for the investigated reaction (scheme **4.26**).[144] Additionally, introduction of a methyl group as a substituent of moderate size in the 6-position of the benzofuran was found to lead to further improvement of the enantiomeric ratio. While installation of a methyl group in the 5-position of the benzofuran led to decreased yield and selectivity, transition to a trifluoromethyl group increased both yield and enantiomeric ratio visibly.
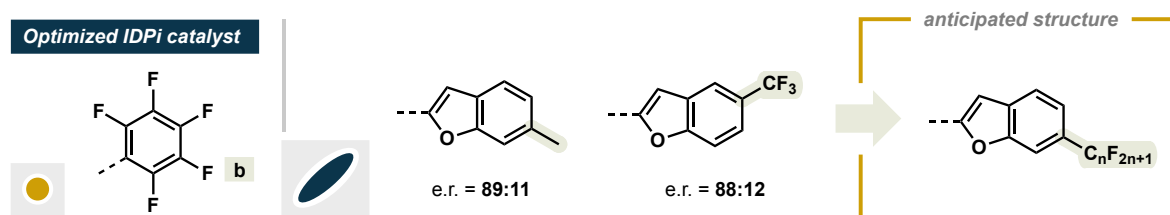
Scheme 4.26: Expected structure of improved IDPi-catalysts.

We consequently envisioned that installation of a perfluoroalkyl group in the 6-position of the benzofuran might lead to a superior catalyst motif through the combination of both, the benefits of the careful introduction of steric bias and a concomitant finetuning of the electronic properties of the IDPi. Consequently, both superior yield and enantiomeric ratio on enol pivalate products might be achievable. In order to gain access to the required benzofuran-substituted IDPis, the synthesis of the catalysts was achieved as described below (Scheme **4.27**).
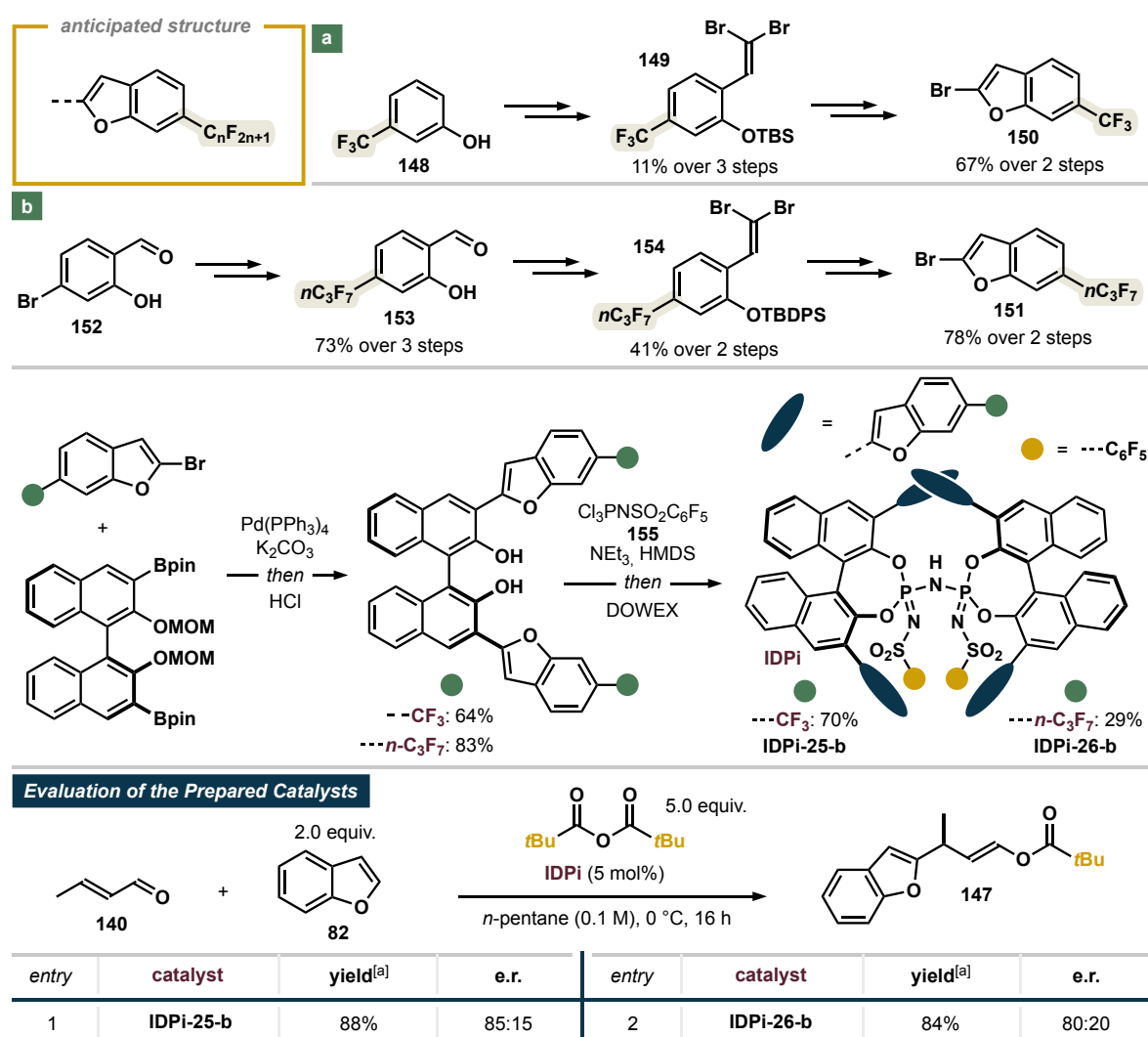
Scheme 4.27: Synthesis of perfluoroalkyl-substituted benzofuran-containing IDPi-catalysts.

4. Results and Discussion

Following preceding studies performed in our laboratories, the 6-trifluoromethylated building block was obtained starting from 3-trifluoromethylphenole (**148**), which was transformed to dibromide **149** and finally, in two further steps, to 2-bromo-6-(trifluoromethyl)benzofuran (**150**). To obtain the perfluoropropylated equivalent **151**, 4-bromosalicylaldehyde (**152**) was transformed to 2-hydroxy-4-(perfluoropropyl)benzaldehyde (**153**) in three steps via Ullmann-coupling sequence. Aldehyde **153** was then transformed to dibromoolefin **154** which could subsequently be cyclized to afford 2-bromobenzofuran **151**. The obtained perfluoroalkylated building blocks **150** and **151** were then introduced into the BINOL backbone via Suzuki-Miyaura coupling to yield the 3,3'-substituted BINOLs. Finally, dimerization of the respective BINOL-building blocks in the presence of HMDS and the pentafluorophenyl-substituted phosphazene reagent **155** gave rise to the desired IDPi-catalysts after acidification over an ion exchange resin. To test the IDPi-catalysts thus prepared, they were subjected to the reaction of (*E*)-crotonaldehyde (**140**) with benzofurane (**82**) (scheme **4.27**). As shown below, both catalysts provided high reactivity, the enantiomeric ratio of enol pivalate **147** was however reduced compared to the results obtained with the previous benchmark catalysts **IDPi-15-b** and **IDPi-18-b**. We therefore chose to use **IDPi-15-b** for the following studies. To further increase the enantioselectivity in the *in situ* Scriabine reaction, we chose to reevaluate the used solvent and to additionally investigate the performance of previously overlooked catalyst motifs.

When chlorinated solvents were used in the *in situ* Scriabine reaction of **140** with **82** as described below, significantly reduced yields on enol pivalate **147** were observed (table **4.13**).

Table 4.13: Solvent screening for the *in situ* Scriabine reaction. [a] = crude NMR yield.

entry	solvent	yield[a]	e.r.	entry	solvent	yield[a]	e.r.
1	CHCl₃ (0.1 M)	16%	78:22	6	CyMe (0.1M)	60%	88:12
2	CH₂Cl₂ (0.1 M)	10%	76:24	7	CypMe (0.1M)	63%	87.5:12.5
3	PhMe (0.1 M)	35%	80:20	8	*n*-pentane (0.1 M)	72%	85.5:14.5
4	Et₂O (0.1M)	51%	83:17	9	*n*-hexane (0.1 M)	57%	87:13
5	CyH (0.1M)	62%	88:12	10	*n*-heptane (0.1 M)	**60%**	**88.5:11.5**

However, when less polar solvents were used, a concomitant increase in yield and enantioselectivity of **147** was obtained (entries 3-5). When various aliphatic hydrocarbon solvents were investigated, *n*-heptane was finally identified as optimal solvent for the reaction. As discussed in our preceding studies on the Scriabine reaction of preformed acylals (see scheme **4.22**), we found that the structure of the acylal moiety is of crucial importance for the enantioselectivity of the reaction. To perform analogous studies on the *in situ* Scriabine reaction, we therefore investigated the influence of the different anhydrides as activating agents under our newly developed reaction conditions (table **4.14**).

Table 4.14: Screening of different anhydride activating agents. [a] = crude NMR yield.

entry	anhydride/equiv.	yield[a]	e.r.	entry	anhydride/equiv.	yield[a]	e.r.
1	Piv$_2$O (2.0 equiv.)	56%	86.5:13.5	3	Piv$_2$O (4.0 equiv.)	68%	86.5:13.5
2	Piv$_2$O (3.0 equiv.)	58%	86.5:13.5	4	Piv$_2$O (5.0 equiv.)	62%	88:12

As shown above, the usage of butyric anhydride (**156**) just like isovaleric anhydride (**157**) led to visibly reduced yield and enantiomeric ratio on the corresponding product which was even undercut when benzoic anhydride was used. Application of the cyclic reagents glutaric anhydride **158** and diglycolic anhydride **159** in both cases led to no visible product formation. Pivalic anhydride (**160**) was consequently found to be the optimal reagent with regard to the yield, the generality and the enantioselectivity of the reaction. Pivalic anhydride furthermore is a non-toxic and inexpensive reagent of no significant odor (unlike many other small aliphatic anhydrides), which contributes to the general practicability of the transformation.

To further optimize the reaction conditions, we then investigated the optimal stoichiometries in the reaction with respect to the applied anhydride activating agent. As described above, no gain in enantiomeric ratio is obtained upon reduction of the amount of pivalic anhydride added, the yield of the reaction however was found to drop while the rate of occurring side reactions

increased. We therefore conclude that the addition of 5 equivalents of pivalic anhydride represents the optimal amount of the activating agent.

With these optimized conditions at hand, we then reinvestigated a broader scope of benzofuran- and benzothiophene-substituted IDPi-catalysts with polyaromatic ring systems to further improve the observed selectivity (table **4.15**).

Table 4.15: Further screening of furan- and thiophene-based catalysts. [a] = crude NMR yield.

entry	catalyst	yield[a]	e.r.	entry	catalyst	yield[a]	e.r.
1	**IDPi-27-b**	50%	83.5:16.5	7	**IDPi-33-b**	85%	86:14
2	**IDPi-28-b**	**82%**	**91:9**	8	**IDPi-33-b$_F$**	>95%	80:20
3	**IDPi-29-b**	68%	90:10	9	**IDPi-34-b**	<5%	n.d.
4	**IDPi-30-b**	39%	79:21	10	**IDPi-35-b$_F$**	81%	77:23
5	**IDPi-31-b**	21%	92.5:7.5	11	**IDPi-36-b$_F$**	75%	81:19
6	**IDPi-32-b**	50%	90:10	12	**IDPi-37-b$_F$**	74%	84:16

To test a broader scope of catalyst structures, the influence of additionally installed perfluoroisopropyl-groups on the 6,6'-positions of the BINOL backbone was studied. Transition from a benzofuran- to a benzothiophene motif was found to only have a minor effect and slightly reduced yield and enantiomeric ratio on the corresponding product **147** was obtained. Usage of **IDPi-28-b** bearing a monochlorinated benzofurane wing led to a significant increase in yield and simultaneously provided the highest enantiomeric ratio on **147** observed thus far

(entry 2). The naphthofuran-system present in **IDPi-29-b** additionally proved to be a highly selective motive as a similarly high enantioenrichment for enol pivalate **147** could be determined (entry 3). While the introduction of another aryl substituent on the naphthofuran-structure, as demonstrated for **IDPi-30-b**, did not lead to any further improvement (entry 4), the use of the 5-methylated analogue gave a slight increase in the enantiomeric ratio at the expanse of the yield of the reaction along with the general chemoselectivity. As a third privileged catalyst structure, thienothiophene-based catalyst **IDPi-32-b** could be identified to be of suitable nature for the investigated reaction as a similarly high enantiomeric ratio was observed for **147** which was obtained with slightly decreased yield (entry 6). Further modification toward a more diverse scope of thiophene-derived 3,3'-substituents was unsuccessful as installation of phenanthrothiophene- (**IDPi-34-b**) or benzodithiophene-substituents (**IDPi-36-b$_F$** and **IDPi-37-b$_F$**) all led to reduced enantiomeric ratios on the corresponding enol pivalate **147**.

Introduction of perfluoroisopropyl substituents in the BINOL's 6,6'-positions was generally found to be detrimental to the enantioselectivity of the reaction while, corresponding to the increased acidity of the catalyst, affording **147** with increased yield. Because of their impact on the reaction, we chose to refrain from the installation of electron withdrawing substituents on the BINOL-backbone of IDPi catalysts for further investigations.

As described above, three privileged catalyst motifs could be identified in the preceding screening which all provided **147** with high yield and enantiomeric excess: the 5-chloro-6-methylbenzofuran structure -**28**, the naphthofuran scaffold -**29** as well as the thienothiophene-based motif -**32**. As the 5-chloro-6-methylbenzofuran-bearing catalyst delivered enol pivalate **147** with both the highest yield as well as enantiomeric ratio observed thus far, the performance of the catalyst was now tested at reduced temperatures of 0 °C and –20 °C for further improvement of the enantiomeric ratio of the reaction (scheme **4.28**). While a significant improvement of the yield and the enantiomeric ratio was observed upon lowering of the temperature to 0 °C, the inverse effect was found at a further decreased temperature of –20 °C. We therefore conclude that 0 °C is the optimal temperature for the reaction to proceed.
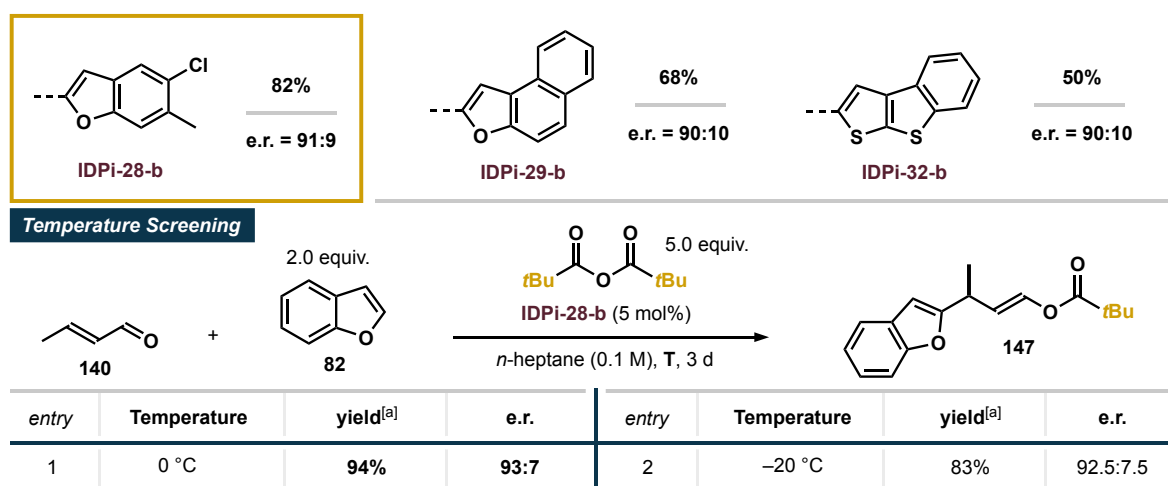
Scheme 4.28: Investigations with **IDPi-28-b** at reduced temperatures.

As shown, we were able to improve the conditions for the asymmetric *in situ* Scriabine reaction of benzofuran (**82**) with (*E*)-crotonaldehyde (**140**) to yield the corresponding product **147** with high yield and enantiomeric ratio. To test the generality of the transformation, we chose to apply the optimized conditions to the reaction of benzothiophene (**81**) and anisole (**26**) with **140** as additional benchmark substrates (scheme **4.29**).
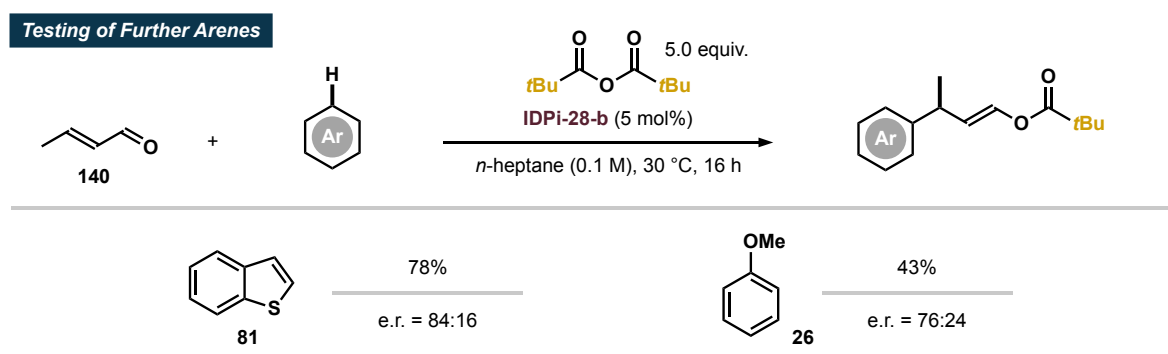
Scheme 4.29: Reactions of alternative arenes.

While the usage of benzothiophene (**81**) gave good yield along with slightly reduced enantiomeric enrichment on the corresponding enol pivalate, the application of anisole (**26**) led to both significantly reduced yield and enantioselectivity on the corresponding Scriabine adduct under analogous conditions.

While good results were already obtained for some *O*- and *S*-containing heterocyclic arenes, further reaction and catalyst optimization is required to enable the general *in situ* Scriabine

reaction of simple alkoxybenzenes or even alkylbenzenes with high selectivity. Investigations on further improvement of the catalytic system are currently ongoing in our laboratory.

5. Summary

The nucleophilicity of aromatic substrates has always been a limiting factor for electrophilic aromatic substitution reactions and unactivated hydrocarbon arenes have required especially harsh reaction conditions to enable their S_EAr reactions. High temperatures and strongly Lewis acidic catalysts have simultaneously complicated the development of asymmetric catalytic Friedel–Crafts reactions of simple alkylbenzenes. In this work, we present the usage of highly acidic and confined IDPi-catalysts to enable the unprecedented asymmetric Friedel–Crafts reaction of only-hydrocarbon alkylbenzenes toward arylglycine esters (scheme **5.1**).
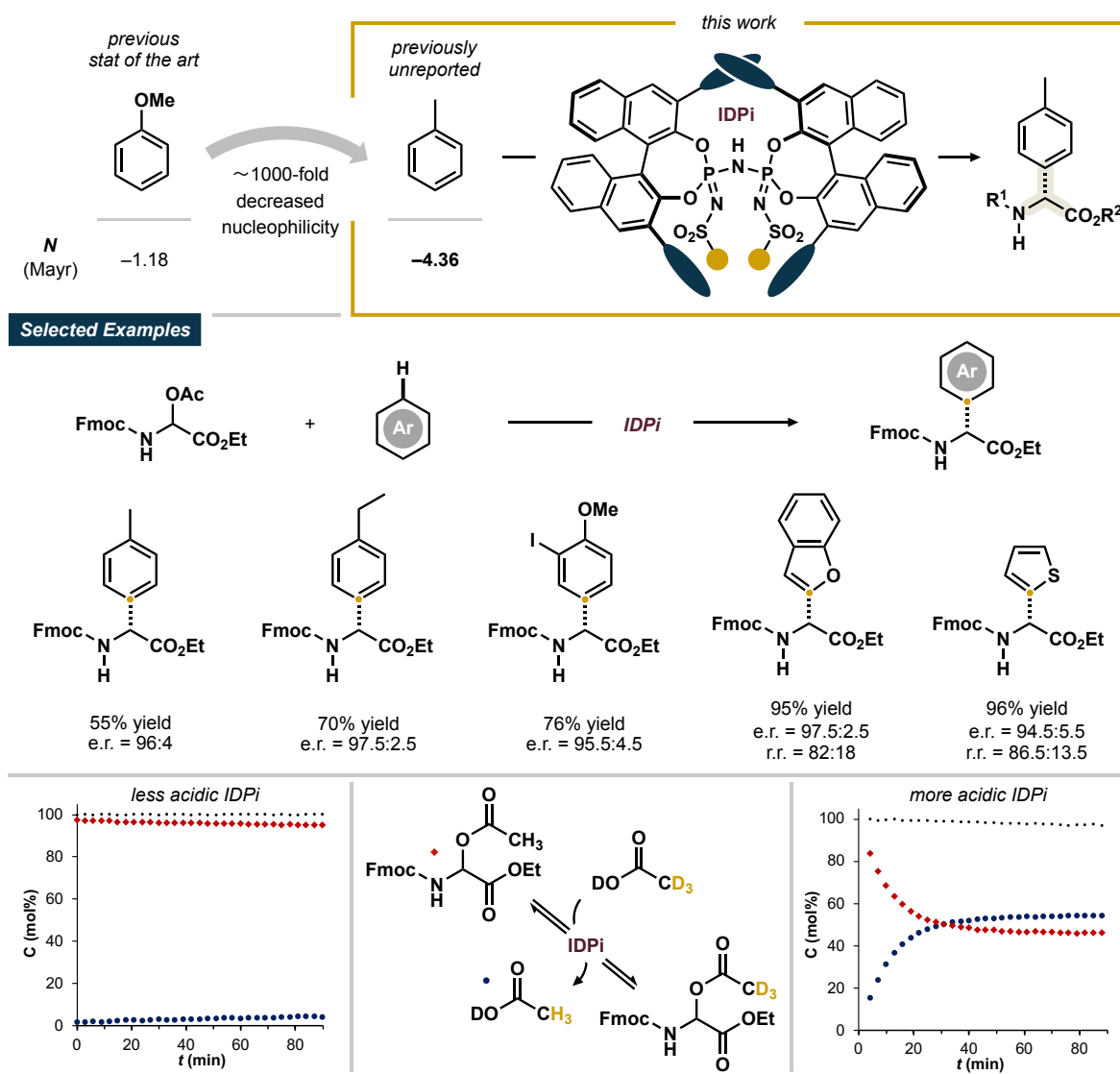
Scheme 5.1: Asymmetric Friedel–Crafts reaction of unactivated arenes toward Arylglycines.

A thorough catalyst screening was performed to identify IDPi-catalysts with sufficient reactivity and durability to allow the proceeding of the reaction under mild reaction conditions. Besides high regio- and stereoselectivities, the discovered reactivity extended to the chemoselective transformation of acid-labile substrates such as cyclopropylbenzene (**60**), which remained intact over the course of the reaction. Slight modifications of the reaction conditions allowed the enantioselective transformation of more functionalized alkoxybenzenes and heteroaromatic substrates.

Intrigued by the high reactivity provided by IDPi catalysts with electron-withdrawing substituents on the 3,3'-positions of the BINOL, we then engaged in the development of experimental tools for the elucidation of the reaction mechanism. Leaving group scrambling experiments were initially performed with isotope labeled reagents to reveal that the reversible formation of iminium ions is significantly decelerated using less acidic IDPi catalysts. This indicates that the insufficient activation of *N,O*-acetals toward corresponding ion pairs limits the scope of applicable catalysts to highly acidic species.

The addition of benzenoids to enals enables the synthesis of 3-arylpropanes, a recurring motif in aroma- and fragrance molecules. However, the direct addition of unreactive arenes to enals toward this highly demanded class of compounds requires exceptionally harsh reaction conditions. Studies by Scriabine already showed that the preceding transformation of enals to corresponding acylals leads to a significant reactivity enhancement effect of the acceptor molecule. The Scriabine reaction has since proven to be a useful tool, but asymmetric versions thereof remained elusive. To contribute an asymmetric organocatalytic Scriabine reaction, we studied the potential activation of acylal reagents with highly acidic IDPi catalysts. Even though a number of aromatic substrates engaged in the asymmetric Scriabine reaction with excellent yield and enantio as well as regioselectivity, the reaction was generally limited to a narrow choice of acylal reagents (scheme **5.2**).
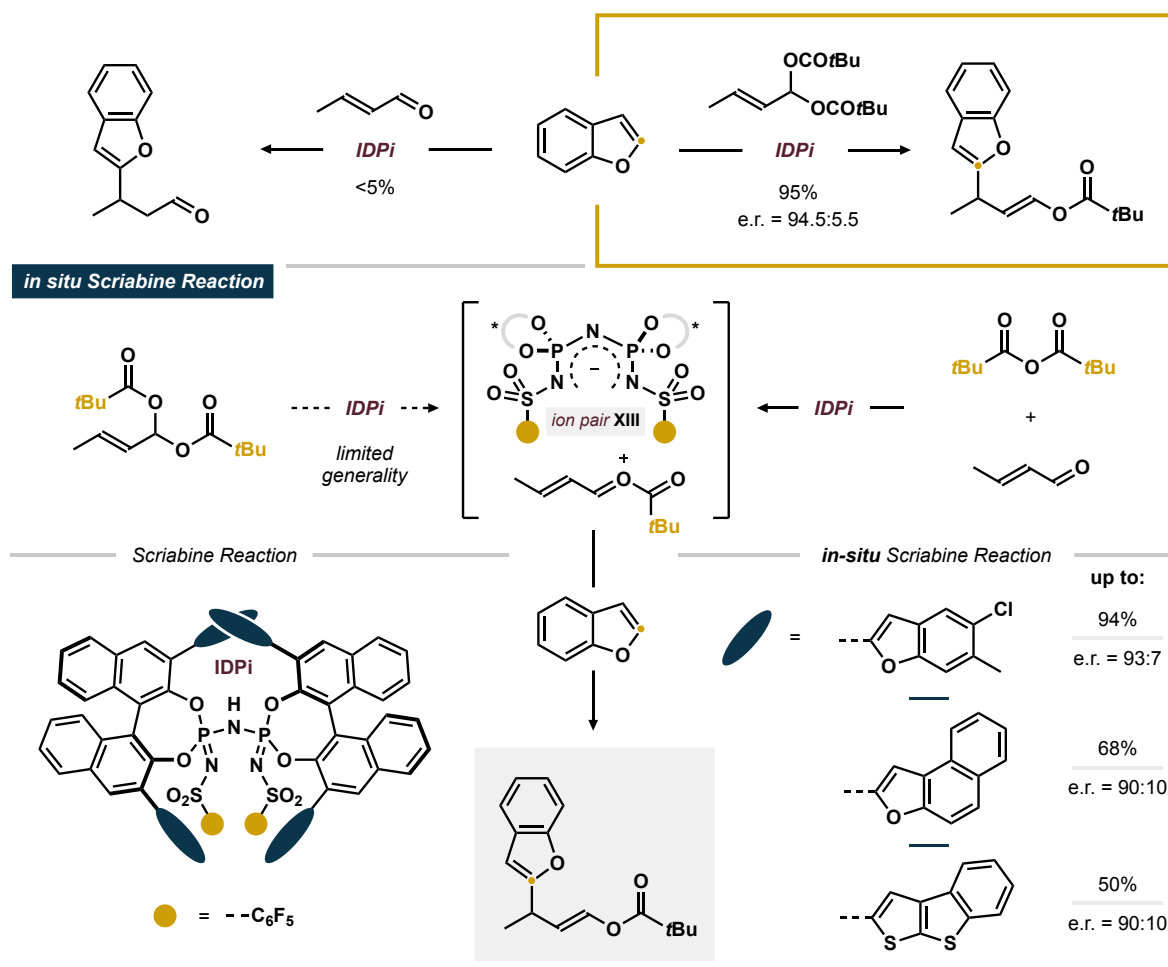
Scheme 5.2: Asymmetric Organocatalytic Scriabine reaction.

Spurred on by this apparent limitation and to avoid the cumbersome transformation of enal reagents to the more activated acylals, we envisioned the direct activation of enals via *in situ* acid-catalyzed acyl transfer to form highly reactive *O*-acyloxocarbenium ion pairs **XIII** and therefore allow the addition of aromatic substrates. The resulting, unprecedented *in situ* Scriabine reaction allowed for the direct addition of a wider range of arenes to a variety of enals and enones in the presence of alkyl anhydrides as activating agents. While the increase in reactivity and generality observed for the *in situ* approach came at the expanse of enantioselectivity, we found a broader scope of IDPi-catalysts to be applicable in the reaction which opened up more possibilities for reaction optimization. Especially 2-benzofuran substituted catalysts, unreactive in the activation of acylal reagents, were now found to give the corresponding acyl enolates with high yields and enantiomeric ratios. Further optimization revealed three different privileged catalysts to afford the corresponding Friedel–Crafts adducts with high yield and enantiomeric ratios.

6. Outlook

6.1 Asymmetric Friedel–Crafts Reaction Toward Arylglycine Esters

Our work on the addition of unactivated arenes to *N*-acyliminium ions has enabled the synthesis of arylglycines with high enantio- and regioselectivities. Despite the predisposition for one of the possible C–H bonds of the aromatic substrate, the regioselectivity of the reaction usually follows substrate-inherent directing effects and overriding the regiochemical outcome of Friedel–Crafts reactions has proven to be a particularly challenging task (scheme **6.1**).[189]
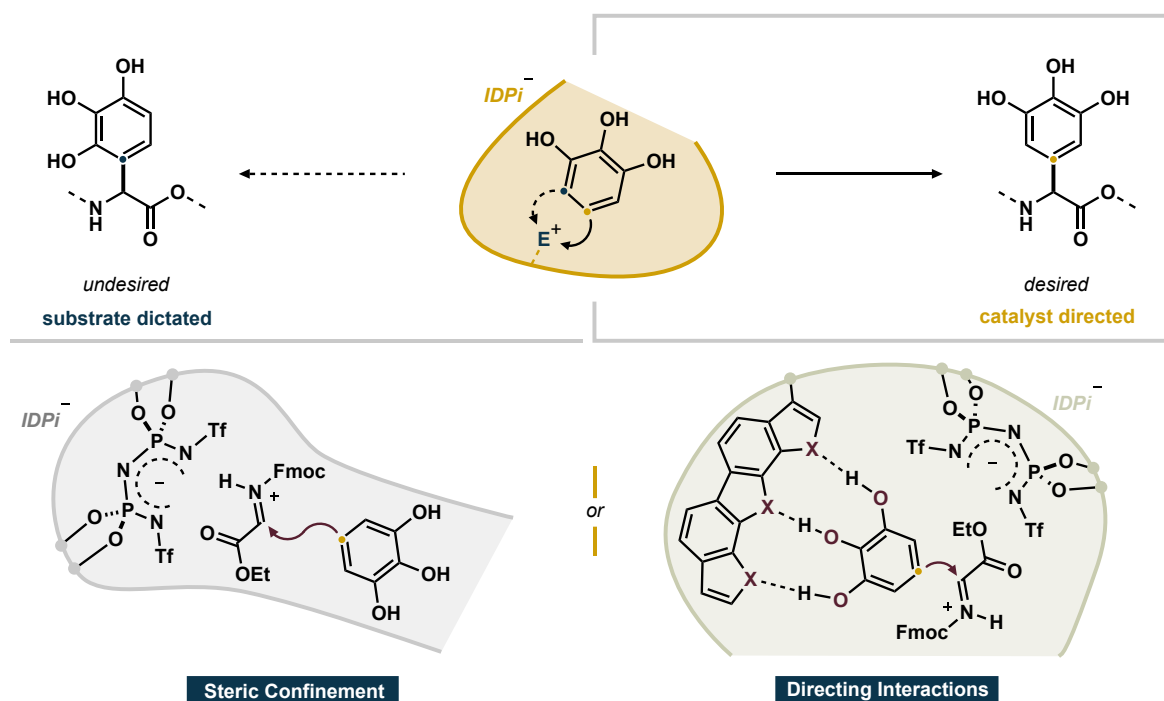
Scheme 6.1: Catalyst controlled regioselective Friedel–Crafts reaction.

As demonstrated by our studies on the synthesis of the arylglycine building blocks of Vancomycin, this approach could enable a particularly efficient synthesis of highly sought-after building blocks. To achieve the regiocontrolled Friedel–Crafts reaction, even more confined, tailor-made catalysts might be used to mimic an enzyme-like microenvironment. Driven by steric bias, this could allow to selectively address intrinsically less activated positions on the aromatic ring. Alternatively, the installation of hydrogen bond donors on the BINOL backbone of the IDPi catalyst might allow to lock the triphenol substrate in a position that supports its regiocontrolled addition to the imidodiphosphorimidate-bound iminium ion.

6.2 Asymmetric Scriabine Reaction

The activation of enals and enones via acyl transfer toward the putative formation of
O-acyloxocarbenium ions allows the selective functionalization of simple acceptor molecules
using cheap and non-toxic alkyl anhydrides. Thus far, however, the proposed
O-acyloxocarbenium ions have not yet been identified analytically which obscures the actual
mode of action as well as the individual mechanistic steps. To elucidate the ongoing reaction
mechanism for potential further improvement of the reaction system, spectroscopic experiments
might be carried out. Among others, KIE experiments might be valuable tools for further
mechanistic studies.

The activation of enals and enones via Brønsted acid-catalyzed acyl transfer has enabled the
addition of otherwise unreactive arenes. Against this background, the addition of other
nucleophiles might be possible to enable the synthesis of a diverse scope of functionalized enol
esters, versatile and stable aldehyde- and ketone surrogates.[190] Olefins or heteroatom-based
nucleophiles might consequently be used as reaction partners with *in situ* generated
O-acyloxocarbenium ions toward β-functionalized products (scheme **6.2**).
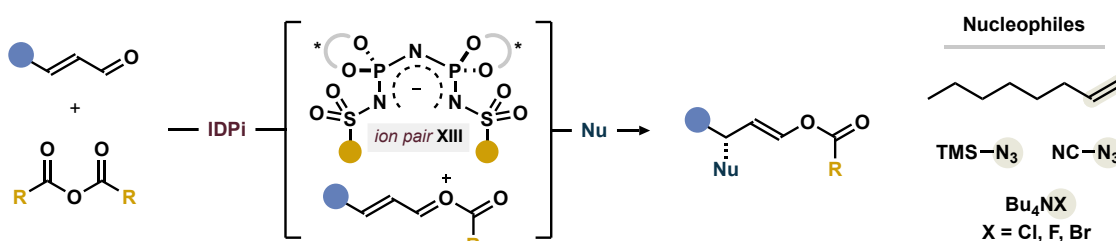
Scheme 6.2: Different nucleophiles for the proposed addition to *O*-acyloxocarbenium ions.

The structure of α,β-unsaturated acylals might also allow the asymmetric transformation thereof
in the absence of an external nucleophile via acid-catalyzed rearrangement toward the acyloxy
enol ester. The same reactivity might consequently be achieved via asymmetric addition of alkyl
anhydrides to enals or enones to yield the disproportionated product which releases the
β-hydroxyaldehydes upon hydrolysis (scheme **6.3**). Following this approach, an alternative
method to reported oxa-Michael procedures could be developed that proceeds under mild
reaction conditions and provides high chemoselectivity. The absence of the toxic reagents or
stoichiometric oxidants usually required in previously reported methods for the asymmetric β-
hydroxylation of enals represents a further benefit of the proposed transformation.[191,192]
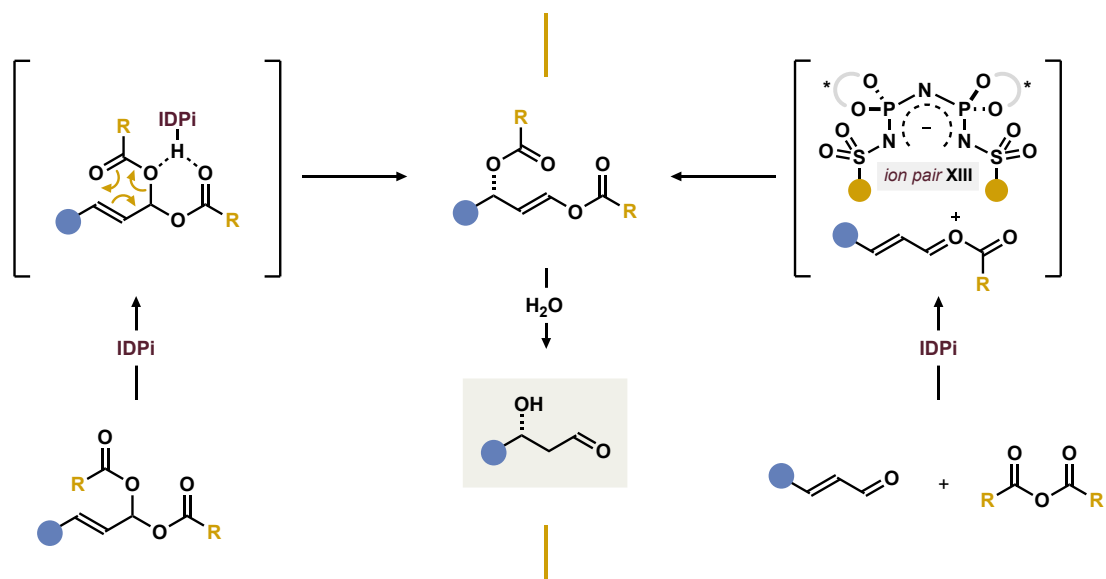
Scheme 6.3: Proposed transformation of acylals and enals to β-hydroxyaldehydes.

7. Experimental Section

Materials and Methods

Chemicals: Unless otherwise indicated, starting materials were obtained from Sigma-Aldrich, ABCR-GmbH, TCI, Acros Co. Ltd., Fluorochem or Deutero GmbH. Commercially available substances were used without further purification.

Solvents: Solvents (Et$_2$O, THF, 1,4-Dioxane, Cyclohexane, CH$_2$Cl$_2$, CHCl$_3$, PhH and PhMe) were dried by distillation from appropriate drying agents in the technical department of the Max-Planck-Institut für Kohlenforschung and obtained in Schlenk flasks under argon atmosphere. Further solvents (CyMe, o-xylene, *n*-hexanes) were obtained from commercial suppliers and stored under an atmosphere of argon in a Schlenk tube.

Inert Gas: Anhydrous argon was purchased from Air Liquide with >99.5% purity.

Thin Layer Chromatography: Thin layer chromatography (TLC) was performed using silica gel pre-coated plastic sheets (Polygram SIL G/UV254, 0.2 mm, with fluorescent indicator; Macherey-Nagel) which was visualized with a UV lamp (254 nm) and/or phosphomolybdic acid (PMA), and/or Cerium Ammonium Molybdate (CAM), and/or ninhydrin. PMA stain: PMA (20 g) in EtOH (200 mL). CAM stain: Ammonium molybdate tetrahydrate (2.5 g), Cerium ammonium sulfate dihydrate (1 g) and Sulfuric acid (10 mL) in Water (90 mL). Ninhydrin stain: ninhydrin (1.5 g) in EtOH (200 mL) with AcOH (3 mL).

Column Chromatography: Column chromatography was carried out using Merck silica gel (60 Å, 230−400 mesh, particle size 0.040−0.063 mm) using technical grade solvents. Elution was accelerated using compressed air. All reported yields, unless otherwise specified, refer to spectroscopically and chromatographically pure compounds.

Nomenclature: Nomenclature follows the suggestions proposed by the computer program ChemBioDraw (12.0.3.1216) of CBD/Cambridgesoft.

Nuclear Magnetic Resonance Spectroscopy: ^{1}H, ^{13}C, ^{19}F, ^{31}P Nuclear magnetic resonance (NMR) spectra for compound characterization were recorded on a Bruker Avance III 500 or a

Bruker Avance Neo 600 MHz NMR spectrometer in a suitable deuterated solvent unless specified otherwise. The solvent employed and the respective measuring frequency are indicated for each experiment. Chemical shifts are reported with tetramethylsilane (TMS) serving as a universal reference of all nuclides. The resonance multiplicity is described as s (singlet), d (doublet), t (triplet), q (quadruplet), p (pentet), h (heptet), m (multiplet), and br (broad). All spectra were recorded at 298 K unless specified differently, processed with MestReNova 14.1.2 suits of program, and coupling constants are reported as observed. The residual deuterated solvent signal relative to tetramethylsilane was used as the internal reference in ^{1}H NMR spectra (e.g. $CDCl_3$ = 7.26 ppm, CD_2Cl_2 = 5.32 ppm). Signals are reported as follows: chemical shift δ in ppm (multiplicity, coupling constant J in Hz, number of protons). All X-nuclei spectra were acquired proton decoupled unless otherwise noted. $^{13}C\{^1H, \,^{19}F\}$ NMR spectra were acquired with a Bruker TBO probe (^{1}H, ^{19}F, BB) with inverse gated decoupling. For ^{1}H waltz16 was used for decoupling. For ^{19}F the decoupling scheme bi_p5m4sp_4sp.2 with adiabatic chirp pulses with an offset at -105 ppm was used to ensure the broadband decoupling on ^{19}F.

Mass Spectrometry: Electrospray ionization (ESI) mass spectrometry was conducted on a Bruker ESQ 3000 spectrometer. High resolution mass spectrometry (HRMS) was performed on a Finnigan MAT 95 (EI) or Bruker APEX III FTMS (7 T magnet, ESI). The ionization method and mode of detection employed is indicated for the respective experiment and all masses are reported in atomic units per elementary charge (m/z) with an intensity normalized to the most intense peak.

Specific Rotations: Specific rotations (α_D^T) were measured with a Rudolph RA Autopol IV automatic polarimeter at the indicated temperature with a sodium lamp (sodium D line, λ = 589 nm). Measurements were performed in an acid resistant 1 mL cell (50 mm length) with concentrations (g/(100 mL)) reported in the corresponding solvent.

High Performance Liquid Chromatography: High performance liquid chromatography (HPLC) was performed on a Shimadzu LC-20AD liquid chromatograph SIL-20AC auto sampler, CMB-20A using Daicel/Merck columns with a chiral stationary phase. All solvents used were HPLC-grade solvents purchased from Sigma-Aldrich. The column employed and the respective solvent mixture are indicated for each experiment.

7.1 Asymmetric Catalytic Synthesis of Arylglycine Esters

7.1.1 Synthesis of Substrates and Reagents

Synthesis of N,O-Acetals

<u>**General Procedure A (GP A):**</u> **Synthesis of Hemiaminals**
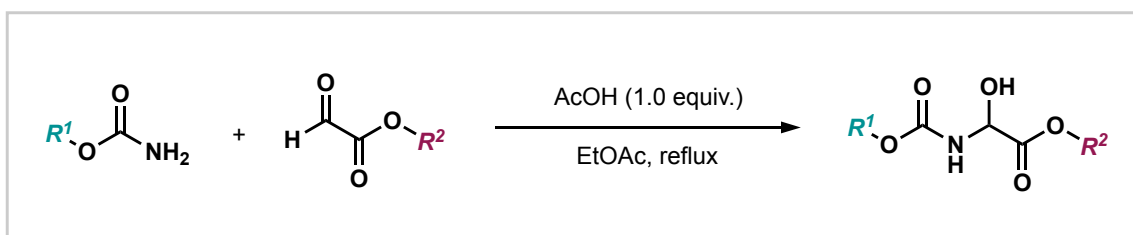
Following a procedure reported by Jacobsen[193], in an oven-dried 500 mL two-neck flask equipped with a reflux condenser, the respective carbamate (14.2 mmol, 1.0 equiv.) was suspended in EtOAc (200 mL) and the alkyl glyoxylate (20.1 mmol, 1.4 equiv., added pure or as solution in PhMe) was added. AcOH (14.2 mmol, 0.8 mL, 1.0 equiv.) was added dropwise under vigorous stirring and the mixture was heated to reflux for 24 to 48 h. When complete conversion of the carbamate was observed via TLC and/or NMR analysis, the mixture was cooled to room temperature and concentrated under reduced pressure. The obtained white residue was dissolved in a minimal amount of warm CH_2Cl_2 (approximately 100 to 200 mL, warmed to 30 °C) and an equal volume of i-hexanes was added slowly under swirling of the flask. The solution was kept at room temperature for two hours whereupon precipitation initiates. The mixture was then cooled to –20 °C overnight and the formed solids were filtered off, washed with i-hexanes and dried under vacuum to yield the desired hemiaminals as white solids.

General Procedure B (GP B): Synthesis of *N,O*-Acetals
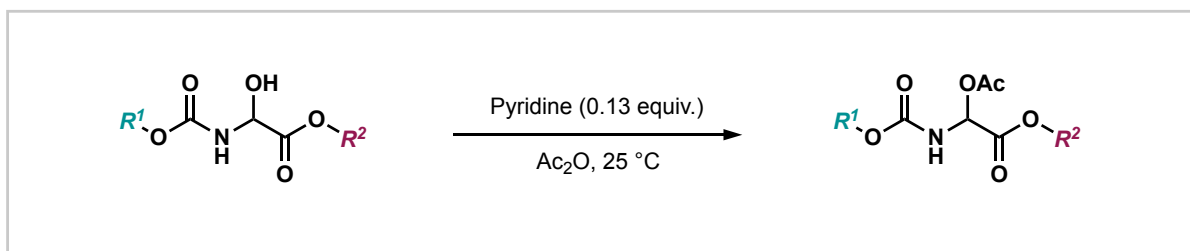
Following a modified procedure reported by Luo[194], the hemiaminal substrate (10 mmol, 1.0 equiv.) was given to a flame dried Schlenk tube followed by acetic anhydride (30 mL) and pyridine (1.3 mmol, 0.10 mL, 0.13 equiv.). The heterogenous mixture was stirred for 20 h under an atmosphere of argon whereupon complete dissolution of the solids was observed. The solution was then concentrated under reduced pressure at 70 °C and the residue was purified via flash column chromatography on silica gel (eluent: *i*-hexanes/EtOAc mixtures) or via recrystallization from CH_2Cl_2/*i*-hexanes to yield the *N,O*-acetals as colorless oils or white solids.

methyl 2-((((9H-fluoren-9-yl)methoxy)carbonyl)amino)-2-hydroxyacetate (167)
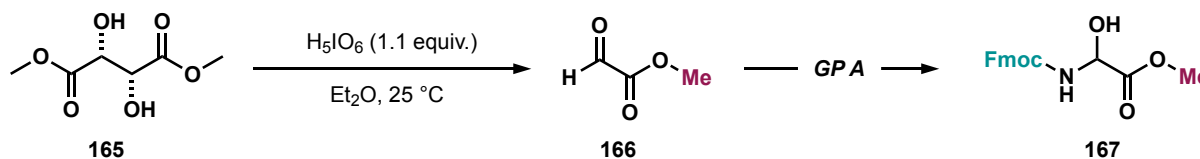
methylglyoxylate (166): Following modified procedure reported by Yus,[195] dimethyl (2*R*,3*R*)-2,3-dihydroxysuccinate (**165**, 1.9 g, 10.7 mmol, 1.0 equiv.) was given to a 50 mL round bottom flask and dissolved in Et_2O (20 mL). H_5IO_6 (2.67 g, 11.7 mmol, 1.1 equiv.) was added slowly, the flask was sealed and the mixture was stirred at 25 °C for 2 h. The solids were filtered off, washed with EtOAc (3 x 40 mL) and the filtrate was dried over $MgSO_4$. The drying agent was filtered off and the solvent was removed under reduced pressure to yield the crude glyoxylate **S2-a** as colorless oil. The spectral data are in agreement with the reported literature[196]. The compound was directly used in the subsequent step.

^{1}H-NMR: (501 MHz, CDCl$_3$): δ = 9.41 (s, 1H), 3.94 (s, 3H).

methyl 2-((((9H-fluoren-9-yl)methoxy)carbonyl)amino)-2-hydroxyacetate (167):

Following GP A, in an oven-dried 250 mL two-neck flask, (9H-fluoren-9-yl)methyl carbamate (**168**, 1.81 g, 7.57 mmol, 1.0 equiv.) was suspended in EtOAc (125 mL) and freshly prepared methylglyoxylate (**166**, 1.00 g, 11.4 mmol, 1.5 equiv.) was added. AcOH (0.43 mL, 7.57 mmol, 1.0 equiv.) was added dropwise under vigorous stirring and the mixture was heated to reflux

for 48 h. The mixture was cooled to room temperature and concentrated under reduced pressure. The obtained white residue was dissolved in warm CH_2Cl_2 (100 mL, warmed in a 30 °C water bath) and an equal volume of i-hexanes was added slowly under swirling of the flask. The solution was kept at room temperature for two hours whereupon initial precipitation was observed. The mixture was then cooled to –20 °C overnight, the formed solids were filtered off, washed with i-hexanes and dried under vacuum to yield the desired hemiaminal **167** (1.51 g, 8.78 mmol, 53% over two steps) as white solid.

TLC:	R_F (i-hexanes/EtOAc 2:1) = 0.36.
¹H-NMR:	(501 MHz, CDCl$_3$): δ = 7.77 (d, J = 7.5 Hz, 2H), 7.58 (d, J = 7.5 Hz, 2H), 7.40 (t, J = 7.4 Hz, 2H), 7.31 (t, J = 7.4 Hz, 2H), 6.06 (s, br, 1H), 5.50 (s, br, 1H), 4.46–4.40 (m, 2H), 4.22 (t, J = 6.9 Hz, 1H), 4.08 (s, br, 1H), 3.83 (s, 3H).
¹³C-NMR:	(126 MHz, CDCl$_3$): δ = 169.82, 155.76, 143.69, 143.64, 141.45, 127.96, 127.26, 125.12, 120.19, 73.70, 67.58, 53.46, 47.09.
ESI-HRMS:	calculated for $C_{18}H_{17}NNaO_5$ ([M+Na]$^+$): 350.10044, found: 350.09972.

isopropyl 2-((((9H-fluoren-9-yl)methoxy)carbonyl)amino)-2-hydroxyacetate (169)
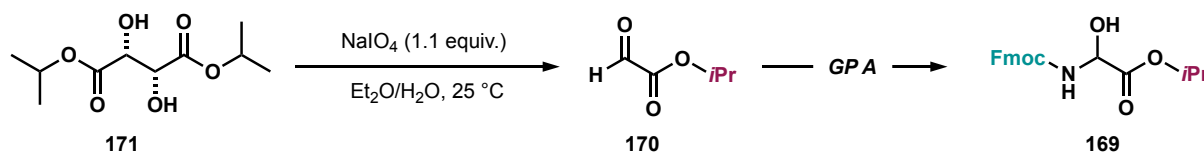
isopropyl 2-oxoacetate (170): Following a modified procedure reported by Xu and Loh,[197] diisopropyl (2R,3R)-2,3-dihydroxysuccinate (**171**, 2.5 g, 10.7 mmol, 1.0 equiv.) was given to a 50 mL round bottom flask, dissolved in Et$_2$O (5 mL) and the solution was cooled to 0°C. A solution of NaIO$_4$ (2.97 g, 13.9 mmol, 1.3 equiv.) in H$_2$O (20 mL) was added dropwise over 20 min, the flask was sealed and the mixture was stirred at 0 °C for 2 h. The mixture was then warmed to 25 °C and EtOAc (20 mL) was added. The layers were separated and the aqueous layer was extracted with EtOAc (5 x 30 mL). The combined organic extracts were dried over Na$_2$SO$_4$, the solids were filtered off and the filtrate was concentrated under reduced pressure to yield the crude glyoxylate **170** as colorless oil. The crude product was directly used in the next step without further purification. The spectral data are in agreement with the reported literature.[198]

¹H-NMR:	(501 MHz, CDCl$_3$): δ = 9.38 (s, 1H), 5.12 (sept, J = 6.4 Hz, 1H), 1.30 (d, J = 6.3 Hz, 6 H).

methyl 2-((((9H-fluoren-9-yl)methoxy)carbonyl)amino)-2-hydroxyacetate (169):
Following GP A, in an oven-dried 250 mL two-neck flask, (9H-fluoren-9-yl)methyl carbamate
(**168**, 1.81 g, 7.57 mmol, 1.0 equiv.) was suspended in EtOAc (125 mL) and freshly prepared
isopropyl 2-oxoacetate (**170**, 1.32 g, 11.4 mmol, 1.5 equiv.) was added. AcOH (0.43 mL,
7.57 mmol, 1.0 equiv.) was added dropwise under vigorous stirring and the mixture was heated
to reflux for 48 h. The mixture was then cooled to room temperature and concentrated under
reduced pressure. The obtained white residue was dissolved in warm CH_2Cl_2 (200 mL, warmed
in a 30 °C water bath) and an equal volume of *i*-hexanes was added slowly under swirling of
the flask. The solution was kept at room temperature for two hours whereupon the initiation of
crystallization was observed. The mixture was then cooled to –20 °C overnight and the formed
solids were filtered off, washed with *i*-hexanes and dried under vacuum to yield **169** (2.10 g,
5.90 mmol, 78% over two steps) as white solid.

¹H-NMR:	(501 MHz, CD_2Cl_2): δ = 7.79 (d, J = 7.6 Hz, 2H), 7.61 (d, J = 7.5 Hz, 2H), 7.42 (t, J = 7.6, 2H), 7.33 (t, J = 7.4, 2H), 5.95 (s, br, 1H), 5.33 (s, br, 1H), 5.09 (p, J = 6.3 Hz, 1H), 4.46–4.37 (m, 2H), 4.25 (t, J = 6.9 Hz, 1H), 3.68 (s, br, 1H), 1.29 (d, J = 6.3 Hz, 3H) 1.27 (d, J = 6.3 Hz, 3H).
¹³C-NMR:	(126 MHz, CD_2Cl_2): δ = 169.30, 144.17, 141.71, 128.17, 127.50, 125.41, 120.39, 74.12, 71.17, 67.59, 47.45, 21.75 (carbamate carbon not detected).
ESI-HRMS:	calculated for $C_{20}H_{21}NNaO_5$ ([M+Na]⁺): 378.13174, found: 378.13146.

ethyl 2-((((9H-fluoren-9-yl)methoxy)carbonyl)amino)-2-hydroxyacetate (172)

Following GP A, in an oven-dried 250 mL two-neck flask equipped with a reflux condenser, (9H-fluoren- 9-yl)methyl carbamate (**168**, 2.1 g, 8.78 mmol, 1.0 equiv.) was suspended in EtOAc (125 mL) and commercial ethyl 2-oxoacetate (**39**, 50% solution in PhMe, 2.7 mL, 13.2 mmol, 1.5 equiv.) was added. AcOH (0.5 mL, 8.78 mmol, 1.0 equiv.) was added dropwise under vigorous stirring and the mixture was heated to reflux for 48 h. The mixture was cooled to room temperature and concentrated under reduced pressure. The obtained white residue was dissolved in warm CH_2Cl_2 (120 mL, warmed in a 30 °C water bath) and an equal volume of *i*-hexanes was added slowly under swirling of the flask. The solution was kept at room temperature for two hours whereupon initiation of the crystallization was observed. The mixture was then cooled to –20 °C overnight and the formed solids were filtered off, washed with *i*-hexanes and dried under vacuum to yield the desired hemiaminal **172** (2.26 g, 6.62 mmol, 75%) as white solid.
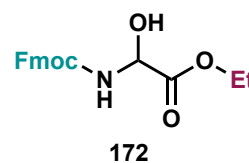
TLC:	R_F (*i*-hexanes/EtOAc 2:1) = 0.26.
¹H-NMR:	(501 MHz, CDCl₃): δ = 7.77 (d, J = 7.6 Hz, 2H), 7.58 (d, J = 7.5 Hz, 2H), 7.41 (t, J = 7.5 Hz, 2H), 7.32 (t, J = 7.4 Hz, 2 H), 5.99 (s, br, 1H), 5.46 (s, br, 1H), 4.48–4.40 (m, 2H), 4.30 (q, J = 7.0 Hz, 2H), 4.24 (t, J = 7.0 Hz, 1H), 3.85 (s, br, 1H), 1.33 (t, J = 7.2 Hz, 3H).
¹³C-NMR:	(126 MHz, MeCN-d₃): δ = 170.50, 156.49, 145.02, 145.00, 142.17, 128.77, 128.16, 126.15, 121.03, 74.44, 67.53, 62.79, 47.90, 14.38.
ESI-HRMS:	calculated for $C_{19}H_{19}NNaO_5$ ([M+Na]⁺): 364.11609, found: 364.11558.

ethyl 2-(((benzyloxy)carbonyl)amino)-2-hydroxyacetate (45)

Following GP A, benzyl carbamate (**44**, 3.00 g, 20.0 mmol, 1.0 equiv.) was given to an oven-dried 50 mL pressure vial, suspended in anhydrous EtOAc (20 mL) and ethyl 2-oxoacetate (**39**, 50% solution in PhMe, 4.86 mL, 23.8 mmol, 1.2 equiv.) was added. The mixture was stirred vigorously and AcOH (0.1 mL, 2.0 mmol, 0.10 equiv.) was added dropwise. The vial was sealed and heated to 75 °C for 48 h. The solution was then cooled to room temperature, concentrated under reduced pressure and the obtained white residue was dissolved in warm CH_2Cl_2 (200 mL, warmed in a 30 °C water bath). An equal volume of *i*-hexanes was added under swirling of the flask and the flask was left at room temperature for 2 h whereupon initiation of the crystallization was observed. The mixture was then cooled to –20 °C overnight and the formed
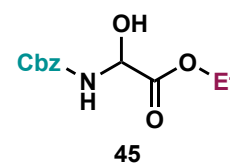
solids were filtered off, washed with *i*-hexanes and dried under vacuum to yield the desired hemiaminal **45** (2.26 g, 8.94 mmol, 45%) as white solid.

TLC:	R$_F$ (*i*-hexanes/EtOAc 2:1) = 0.54.
^{1}H-NMR:	(501 MHz, CDCl$_3$): δ = 7.40 – 7.30 (m, 5H), 6.04 (s, br, 1H), 5.47 (d, J = 8.0 Hz, 1H), 5.14 (s, 2H), 4.27 (q, J = 7.2 Hz, 2H), 4.09 (s, br, 1H), 1.30 (t, J = 7.1 Hz, 3H).
^{13}C-NMR:	(126 MHz, CDCl$_3$): δ = 169.40, 155.74, 135.84, 128.72, 128.52, 128.35, 73.78, 67.56, 62.81, 14.13.
ESI-HRMS:	calculated for C$_{12}$H$_{15}$NNaO$_5$ ([M+Na]$^+$): 276.08479, found: 276.08424.

ethyl 2-benzamido-2-hydroxyacetate (41)

Following a procedure reported by Ciufolini, benzamide (**38**, 3.0 g, 24.7 mmol, 1.0 equiv.) was given to a flame dried Schlenk tube and dissolved in anhydrous THF (100 mL).[199] Ethyl glyoxylate (**39**, 50% solution in PhMe, 5.14 mL, 25.3 mmol, 1.02 equiv.) was added under stirring. The mixture was heated to 80 °C with an attached reflux condenser for 20 h and then cooled to room temperature. The solution was concentrated under reduced pressure, adsorbed on celite and purified via flash column chromatography on silica gel (eluent: *i*-hexanes/EtOAc 3:1 → 1:1) to yield hemiaminal **41** (4.37 g, 19.6 mmol, 79%) as white solid. The measured analytical data is in accordance with the reported literature.[199]
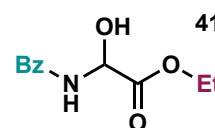
^{1}H-NMR:	(501 MHz, CDCl3): δ = 7.83–7.80 (m, 2H), 7.57–7.51 (m, 1H), 7.50–7.41 (m, 3H), 5.80 (d, J = 7.3 Hz, 1H), 4.47 (s, br, 1H), 4.33 (q, J = 7.1 Hz, 2H), 1.34 (t, J = 7.1 Hz, 3H).

methyl 2-(((((9H-fluoren-9-yl)methoxy)carbonyl)amino)-2-acetoxyacetate (53)

Following GP B, methyl 2-(((((9H-fluoren-9-yl)methoxy)carbonyl)amino)-2-hydroxyacetate (**167**, 1.0 g, 3.06 mmol, 1.0 equiv.) was given to a flame dried 25 mL Schlenk tube followed by acetic anhydride (9 mL) and anhydrous pyridine (30 μL, 0.40 mmol, 0.13 equiv.). The heterogenous mixture was stirred at 25 °C for 20 h under an atmosphere of argon whereupon a clear homogenous solution was obtained. The mixture was then concentrated under reduced pressure at 70 °C and the residue was purified via flash column
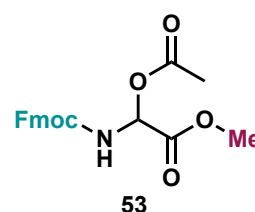
chromatography on silica gel (eluent: *i*-hexanes/EtOAc 4:1 → 3:1) to yield the desired *N,O*-acetal **53** (761 mg, 2.06 mmol, 67%) as white solid.

TLC:	R_f (*i*-hexanes/EtOAc 3:1) = 0.27.
^{1}H-NMR:	(501 MHz, CDCl$_3$): δ = 7.77 (d, J = 7.6, 2H), 7.59 (d, 7.8 Hz, 2H), 7.41 (t, J = 7.5, 2H), 7.32 (td, J = 7.5, 1.2 Hz, 2H) 6.29 (d, J = 9.4 Hz, 1H), 6.20 (s, br, 1H), 4.49–4.41 (m, 2H), 4.24 (t, J = 7.0 Hz, 1H), 3.83 (s, 3H), 2.13 (s, 3H).
^{13}C-NMR:	(126 MHz, CDCl$_3$): δ = 170.37, 166.96, 155.00, 143.65, 143.58, 141.46, 127.98, 127.26, 125.16, 125.14, 120.21, 74.50, 67.90, 53.52, 47.07, 20.83.
ESI-HRMS:	calculated for C$_{20}$H$_{19}$NNaO$_6$ ([M+Na]$^+$): 392.11101, found: 392.11066.

ethyl 2-((((9H-fluoren-9-yl)methoxy)carbonyl)amino)-2-acetoxyacetate (54)

Following GP B, ethyl 2-((((9H-fluoren-9-yl)methoxy)carbonyl)amino)-2-hydroxyacetate (**172**, 860 mg, 2.52 mmol, 1.0 equiv.) was given to a flame dried 25 mL Schlenk tube followed by acetic anhydride (7.5 mL) and anhydrous pyridine (27 µL, 0.33 mmol, 0.13 equiv.). The heterogenous mixture was stirred at 25 °C for 20 h under an atmosphere of argon whereupon a clear homogenous solution was obtained. The mixture was then concentrated under reduced pressure at 70 °C and the residue was purified via flash column chromatography on silica gel (eluent: *i*-hexanes/EtOAc 4:1 → 3:1) to yield the desired acetate **54** (819 mg, 2.14 mmol, 96%) as white solid.
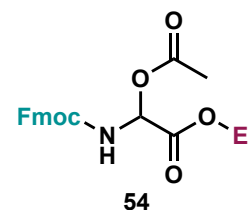
TLC:	R_f (*i*-hexanes/EtOAc 3:1) = 0.46.
^{1}H-NMR:	(501 MHz, CDCl$_3$): δ = 7.77 (d, J = 7.6, 2H), 7.59 (d, J = 7.7 Hz, 2H), 7.41 (t, J = 7.5, 2H), 7.32 (td, J = 7.4, 1.1 Hz, 2H), 6.26 (d, J = 9.4 Hz, 1H), 6.22–6.17 (m, 1H), 4.49–4.42 (m, 2H), 4.29 (q, J = 7.2 Hz, 2H), 4.24 (t, J = 7.1 Hz, 1H), 2.13 (s, 3H), 1.31 (t, J = 7.1 Hz, 3H).
^{13}C-NMR:	(126 MHz, CDCl$_3$): δ = 170.34, 166.44, 155.05, 143.66, 143.60, 141.44, 127.97, 127.25, 125.17, 125.15, 120.20, 74.67, 67.86, 62.87, 47.06, 20.82, 14.11.
ESI-HRMS:	calculated for C$_{21}$H$_{21}$NNaO$_6$ ([M+Na]$^+$): 406.12666, found: 406.12630.

isopropyl 2-(((((9H-fluoren-9-yl)methoxy)carbonyl)amino)-2-acetoxyacetate (55)

Following GP B, isopropyl 2-(((((9H-fluoren-9-yl)methoxy)carbonyl)amino)-2-hydroxyacetate (**169**, 1.0 g, 2.81 mmol, 1.0 equiv.) was given to a flame dried 25 mL Schlenk tube followed by acetic anhydride (8 mL) and anhydrous pyridine (30 µL, 0.37 mmol, 0.13 equiv.). The heterogenous mixture was stirred at 25 °C for 20 h under an atmosphere of argon whereupon a clear homogenous solution was obtained. The mixture was then concentrated under reduced pressure at 70 °C and the residue was purified via flash column chromatography on silica gel (eluent: *i*-hexanes/EtOAc 4:1 → 3:1) to yield the desired acetate **55** (660 mg, 1.66 mmol, 59%) as white solid.
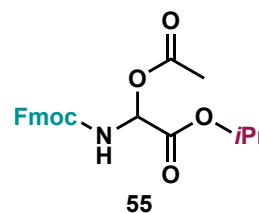
TLC:	R_f (*i*-hexanes/MTBE 2:1) = 0.48.
¹H-NMR:	(501 MHz, CDCl₃): δ = 7.77 (d, J = 7.6, 2H), 7.59 (d, J = 7.5 Hz, 2H), 7.41 (t, J = 7.5, 2H), 7.32 (td, J = 7.5, 1.2 Hz, 2H), 6.22–6.16 (m, 2H), 5.11 (hept, J = 6.2 Hz, 1H), 4.50–4.39 (m, 2H), 4.25 (t, J = 7.1 Hz, 1H), 2.12 (s, 3H), 1.30 (d, J = 6.3 Hz, 3H), 1.28 (d, J = 6.2 Hz, 3H).
¹³C-NMR:	(126 MHz, CDCl₃): δ = 170.36, 165.93, 155.07, 143.68, 143.63, 141.45, 127.97, 127.25, 125.19, 125.17, 120.20, 74.89, 70.97, 67.85, 47.07, 21.72, 21.64, 20.81.
ESI-HRMS:	calculated for C₂₂H₂₃NNaO₆ ([M+Na]⁺): 420.14231, found: 420.14156.

ethyl 2-acetoxy-2-(((benzyloxy)carbonyl)amino)acetate (46)

Following GP B, ethyl 2-(((benzyloxy)carbonyl)amino)-2-hydroxyacetate (**45**, 1.0 g, 3.95 mmol, 1.0 equiv.) was given to a flame dried 25 mL Schlenk tube followed by acetic anhydride (12 mL) and anhydrous pyridine (42 µL, 0.51 mmol, 0.13 equiv.). The homogeneous mixture was stirred at 25 °C for 20 h under an atmosphere of argon and subsequently concentrated under reduced pressure at 70 °C. The residue was purified via flash column chromatography on silica gel (eluent: *i*-hexanes/EtOAc 4:1 → 3:1) to yield the desired acetate **46** (1.0 g, 3.39 mmol, 86%) as colorless oil.
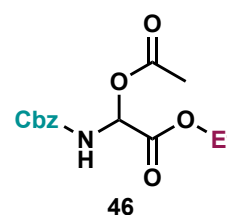
TLC:	R_f (*i*-hexanes/MTBE 2:1) = 0.28.
¹H-NMR:	(501 MHz, CDCl₃): δ = 7.41–7.29 (m, 5H), 6.25 (d, J = 9.4 Hz, 1H), 6.22 (s, br, 1H), 5.18–5.13 (m, 2H), 4.25 (q, J = 7.1 Hz, 2H), 2.10 (s, 3H), 1.28 (t, J = 7.2 Hz, 3H).

¹³C-NMR: (126 MHz, CDCl₃): δ = 170.31, 166.39, 155.01, 135.68, 128.71, 128.56, 128.42, 74.67, 67.81, 62.80, 20.77, 14.07.

ESI-HRMS: calculated for $C_{14}H_{17}NNaO_6$ ([M+Na]⁺): 318.09536, found: 318.09473.

ethyl 2-acetoxy-2-((*tert*-butoxycarbonyl)amino)acetate (52)
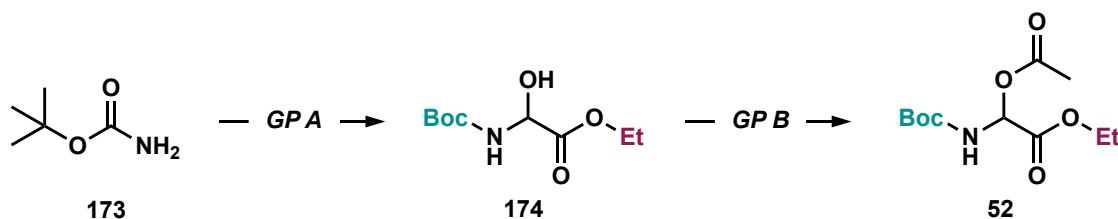
Following GP A, *tert*-butylcarbamate (**173**, 351 mg, 3.0 mmol, 1.0 equiv.) was given to a 100 mL two-neck flask equipped with a reflux condenser. Anhydrous EtOAc (30 mL) was added followed by commercial ethyl glyoxylate (50% in PhMe, 0.80 mL, 3.90 mmol, 1.3 equiv.). The mixture was stirred vigorously, AcOH (20.0 µL, 0.30 mmol, 0.10 equiv.) was added dropwise and the mixture was then heated to reflux for 24 h. The mixture was cooled to room temperature and concentrated under reduced pressure. The crude material was directly used for the subsequent acetylation step.

Following GP B, crude ethyl 2-((tert-butoxycarbonyl)amino)-2-hydroxyacetate (**174**) was given to a flame dried 10 mL Schlenk tube followed by acetic anhydride (3.5 mL) and anhydrous pyridine (12 µL, 0.15 mmol, 0.13 equiv.). The homogeneous mixture was stirred at 25 °C for 20 h under an atmosphere of argon and subsequently concentrated under reduced pressure at 70 °C. The residue was purified via flash column chromatography on silica gel (eluent: *i*-hexanes/EtOAc 7:1 → 3:1) to yield acetate **52** (208 mg, 0.80 mmol, 27% over two steps) as colorless oil.

TLC: R$_f$ (*i*-hexanes/EtOAc 3:1) = 0.52

¹H-NMR: (501 MHz, CDCl₃): δ = 6.18 (d, J = 9.4 Hz, 1H), 5.91 (s, br, 1H), 4.25 (q, J = 7.1 Hz, 2H), 2.11 (s, 3H), 1.46 (s, 9H), 1.29 (t, J = 7.1 Hz, 3H).

¹³C-NMR: (126 MHz, CDCl₃): δ = 170.45, 166.75, 154.12, 81.44, 74.65, 62.67, 28.30, 20.87, 14.12.

ESI-HRMS: calculated for $C_{11}H_{19}NNaO_6$ ([M+Na]⁺): 284.11101, found: 284.11055.

Synthesis of Arene Substrates

(2-methoxyphenyl)trimethylsilane (75)

Following a modified procedure reported by Schoenebeck,[200] 2-bromoanisole (**175**, 1.4 mL, 11.2 mmol, 1.0 equiv.) was given to a flame dried Schlenk tube under an atmosphere of argon, dissolved in anhydrous THF (23 mL) and cooled to –78 °C. A solution of n-BuLi (2.5 M in hexanes, 5.0 mL, 12.4 mmol, 1.1 equiv.) was added dropwise and the mixture was stirred for 1 h at –78 °C. TMSCl (1.71 mL, 13.5 mmol, 1.2 equiv.) was added dropwise, the mixture was slowly warmed to room temperature and stirred for 18 h at room temperature. The mixture was poured onto Et_2O (100 mL), washed with H_2O (3x 20 mL) and brine (20 mL), dried over anhydrous Na_2SO_4, filtered and concentrated under reduced pressure to yield anisole **75** (2.0 g, 11.1 mmol, 98%) as colorless oil. The spectral data are in agreement with the reported literature.[200]
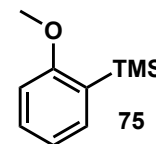
^{1}H-NMR: (501 MHz, $CDCl_3$): δ = 7.38 (dd, J = 7.1, 1.8 Hz, 1H), 7.35 (ddd, J = 8.1, 7.3, 1.8 Hz, 1H), 6.95 (td, J = 7.2, 0.9 Hz, 1H), 6.83 (d, J = 8.1 Hz, 1H), 3.81 (s, 3H), 0.27 (s, 9H).

(2-azidoethoxy)benzene (76)

Following a modified procedure reported by Elmali,[201] (2-bromoethoxy)benzene (**176**, 2.0 g, 9.95 mmol, 1.0 equiv.) and NaN_3 (1.29 g, 19.9 mmol, 2.0 equiv.) were given to a 250 mL round bottom flask with an attached pressure compensation bubbler and dissolved in anhydrous DMF (100 mL). The mixture was heated to 100 °C for 16 h, then cooled to room temperature and poured onto water (100 mL). The mixture was extracted with CH_2Cl_2 (3x 25 mL) and concentrated under reduced pressure. The residue was filtered over a short plug of silica gel (eluent: i-hexanes) and concentrated under reduced pressure to yield anisole **76** (1.50 g, 9.21 mmol, 93%) as colorless oil. The compound was stored in an aluminum foil coated vial at 4 °C. The spectral data are in agreement with the reported literature.[201]
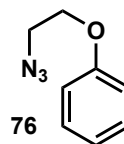
^{1}H-NMR: (501 MHz, $CDCl_3$): δ = 7.35 – 7.27 (m, 2H), 6.99 (tt, J = 7.4, 1.1 Hz, 1H), 6.96–6.92 (m, 2H), 4.16 (t, J = 5.1 Hz, 2H), 3.60 (t, J = 5.0 Hz, 2H).

2-methoxy-1,3-phenylene diacetate (100)

2-methoxybenzene-1,3-diol (**177**, 280 mg, 2.0 mmol, 1.0 equiv.) was given to a flame dried 10 mL microwave vial under an atmosphere of Ar followed by acetic anhydride (1.0 mL, 10.4 mmol, 5.2 equiv.) and one drop of concentrated sulfuric acid. The vial was sealed and the mixture was heated to 80 °C for 16 h. The vial was then cooled to room temperature and the mixture was poured onto ice water. EtOAc (50 mL) were added, the layers were separated and the aqueous layer was extracted with EtOAc (3x50 mL). The combined organic layers were washed with brine, dried over anhydrous Na$_2$SO$_4$ and concentrated under reduced pressure. The crude product was purified via flash column chromatography on silica gel (eluent: i-hexanes/EtOAc 10:1 → 8:1) to yield diacetate **100** (318 mg, 1.42 mmol, 71%) as colorless oil.
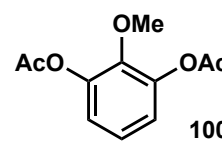
TLC:	R$_f$ (*i*-hexanes/EtOAc 10:1) = 0.25.
^{1}H-NMR:	(501 MHz, CDCl$_3$): δ = 7.08 (dd, J = 8.8, 7.5 Hz, 1H), 6.98 – 6.95 (m, 2H), 3.81 (s, 3H), 2.33 (s, 6H).
^{13}C-NMR:	(126 MHz, CDCl$_3$): δ = 168.89, 144.60, 144.26, 123.50, 121.07, 61.15, 20.88.
GC-EI:	calculated for C$_{11}$H$_{12}$O$_5$ ([M]$^+$): 224.06793, found: 224.06774.

2-methoxy-1,3-phenylene bis(2,2-dimethylpropanoate) (101)

To a flame dried round bottom flask under an atmosphere of Ar was added 2-methoxybenzene-1,3-diol (**177**, 280 mg, 2.0 mmol, 1.0 equiv.) followed by 4-(dimethylamino)-pyridine (122 mg, 1.0 mmol, 0.5 equiv.) and CH$_2$Cl$_2$ (20 mL). To the stirred solution was then added pyridine (0.4 mL, 5.0 mmol, 2.5 equiv.) and pivalic acid anhydride (1.62 mL, 8 mmol, 4 equiv.). The mixture was stirred at 30 °C for 16 h, then poured onto a concentrated solution of NaHCO$_3$ (20 mL) and CH$_2$Cl$_2$ (20 mL) was added. The layers were separated, the aqueous layer was extracted with CH$_2$Cl$_2$ (3x20 mL) and the combined organic layers were washed with brine, dried over anhydrous Na$_2$SO$_4$ and concentrated under reduced pressure. The crude product was purified via flash column chromatography on silica gel (eluent: *i*-hexanes/EtOAc 30:1 → 20:1) to yield the desired pivalate **101** (419 mg, 1.36 mmol, 68%) as colorless solid.
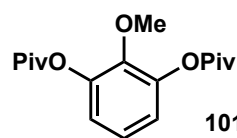
^{1}H-NMR:	(501 MHz, CDCl$_3$): δ = 7.07 (t, J = 8.2 Hz, 1H), 6.92 (d, J = 8.1 Hz, 2H), 3.76 (s, 3H), 1.38 (s, 18H).
^{13}C-NMR:	(126 MHz, CDCl$_3$): δ = 176.61, 145.22, 144.40, 123.57, 120.85, 61.44, 39.27, 27.32.

((2-methoxy-1,3-phenylene)bis(oxy))bis(triisopropylsilane) (102)

To a flame dried 25 mL round bottom flask under an Ar atmosphere was added 2-methoxybenzene-1,3-diol (**177**, 280 mg, 2.0 mmol, 1.0 equiv.) followed by anhydrous DMF (3.3 mL). Imidazole (1.36 g, 20 mmol, 10 equiv.) was added followed by triisopropylsilylchloride (2.14 mL, 10 mmol, 5 equiv.) and the mixture was stirred at 30 °C for 20 h. Et$_2$O (20 mL) was added and the mixture was washed with water (3x20 mL) and brine (2x20 mL) and then dried over anhydrous Na$_2$SO$_4$ and concentrated under reduced pressure. The crude product was purified via flash column chromatography on silica gel (*i*-hexanes/EtOAc 100:1 → 50:1) to yield the desired silyl ether **102** (706 mg, 1.56 mmol, 78%) as colorless oil.
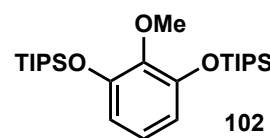
^{1}H-NMR:	(501 MHz, CD$_2$Cl$_2$): δ = 6.77 – 6.72 (m, 1H), 6.50 (d, J = 8.2 Hz, 2H), 3.76 (s, 3H), 1.31 – 1.22 (m, 6H), 1.10 (d, J = 7.4 Hz, 36H).
ESI-HRMS:	calculated for C$_{25}$H$_{48}$NaO$_3$Si$_2$ ([M+Na]$^+$): 475.30342, found: 475.30392.

2-(benzyloxy)benzene-1,3-diol (178)

Following a procedure reported by Suzuki, a flame dried 250 mL flask under an atmosphere of Ar was added pyrogallol (**179**, 2.54 g, 20.2 mmol, 1.0 equiv.) followed by anhydrous acetone (100 mL).[202] The mixture was cooled to 0 °C and K$_2$CO$_3$ (2.78 g, 20.2 mmol, 1.0 equiv.) was added followed by the dropwise addition of benzylbromide (2.4 mL, 20.2 mol, 1.0 equiv.). The mixture was allowed to warm to 30 °C and stirred for 20 h. Et$_2$NH (0.2 mL) was added and the mixture was filtered over a plug of celite. The filtrate was concentrated and the crude product was purified via flash column chromatography on silica gel (eluent: *i*-hexanes/EtOAc 10:1 → 5:1) to yield the desired phenole **178** (1.60 g, 7.4 mmol, 37%) as a yellow oil.
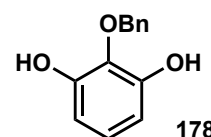
TLC:	R$_f$ (*i*-hexanes/EtOAc 3:1) = 0.55.
^{1}H-NMR:	(501 MHz, CDCl$_3$): δ = 7.49 – 7.35 (m, 5H), 6.87 (t, J = 8.2 Hz, 1H), 6.49 (d, J = 8.2 Hz, 2H), 5.20 (s, 2H), 5.02 (s, 2H).
GC-EI:	calculated for C$_{13}$H$_{12}$O$_3$ ([M]$^+$): 216.07810, found: 216.07794.

The spectroscopic data is in agreement with the reported literature.[202]

((2-(benzyloxy)-1,3-phenylene)bis(oxy))bis(triisopropylsilane) (180)

To a flame dried 25 mL round bottom flask under an atmosphere of argon was added 2-(benzyloxy)benzene-1,3-diol (**178**, 530 mg, 2.45 mmol, 1.0 equiv.) followed by anhydrous DMF (4.2 mL). Imidazole (1.67 g, 24.5 mmol, 10 equiv.) were added followed by triisopropylsilylchloride (2.63 mL, 12.3 mmol, 5.0 equiv.). The flask was sealed and stirred for 16 h at 30 °C, then Et_2O (15 mL) was added and the mixture was washed with water (3x15 mL) and brine (2x15 mL) and then dried over anhydrous Na_2SO_4 and concentrated under reduced pressure. The crude product was purified via flash column chromatography on silica gel (*i*-hexanes/EtOAc 50:1 → 20:1) to yield the desired silyl ether **180** (725 mg, 1.37 mmol, 56%) as colorless oil.
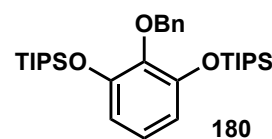
TLC:	R_f (*i*-hexanes/EtOAc 3:1) = 0.55.
^{1}H-NMR:	(501 MHz, CDCl$_3$): δ = 7.46 – 7.42 (m, 2H), 7.35 – 7.29 (m, 2H), 7.28 – 7.22 (m, 1H), 6.75 (t, J = 8.2 Hz, 1H), 6.51 (d, J = 8.2 Hz, 2H), 5.03 (s, 2H), 1.31 – 1.18 (m, 6H), 1.08 – 1.04 (m, 36H).
^{13}C-NMR:	(126 MHz, CDCl$_3$): δ = 150.85, 138.72, 128.02, 127.55, 127.26, 122.95, 113.46, 74.13, 18.08, 17.85, 13.07.

2,6-bis((triisopropylsilyl)oxy)phenol (93)

To a 250 mL round bottom flask under an atmosphere of Ar was added Pd on charcoal (10%, 266 mg) followed by anhydrous MeOH (100 mL). ((2-(benzyloxy)-1,3-phenylene)bis(oxy))bis(triisopropylsilane) (**180**, 1.22 g, 2.30 mmol, 1.0 equiv.) was transferred to the mixture and the flask was charged with H_2 (via attached H_2-balloon, 1 atm). The mixture was then stirred at 30 °C for 2h, whereupon full conversion of the benzyl ether was observed. The mixture was filtered over a plug of celite, rinsed with acetone (50 mL) and the filtrate was concentrated under reduced pressure. The Pd-containing waste was discarded as aqueous suspension. The crude product was then purified via flash column chromatography on silica gel (eluent: *i*-hexanes/CH_2Cl_2 20:1 → 10:1) to yield the desired phenol **93** (817 mg, 1.86 mmol, 81%) as colorless oil.
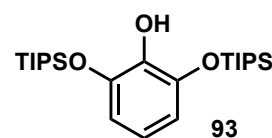
^{1}H-NMR:	(501 MHz, CDCl$_3$): δ = 6.58 – 6.47 (m, 3H), 5.40 (s, 1H), 1.30 (tt, J = 8.5, 6.9 Hz, 6H), 1.11 (d, J = 7.5 Hz, 36H).
^{13}C-NMR:	(126 MHz, CDCl$_3$): δ = 167.54, 162.48, 141.89, 136.26, 41.40, 36.54.

GC-EI: calculated for $C_{11}H_{12}O_5$ ([M]$^+$): 437.29127, found: 437.29143.

7.1.2 Synthesis of IDPi Catalysts

(*S*,*S*)-IDPi catalysts **4a**, **4b**, **4c**, **4d**, **4e** and **4g** were prepared according to reported literature procedures.[66,68,203] Phosphazene reagents **S9-a**[68] and **S9-b**[203] were prepared following reported literature procedures.

General Remark on the Synthesis of (*S*,*S*)-IDPi Catalysts: Our group recently reported an alternative synthesis for the preparation of IDPi catalysts based on the usage of hexachlorobisphosphazonium salts.[204] While this route has proven its versatility in the modular synthesis of broad IDPi libraries, we chose to follow the previously established phosphazene-route as a variety of phosphazene reagents are regularly prepared on large scales in our laboratory which consequentially facilitates the reaction setup.

Synthesis of substituted (S)-BINOLs
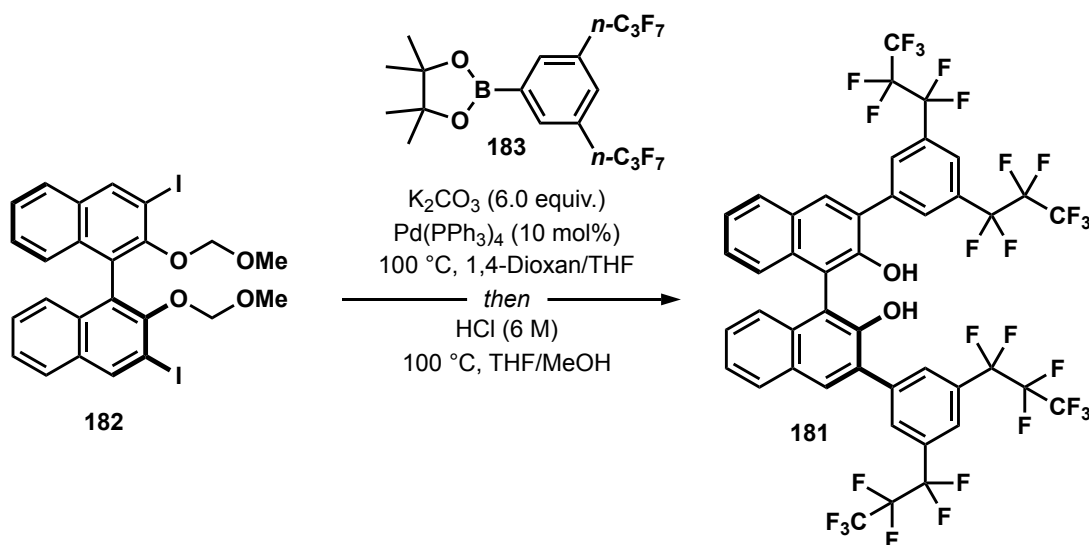
(S)-3,3'-bis(3,5-bis(perfluoropropyl)phenyl)-[1,1'-binaphthalene]-2,2'-diol (181)

A Schlenk tube was charged with (*S*)-3,3'-diiodo-2,2'-bis(methoxymethoxy)-1,1'-binaphthalene (**182**, 1.35 g, 2.16 mmol, 1.0 equiv.), 2-(3,5-bis(perfluoropropyl)phenyl)-4,4,5,5-tetramethyl-1,3,2-dioxaborolane (**183**, 3.5 g, 6.48 mmol, 3.0 equiv.) and K_2CO_3 (1.79 g, 13.0 mmol, 6.0 equiv.). A 4:1 (*v:v*) mixture of H_2O and 1,4-dioxane (28 mL) was added and the mixture was degassed in a constant stream of Ar bubbling through the mixture under stirring for 20 min. Pd(PPh$_3$)$_4$ (250 mg, 0.22 mmol, 10 mol%) was added, the tube was sealed and heated to 110 °C for 16 h. The mixture was then cooled to room temperature, diluted with CH_2Cl_2 (100 mL) and

water (100 mL) was added. The layers were separated, the aqueous layer was extracted with CH$_2$Cl$_2$ (3 x 70 mL) and the combined organic extracts were concentrated under reduced pressure.

The obtained residue was dissolved in a 6:1 (*v:v*) mixture of THF and MeOH (42 mL) and then treated with HCl (6.0 M, 13 mL). The mixture was transferred to two separate microwave reaction vials and heated to 100 °C for 1 h in a microwave reactor, respectively. The vials were cooled to 25 °C, combined and diluted with H$_2$O (100 mL) and CH$_2$Cl$_2$ (100 mL) and the layers were separated. The aq. layers were extracted with CH$_2$Cl$_2$ (3 x 70 mL), the combined organic extracts were washed with brine (100 mL) and dried over anhydrous Na$_2$SO$_4$. The solids were filtered off, the filtrate was adsorbed on celite® and the solvent was removed under reduced pressure. The crude mixture was purified via flash column chromatography on silica gel (eluent: *i*-hexanes/CH$_2$Cl$_2$ 98:2 → 95:5) to yield (*S*)-BINOL **181** (1.99 g, 1.79 mmol, 83%) as white solid. The analytical data are in agreement with the reported literature.[68]

TLC:	R$_f$ (*i*-hexanes/CH$_2$Cl$_2$ 10:1) = 0.32.
^{1}H-NMR:	(501 MHz, CDCl$_3$): δ = 8.25 (s, 4H), 8.13 (s, 2H), 8.02 (d, J = 8.1 Hz, 2H), 7.84 (s, 2H), 7.50 (ddd, J = 8.0, 6.8, 1.3 Hz, 2H), 7.44 (ddd, J = 8.3, 6.9, 1.4 Hz, 2H), 7.25 (d, J = 8.0 Hz, 2H), 5.40 (s, 2H).
^{13}C-NMR:	(126 MHz, CDCl$_3$): δ = 150.08, 139.47, 133.52, 132.63, 131.79, 131.75, 131.69, 130.18, 129.99, 129.79, 129.66, 129.10, 128.89, 127.76, 125.40, 124.39, 124.19, 121.51, 119.50, 119.23, 118.96, 117.21, 116.95, 116.70, 115.17, 114.92, 114.67, 113.13, 112.89, 112.64, 111.97, 111.36, 111.06, 110.75, 110.45, 109.26, 108.96, 108.65, 108.35, 107.16, 106.86, 106.55, 106.25, 77.41, 77.37, 77.16, 76.91.
^{19}F-NMR:	(471 MHz, CDCl$_3$) δ = –79.94 (t, J = 9.8 Hz), –111.90 (q, J = 10.0 Hz), –126.16.
ES-HRMS:	calculated for C$_{44}$H$_{17}$F$_{28}$O$_2$ [(M-H)$^-$]: 1109.07869, found: 1109.07881.

(S)-3,3'-bis(3,5-bis(pentafluoro-λ^6-sulfaneyl)phenyl)-[1,1'-binaphthalene]-2,2'-diol (184)
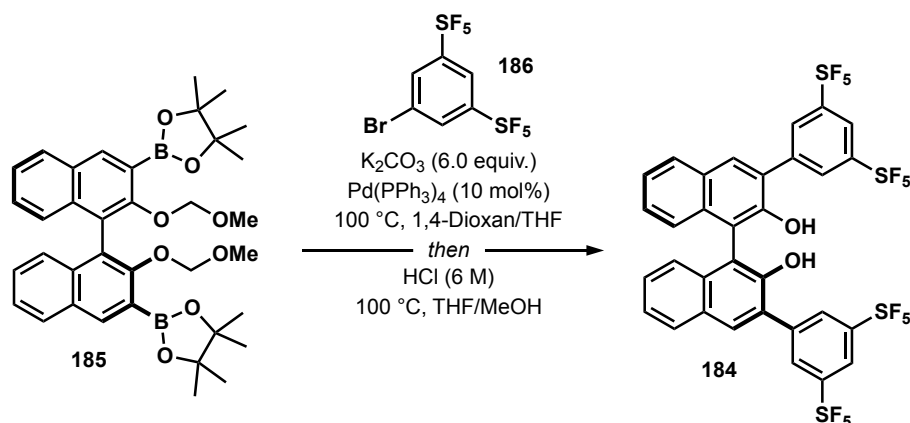
A Schlenk tube was charged with (S)-2,2'-(2,2'-bis(methoxymethoxy)-[1,1'-binaphthalene]-3,3'-diyl)bis(4,4,5,5-tetramethyl-1,3,2-dioxaborolane) (**185**, 250 mg, 0.40 mmol, 1.0 equiv.), (5-bromo-1,3-phenylene)bis(pentafluoro-λ^6-sulfane) (**186**, 375 mg, 0.92 mmol, 2.3 equiv.) and K$_2$CO$_3$ (331 mg, 2.4 mmol, 6.0 equiv.). A 6:1 (*v:v*) mixture of H$_2$O and 1,4-dioxane (6 mL) was added and the mixture was degassed in a constant stream of Ar bubbling through the mixture under stirring for 20 min. Pd(PPh$_3$)$_4$ (46 mg, 0.04 mmol, 10 mol%) was added, the tube was sealed and heated to 110 °C for 16 h. The mixture was then cooled to room temperature, diluted with CH$_2$Cl$_2$ (10 mL) and water (10 mL) was added. The layers were separated, the aqueous layer was extracted with CH$_2$Cl$_2$ (3 x 10 mL) and the combined organic extracts were concentrated under reduced pressure.

The obtained residue was dissolved in a 6:1 (*v:v*) mixture of THF and MeOH (8.5 mL) and then treated with HCl (6.0 M, 1.2 mL). The mixture was transferred to a microwave reaction vial and heated to 100 °C for 1 h in a microwave reactor. The vial was cooled to room temperature, diluted with H$_2$O (10 mL) and CH$_2$Cl$_2$ (10 mL) and the layers were separated. The aqueous layer was extracted with CH$_2$Cl$_2$ (3 x 10 mL), the combined organic extracts were washed with brine (10 mL) and dried over anhydrous Na$_2$SO$_4$. The solids were filtered off, the filtrate was adsorbed on celite® and the solvent was removed under reduced pressure. The crude mixture was purified via flash column chromatography on silica gel (eluent: *i*-hexanes/CH$_2$Cl$_2$ 3:1 $\rightarrow$ 2:1) to yield (S)-BINOL **184** (239 mg, 0.25 mmol, 64%) as white solid. The analytical data are in agreement with the reported literature.[68]

TLC: R$_f$ (*i*-hexanes/EtOAc 20:1) = 0.58.

^{1}H-NMR: (501 MHz, CDCl$_3$): δ = 8.33 (d, J = 2.1 Hz, 4H), 8.16 (t, J = 2.1 Hz, 2H), 8.08 (s, 2H), 8.00 (d, J = 8.0 Hz, 2H), 7.47 (ddd, J = 8.6, 7.6, 0.97 Hz,

	2H), 7.41 (ddd, J = 8.9, 8.0, 1.0 Hz, 2H), 7.21 (d, J = 8.3 Hz, 2H), 5.84 (s, 2H).
^{13}C-NMR:	(126 MHz, CDCl$_3$): δ = 153.55 (p, J = 19.0 Hz), 149.95, 139.77, 133.71, 132.42, 130.41, 129.44, 129.03, 128.95, 127.31, 125.40, 124.18, 123.03, 112.37.
^{19}F-NMR	(471 MHz, CDCl$_3$): δ = 81.98 (p, J = 150.6 Hz), 63.08 (d, J = 150.6 Hz).
ES-HRMS:	calculated for C$_{32}$H$_{17}$F$_{20}$O$_2$S$_4$ [(M-H)$^-$]: 940.97975, found: 940.97990.

Synthesis of (S,S)-IDPi Catalysts from 3,3'-disubstituted BINOLs

(*S,S*)-IDPi catalysts were prepared following a modified procedure reported by our group:
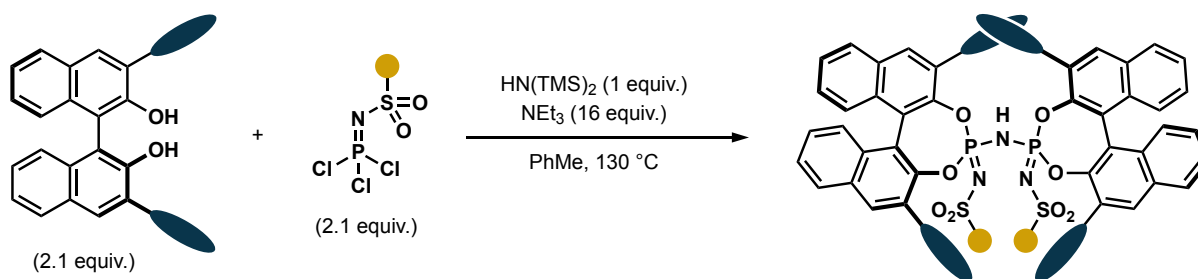
General Procedure C (GP C): Synthesis of (*S,S*)-IDPi Catalysts

Following a modified procedure reported by List, the respective 3,3'-disubstituted (*S*)-BINOL (2.1 equiv.) was given to a flame dried Schlenk tube under an atmosphere of argon and dissolved in anhydrous PhMe.[203] Phosphazene reagent (2.1 equiv.) was added followed by NEt$_3$ (16 equiv.) and the mixture was stirred at room temperature for 30 min. Hexamethyldisilazane (1.0 equiv.) was added, the mixture was stirred for another 20 min at room temperature and subsequently heated to 130 °C for 3 days. The tube was then cooled to room temperature, diluted with CH$_2$Cl$_2$ and quenched via the addition of HCl (10%). The layers were separated and the aqueous layer was extracted with CH$_2$Cl$_2$, the combined organic extracts dried over anhydrous Na$_2$SO$_4$ and concentrated under reduced pressure. The crude residue was purified via flash column chromatography on silica gel to yield the salts of the (*S,S*)-IDPis which were acidified via filtration over a short plug of DOWEX 50WX8 (H-form, eluted with CH$_2$Cl$_2$) to yield (*S,S*)-IDPis as white or off-white solids.

(*S*,*S*)-(3,5-bis-perfluoropropylphenyl)-C$_2$F$_5$ IDPi (IDPi-10-c)

Prepared according to GP C: (*S*)-3,3'-bis(3,5-bis(perfluoropropyl)-phenyl)-[1,1'-binaphthalene]-2,2'-diol (**181**, 671 mg, 0.60 mmol, 2.1 equiv.) was given to a flame dried Schlenk tube under an atmosphere of argon and dissolved in anhydrous PhMe (6.5 mL). ((perfluoroethyl)sulfonyl)phosphorimidoyl trichloride (**187,** 202 mg, 0.60 mmol, 2.1 equiv.) was added followed by triethylamine (0.64 mL, 4.60 mmol, 16 equiv.) and the mixture was stirred at room temperature for 30 min. Hexamethyldisilazane (60 μL, 0.29 mmol, 1.0 equiv.) was added, the mixture was stirred for another 20 min at room temperature and subsequently heated to 130 °C for 3 days. The tube was then cooled to room temperature, diluted with CH$_2$Cl$_2$ (30 mL) and quenched via the addition of HCl (10%, 30 mL). The layers were separated, and the aqueous layer was extracted with CH$_2$Cl$_2$ (3 x 30 mL), the combined organic extracts were dried over anhydrous Na$_2$SO$_4$ and concentrated under reduced pressure. The crude residue was purified via flash column chromatography on silica gel (eluent: *i*-hexanes/CH$_2$Cl$_2$ 1:1 → CH$_2$Cl$_2$/EtOAc 99:1) and the isolated salt was acidified via filtration over a short plug of DOWEX 50WX8 (H-form, eluted with CH$_2$Cl$_2$) to yield (***S*,*S*)-IDPi-10-c** (570 mg, 0.21 mmol, 74%) as off-white solid.
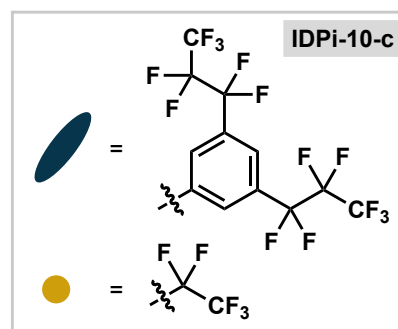
TLC:	R$_F$ (i-hexanes/EtOAc 3:1) = 0.72.
^{1}H-NMR:	(501 MHz, CDCl$_3$): δ = 8.10 (s, 2H), 8.09 (d, J = 8. Hz, 2H), 7.90 (d, J = 3.9 Hz, 4H), 7.74 (s, 4H) 7.72 (d, J = 8.9 Hz, 2H), 7.69–7.65 (m, 6H), 7.62 (t, J = 7.5 Hz 2H), 7.38 (ddd, J = 8.4, 6.8, 1.2 Hz, 2H), 7.32 (s, 4H), 7.10 (d, J = 8.6 Hz, 2H), 6.57 (s, 2H), 5.99 (s, br, 1H).
^{13}C{^{1}H, ^{19}F}-NMR:	(126 MHz, CDCl$_3$): δ = 143.86 (t, J = 5.4 Hz), 141.75 (t, J = 5.1 Hz), 138.14, 137.96, 133.94, 132.22, 131.97 (d, J = 8.3 Hz), 131.96, 131.50, 131.13, 130.86, 130.73, 130.18, 130.14, 129.86, 129.24, 128.64, 128.00, 127.23, 127.08, 126.74, 125.35 (d, J = 12.5 Hz), 123.67, 121.47, 118.02, 117.79, 117.05, 114.42 (d, J = 10.7 Hz), 111.29, 108.70, 108.39.
^{19}F-NMR:	(471 MHz, CDCl$_3$): δ = –79.00 (s), –79.98 (t, J = 9.5 Hz), –80.14 (t, J = 9.6 Hz), –112.06 (s), –112.65 (s), –113.92 (d, J = 277.8 Hz), –116.50 (s), –126-04 (s), –126.55 (d, J = 291.3 Hz).
^{31}P-NMR:	(202 MHz, CDCl$_3$) δ = –14.27.
ESI-HRMS:	calculated for C$_{92}$H$_{32}$F$_{66}$N$_3$O$_8$P$_2$S$_2$ ([M-H]$^-$): 2686.00522, found: 2686.00395.

$[\propto]_D^{25}$:	184.3 (c = 0.13, CHCl$_3$).

(S,S)-(3,5-bis-(pentafluoro-λ^6-sulfaneyl)phenyl)-C$_6$F$_{13}$ IDPi-13-f

Prepared according to GP C: (*S*)-3,3'-bis(3,5-bis(pentafluoro-λ^6-sulfaneyl)phenyl)-[1,1'-binaphthalene]-2,2'-diol (**184**, 64 mg, 68 µmol, 2.1 equiv.) was given to a flame dried Schlenk tube under an atmosphere of argon and dissolved in anhydrous PhMe (1.2 mL). ((perfluorohexyl)sulfonyl)phosphorimidoyl trichloride (**188**, 36 mg, 68 µmol, 2.1 equiv.) was added followed by triethylamine (72 µL, 0.52 mmol, 16 equiv.) and the mixture was stirred at room temperature for 30 min. Hexamethyldisilazane (6.7 µL, 32 µmol, 1.0 equiv.) was added, the mixture was stirred for another 20 min at room temperature and subsequently heated to 130 °C for 3 days. The tube was then cooled to room temperature, diluted with CH$_2$Cl$_2$ (10 mL) and quenched via the addition of HCl (10%, 10 mL). The layers were separated, and the aqueous layer was extracted with CH$_2$Cl$_2$ (3 x 10 mL), the combined organic extracts dried over anhydrous Na$_2$SO$_4$ and concentrated under reduced pressure. The crude residue was purified via flash column chromatography on silica gel (eluent: CH$_2$Cl$_2$/EtOAc 99.75:0.25 → 99:1) and the isolated salt was acidified via filtration over a short plug of DOWEX 50WX8 (H-form, eluted with CH$_2$Cl$_2$) to yield (*S*,*S*)-IDPi-13-f (57 mg, 21 µmol, 64%) as off-white solid.

TLC:	R$_F$ (CH$_2$Cl$_2$/EtOAc 99:1) = 0.63.
¹H-NMR:	(501 MHz, CDCl$_3$): δ = 8.18 (s, 2H), 8.14 (d, H = 1.6 Hz, 2H), 8.13 (d, J = 4.5 Hz, 2H), 8.09 (t, J = 1.9 Hz, 2H), 7.96–7.87 (m, 4H), 7.82 (s, 4H), 7.81–7.76 (m, 2H), 7.73 (ddd, J = 8.3, 6.2, 1.7 Hz, 2H), 7.65 (t, J = 7.5 Hz, 2H), 7.47–7.37 (m, 6H), 7.07 (d, J = 8.6 Hz, 2H), 6.55 (s, 2H).
¹³C{¹H, ¹⁹F}-NMR:	(126 MHz, CDCl$_3$): δ = 153.71 (q, J = 19.1 Hz), 143.50 (t, J = 5.4 Hz), 141.29 (t, J = 5.1 Hz), 138.25, 137.29, 133.89, 132.58, 132.29, 132.08, 131.00, 130.36, 130.18, 129.85, 129.52, 129.14, 128.49, 127.53, 127.47, 127.18, 126.69, 124.31, 124.01, 123.93, 121.60, 117.23, 113.15, 110.60, 110.44, 110.17, 108.38, 100.12.
¹⁹F-NMR:	(471 MHz, CDCl$_3$): δ = 80.97 (p, J = 149.6 Hz), 63.29 (d, J = 149.7 Hz), 62.35 (d, J = 150.0 Hz), -81.01 (t, J = 9.9 Hz), -111.97 (d, J = 258.8 Hz),

-113.35 (d, J = 258.7 Hz), -119.93 (dt, J = 34.3, 15.8 Hz), -122.03 (d, J = 82.4 Hz), -123.08 (d, J = 86.3 Hz), -126.36 (dt, J = 28.9, 14.6 Hz).

^{31}P-NMR: (203 MHz, CDCl$_3$) δ = –14.34.

ESI-HRMS: calculated for C$_{76}$H$_{32}$F$_{66}$N$_3$O$_8$P$_2$S$_{10}$ ([M-H]$^-$): 2749.78178, found: 2749.78287.

$[\alpha]_D^{25}$: 267.2 (c = 0.13, CHCl$_3$).

7.1.3 Reaction Development

Reaction conditions for the conversion of hydrocarbon arenes were optimized as described below using toluene (**3**) as representative substrate: An oven dried 1 mL screwcap vial equipped with a magnetic stirring bar was charged with the respective catalyst (5 mol%) and *N,O*-acetal **54** (1.0 equiv., 0.025 mmol). The vial was evacuated and placed under an atmosphere of argon. Anhydrous PhMe (**3**, 0.25 mL) was added via syringe, the vial was sealed and the mixture was stirred at 30 °C for 16 h if not indicated otherwise. The reaction was then quenched via addition of triethylamine (0.3 M solution in PhMe, 50 µL), dimethylsulfone (2.0 M solution in MeCN, 12.5 µL, 1.0 equiv.) was added as internal standard and the mixture was diluted with CH$_2$Cl$_2$ (0.2 mL). An aliquot of the reaction was diluted with CDCl$_3$ (0.6 mL) and analyzed via ^{1}H-NMR for the determination of the reaction's yield. The remaining solution was purified via preparative thin layer chromatography (PTLC) and analyzed via HPLC for the determination of the regioisomeric ratio as well as the enantiomeric ratio.

Asymmetric Friedel–Crafts Reactions toward Arylglycines
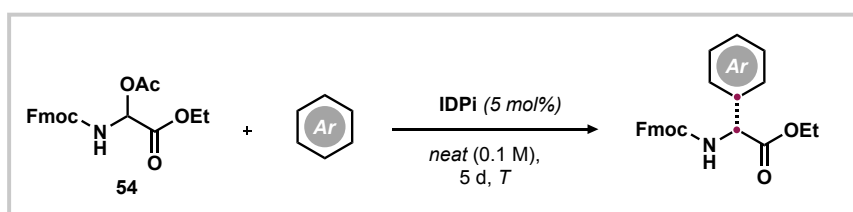
General Procedure D (GP D): Friedel–Crafts Reaction of Only Hydrocarbon Arenes

A flame-dried 5 mL finger Schlenk tube under an atmosphere of argon equipped with a magnetic stirring bar was charged with *N,O*-acetal **54** (38.3 mg, 0.1 mmol, 1.0 equiv.) and an (*S,S*)-IDPi catalyst (5 µmol, 5 mol%). The respective hydrocarbon arene (1.0 mL) was then added via syringe. If the reaction was performed at temperatures below 30 °C, the tube was cooled on dry ice during the addition of the respective arene substrate. The tube was sealed and

the reaction was stirred at the indicated temperature for the indicated reaction time. The mixture was then quenched with triethylamine (0.3 M solution in PhMe, 200 µL) and applied directly on a silica gel column equilibrated with *i*-hexanes. The mixture was flushed with *i*-hexanes (100 mL) and then purified via flash column chromatography on silica gel (*i*-hexanes/MTBE eluents) to yield the arylglycines as white solids. Regioisomeric ratios were determined either via ^{1}H-NMR- or HPLC analysis. *Deviations from the general protocol are indicated at the respective entry.*
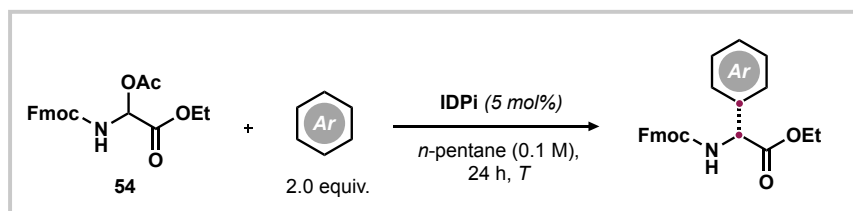
General Procedure E (GP E): Friedel–Crafts Reaction of Anisoles and Heteroarenes

A flame-dried 5 mL finger Schlenk tube under an atmosphere of argon and equipped with a magnetic stir bar was charged with *N,O*-acetal **54** (38.3 mg, 0.1 mmol, 1.0 equiv.) and an (*S,S*)-IDPi catalyst (5 µmol, 5 mol%). *n*-pentane (1.0 mL) or CyMe (1.0 mL) was added via syringe followed by the respective arene substrate (0.2 mmol, 2.0 equiv.). If the reaction was performed at temperatures below 30 °C, the tube was cooled on dry ice during the addition of the arene. The tube was sealed and the reaction was stirred at the respective temperature for the indicated reaction time. The mixture was then quenched with NEt$_3$ (0.3 M solution in PhMe, 200 µL) and applied directly on a silica gel column equilibrated with *i*-hexanes. The mixture was flushed with *i*-hexanes (100 mL) and then purified via flash column chromatography on silica gel (*i*-hexanes/MTBE eluents) to yield the arylglycines as white solids. Regioisomeric ratios were determined either via ^{1}H-NMR- or HPLC analysis. *Deviations from the general protocol are indicated at the respective entry.*

Preparation of Racemic Reference Samples

Racemic reference samples for the determination of the enantiomeric ratios of the arylglycine derivates were prepared using bistriflimide (HNTf$_2$, added as stock solution in CH$_2$Cl$_2$: 0.2 M, 50 µL, 10 µmol, 10 mol%) instead of (*S,S*)-IDPi catalysts under the reaction conditions described in General Procedures D and E. *Deviations from the general protocol are indicated at the respective entry.*

7.1.4 Friedel–Crafts Reaction of Only-Hydrocarbon Arenes

ethyl (*R*)-2-((((9H-fluoren-9-yl)methoxy)carbonyl)amino)-2-(p-tolyl)acetate (56)

Prepared following *General Procedure D*, from *N,O*-acetal **54** (38.4 mg, 0.1 mmol, 1.0 equiv.) and toluene (**3**, 1.0 mL) using **IDPi-13-c** (11.7 mg, 5 µmol, 5 mol%) over 5 d reaction time at 15 °C. Purification by silica gel flash column chromatography (eluent: *i*-hexanes/MTBE 4:1) gave **56** as white solid (23 mg, 55 µmol, 55%).
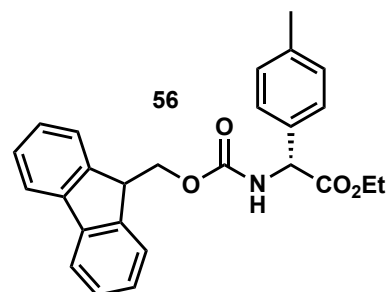
TLC:	R_f (*i*-hexanes/MTBE 2:1) = 0.71.
^{1}H-NMR:	(501 MHz, CDCl$_3$): mixture of two rotamers with a ratio of 1:0.20. δ = 7.76 (d, J = 7.6 Hz, 2H), 7.58 (d, J = 7.5 Hz, 2H), 7.40 (t, J = 7.6 Hz, 2H), 7.34–7.23 (m, 4H), 7.18 (d, J = 6.9 Hz, 2H), 5.82 (d, J = 6.8 Hz, 1H$_{maj}$), 5.70 (s, 1H$_{min}$), 5.33 (d, J = 6.9 Hz, 1H$_{maj}$), 5.12 (s, 1H$_{min}$), 4.44–4.32 (m, 2H), 4.30–4.10 (m, 3H), 2.35 (s, 3H), 1.22 (t, J = 6.7 Hz, 3H).
^{13}C-NMR:	(126 MHz, CDCl3): δ = 171.15, 155.51, 144.03, 143.93, 141.43, 138.55, 133.91, 129.78, 127.83, 127.20, 125.24, 120.12, 67.26, 62.06, 57.88, 47.30, 21.31, 14.16.
ESI-HRMS:	calculated for C$_{26}$H$_{25}$NNaO$_4$ ([M+Na]$^+$): 438.16813, found: 438.16767.
HPLC:	(Chiralpak IG-3, *n*-heptane/*i*-PrOH 95:5, 298 K, 254 nm): t_R (major) = 32.0 min, t_R (minor) = 36.1 min, e.r. = 96:4 (92% e.e.).
$[\alpha]_D^{25}$:	–76.9 (c = 0.14, CHCl$_3$).
r.r.:	>20:1 (favoring the *para* isomer), determined via HPLC analysis.

ethyl (*R*)-2-((((9H-fluoren-9-yl)methoxy)carbonyl)amino)-2-(4-ethylphenyl)acetate (189)

Prepared following *General Procedure D*, from *N,O*-acetal **54** (38.4 mg, 0.1 mmol, 1.0 equiv.) and ethylbenzene (**4**, 1.0 mL) using **IDPi-13-c** (11.7 mg, 5 μmol, 5 mol%) over 5 d reaction time at 30 °C. Purification by silica gel flash column chromatography (eluent: *i*-hexanes/MTBE 4:1) gave **189** as white solid (30 mg, 70 μmol, 70%).
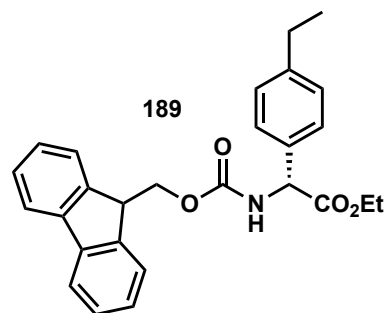
TLC:	R_f (*i*-hexanes/MTBE 2:1) = 0.62.
^{1}H-NMR:	(501 MHz, CDCl$_3$): mixture of two rotamers with a ratio of 1:0.18. δ = 7.77 (d, J = 7.6 Hz, 2H), 7.60 (d, J = 7.5 Hz, 2H), 7.40 (t, J = 7.5 Hz, 2H), 7.35–7.26 (m, 4H), 7.21 (d, J = 7.6 Hz, 2H), 5.85 (d, J = 7.5 Hz, 1H$_{maj}$), 5.73 (s, 1H$_{min}$), 5.36 (d, J = 7.5 Hz, 1H$_{maj}$), 5.16 (s, 1H$_{min}$), 4.43–4.36 (m, 2H), 4.31–4.11 (m, 3H), 2.66 (q, J = 7.6 Hz, 2H), 1.25 (t, J = 7.6 Hz, 3 H), 1.24 (t, J = 7.0 Hz, 3H).
^{13}C-NMR:	(126 MHz, CDCl$_3$): δ = 171.15, 155.52, 144.78, 144.01, 143.90, 141.41, 134.03, 128.57, 127.81, 127.23, 127.18, 125.22, 120.09, 67.23, 62.01, 57.88, 47.28, 28.65, 15.50, 14.15.
ESI-HRMS:	calculated for C$_{27}$H$_{27}$NNaO$_4$ ([M+Na]$^+$): 452.18378, found: 452.18319.
HPLC:	(Chiralpak IB-3 column, *n*-heptane/*i*-PrOH 95:5, 298 K, 254 nm): t_R (minor) = 11.1 min, t_R (major) = 14.7 min, e.r. = 97.5:2.5 (95% e.e.).
$[\alpha]_D^{25}$:	–64.4 (c = 0.17, CHCl$_3$).
r.r.:	>20:1 (favoring the *para* isomer), determined via ^{1}H-NMR analysis.

ethyl (*R*)-2-((((9H-fluoren-9-yl)methoxy)carbonyl)amino)-2-(4-propylphenyl)acetate (190)

Prepared following *General Procedure D*, from *N,O*-acetal **54** (38.4 mg, 0.1 mmol, 1.0 equiv.) and *n*-propylbenzene (**57**, 1.0 mL) using **IDPi-13-c** (11.7 mg, 5 μmol, 5 mol%) over 5 d reaction time at 30 °C. Purification by silica gel flash column chromatography (eluent: *i*-hexanes/MTBE 4:1) gave **190** as white solid (21 mg, 47 μmol, 47%).

TLC:	R_f (*i*-hexanes/EtOAc 3:1) = 0.68.

^{1}H-NMR:	(501 MHz, CDCl$_3$): mixture of two rotamers with a ratio of 1:0.19. δ = 7.76 (d, J = 7.6 Hz, 2H), 7.59 (d, J = 7.5 Hz, 2H), 7.39 (t, J = 7.5 Hz, 2H), 7.33–7.20 (m, 4H), 7.18 (d, J = 7.7 Hz, 3H), 5.80 (d, J = 7.5 Hz, 1H$_{maj}$), 5.67 (s, 1H$_{min}$), 5.34 (d, J = 7.5 Hz, 1H$_{maj}$), 5.14 (s, 1H$_{min}$), 4.39 (qd, J = 10.7, 7.2 Hz, 2H), 4.29–4.10 (m, 3H), 2.58 (t, J = 7.7 Hz, 2H), 1.64 (h, J = 7.4 Hz, 2H), 1.23 (t, J = 7.1 Hz, 3H), 0.94 (t, J = 7.3 Hz, 3H).
^{13}C-NMR:	(126 MHz, CDCl$_3$): δ = 171.18, 155.55, 144.03, 143.92, 143.32, 141.43, 134.02, 129.19, 127.84, 127.21, 127.15, 125.24, 120.12, 67.26, 62.03, 57.90, 47.30, 37.86, 24.56, 14.18, 14.00.
ESI-HRMS:	calculated for C$_{28}$H$_{29}$NNaO$_4$ ([M+Na]$^+$): 466.19943, found: 466.19925.
HPLC:	(Chiralpak IB-3 column, *n*-heptane/*i*-PrOH 96:4, 298 K, 254 nm): t$_R$ (minor) = 12.4 min, t$_R$ (major) = 17.1 min, e.r. = 95:5 (90% e.e.).
$[\propto]_D^{25}$:	–56.0 (c = 0.10, CHCl$_3$).
r.r.	>20:1 (favoring the *para* isomer), determined via ^{1}H-NMR analysis.

ethyl (*R*)-2-((((9H-fluoren-9-yl)methoxy)carbonyl)amino)-2-(4-butylphenyl)acetate (191)

Prepared following *General Procedure D*, from *N,O*-acetal **54** (38.4 mg, 0.1 mmol, 1.0 equiv.) and *n*-butylbenzene (**3d**, 1.0 mL) using **IDPi-13-c** (11.7 mg, 5 µmol, 5 mol%) over 5 d reaction time at 30 °C. Purification by silica gel flash column chromatography (eluent: *i*-hexanes/MTBE 4:1) gave **191** as white solid (22 mg, 48 µmol, 48%).

TLC:	R$_f$ (*i*-hexanes/MTBE 2:1) = 0.83.
^{1}H-NMR:	(501 MHz, CDCl$_3$): mixture of two rotamers with a ratio of 1:0.19. δ = 7.76 (d, J = 7.6 Hz, 2H), 7.59 (d, J = 7.5 Hz, 2H), 7.40 (t, J = 7.5 Hz, 2H), 7.34–7.26 (m, 4H), 7.18 (d, J = 7.7 Hz, 2H), 5.81 (d, J = 7.5 Hz, 1H$_{maj}$), 5.68 (s, 1H$_{min}$), 5.35 (d, J = 7.5 Hz, 1H$_{maj}$), 5.14 (s, 1H$_{min}$), 4.39 (qd, J = 10.7, 7.2 Hz, 2H), 4.31–4.11 (m, 3H), 2.61 (t, J = 7.8 Hz, 2H), 1.60 (p, J = 7.6 Hz, 2H), 1.36 (h, J = 7.4 Hz, 2H), 1.23 (t, J = 7.1 Hz, 3H), 0.93 (t, J = 7.3 Hz, 3H).
^{13}C-NMR:	(126 MHz, CDCl$_3$): δ = 171.18, 155.54, 144.03, 143.91, 143.53, 141.43, 133.98, 129.13, 127.83, 127.20, 127.16, 125.24, 120.11, 67.26, 62.02, 57.90, 47.30, 35.47, 33.61, 22.52, 14.17, 14.08.
ESI-HRMS:	calculated for C$_{29}$H$_{31}$NNaO$_4$ ([M+Na]$^+$): 480.21508, found: 480.21486.

HPLC:	(Chiralpak IB-3 column, *n*-heptane/*i*-PrOH 95:5, 298 K, 254 nm): t_R (minor) = 10.4 min, t_R (major) = 13.9 min, e.r. = 96:4 (92% e.e.).
$[\propto]_D^{25}$:	–63.9 (c = 0.12, CHCl$_3$).
r.r.	>20:1 (favoring the *para* isomer), determined via ^{1}H-NMR analysis.

ethyl (*R*)-2-((((9H-fluoren-9-yl)methoxy)carbonyl)amino)-2-(4-isopropylphenyl)acetate (192)

Prepared following *General Procedure D* with deviation, from *N*,*O*-acetal **54** (38.4 mg, 0.1 mmol, 1.0 equiv.) and cumene (**5**, 1.0 mL) using **IDPi-13-c** (13.4 mg, 5 µmol, 5 mol%) over 3 d reaction time in a 4 mL screwcap vial under an atmosphere of argon. Purification by silica gel flash column chromatography (eluent: *i*-hexanes/MTBE 4:1) gave **192** as white solid (25 mg, 56 µmol, 56%).

192
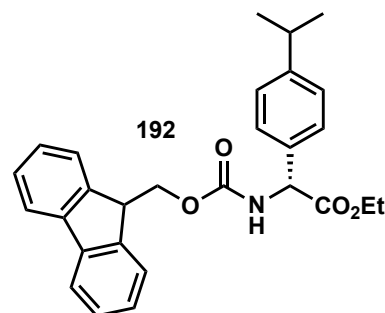
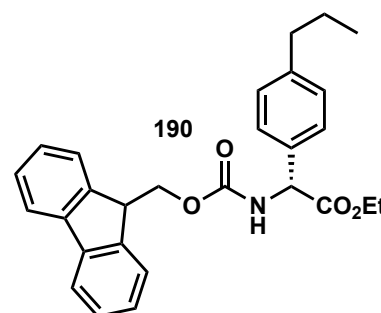|	
TLC:	R$_f$ (*i*-hexanes/MTBE 2:1) = 0.69.
^{1}H-NMR:	(501 MHz, CDCl$_3$): mixture of two rotamers with a ratio of 1.0:0.21. δ = 7.76 (d, J = 7.6 Hz, 2H), 7.59 (d, J = 7.5 Hz, 2H), 7.40 (t, J = 7.5 Hz, 2H), 7.34–7.24 (m, 4H), 7.23 (d, J = 7.9 Hz, 2H), 5.80 (d, J = 7.4 Hz, 1H$_{maj}$), 5.67 (s, 1H$_{min}$), 5.35 (d, J = 7.5 Hz, 1H$_{maj}$), 5.15 (s, 1H$_{min}$), 4.39 (qd, J = 10.7, 7.2 Hz, 2H), 4.31–4.08 (m, 3H), 2.91 (hept, J = 7.0 Hz, 1H), 1.31 – 1.20 (m, 9H).
^{13}C-NMR:	(126 MHz, CDCl$_3$): δ = 171.18, 155.55, 149.40, 144.03, 143.91, 141.43, 134.08, 127.83, 127.21, 127.18, 125.24, 120.11, 67.26, 62.03, 57.89, 47.30, 33.96, 24.03, 14.18.
ESI-HRMS:	calculated for C$_{28}$H$_{29}$NNaO$_4$ ([M+Na]$^+$): 466.19888, found: 466.19887.
HPLC:	(Chiralpak IB-3 column, *n*-heptane/*i*-PrOH 95:5, 298 K, 254 nm): t_R (minor) = 10.7 min, t_R (major) = 15.4 min, e.r. = 97:3 (94% e.e.).

ethyl (*R*)-2-((((9H-fluoren-9-yl)methoxy)carbonyl)amino)-2-(4-(tert-butyl)phenyl)acetate (193)

Prepared following *General Procedure D*, from *N,O*-acetal **54** (38.4 mg, 0.1 mmol, 1.0 equiv.) and *t*-butylbenzene (**59**, 1.0 mL) using **IDPi-13-c** (11.7 mg, 5 µmol, 5 mol%) over 5 d reaction time at 30 °C. Purification by silica gel flash column chromatography (eluent: *i*-hexanes/MTBE 4:1) gave **193** as white solid (16 mg, 35 µmol, 35%).
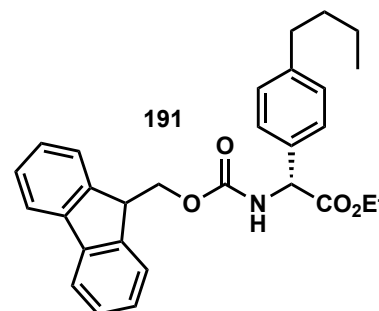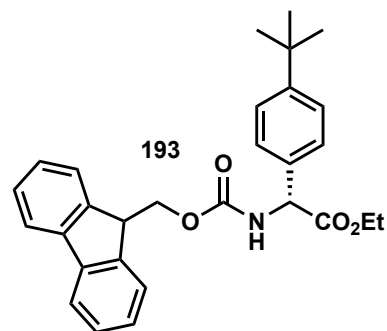
TLC:	R_f (*i*-hexanes/MTBE 2:1) = 0.78.
¹H-NMR:	(501 MHz, CDCl3): mixture of two rotamers with a ratio of 1.0:0.20. δ = 7.76 (d, J = 7.6 Hz, 2H), 7.59 (d, J = 7.5 Hz, 2H), 7.42–7.36 (m, 4H), 7.34–7.28 (m, 4H), 5.80 (d, J = 7.6 Hz, $1H_{maj}$), 5.66 (s, $1H_{min}$), 5.36 (d, J = 7.5 Hz, $1H_{maj}$), 5.16 (s, $1H_{min}$), 4.39 (qd, J = 10.7, 7.2 Hz, 2H), 4.32–4.11 (m, 3H), 1.32 (s, 9H), 1.24 (t, J = 7.1 Hz, 3H).
¹³C-NMR:	(126 MHz, CDCl₃): δ = 171.17, 155.57, 151.67, 144.03, 143.91, 141.43, 133.68, 127.83, 127.21, 126.94, 126.06, 125.24, 120.11, 67.26, 62.03, 57.80, 47.30, 34.74, 31.43, 14.19.
ESI-HRMS:	calculated for $C_{29}H_{31}NNaO_4$ ([M+Na]⁺): 480.21508, found: 480.21474.
HPLC:	(Chiralpak IB-3 column, *n*-heptane/*i*-PrOH 96:4, 298 K, 254 nm): t_R (minor) = 11.4 min, t_R (major) = 17.3 min, e.r. = 97:3 (94% e.e.).
$[\alpha]_D^{25}$**:**	–71.2 (c = 0.12, CHCl₃).
r.r.	93.5:6.5 (favoring the *para* isomer), determined via HPLC analysis.

ethyl (*R*)-2-((((9H-fluoren-9-yl)methoxy)carbonyl)amino)-2-(4-cyclopropylphenyl)acetate (194)

Prepared following *General Procedure D*, from *N,O*-acetal **54** (38.4 mg, 0.1 mmol, 1.0 equiv.) and cyclopropylbenzene (**60**, 1.0 mL) using **IDPi-13-c** (11.7 mg, 5 μmol, 5 mol%) over 6 d reaction time at 20 °C. Purification by silica gel flash column chromatography (eluent: *i*-hexanes/MTBE 4:1) gave **194** as white solid (34 mg, 77 μmol, 77%).
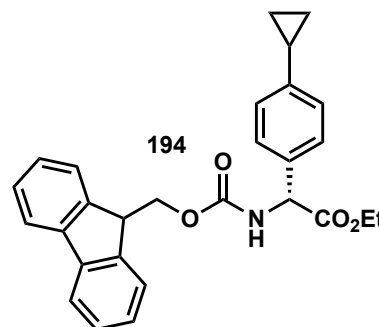
|	
TLC:	R_f (*i*-hexanes/MTBE 2:1) = 0.63.
¹H-NMR:	(501 MHz, CDCl₃): mixture of two regioisomers with a ratio of 1.0:0.05 and two rotamers of the main regioisomer with a ratio of 1.0:0.21. δ = 7.76 (d, J = 7.6 Hz, 2H), 7.58 (d, J = 7.6 Hz, 2H), 7.40 (t, J = 7.6 Hz, 2H), 7.34–7.15 (m, 4H), 7.06 (d, J = 7.8 Hz, 2H), 5.87 (d, J = 9.7 Hz, 1H$_{min}$), 5.81 (d, J = 7.4 Hz, 1H$_{maj}$), 5.70 (s, 1H$_{min}$), 5.40 (d, J = 9.7 Hz, 1H$_{min}$), 5.32 (d, J = 7.4 Hz, 1H$_{maj}$), 5.12 (s, 1H$_{min}$), 4.49 (s, 1H$_{min}$), 4.38 (qd, J = 10.8, 7.2 Hz, 2H$_{maj}$), 4.30–4.10 (m, 3H$_{maj}$), 3.68 (s, 1H$_{min}$), 1.89 (tt, J = 8.6, 4.9 Hz, 1H), 1.33 (t, J = 7.4 Hz, 3H$_{min}$), 1.23 (t, J = 7.2 Hz, 3H$_{maj}$), 1.01–0.94 (m, 2H), 0.73–0.66 (m, 2H).
¹³C-NMR:	(126 MHz, CDCl₃): δ = 171.13, 155.50, 144.72, 144.01, 143.91, 141.41, 133.78, 127.93 (C$_{min}$), 127.82 (C$_{maj}$), 127.20, 126.31, 125.23, 120.10, 67.24, 62.29 (C$_{min}$), 62.03 (C$_{maj}$), 57.84, 47.29, 15.30, 14.16, 9.54.
ESI-HRMS:	calculated for $C_{28}H_{27}NNaO_4$ ([M+Na]⁺): 464.18322, found: 464.18325.
HPLC:	(Chiralpak IB-3 column, *n*-heptane/*i*-PrOH 95:5, 298 K, 254 nm): t_R (minor) = 14.4 min, t_R (major) = 17.8 min, e.r. = 96:4 (92% e.e.).
$[\alpha]_D^{25}$:	–82.0 (c = 0.18, CHCl₃).
r.r.	95:5 (favoring the *para* isomer), determined via ¹H-NMR analysis.

ethyl (*R*)-2-((((9H-fluoren-9-yl)methoxy)carbonyl)amino)-2-(3,4-dimethylphenyl)acetate (195)

Prepared following *General Procedure D*, from *N,O*-acetal **54** (38.4 mg, 0.1 mmol, 1.0 equiv.) and *o*-xylene (**61**, 1.0 mL) using **IDPi-13-c** (11.7 mg, 5 μmol, 5 mol%) over 6 d reaction time at 0 °C. Purification by silica gel flash column chromatography (eluent: *i*-hexanes/MTBE 4:1) gave **195** as white solid (34 mg, 77 μmol, 77%).

TLC:	R_f (*i*-hexanes/MTBE 2:1) = 0.64.
^{1}H-NMR:	(501 MHz, CDCl$_3$): mixture of two rotamers with a ratio of 1:0.20. δ = 7.76 (d, J = 7.6 Hz, 2H), 7.59 (d, J = 7.4 Hz, 2H), 7.39 (t, J = 7.5 Hz, 2H), 7.34–7.23 (m, 2H), 7.18–7.02 (m, 3H), 5.80 (d, J = 7.5 Hz, 1H$_{maj}$), 5.67 (s, 1H$_{min}$), 5.30 (d, J = 7.4 Hz, 1H$_{maj}$), 5.12 (s, 1H$_{min}$), 4.44–4.32 (m, 2H), 4.30–4.09 (m, 3H), 2.27 (s, 3H), 2.25 (s, 3H), 1.23 (t, J = 7.1 Hz, 3H).
^{13}C-NMR:	(126 MHz, CDCl$_3$): δ = 171.25, 155.52, 144.03, 143.94, 141.41, 137.43, 137.24, 134.22, 130.31, 128.51, 127.82, 127.19, 125.24, 124.66, 120.10, 67.26, 62.01, 57.92, 47.28, 19.97, 19.64, 14.18.
ESI-HRMS:	calculated for C$_{27}$H$_{27}$NNaO$_4$ ([M+Na]$^+$): 452.18323, found: 452.18340.
HPLC:	(Chiralpak IB-3 column, *n*-heptane/*i*-PrOH 96:4, 298 K, 254 nm): t_R (minor) = 13.3 min, t_R (major) = 18.1 min, e.r. = 94.5:4.5 (89% e.e.).
$[\alpha]_D^{25}$:	–81.0 (c = 0.11, CHCl$_3$).
r.r.	>20:1 (favoring the *para* isomer), determined via HPLC analysis and ^{1}H-NMR analysis.

ethyl (*R*)-2-((((9H-fluoren-9-yl)methoxy)carbonyl)amino)-2-(3,4-diethylphenyl)acetate (196)

Prepared following *General Procedure D*, from *N,O*-acetal **54** (38.4 mg, 0.1 mmol, 1.0 equiv.) and 1,2-diethylbenzene (**62**, 1.0 mL) using **IDPi-13-c** (11.7 mg, 5 μmol, 5 mol%) over 6 d reaction time at 0 °C. Purification by silica gel flash column chromatography (eluent: *i*-hexanes/MTBE 4:1) gave **196** as white solid (38 mg, 79 μmol, 79%).
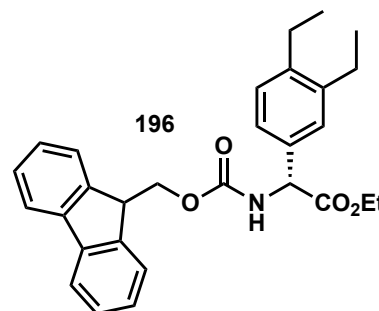
TLC:	R_f (*i*-hexanes/MTBE 2:1) = 0.74.

|	
^{1}H-NMR:	(501 MHz, CDCl$_3$): mixture of two rotamers with a ratio of 1:0.21. δ = 7.76 (d, J = 7.7 Hz, 2H), 7.60 (d, J = 7.5 Hz, 2H), 7.40 (t, J = 7.5 Hz, 2H), 7.34–7.28 (m, 2H), 7.23–7.09 (m, 3H), 5.79 (d, J = 7.5 Hz, 1H$_{maj}$), 5.66 (s, 1H$_{min}$), 5.34 (d, J = 7.6 Hz, 1H$_{maj}$), 5.18 (s, 1H$_{min}$), 4.39 (dt, J = 18.2, 9.1 Hz, 2H), 4.31–4.12 (m, 3H), 2.70–2.61 (m, 4H), 1.29–1.19 (m, 9H).
^{13}C-NMR:	(126 MHz, CDCl$_3$): δ = 171.28, 155.57, 144.03, 143.93, 142.60, 142.32, 141.41, 134.10, 128.96, 127.81, 127.19, 125.27, 125.24, 124.71, 120.10, 67.27, 61.95, 57.98, 47.28, 25.65, 25.31, 15.29, 15.19, 14.18.
ESI-HRMS:	calculated for C$_{29}$H$_{31}$NNaO$_4$ ([M+Na]$^+$): 480.21453, found: 480.21494.
HPLC:	(Chiralpak IB-3 column, *n*-heptane/*i*-PrOH 95:5, 298 K, 254 nm): t$_R$ (minor) = 9.7 min, t$_R$ (major) = 12.7 min, e.r. = 96.5:3.5 (93% e.e.).
$[\alpha]_D^{25}$:	–74.8 (c = 0.11, CHCl$_3$).
r.r.	>20:1 (favoring the *para* isomer), determined via HPLC analysis and ^{1}H-NMR analysis.

ethyl (*R*)-2-((((9H-fluoren-9-yl)methoxy)carbonyl)amino)-2-phenylacetate (63)

Prepared following *General Procedure D* with some deviations, from *N,O*-acetal **54** (9.6 mg, 0.025 mmol, 1.0 equiv.) and benzene (**1**, 0.25 mL) using **IDPi-13-f** (6.9 mg, 2.5 μmol, 10 mol%) over 5 d reaction time at 60 °C in a 1 mL pressure vial. Purification by preparative TLC (eluent: *i*-hexanes/EtOAc 3:1) gave **63** as white solid (5.3 mg, 13 μmol, 53%).
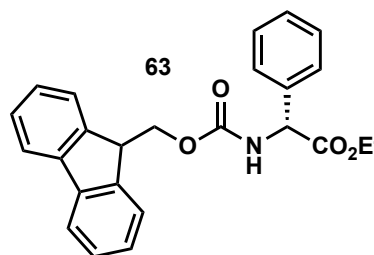
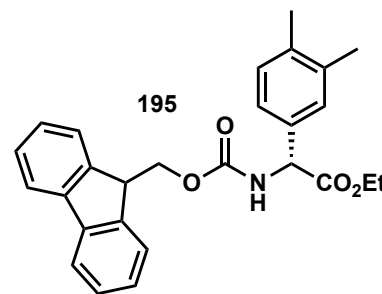|	
TLC:	R$_f$ (*i*-hexanes/EtOAc 3:1) = 0.63.
^{1}H-NMR:	(501 MHz, CDCl$_3$): mixture of two rotamers with a ratio of 1:0.19. δ = 7.76 (d, J = 7.6 Hz, 2H), 7.59 (d, J = 7.5 Hz, 2H), 7.44–7.28 (m, 9H), 5.86 (d, J = 7.4 Hz, 1H$_{maj}$), 5.75 (s, 1H$_{min}$), 5.38 (d, J = 7.5 Hz, 1H$_{maj}$), 5.15 (s, 1H$_{min}$), 4.40 (tt, J = 8.1, 7.4 Hz, 2H), 4.31–4.09 (m, 3H), 1.23 (t, J = 7.1 Hz, 3H).
^{13}C-NMR:	(126 MHz, CDCl$_3$): δ = 170.98, 155.51, 144.00, 143.88, 141.43, 136.87, 129.09, 128.67, 127.84, 127.26, 127.21, 125.22, 120.12, 67.27, 62.12, 58.13, 47.30, 14.14.
ESI-HRMS:	calculated for C$_{25}$H$_{23}$NNaO$_4$ ([M+Na]$^+$): 424.15193, found: 424.15206.
HPLC:	(Chiralpak IB-3 column, *n*-heptane/*i*-PrOH 95:5, 298 K, 254 nm): t$_R$ (minor) = 13.3 min, t$_R$ (major) = 19.3 min, e.r. = 81:19 (62% e.e.).

$[\propto]_D^{25}$:   −79.4 (c = 0.19, CHCl₃).

ethyl   2-((((9H-fluoren-9-yl)methoxy)carbonyl)amino)-2-(2,4-dimethylphenyl)acetate (197)

Prepared following *General Procedure D* with some deviations, from *N,O*-acetal **54** (76.7 mg, 0.2 mmol, 1.0 equiv.) and *m*-xylene (**64**, 2.0 mL, 0.1 M) using **IDPi-01-a** (17.9 mg, 10 µmol, 5 mol%) over 16 h reaction time at 30 °C in a flame dried Schlenk tube. Purification by silica gel flash column chromatography (eluent: *i*-hexanes/MTBE 4:1) gave **197** as white solid (68.7 mg, 0.16, 80%).
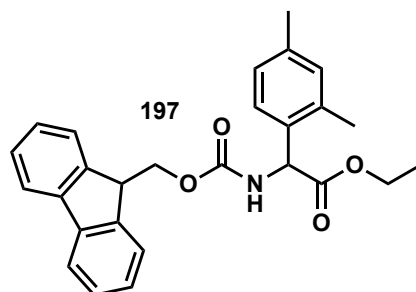
|	
TLC:	R*f* (*i*-hexanes/MTBE 2:1) = 0.60.
¹H-NMR:	(600 MHz, MeCN-d₃): δ = 7.82 (dt, J = 7.7, 1.0 Hz, 2H), 7.65 (dt, J = 7.5, 0.9 Hz, 2H), 7.42 – 7.38 (m, 2H), 7.31 (dtd, J = 13.4, 7.5, 1.1 Hz, 2H), 7.07 – 6.99 (m, 3H), 6.54 (d, J = 7.6 Hz, 1H), 5.39 (d, J = 7.6 Hz, 1H), 4.34 – 4.24 (m, 2H), 4.21 (t, J = 7.2 Hz, 1H), 4.11 (ddq, J = 38.1, 10.8, 7.1 Hz, 2H), 2.33 (s, 3H), 2.27 (s, 3H), 1.13 (t, J = 7.1 Hz, 3H).
¹³C-NMR:	(126 MHz, CDCl₃): δ = 171.98, 156.25, 144.65, 144.44, 141.61, 141.60, 138.94, 137.22, 132.59, 131.94, 128.32, 128.31, 127.71, 127.69, 127.53, 127.47, 125.84, 125.80, 120.62, 66.91, 62.03, 55.08, 47.31, 20.68, 19.04, 13.94.
ESI-HRMS:	calculated for C₂₇H₂₇N₁NaO₄ ([M+Na]⁺): 452.18323, found: 452.18285.
HPLC:	(Chiralpak IB-3 column, *n*-heptane/*i*-PrOH 95:5, 298 K, 254 nm): t_R (minor) = 13.3 min, t_R (major) = 19.3 min, e.r. = 60:40 (20% e.e.).

ethyl 2-((((9H-fluoren-9-yl)methoxy)carbonyl)amino)-2-mesitylacetate (198)

Prepared following *General Procedure D* with some deviations, from *N,O*-acetal **54** (9.6 mg, 0.025 mmol, 1.0 equiv.) and *m*-xylene (**65**, 0.25 mL, 0.1 M) using **IDPi-01-a** (2.23 mg, 1.25 µmol, 5 mol%) over 16 h reaction time at 30 °C in an oven dried screwcap vial. Purification by preparative thin layer chromatography (eluent: *i*-hexanes/MTBE 2:1) gave **198** as white solid (9.2 mg, 21 µmol, 83%).
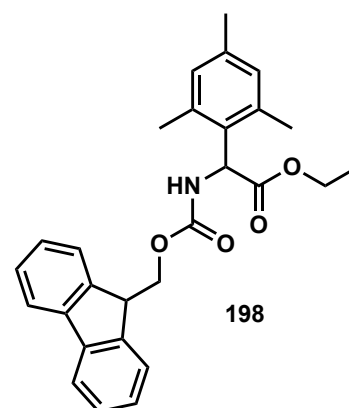
¹H-NMR: (600 MHz, MeCN-d₃): δ = 7.82 (d, J = 7.6 Hz, 2H), 7.68 – 7.63 (m, 2H), 7.44 – 7.37 (m, 2H), 7.34 – 7.24 (m, 2H), 6.87 (s, 2H), 6.30 (s, 1H), 5.70 (d, J = 7.2 Hz, 1H), 4.33 (t, J = 7.8 Hz, 2H), 4.22 (t, J = 6.9 Hz, 1H), 4.15 (dd, J = 29.0, 7.4 Hz, 2H), 2.29 (s, 6H), 2.24 (s, 3H), 1.15 (t, J = 7.1 Hz, 3H).

¹³C-NMR: (126 MHz, CDCl₃): δ = 171.63, 155.62, 143.79, 141.29, 137.74, 136.85, 131.01, 130.01, 127.67, 127.05, 126.91, 125.11, 119.97, 67.14, 61.97, 53.61, 47.18, 21.21, 20.89, 20.22, 14.10.

ESI-HRMS: calculated for $C_{28}H_{29}N_1NaO_4$ ([M+Na]⁺): 466.19888, found: 466.19886.

HPLC: (Chiralpak OD-3 column, *n*-heptane/*i*-PrOH 90:10, 298 K, 254 nm): t_R (minor) = 27.4 min, t_R (major) = 9.3 min, e.r. = 55:45 (10% e.e.).

ethyl 2-((((9H-fluoren-9-yl)methoxy)carbonyl)amino)-2-(2,5-dimethylphenyl)acetate (199)

Prepared following *General Procedure D* with some deviations, from *N,O*-acetal **54** (9.6 mg, 0.025 mmol, 1.0 equiv.) and *p*-xylene (**6**, 0.25 mL, 0.1 M) using **IDPi-01-a** (2.23 mg, 1.25 µmol, 5 mol%) over 16 h reaction time at 30 °C in an oven dried screwcap vial. Purification by preparative thin layer chromatography (eluent: *i*-hexanes/MTBE 2:1) gave **199** as white solid (2.7 mg, 6.2 µmol, 25%).
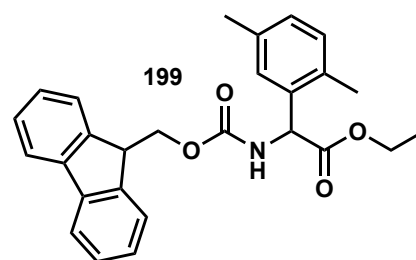
¹H-NMR: (600 MHz, MeCN-d₃): δ = 7.76 (d, J = 7.6 Hz, 2H), 7.59 (d, J = 7.5 Hz, 2H), 7.39 (t, J = 7.5 Hz, 2H), 7.30 (td, J = 7.4, 4.4 Hz, 2H), 7.14 – 7.02 (m, 3H), 5.72 (d, J = 7.5 Hz, 1H), 5.56 (d, J = 7.5 Hz, 1H), 4.44 – 4.32 (m, 2H), 4.29

            – 4.20 (m, 1H), 4.19 – 4.10 (m, 1H), 2.44 (s, 3H), 2.31 (d, J = 1.9 Hz, 5H), 1.22 (t, J = 7.1 Hz, 3H).

^{13}C-NMR: (126 MHz, CDCl$_3$): δ = 171.66, 155.65, 143.90, 141.43, 136.22, 135.06, 133.74, 131.01, 129.40, 127.83, 127.20, 127.06, 125.26, 120.11, 67.28, 61.97, 54.76, 47.29, 31.06, 29.85, 19.08.

ESI-HRMS: calculated for C$_{27}$H$_{27}$N$_1$NaO$_4$ ([M+Na]$^+$): 452.18323, found: 452.18357.

HPLC: (Chiralpak IB-3 column, *n*-heptane/*i*-PrOH 95:5, 298 K, 254 nm): t$_R$ (minor) = 10.3 min, t$_R$ (major) = 13.9 min, e.r. = 60:40 (20% e.e.).

ethyl 2-((((9H-fluoren-9-yl)methoxy)carbonyl)amino)-2-(azulen-1-yl)acetate (68)

Prepared following *General Procedure D* with some deviations, from *N,O*-acetal **54** (9.6 mg, 0.025 mmol, 1.0 equiv.) and azulene (**67**, 0.25 mL, 0.1 M) using **IDPi-01-a** (2.23 mg, 1.25 µmol, 5 mol%) in CyMe (0.25 mL, 0.1 M) over 24 h reaction time at 30 °C in an oven dried screwcap vial. Purification by preparative thin layer chromatography (eluent: *i*-hexanes/MTBE 2:1) gave **68** as blue solid (10.7 mg, 23.8 µmol, 95%).
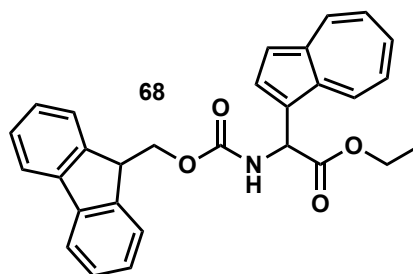
^{1}H-NMR: (600 MHz, MeCN-d$_3$): δ = 8.41 (t, J = 10.2 Hz, 2H), 8.35 – 8.32 (m, 1H), 8.32 – 8.29 (m, 2H), 8.29 – 8.26 (m, 2H), 7.87 (d, J = 3.9 Hz, 1H), 7.76 (d, J = 3.9 Hz, 1H), 7.57 (tdq, J = 9.8, 1.8, 0.9 Hz, 3H), 7.54 – 7.48 (m, 1H), 7.31 (d, J = 3.9 Hz, 1H), 7.27 (d, J = 4.0 Hz, 1H), 7.16 – 7.08 (m, 5H), 7.04 (dt, J = 13.2, 10.0 Hz, 2H), 6.28 (d, J= 8.2 Hz, 2H), 4.19 (qd, J = 7.1, 4.8 Hz, 3H), 4.13 (qd, J = 7.1, 1.0 Hz, 2H), 1.10 (t, J = 7.1 Hz, 3H).

^{13}C-NMR: (126 MHz, CDCl$_3$): δ = 172.97, 172.94, 141.19, 137.88, 137.84, 137.81, 137.69, 137.65, 137.48, 136.90, 136.88, 136.49, 136.42, 135.33, 133.51, 133.41, 133.18, 126.97, 126.95, 125.75, 125.67, 122.93, 122.91, 122.58, 122.38, 117.04, 61.14, 43.76, 43.68, 14.21, 14.07.

ESI-HRMS: calculated for C$_{29}$H$_{25}$N$_1$NaO$_4$ ([M+Na]$^+$): 474.16758, found: 474.16752.

HPLC: (Chiralpak IA-3 column, *n*-heptane/*i*-PrOH 80:20, 298 K, 254 nm): t$_R$ (1) = 7.4 min, t$_R$ (major) = 9.7 min, e.r. = 50:50 (0% e.e.).

7.1.5 Friedel–Crafts Reaction of Alkoxybenzenes and Heteroarenes

ethyl (R)-2-((((9H-fluoren-9-yl)methoxy)carbonyl)amino)-2-(4-methoxyphenyl)acetate (69)

Prepared following *General Procedure E*, from *N,O*-acetal **54** (38.4 mg, 0.1 mmol, 1.0 equiv.) and anisole (**26**, 22 µL, 0.2 mmol, 2.0 equiv.) in *n*-pentane (1.0 mL) using catalyst **IDPi-10-c** (13.4 mg, 5 µmol, 5 mol%) over 20 h reaction time at 30 °C. Purification by silica gel flash column chromatography (eluent: *i*-hexanes/EtOAc 10:1 → 3:1) gave **69** as white solid (40 mg, 92 µmol, 92%).
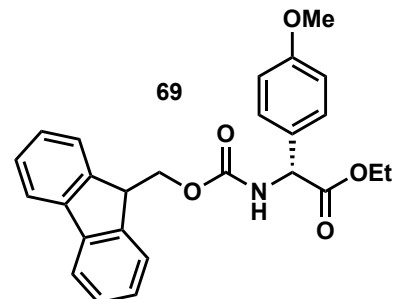
TLC: R_f (*i*-hexanes/EtOAc 3:1) = 0.55.

¹H-NMR: (501 MHz, CD$_2$Cl$_2$): mixture of two regioisomers with a ratio of 1:0.02 and two rotamers of the main regioisomer with a ratio of 1:0.17. δ = 7.78 (d, J = 7.6 Hz, 2H), 7.61 (d, J = 7.5 Hz, 2H), 7.41 (t, J = 7.5 Hz, 2H), 7.35–7.17 (m, 4H), 6.90 (d, J = 8.3 Hz, 2H), 5.95 (d, J = 8.6 Hz, 1H$_{min}$), 5.86 (d, J = 7.3 Hz, 1H$_{maj}$), 5.64 (s, 1H$_{min}$), 5.46 (d, J = 8.6 Hz, 1H$_{min}$), 5.26 (d, J = 7.2 Hz, 1H$_{maj}$), 5.06 (s, 1H$_{min}$), 4.44–4.33 (m, 2H), 4.26–4.09 (m, 3H), 3.84 (s, 3H$_{min}$), 3.80 (s, 3H$_{maj}$), 1.21 (t, J = 7.2 Hz, 3H).

Exemplary experiment at decreased temperature for detailed analysis of rotamers:

(600 MHz, CD$_2$Cl$_2$, 233 K): mixture of two regioisomers with a ratio of 1.0:0.02 and two rotamers of the main regioisomer with a ratio of 1.0:0.13. δ = 7.78 (dt, J = 7.6, 1.0 Hz, 2H$_{maj}$), 7.75 (dt, J = 7.6, 0.9 Hz, 2H$_{min}$) 7.59 (ddq, J = 7.4, 1.9, 0.9 Hz, 2H), 7.40 (t, J = 7.4 Hz, 2H$_{maj}$), 7.37 (t, J = 7.5 Hz, 2H$_{min}$), 7.30 (tdd, J = 7.3, 4.5, 1.0 Hz, 2H$_{maj}$), 7.29–7.26 (m, 2H$_{maj}$), 7.25–7.21 (m, 2H$_{min}$), 7.20–7.16 (m, 2H$_{min}$), 6.95 (td, J = 7.4, 1.0 Hz, 2H$_{min}$) 6.91–6.83 (m, 2H$_{maj}$), 6.02 (d, J = 7.0 Hz, 1H$_{maj}$), 5.87 (d, J = 6.6 Hz, 1H$_{min}$), 5.37 (d, J = 8.7 Hz, 1H$_{min}$), 5.21 (d, J = 6.9 Hz, 1H$_{maj}$), 5.09 (d, J = 7.5 Hz, 1H$_{min}$), 5.06 (d, J = 6.6 Hz, 1H$_{min}$), 4.39–4.34 (m, 1H), 4.33–4.28 (m, 1H), 4.22 – 4.12 (m, 2H), 4.06 (dq, J = 10.8, 7.1 Hz, 1H), 3.78 (s, 3H$_{min}$), 3.76 (s, 3H$_{maj}$), 1.16 (t, J = 7.2 Hz, 3H$_{maj}$), 1.15 (t, J = 7.1 Hz, 3H$_{min}$).

¹³C-NMR:	(126 MHz, CD_2Cl_2): δ = 171.30, 160.20, 155.64, 144.41, 144.33, 141.68, 129.36, 128.77, 128.06, 127.44, 125.45, 120.33, 114.59, 67.27, 62.27, 57.88, 55.69, 47.60, 14.22.

Exemplary experiment at decreased temperature for detailed analysis of rotamers:

(151 MHz, CD_2Cl_2, 233 K): δ = 170.93 (C_{maj}), 170.64 (C_{min}), 159.41 (C_{maj}), 159.37 (C_{min}), 155.06 (C_{maj}), 154.70 (C_{min}), 143.75 (d, J = 19.0 Hz, C_{maj}), 143.70 (d, J = 19.1 Hz, C_{min}), 141.06 (d, J = 2.6 Hz, C_{maj}), 140.99 (d, J = 14.4 Hz, C_{min}), 129.02 (C_{min}), 128.60 (C_{min}), 128.42 (C_{maj}), 128.25 (C_{min}), 127.65 (C_{maj}), 127.60 (d, J = 5.5 Hz, C_{min}), 127.02 (d, J = 2.3 Hz, C_{maj}), 126.97 (C_{min}), 125.05 (d, J = 2.9 Hz, C_{maj}), 124.94 (d, J = 11.0 Hz, C_{min}), 119.98 (C_{maj}), 119.96 (C_{min}), 119.88 (C_{min}), 113.93 (C_{min}), 113.91 (C_{maj}), 67.19 (C_{min}), 66.61 (C_{maj}), 62.22 (C_{min}), 62.09 (C_{maj}), 57.52 (C_{min}), 57.15 (C_{maj}), 55.30, 46.77 (C_{maj}), 46.67 (C_{min}), 13.83 (C_{maj}), 13.82 (C_{min}).

ESI-HRMS:	calculated for $C_{26}H_{25}NNaO_5$ ([M+Na]⁺): 454.16249, found: 454.16295.
2D-LC:	(1. dimension: 100 mm Zorbax RX-SIL, *n*-heptane/*i*-PrOH 99:1, 308 K, 220 nm): t_R (major regioisomer) = 3.2 min, t_R (minor regioisomer) = 3.8 min.
	(2. dimension: Chiralpak IC-3, *n*-heptane/*i*-PrOH 70:30, 298 K, 220 nm): t_R (minor enantiomer) = 8.0 min, t_R (major enantiomer) = 12.6 min, e.r. = 97.5:2.5 (95% e.e.).
$[\propto]_D^{25}$:	–86.6 (c = 0.13, CHCl₃).
r.r.	72:1 (favoring the *para* isomer), determined via HPLC analysis.

ethyl (*R*)-2-((((9H-fluoren-9-yl)methoxy)carbonyl)amino)-2-(4-(methoxy-*d₃*)phenyl)acetate (200)

Prepared following *General Procedure E*, from *N,O*-acetal **54** (38.4 mg, 0.1 mmol, 1.0 equiv.) and (methoxy-*d₃*)benzene (**70**, 22 μL, 0.2 mmol, 2.0 equiv.) in *n*-pentane (1.0 mL) using catalyst **IDPi-10-c** (13.4 mg, 5 μmol, 5 mol%) over 20 h reaction time at 30 °C. Purification by silica gel flash column chromatography (eluent: *i*-hexanes/EtOAc 10:1 → 3:1) gave **200** as white solid (41 mg, 95 μmol, 95%).
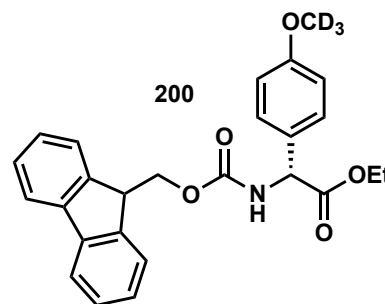
TLC:	R_f (*i*-hexanes/EtOAc 3:1) = 0.55.
¹H-NMR:	(501 MHz, CDCl₃): mixture of two rotamers with a ratio of 1:0.18. δ = 7.76 (d, J = 7.6 Hz, 2H), 7.59 (d, J = 7.5 Hz, 2H), 7.40 (t, J = 7.5 Hz, 2H), 7.35–7.17 (m, 4H), 6.89 (d, J = 8.3 Hz, 2H), 5.81 (d, J = 7.2 Hz, 1H$_{maj}$), 5.68 (s, 1H$_{min}$), 5.31 (d, J = 7.3 Hz, 1H$_{maj}$), 5.08 (s, 1H$_{min}$), 4.45–4.34 (m, 2H), 4.30–4.10 (m, 3H), 1.23 (t, J = 7.2 Hz, 3H).
¹³C-NMR:	(126 MHz, CDCl3): δ 171.22, 159.86, 155.50, 144.02, 143.91, 141.43, 128.94, 128.53, 127.83, 127.20, 125.23, 120.11, 114.46, 67.23, 62.03, 57.57, 47.30, 14.17.
ESI-HRMS:	calculated for $C_{26}H_{22}D_3NNaO_5$ ([M+Na]⁺): 457.18187, found: 457.18131.
2D-LC:	(1. dimension: 100 mm Zorbax RX-SIL, *n*-heptane/*i*-PrOH 99:1, 308 K, 220 nm): t$_R$ (major regioisomer) = 3.2 min, t$_R$ (minor regioisomer) = 3.8 min. (2. dimension: Chiralpak IC-3, *n*-heptane/*i*-PrOH 65:35, 298 K, 220 nm): t$_R$ (minor enantiomer) = 7.1 min, t$_R$ (major enantiomer) = 11.0 min, e.r. = 97.5:2.5 (95% e.e.).
$[\propto]_D^{25}$:	–85.3 (c = 0.12, CHCl₃).
r.r.	68:1 (favoring the *para* isomer), determined via HPLC analysis.

ethyl (*R*)-2-((((9H-fluoren-9-yl)methoxy)carbonyl)amino)-2-(4-(methylthio)phenyl)acetate (201)

Prepared following *General Procedure E*, from *N,O*-acetal **54** (38.4 mg, 0.1 mmol, 1.0 equiv.) and methyl(phenyl)sulfane (**71**, 24 µL, 0.2 mmol, 2.0 equiv.) in *n*-pentane (1.0 mL) using **IDPi-10-c** (13.4 mg, 5 µmol, 5 mol%) over 36 h reaction time at 30 °C. Purification by silica gel flash column chromatography (eluent: *i*-hexanes/EtOAc 10:1 → 3:1) gave **201** as white solid (33 mg, 74 µmol, 74%).
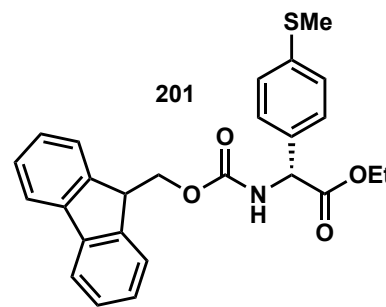
TLC:	R_f (*i*-hexanes/MTBE 2:1) = 0.58.
^{1}H-NMR:	(501 MHz, CDCl$_3$): mixture of two rotamers with a ratio of 1:0.22. δ = 7.76 (d, J = 7.6 Hz, 2H), 7.58 (d, J = 7.6 Hz, 2H), 7.40 (t, J = 7.5 Hz, 2H), 7.34–7.27 (m, 4H), 7.26–7.16 (m, 4H), 5.87 (d, J = 7.3 Hz, 1H$_{maj}$), 5.76 (s, 1H$_{min}$), 5.33 (d, J = 7.3 Hz, 1H$_{maj}$), 5.07 (s, 1H$_{min}$), 4.48–4.33 (m, 2H), 4.29–4.10 (m, 3H), 2.48 (s, 3H), 1.23 (t, J = 7.1 Hz, 3H).
^{13}C-NMR:	(126 MHz, CDCl$_3$): δ = 170.86, 155.45, 143.96, 143.86, 141.42, 139.32, 133.59, 127.84, 127.69, 127.19, 126.88, 125.19, 120.12, 67.24, 62.17, 57.67, 47.28, 15.73, 14.14.
ESI-HRMS:	calculated for C$_{26}$H$_{25}$NNaO$_4$S ([M+Na]$^+$): 470.13965, found: 470.13952.
2D-LC:	(1. dimension: 250 mm PVA-SIL, *n*-heptane/*i*-PrOH 99:1, 308 K, 220 nm): t$_R$ (major regioisomer) = 16.3 min, t$_R$ (minor regioisomer) = 17.5 min.
	(2. dimension: Chiralpak IC-3, *n*-heptane/*i*-PrOH 65:35, 298 K, 220 nm): t$_R$ (minor enantiomer) = 7.1 min, t$_R$ (major enantiomer) = 9.2 min, e.r. = 97:3 (94% e.e.).
$[\alpha]_D^{25}$:	–99.0 (c = 0.10, CHCl$_3$).
r.r.	42:1 (favoring the *para* isomer), determined via HPLC analysis.

ethyl (*R*)-2-((((9H-fluoren-9-yl)methoxy)carbonyl)amino)-2-(4-methoxy-3-methylphenyl)acetate (202)

Prepared following *General Procedure E,* from *N,O*-acetal **54** (38.4 mg, 0.1 mmol, 1.0 equiv.) and 1-methoxy-2-methylbenzene (**72**, 25 μL, 0.2 mmol, 2.0 equiv.) in *n*-pentane (1.0 mL) **IDPi-10-c** (13.4 mg, 5 μmol, 5 mol%) over 16 h reaction time at 30 °C. Purification by silica gel flash column chromatography (eluent: *i*-hexanes/EtOAc 10:1 → 3:1) gave **202** as white solid (42 mg, 94 μmol, 94%).
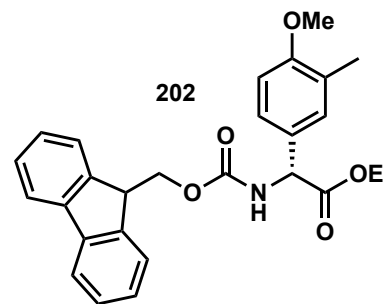
TLC:	R_f (*i*-hexanes/EtOAc 3:1) = 0.55.
^{1}H-NMR:	(501 MHz, CDCl$_3$): mixture of two rotamers with a ratio of 1:0.20. δ = 7.76 (d, J = 7.6 Hz, 2H), 7.59 (d, J = 7.5 Hz, 2H), 7.39 (t, J = 7.5 Hz, 2H), 7.34–7.27 (m, 2H), 7.23–7.07 (m, 2H), 6.80 (d, J = 8.4 Hz, 1H), 5.77 (d, J = 7.3 Hz, 1H$_{maj}$), 5.65 (s, 1H$_{min}$), 5.27 (d, J = 7.4 Hz, 1H$_{maj}$), 5.09 (s, 1H$_{min}$), 4.46–4.33 (m, 2H), 4.31–4.09 (m, 3H), 3.83 (s, 3H), 2.22 (s, 3H), 1.23 (t, J = 7.1 Hz, 3H).
^{13}C-NMR:	(126 MHz, CDCl$_3$): δ = 171.38, 158.08, 155.52, 144.05, 143.95, 141.43, 129.52, 128.39, 127.83, 127.50, 127.20, 125.91, 125.24, 120.11, 110.22, 67.24, 61.98, 57.66, 55.51, 47.30, 16.45, 14.19.
ESI-HRMS:	calculated for C$_{27}$H$_{27}$NNaO$_5$ ([M+Na]$^+$): 468.17814, found: 468.17859.
HPLC:	(Chiralpak AD-3 column, *n*-heptane/*i*-PrOH 94:6, 298 K, 254 nm): t_R (minor) = 19.1 min, t_R (major) = 20.5 min, e.r. = 95.5:4.5 (91% e.e.).
$[\alpha]_D^{25}$:	–90.8 (c = 0.13, CHCl$_3$).
r.r.	>20:1 (favoring the *para* isomer), determined via ^{1}H-NMR analysis.

ethyl (*R*)-2-((((9H-fluoren-9-yl)methoxy)carbonyl)amino)-2-(benzo[*d*][1,3]dioxol-5-yl)acetate (203)

Prepared following *General Procedure E*, from *N,O*-acetal **54** (38.4 mg, 0.1 mmol, 1.0 equiv.) and benzo[*d*][1,3]dioxole (**74**, 23 µL, 0.2 mmol, 2.0 equiv.) in *n*-pentane (1.0 mL) using **IDPi-10-c** (13.4 mg, 5 µmol, 5 mol%) over 36 h reaction time at 30 °C. Purification by silica gel flash column chromatography (eluent: *i*-hexanes/EtOAc 10:1 → 3:1) gave **203** as white solid (42 mg, 94 µmol, 94%).

TLC:	R_f (*i*-hexanes/EtOAc 3:1) = 0.53.
¹H-NMR:	(501 MHz, CDCl₃): mixture of two rotamers with a ratio of 1:0.20. δ = 7.76 (d, J = 7.6 Hz, 2H), 7.58 (d, J = 7.5 Hz, 2H), 7.40 (t, J = 7.5 Hz, 2H), 7.31 (t, J = 7.5 Hz, 2H), 6.90–6.69 (m, 3H), 5.97 (s, 2H), 5.83 (d, J = 7.2 Hz, 1H$_{maj}$), 5.67 (s, 1H$_{min}$), 5.26 (d, J = 7.2 Hz, 1H$_{maj}$), 4.99 (s, 1H$_{min}$), 4.51–4.33 (m, 2H), 4.29–4.08 (m, 3H), 1.24 (t, J = 7.2 Hz, 3H).
¹³C-NMR:	(126 MHz, CDCl₃): δ = 170.96, 155.44, 148.21, 147.95, 143.98, 143.87, 141.43, 130.66, 127.84, 127.20, 125.21, 120.96, 120.12, 108.70, 107.65, 101.45, 67.25, 62.16, 57.81, 47.28, 14.16.
ESI-HRMS:	calculated for $C_{26}H_{23}NNaO_6$ ([M+Na]⁺): 468.14175, found: 468.14216.
HPLC:	(Chiralpak IB-3 column, *n*-heptane/*i*-PrOH 95:5, 298 K, 254 nm): t_R (minor) = 20.6 min, t_R (major) = 24.1 min, e.r. = 96:4 (92% e.e.).
$[\alpha]_D^{25}$**:**	–70.5 (c = 0.11, CHCl₃).
r.r.	>20:1 (favoring the *para* isomer), determined via ¹H-NMR analysis.

ethyl (*R*)-2-((((9H-fluoren-9-yl)methoxy)carbonyl)amino)-2-(3-iodo-4-methoxyphenyl)acetate (204)

Prepared following *General Procedure E*, from *N,O*-acetal **54** (38.4 mg, 0.1 mmol, 1.0 equiv.) and 1-iodo-2-methoxybenzene (**73**, 26 µL, 0.2 mmol, 2.0 equiv.) in CyMe (1.0 mL) using **IDPi-10-c** (13.4 mg, 5 µmol, 5 mol%) over 6 d reaction time at 30 °C. Purification by silica gel flash column chromatography (eluent: *i*-hexanes/MTBE 4:1 → 2:1) gave **204** as white solid (42 mg, 75 µmol, 75%).

TLC:	R_f (*i*-hexanes/EtOAc 3:1) = 0.52.
^{1}H-NMR:	(501 MHz, CDCl$_3$): mixture of two regioisomers with a ratio of 1:0.02 and two rotamers of the main regioisomer with a ratio of 1:0.17. δ = 7.84–7.70 (m, 3H), 7.59 (d, J = 7.5 Hz, 2H), 7.40 (t, J = 7.5 Hz, 2H), 7.36–7.15 (m, 1H), 7.32 (q, J = 7.8 Hz, 2H), 6.79 (d, J = 8.4 Hz, 1H), 5.95 (d, J = 7.4 Hz, 1H$_{min}$), 5.87 (d, J = 7.2 Hz, 1H$_{maj}$), 5.71 (s, 1H$_{min}$), 5.44 (d, J = 7.2 Hz, 1H$_{min}$), 5.27 (d, J = 7.2 Hz, 1H$_{maj}$), 4.99 (s, 1H$_{min}$), 4.53–4.33 (m, 2H), 4.32–4.09 (m, 3H), 3.88 (s, 3H), 1.23 (t, J = 7.1 Hz, 3H).
^{13}C-NMR:	(126 MHz, CDCl3): δ = 170.70, 158.40, 155.40, 143.93, 143.84, 141.42, 138.06, 131.06, 128.70, 127.85, 127.23, 125.20, 120.12, 111.03, 86.47, 67.30, 62.28, 56.84, 56.57, 47.26, 14.16.
ESI-HRMS:	calculated for C$_{26}$H$_{24}$NNaO$_5$I ([M+Na]$^+$): 580.05914, found: 580.05978.
HPLC:	(Chiralpak IB-3 column, *n*-heptane/*i*-PrOH 97:3, 298 K, 254 nm): t$_R$ (minor) = 36.1 min, t$_R$ (major) = 40.1 min, e.r. = 95.5:4.5 (91% e.e.).
$[\alpha]_D^{25}$:	–66.7 (c = 0.11, CHCl$_3$).
r.r.	>20:1 (favoring the *para* isomer), determined via ^{1}H-NMR analysis.

ethyl (*R*)-2-((((9H-fluoren-9-yl)methoxy)carbonyl)amino)-2-(4-methoxy3 (trimethylsilyl)-phenyl)acetate (205)

Prepared following *General Procedure E*, from *N,O*-acetal **54** (38.4 mg, 0.1 mmol, 1.0 equiv.) and (2-methoxyphenyl)trimethylsilane (**75**, 38 µL, 0.2 mmol, 2.0 equiv.) in CyMe (1.0 mL) using **IDPi-10-c** (13.4 mg, 5 µmol, 5 mol%) over 20 h reaction time at 30 °C. Purification by silica gel flash column chromatography (eluent: *i*-hexanes/MTBE 3:1) gave **205** as white solid (42 mg, 83 µmol, 83%). *Since usage of bistriflimide as catalyst for the synthesis of a racemic sample exclusively gave the protodesilylated product **69**, HOTf was used as achiral acid catalyst.*

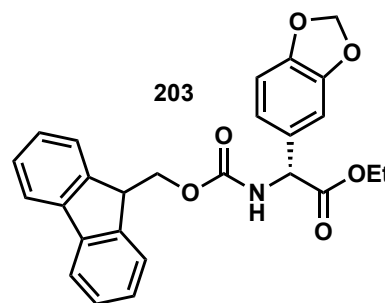|	
TLC:	R_f (*i*-hexanes/MTBE 2:1) = 0.55.
¹H-NMR:	(501 MHz, CDCl₃): mixture of two rotamers with a ratio of 1:0.19. δ = 7.77 (d, J = 7.6 Hz, 2H), 7.60 (dd, J = 7.5, 2.7 Hz, 2H), 7.40 (t, J = 7.5 Hz, 2H), 7.37–7.28 (m, 4H), 6.81 (d, J = 9 Hz, 1H), 5.77 (d, J = 7.5 Hz, 1H$_{maj}$), 5.64 (s, 1H$_{min}$), 5.34 (d, J = 7.5 Hz, 1H$_{maj}$), 5.19 (s, 1H$_{min}$), 4.40 (qd, J = 10.7, 7.2 Hz, 2H), 4.30–4.13 (m, 3H), 3.81 (s, 3H), 1.25 (t, J = 7.1 Hz, 3H), 0.28 (s, 9H).
¹³C-NMR:	(126 MHz, CDCl₃): δ = 171.37, 164.61, 155.56, 144.03, 143.93, 141.41, 133.99, 129.65, 129.05, 128.32, 127.82, 127.19, 125.26, 125.23, 120.10, 109.84, 67.26, 61.92, 57.72, 55.29, 47.28, 14.19, –0.91.
ESI-HRMS:	calculated for $C_{29}H_{33}NNaO_5Si$ ([M+Na]⁺): 526.20202, found: 526.20223.
HPLC:	(Chiralpak IB-3 column, *n*-heptane/*i*-PrOH 95:5, 298 K, 254 nm): t$_R$ (minor) = 9.7 min, t$_R$ (major) = 11.9 min, e.r. = 96:4 (92% e.e.).
$[\alpha]_D^{25}$**:**	–71.3 (c = 0.12, CHCl₃).
r.r.	>20:1 (favoring the *para* isomer), determined via ¹H-NMR analysis.

ethyl (*R*)-2-((((9H-fluoren-9-yl)methoxy)carbonyl)amino)-2-(4-(2-bromoethoxy)phenyl)acetate (206)

Prepared following *General Procedure E*, from *N,O*-acetal **54** (38.4 mg, 0.1 mmol, 1.0 equiv.) and (2-bromoethoxy)benzene (**76**, 40 mg, 0.2 mmol, 2.0 equiv.) in *n*-pentane (1.0 mL) using **IDPi-10-c** (13.4 mg, 5 μmol, 5 mol%) over 3 d reaction time at 30 °C. Purification by silica gel flash column chromatography (eluent: *i*-hexanes/MTBE 3:1 → 2:1) gave **206** as white solid (50 mg, 95 μmol, 95%).

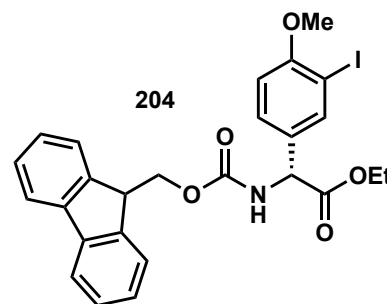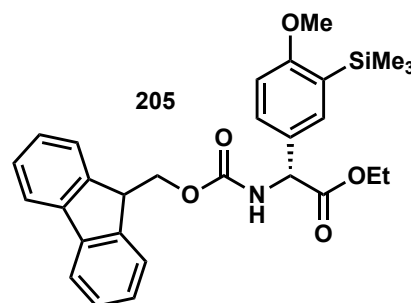|	
TLC:	R_f (*i*-hexanes/EtOAc 2:1) = 0.68.
^{1}H-NMR:	(501 MHz, CDCl$_3$): mixture of two rotamers with a ratio of 1:0.23. δ = 7.76 (d, J = 7.6 Hz, 2H), 7.58 (d, J = 7.5 Hz, 2H), 7.40 (t, J = 7.5 Hz, 2H), 7.35–7.17 (m, 4H), 6.90 (d, J = 8.4 Hz, 2H), 5.83 (d, J = 7.3 Hz, 1H$_{maj}$), 5.70 (s, 1H$_{min}$), 5.31 (d, J = 7.2 Hz, 1H$_{maj}$), 5.06 (s, 1H$_{min}$), 4.45–4.34 (m, 2H), 4.29 (t, J = 6.2 Hz, 2H), 4.27–4.10 (m, 3H), 3.63 (t, J = 6.2 Hz, 2H), 1.22 (t, J = 7.1 Hz, 3H).
^{13}C-NMR:	(126 MHz, CDCl$_3$): δ = 171.09, 158.36, 155.47, 143.99, 143.89, 141.43, 129.84, 128.64, 127.84, 127.20, 125.21, 120.12, 115.25, 68.03, 67.24, 62.10, 57.51, 47.29, 29.10, 14.16.
ESI-HRMS:	calculated for C$_{27}$H$_{26}$BrNNaO$_5$ ([M+Na]$^+$): 546.08866, found: 546.08899.
HPLC:	(Chiralpak AD-3 column, *n*-heptane/*i*-PrOH 92:8, 298 K, 254 nm): t$_R$ (minor) = 40.0 min, t$_R$ (major) = 44.7 min, e.r. = 98:2 (96% e.e.).
$[\propto]_D^{25}$:	–61.2 (c = 0.24, CHCl$_3$).
r.r.	>20:1 (favoring the *para* isomer), determined via ^{1}H-NMR analysis.

ethyl (R)-2-((((9H-fluoren-9-yl)methoxy)carbonyl)amino)-2-(4-(2-azidoethoxy)phenyl)acetate (207)

Prepared following *General Procedure E*, from *N,O*-acetal **54** (38.4 mg, 0.1 mmol, 1.0 equiv.) and (2-azidoethoxy)benzene (**77**, 32.6 mg, 0.2 mmol, 2.0 equiv.) in *n*-pentane (1.0 mL) using **IDPi-10-c** (13.4 mg, 5 μmol, 5 mol%) over 3 d reaction time at 30 °C. Purification by silica gel flash column chromatography (eluent: *i*-hexanes/MTBE 3:1) gave **207** as white solid (42 mg, 86 μmol, 86%).

TLC:	R_f (*i*-hexanes/EtOAc 2:1) = 0.53.
^{1}H-NMR:	(501 MHz, CDCl$_3$): mixture of two rotamers with a ratio of 1:0.28. δ = 7.76 (d, J = 7.7 Hz, 2H), 7.58 (d, J = 7.6 Hz, 2H), 7.40 (t, J = 7.5 Hz, 2H), 7.36–7.17 (m, 4H), 6.91 (d, J = 8.4 Hz, 2H$_{maj}$), 6.16 (s, 2H$_{min}$), 5.83 (d, J = 7.3 Hz, 1H$_{maj}$), 5.69 (s, 1H$_{min}$), 5.31 (d, J = 7.3 Hz, 1H$_{maj}$), 5.07 (s, 1H$_{min}$), 4.48–4.34 (m, 2H), 4.31–4.17 (m, 3H), 4.15 (t, J = 5.0 Hz, 2H), 3.60 (t, J = 4.9 Hz, 2H), 1.33 (t, J = 7.2 Hz, 3H$_{min}$), 1.22 (t, J = 7.1 Hz, 3H$_{maj}$).
^{13}C-NMR:	(126 MHz, CDCl$_3$): δ = 171.12, 158.51, 155.49, 144.00, 143.90, 141.44, 129.79, 128.63, 127.85, 127.21, 125.22, 120.13, 115.13, 67.25, 67.19, 62.10, 57.53, 50.26, 47.30, 14.17.
ESI-HRMS:	calculated for C$_{27}$H$_{26}$N$_4$NaO$_5$ ([M+Na]$^+$): 509.17954, found: 509.17994.
HPLC:	*achiral HPLC (for the determination of the regioisomeric ratio):* (Eclipse Plus C18, MeOH/H$_2$O – gradient: 60:40 – 5' – 90:10, 308 K, 220 nm): t$_R$ (minor) = 4.60 min, t$_R$ (major) = 4.7 min, r.r. = 98.5:1.5. *chiral HPLC (for the determination of the enantiomeric ratio):* (Chiralpak OJ-3 column, MeOH 100%, 298 K, 2204 nm): t$_R$ (major) = 6.9 min, t$_R$ (minor) = 10.4 min, e.r. = 98:2 (96% e.e.).
[∝]$_D^{25}$:	–81.1 (c = 0.11, CHCl$_3$).
r.r.	98.1:1.5 (favoring the *para* isomer), determined via HPLC analysis.

ethyl (*R*)-2-((((9H-fluoren-9-yl)methoxy)carbonyl)amino)-2-(4-(allyloxy)phenyl)acetate (208)

Prepared following *General Procedure E*, from *N,O*-acetal **54** (38.4 mg, 0.1 mmol, 1.0 equiv.) and (allyloxy)benzene (**78**, 27 μL, 0.2 mmol, 2.0 equiv.) in *n*-pentane (1.0 mL) using **IDPi-10-c** (13.4 mg, 5 μmol, 5 mol%) over 16 h reaction time at 30 °C. Purification by silica gel flash column chromatography (eluent: *i*-hexanes/MTBE 5:1 → 3:1) gave **208** as white solid (42 mg, 92 μmol, 92%).
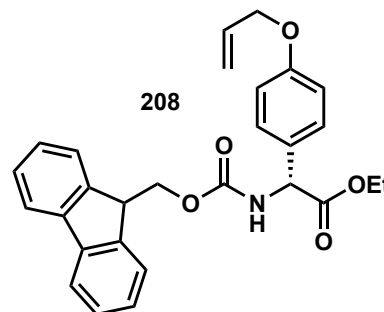
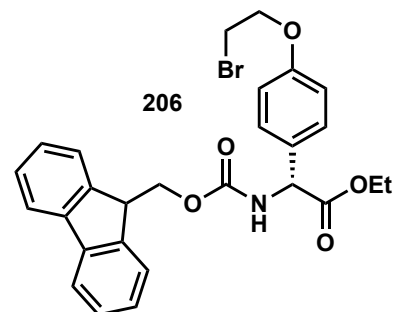|	
TLC:	R_f (*i*-hexanes/MTBE 2:1) = 0.67.
^{1}H-NMR:	(501 MHz, CDCl$_3$): mixture of two rotamers with a ratio of 1:0.21. δ = 7.76 (d, J = 7.6 Hz, 2H), 7.59 (d, J = 7.5 Hz, 2H), 7.40 (t, J = 7.5 Hz, 2H), 7.34–7.16 (m, 4H), 6.91 (d, J = 8.3 Hz, 2H), 6.05 (ddt, J = 16.2, 10.5, 5.3 Hz, 1H), 5.80 (d, J = 7.3 Hz, 1H$_{maj}$), 5.67 (s, 1H$_{min}$), 5.41 (d, J = 17.3 Hz, 1H), 5.35–5.26 (m, 2H), 5.08 (s, 1H$_{min}$), 4.54 (dt, J = 5.3, 1.6 Hz, 2H), 4.47–4.34 (m, 2H), 4.32–4.07 (m, 3H), 1.22 (t, J = 7.1 Hz, 3H).
^{13}C-NMR:	(126 MHz, CDCl$_3$): δ = 171.21, 158.91, 155.51, 144.02, 143.91, 141.43, 133.21, 129.10, 128.51, 127.83, 127.21, 125.23, 120.12, 117.97, 115.26, 69.00, 67.23, 62.03, 57.55, 47.30, 14.17.
ESI-HRMS:	calculated for C$_{28}$H$_{27}$N$_1$NaO$_5$ ([M+Na]$^+$): 480.17814, found: 480.17845.
HPLC:	(Chiralpak AD-3 column, *n*-heptane/*i*-PrOH 92:8, 298 K, 254 nm): t_R (minor) = 21.4 min, t_R (major) = 23.2 min, e.r. = 96.5:3.5 (93% e.e.).
$[\alpha]_D^{25}$:	–80.0 (c = 0.14, CHCl$_3$).
r.r.	>20.1 (favoring the *para* isomer), determined via ^{1}H-NMR analysis.

ethyl (*R*)-2-((((9H-fluoren-9-yl)methoxy)carbonyl)amino)-2-(4-(prop-2-yn-1-yloxy)phenyl)acetate (209)

Prepared following *General Procedure E*, from *N,O*-acetal **54** (38.4 mg, 0.1 mmol, 1.0 equiv.) and (prop-2-yn-1-yloxy)benzene)benzene (**79**, 25.7 µL, 0.2 mmol, 2.0 equiv.) in *n*-pentane (1.0 mL) using **IDPi-10-c** (13.4 mg, 5 µmol, 5 mol%) over 3 d reaction time at 30 °C. Purification by silica gel flash column chromatography (eluent: *i*-hexanes/MTBE 3:1) gave **209** as white solid (45 mg, 98 µmol, 98%).

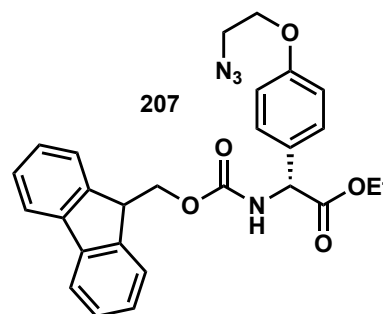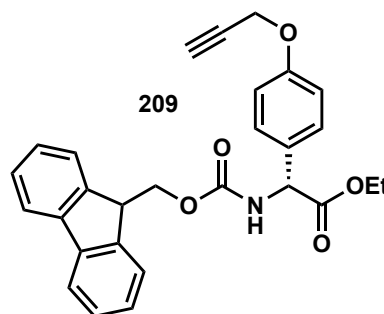|	
TLC:	R_f (*i*-hexanes/EtOAc 2:1) = 0.65.
^{1}H-NMR:	(501 MHz, CDCl$_3$): mixture of two rotamers with a ratio of 1:0.20. δ = 7.76 (d, J = 7.6 Hz, 2H), 7.58 (d, J = 7.5 Hz, 2H), 7.40 (t, J = 7.5 Hz, 2H), 7.36–7.17 (m, 4H), 6.97 (d, J = 8.3 Hz, 2H), 5.82 (d, J = 7.3 Hz, 1H$_{maj}$), 5.69 (s, 1H$_{min}$), 5.32 (d, J = 7.3 Hz, 1H$_{maj}$), 5.08 (s, 1H$_{min}$), 4.69 (d, J = 2.4 Hz, 2H), 4.50–4.33 (m, 2H), 4.31–4.07 (m, 3H), 2.53 (t, J = 2.4 Hz, 1H), 1.23 (t, J = 7.1 Hz, 3H).
^{13}C-NMR:	(126 MHz, CDCl$_3$): δ = 171.10, 157.83, 155.49, 144.00, 143.88, 141.43, 129.92, 128.55, 127.84, 127.21, 125.22, 120.12, 115.40, 78.49, 75.86, 67.23, 62.09, 57.52, 55.97, 47.30, 14.16.
ESI-HRMS:	calculated for C$_{28}$H$_{25}$N$_1$NaO$_5$ ([M+Na]$^+$): 478.16249, found: 478.16271.
HPLC:	(Chiralpak AD-3 column, *n*-heptane/*i*-PrOH 92:8, 298 K, 254 nm): t_R (minor) = 35.0 min, t_R (major) = 41.2 min, e.r. = 98:2 (96% e.e.).
$[\alpha]_D^{25}$:	–78.6 (c = 0.20, CHCl$_3$).
r.r.	>20:1 (favoring the *para* isomer), determined via HPLC analysis.

ethyl 2-((((9H-fluoren-9-yl)methoxy)carbonyl)amino)-2-(3-hydroxy-2,4-bis((triisopropylsilyl)oxy)phenyl)acetate (210)

Prepared following *General Procedure E,* from *N,O*-acetal **54** (38.4 mg, 0.1 mmol, 1.0 equiv.) and 2,6-bis((triisopropylsilyl)oxy)phenol (**93**, 87.8.0 mg, 0.2 mmol, 2.0 equiv.) in CyMe (1.0 mL) using **IDPi-01-a** (8.9 mg, 5 μmol, 5 mol%) over 20 h reaction time at 30 °C. Purification by silica gel flash column chromatography (eluent: *i*-hexanes/MTBE 3:1) gave a mixture of the regioisomers **210-a** and **210-b** as white solid (46 mg, 0.061 mmol, 61%).
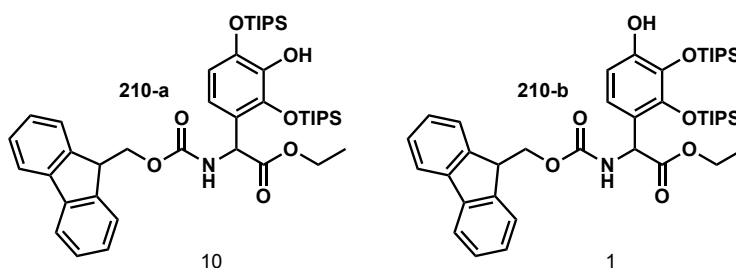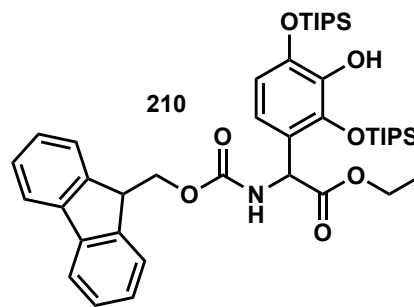
Formed regioisomers **210-a** and **210-b**.

¹H-NMR: (600 MHz, CDCl₃): mixture of two regioisomers **210-a** and **210-b** in a ratio of 10:1 and additional rotamers for each regioisomer. δ = 7.79 – 7.74 (m, 4H), 7.78 – 7.75 (m, 2H), 7.62 (dq, J = 7.6, 1.0 Hz, 1H), 7.59 (dq, J = 7.6, 0.9 Hz, 1H), 7.42 – 7.38 (m, 3H), 7.30 (tt, J = 7.5, 1.3 Hz, 2H), 6.69 (d, J = 8.6 Hz, 0H), 6.61 (d, J = 8.5 Hz, 1H), 6.45 (d, J = 8.4 Hz, 1H), 6.40 (d, J = 8.5 Hz, 0H), 6.11 (d, J = 8.6 Hz, 0H), 5.61 (s, 2H), 5.50 (s, 1H), 5.42 (d, J = 8.5 Hz, 0H), 5.39 (d, J = 6.6 Hz, 0H), 4.39 (dd, J = 10.5, 7.4 Hz, 0H), 4.36 (d, J = 0.9 Hz, 1H), 4.35 (s, 1H), 4.33 – 4.26 (m, 0H), 4.23 (t, J = 7.7 Hz, 1H), 4.23 (t, J = 7.5 Hz, 1H), 4.20 (d, J = 10.6 Hz, 0H), 4.20 (dd, J = 10.7, 7.1 Hz, 1H), 4.11 (d, J = 10.7 Hz, 0H), 4.11 (dd, J = 10.8, 7.2 Hz, 1H), 3.48 (q, J = 7.0 Hz, 2H), 1.39 (p, J= 7.5 Hz, 2H), 1.35 – 1.29 (m, 0H), 1.31 (dt, J = 14.9, 7.5 Hz, 3H), 1.21 (t, J = 7.0 Hz, 3H), 1.17 (t, J = 7.1 Hz, 1H), 1.17 (t, J = 7.1 Hz, 3H), 1.10 (d, J = 7.6 Hz, 10H), 1.09 (dt, J = 7.5, 1.0 Hz, 32H).

¹³C-NMR: (151 MHz, CDCl₃): δ = 171.91, 171.49, 156.17, 155.69, 147.52, 146.60, 143.92, 143.85, 143.83, 143.81, 143.78, 141.94, 141.20, 141.15, 141.12, 137.35, 134.84, 127.75, 127.69, 127.13, 127.09, 125.37, 125.34, 125.29, 125.28, 121.25, 120.51, 120.05, 120.01, 117.88, 116.04, 111.50, 110.00, 77.37, 77.16, 76.95, 67.28, 67.05, 66.13, 61.77, 61.65, 54.65, 52.89, 46.94, 46.92, 18.20, 18.20, 17.97, 17.97, 15.46, 14.27, 14.26, 14.10, 14.08, 13.59, 12.69.

ethyl 2-((((9H-fluoren-9-yl)methoxy)carbonyl)amino)-2-(4-acetoxybenzo[d][1,3]dioxol-5-yl)acetate (211)

Prepared following *General Procedure E*, from *N,O*-acetal **54** (38.4 mg, 0.1 mmol, 1.0 equiv.) and benzo[d][1,3]dioxol-4-yl acetate (**94**, 36 mg, 0.2 mmol, 2.0 equiv.) in CyMe (1.0 mL) using **IDPi-01-a** (8.9 mg, 5 μmol, 5 mol%) over 4 d reaction time at 30 °C. Purification by silica gel flash column chromatography (eluent: *i*-hexanes/EtOAc 10:1 → 3:1) gave **211** as white solid (25 mg, 49 μmol, 49%).
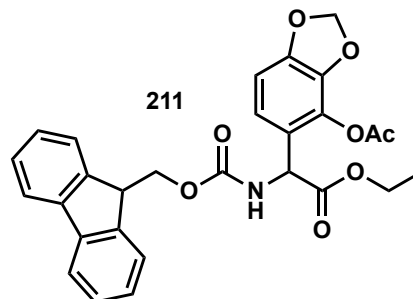
TLC: R_f (*i*-hexanes/EtOAc 3:1) = 0.55.

^{1}H-NMR: (501 MHz, CDCl$_3$): mixture of three regioisomers in a ratio of 3:2:1. δ = 7.78 (dd, J = 7.6, 1.0 Hz, 2H), 7.60 (d, J = 7.4 Hz, 2H), 7.40 (tq, J = 7.5, 1.0 Hz, 2H), 7.35 – 7.27 (m, 2H), 6.86 (d, J = 8.1 Hz, 1H), 6.78 (s, 2H$_{min}$), 6.74 (d, J = 8.1 Hz, 1H), 6.68 (s, 2H), 6.64 (d, J = 8.6 Hz, 1H), 6.04 (d, J = 7.7 Hz, 1H), 6.01 (q, J = 1.3 Hz, 2H), 5.92 (dd, J = 21.1, 7.5 Hz, 1H), 5.84 (d, J = 7.8 Hz, 1H), 5.43 (d, J = 7.8 Hz, 1H), 5.22 (d, J = 7.2 Hz, 0H), 4.37 (ddd, J = 17.1, 7.7, 4.0 Hz, 2H), 4.21 (q, J= 9.3 Hz, 2H), 4.08 (q, J = 7.1 Hz, 2H), 2.28 (d, J = 2.6 Hz, 3H), 2.01 (s, 3H), 2.01 (s, 2H), 1.23 (t, J = 7.1 Hz, 3H).

ESI-HRMS: calculated for $C_{28}H_{25}N_1NaO_8$ ([M+Na]$^+$): 526.14724, found: 526.14759.

ethyl (*R*)-2-((((9H-fluoren-9-yl)methoxy)carbonyl)amino)-2-(thipohen-2-yl)acetate (212)

Prepared following *General Procedure E*, from *N,O*-acetal **54** (38.4 mg, 0.1 mmol, 1.0 equiv.) and thiophene (**80**, 16 μL, 0.2 mmol, 2.0 equiv.) in CyMe (1.0 mL) using **IDPi-10-c** (13.4 mg, 5 μmol, 5 mol%) over 5 d reaction time at 30 °C. Purification by silica gel flash column chromatography (eluent: *i*-hexanes/MTBE 4:1) gave **212** as white solid (39 mg, 96 μmol, 96%).
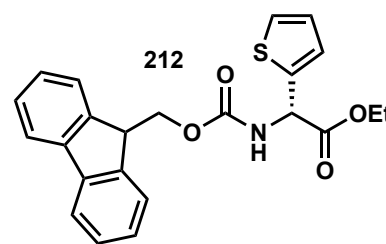
|	
TLC:	R$_f$ (*i*-hexanes/EtOAc 2:1) = 0.74.
^{1}H-NMR:	(600 MHz, CDCl$_3$, 253 K): mixture of two regioisomers with a ratio of 1:0.15 and two rotamers of the main regioisomer with a ratio of 1:0.19. δ = 7.78 (d, J = 7.6 Hz, 2H), 7.62–7.57 (m, 2H), 7.42 (t, J = 7.5 Hz, 2H), 7.33 (dddd, J = 8.5, 7.5, 2.0, 1.2 Hz, 2H), 7.29 (dd, J = 5.2, 1.2 Hz, 1H), 7.07 (dt, J = 3.6, 1.1 Hz, 1H), 6.99 (dd, J = 5.1, 3.6 Hz, 1H), 5.92 (d, J = 7.7 Hz, 1H$_{maj}$), 5.82 (d, J =7.7 Hz, 1H$_{min}$), 5.80 (d, J = 7.2 Hz, 1H$_{min}$), 5.74 (d, J = 7.2 Hz, 1H$_{min}$), 5.65 (dd, J = 7.7, 0.9 Hz, 1H$_{maj}$), 5.49 (d, J = 7.0 Hz, 1H$_{min}$), 5.48 (d, J = 7.7 Hz, 1H$_{min}$), 5.28 (d, J = 7.1 Hz, 1H$_{min}$), 4.48–4.34 (m, 2H), 4.32–4.15 (m, 3H), 1.28 (t, J = 7.1 Hz, 3H$_{maj}$), 1.26 (t, J = 7.3 Hz, 3H$_{min}$).
^{13}C-NMR:	(126 MHz, CDCl$_3$ at 253 K): δ = 170.65 (C$_{min}$), 170.05, 169.45 (C$_{min}$), 155.45 (C$_{min}$), 155.33, 154.69 (C$_{min}$), 143.75 (C$_{min}$), 143.67, 143.60, 143.59 (C$_{min}$), 143.54 (C$_{min}$), 141.27 (C$_{min}$), 141.25, 141.24, 141.22 (C$_{min}$), 139.51 (C$_{min}$), 138.82, 136.63 (C$_{min}$), 127.83, 127.79 (C$_{min}$), 127.77 (C$_{min}$), 127.31 (C$_{min}$), 127.28, 127.17, 126.99 (C$_{min}$), 126.26, 126.20 (C$_{min}$), 126.06, 126.04 (C$_{min}$), 125.98 (C$_{min}$), 125.22, 125.19, 125.17 (C$_{min}$), 125.15 (C$_{min}$), 125.06 (C$_{min}$), 125.03 (C$_{min}$), 123.26 (C$_{min}$), 120.13, 120.08 (C$_{min}$), 67.72 (C$_{min}$), 67.23, 67.02 (C$_{min}$), 62.73 (C$_{min}$), 62.60, 62.31 (C$_{min}$), 54.12 (C$_{min}$), 53.72 (C$_{min}$), 53.46, 46.97 (C$_{min}$), 46.91, 46.83 (C$_{min}$), 14.18 (C$_{min}$), 14.15.
ESI-HRMS:	calculated for C$_{23}$H$_{21}$N$_1$NaO$_4$S ([M+Na]$^+$): 430.10835, found: 430.10874.
HPLC:	(Chiralpak IB-3 column, *n*-heptane/*i*-PrOH 95:5, 298 K, 254 nm): t$_R$ (minor) = 14.1 min, t$_R$ (major) = 19.2 min, e.r. = 94.5:5.5 (89% e.e.).
[∝]$_D^{25}$:	–51.9 (c = 0.13, CHCl$_3$).
r.r.	86.5:13.5 (favoring the 2-position), determined via HPLC analysis. The connectivity of the thiophene ring of the major regioisomer to the glycine

scaffold was determined based on the coupling of the signals of the thiophene ring in the ^{1}H-NMR (signals at 7.29, 7.07 and 6.99 ppm).

ethyl (*R*)-2-((((9H-fluoren-9-yl)methoxy)carbonyl)amino)-2-(benzo[*b*]thiophen-2-yl)acetate (213)

Prepared following *General Procedure E*, from *N,O*-acetal **54** (38.4 mg, 0.1 mmol, 1.0 equiv.) and benzo[*b*]thiophen (**81**, 23 µL, 0.2 mmol, 2.0 equiv.) in *n*-pentane (1.0 mL) using **IDPi-10-c** (13.4 mg, 5 µmol, 5 mol%) over 4 d reaction time at 30 °C. Purification by silica gel flash column chromatography (eluent: *i*-hexanes/MTBE 4:1) gave **213** as white solid (45 mg, 98 µmol, 98%).
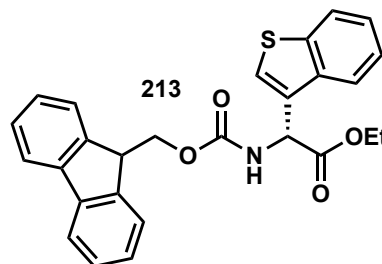
TLC:	R_f (*i*-hexanes/EtOAc 3:1) = 0.58.
^{1}H-NMR:	(600 MHz, CDCl$_3$, 233 K): mixture of two regioisomers with a ratio of 1:0.12 and two rotamers of the main regioisomer with a ratio of 1:0.16. δ = 7.92 (ddd, J = 7.9, 1.4, 0.7 Hz, 1H), 7.90 (ddd, J = 7.7, 1.3, 0.6 Hz, 1H), 7.77 (dd, J = 7.6, 0.9 Hz, 2H), 7.72 (t, J = 7.8 Hz, 1H$_{min}$), 7.61 (td, J = 7.7, 0.9 Hz, 1H$_{min}$), 7.58 (ddd, J = 7.5, 1.9, 1.0 Hz, 2H), 7.47–7.43 (m, 2H$_{min}$), 7.42 (d, J = 0.7 Hz, 1H), 7.39–7.33 (m, 2H$_{min}$), 7.30 (dtd, J = 10.8, 7.5, 1.1 Hz, 2H), 7.22–7.20 (m, 1H$_{min}$), 7.11–7.07 (m, 1 H$_{min}$), 6.92 (td, J = 7.5, 1.1 Hz, 1H$_{min}$), 6.80 (td, J = 7.5, 1.1 Hz, 1H$_{min}$), 6.10 (d, J = 7.5 Hz, 1H$_{min}$), 6.04 (d, J = 6.5 Hz, 1H$_{min}$), 5.92 (d, J = 6.8 Hz, 1H$_{min}$), 5.89 (d, J = 7.7 Hz, 1H$_{maj}$), 5.79 (dd, J = 7.7, 0.7 Hz, 1H, $_{maj}$), 5.73 (dd, 7.5, 0.9 Hz, 1H$_{min}$), 5.53 (dd, J = 6.5, 1.0 Hz, 1H$_{min}$), 5.45 (dd, J = 6.7, 0.8 Hz, 1H$_{min}$), 4.51–4.43 (m, 2H$_{min}$), 4.43–4.35 (m, 2H), 4.29 (dd, J = 10.8, 7.2 Hz, 1H), 4.23–4.20 (m, 1H), 4.16 (dd, J = 10.8, 7.1 Hz, 1H), 4.06 (dq, J = 10.8, 7.1 Hz, 1H$_{min}$), 1.29 (t, J = 7.2 Hz, 3H$_{min}$), 1.22 (t, J = 7.1 Hz, 3H, 27) 1.16 (t, J = 7.1 Hz, 3H$_{min}$).
^{13}C-NMR:	(151 MHz, CDCl$_3$ at 233 K): δ = 170.70, 169.76 (C$_{min}$), 169.61 (C$_{min}$), 155.51, 155.26 (C$_{min}$), 154.84 (C$_{min}$), 143.62, 143.51 (C$_{min}$), 143.50 (C$_{min}$), 143.42, 143.39 (C$_{min}$), 143.38 (C$_{min}$), 141.15, 141.13, 141.09 (C$_{min}$), 141.05 (C$_{min}$), 140.58 (C$_{min}$), 140.36, 139.62 (C$_{min}$), 139.38 (C$_{min}$), 139.04 (C$_{min}$),

136.73, 136.37 (C_{min}), 131.01 (C_{min}), 130.53, 127.79, 127.78, 127.70 (C_{min}), 127.67 (C_{min}), 127.13, 127.11, 127.03 (C_{min}), 125.74, 125.66 (C_{min}), 125.16, 125.21 (C_{min}), 125.16, 124.95, 124.85 (C_{min}), 124.82 (C_{min}), 124.77 (C_{min}), 124.73 (C_{min}), 124.68, 124.62 (C_{min}), 124.55 (C_{min}), 123.90 (C_{min}), 123.08 (C_{min}), 123.05, 123.01 (C_{min}), 122.44 (C_{min}), 122.14 (C_{min}), 122.00, 120.11, 120.14 (C_{min}), 120.09, 120.06 (C_{min}), 67.16 (C_{min}), 67.12 (C_{min}), 67.09, 62.91 (C_{min}), 62.68 (C_{min}), 62.50, 54.05 (C_{min}), 53.28 (C_{min}), 52.48, 46.75, 46.69 (C_{min}), 14.13, 14.07 (C_{min}).

ESI-HRMS: calculated for $C_{27}H_{23}N_1NaO_4S$ ([M+Na]$^+$): 480.12400, found: 480.12392.

2D-LC (1. dimension: 250 mm PVA-SIL, *n*-heptane/*i*-PrOH 95:5, 308 K, 220 nm): t_R (minor regioisomer) = 7.2 min, t_R (major regioisomer) = 7.7 min.

(2. dimension: Chiralpak IB-3, *n*-heptane/*i*-PrOH 80:20, 298 K, 220 nm): t_R (minor enantiomer) = 7.3 min, t_R (major enantiomer) = 8.4 min, e.r. = 96.5:3.5 (93% e.e.).

$[\alpha]_D^{25}$: –84.1 (c = 0.18, CHCl$_3$).

r.r. 85.5:15.5 (favoring the 3-position), determined via ^{1}H-NMR analysis and HPLC analysis. The connectivity of the benzothiophene ring of the major regioisomer to the glycine scaffold was determined based on the following characteristic cross peaks: HMBC (C19 to H16); NOESY (H16 to H20), see section 11 for further details.

ethyl (*R*)-2-((((9H-fluoren-9-yl)methoxy)carbonyl)amino)-2-(benzofuran-2-yl)acetate (214)

Prepared following *General Procedure E*, from *N,O*-acetal **54** (38.4 mg, 0.1 mmol, 1.0 equiv.) and benzofuran (**82**, 22 μL, 0.2 mmol, 2.0 equiv.) in CyMe (1.0 mL) using **IDPi-10-c** (13.4 mg, 5 μmol, 5 mol%) over 3 d reaction time at 30 °C. Purification by silica gel flash column chromatography (eluent: *i*-hexanes/MTBE 4:1) gave **214** as off-white solid (42 mg, 95 μmol, 95%).
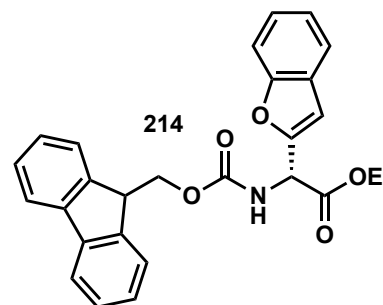
TLC:	R_f (*i*-hexanes/MTBE 2:1) = 0.44.
^{1}H-NMR:	(600 MHz, CDCl$_3$, 233 K): mixture of two regioisomers with a ratio of 1:0.13 and two rotamers of the main regioisomer with a ratio of 1:0.09. δ 7.78 (dd, J = 7.6, 0.9 Hz, 2H), 7.62 – 7.58 (m, 3H), 7.57–7.52 (m, 2H$_{min}$), 7.52–7.45 (m, 1H), 7.43–7.39 (m, 2H), 7.39–7.36 (m, 1H$_{min}$), 7.35–7.29 (m, 3H), 7.29–7.24 (m, 1H$_{min}$), 7.17 (td, J = 7.5, 1.1 Hz, 1H$_{min}$), 7.09 (td, J = 7.5, 1.1 Hz, 1H$_{min}$), 6.81 (s, 1H), 6.24 (s, 1H$_{min}$), 6.08 (d, J = 8.0 Hz, 1H), 5.94 (d, J = 7.4 Hz, 1H$_{min}$), 5.88 (d, J = 7.1 Hz, 1H$_{min}$), 5.65 (d, J= 7.9 Hz, 1H), 5.62 (dd, J = 7.4, 0.7 Hz, 1H$_{min}$), 5.25 (d, J = 7.1 Hz, 1H$_{min}$), 4.53–4.46 (m, 2H$_{min}$), 4.43–4.36 (m, 2H), 4.34–4.29 (m, 1H), 4.23 (t, J = 6.7 Hz, 1H), 4.21–4.17 (m, 1H), 1.25 (t, J = 7.2 Hz, 3H).
^{13}C-NMR:	(151 MHz, CDCl$_3$ at 233 K): δ = 170.35 (C$_{min}$), 168.54, 167.89 (C$_{min}$), 155.43 (C$_{min}$), 155.39, 155.29 (C$_{min}$), 154.67, 154.64 (C$_{min}$), 154.60 (C$_{min}$), 151.31 (C$_{min}$), 150.88, 143.58 (C$_{min}$), 143.54, 143.52 (C$_{min}$), 143.45, 143.43 (C$_{min}$), 143.40 (C$_{min}$), 143.38 (C$_{min}$), 141.19 (C$_{min}$), 141.15, 141.14, 141.07 (C$_{min}$), 127.80, 127.75 (C$_{min}$), 127.73 (C$_{min}$), 127.63, 127.13, 127.09 (C$_{min}$), 125.19, 125.16, 125.11 (C$_{min}$), 125.04 (C$_{min}$), 124.92, 124.86 (C$_{min}$), 124.73 (C$_{min}$), 123.18, 123.15 (C$_{min}$), 121.53, 120.17 (C$_{min}$), 120.12, 120.10, 116.13 (C$_{min}$), 111.93 (C$_{min}$), 111.57 (C$_{min}$), 111.52, 105.94, 105.38 (C$_{min}$), 67.23, 67.19 (C$_{min}$), 67.03 (C$_{min}$), 63.12 (C$_{min}$), 62.96, 62.62 (C$_{min}$), 52.58 (C$_{min}$), 52.16, 49.67 (C$_{min}$), 46.76 (C$_{min}$), 46.71, 46.62 (C$_{min}$).
ESI-HRMS:	calculated for C$_{27}$H$_{23}$N$_1$NaO$_5$ ([M+Na]$^+$): 464.14684, found: 464.14681.

2D-LC:	(1. dimension: 100 mm Zorbax RX-Sil, *n*-heptane/*i*-PrOH 99.5:0.5, 308 K, 220 nm): t_R (major regioisomer) = 3.1 min, t_R (minor regioisomer) = 3.3 min, r.r. = 82:18.

(2. dimension: Chiralpak IB-3, *n*-heptane/*i*-PrOH 80:20, 298 K, 220 nm): t_R (minor enantiomer) = 5.9 min, t_R (major enantiomer) = 6.9 min, e.r. = 97.5:2.5 (95% e.e.).

$[\alpha]_D^{25}$:	–95.8 (c = 0.12, CHCl$_3$).
r.r.	82:18 (favoring the 2-position), determined via ^{1}H-NMR analysis and HPLC analysis. The connectivity of the benzofurane ring of the major regioisomer to the glycine scaffold was determined based on the following characteristic cross peak: HMBC (C20 to H18), see section 11 for further details.

ethyl 2-((((9H-fluoren-9-yl)methoxy)carbonyl)amino)-2-(furan-2-yl)acetate (215)

Prepared following *General Procedure E*, from *N,O*-acetal **54** (38.4 mg, 0.1 mmol, 1.0 equiv.) and furan (**83**, 16 µL, 0.2 mmol, 2.0 equiv.) in CyMe (1.0 mL) using **IDPi-10-c** (13.4 mg, 5 µmol, 5 mol%) over 5 d reaction time at 30 °C. Purification by silica gel flash column chromatography (eluent: *i*-hexanes/MTBE 4:1) gave **215** as white solid (20 mg, 40 µmol, 40%).
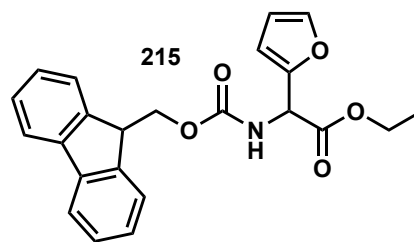
^{1}**H-NMR:**	(501 MHz, CDCl$_3$): δ = 7.84 (dd, J = 7.5, 1.0 Hz, 2H), 7.67 (d, J = 7.5 Hz, 2H), 7.48 (s, 1H), 7.42 (tt, J = 7.5, 0.9 Hz, 2H), 7.34 (tdd, J = 7.5, 2.1, 1.1 Hz, 2H), 6.49 (d, J = 8.0 Hz, 1H), 6.40 (d, J = 13.0 Hz, 2H), 5.40 (d, J = 8.0 Hz, 1H), 4.36 (p, J = 10.1 Hz, 2H), 4.24 (t, J = 6.9 Hz, 1H), 4.21 – 4.15 (m, 2H), 1.20 (t, J = 7.1 Hz, 3H).
^{13}**C-NMR:**	(126 MHz, CDCl$_3$): δ = 169.70, 145.04, 144.06, 142.13, 128.71, 128.10, 126.17, 120.97, 111.68, 109.54, 67.59, 62.84, 55.28, 53.24, 47.93, 30.85, 14.33.
ESI-HRMS:	calculated for C$_{23}$H$_{21}$N$_1$NaO$_5$ ([M+Na]$^+$): 414.13119, found: 414.13156.
HPLC:	(Chiralpak IB-3 column, *n*-heptane/*i*-PrOH 95:5, 298 K, 254 nm): t_R (minor) = 7.0 min, t_R (major) = 11.1 min, e.r. = 80:20 (60% e.e.).

7.1.6 Friedel–Crafts Reaction with Differing N,O-acetals

ethyl (*R*)-2-(((benzyloxy)carbonyl)amino)-2-(p-tolyl)acetate (216)

Prepared following *General Procedure D*, from *N,O*-acetal **46** (29.5 mg, 0.1 mmol, 1.0 equiv.) and toluene (**3**, 1.0 mL) using **IDPi-01-a** (8.9 mg, 5 μmol, 5 mol%) over 24 h reaction time at 30 °C. Purification by silica gel flash column chromatography (eluent: *i*-hexanes/MTBE 4:1) gave **216** as colorless oil (15.7 mg, 48.0 μmol, 48%).
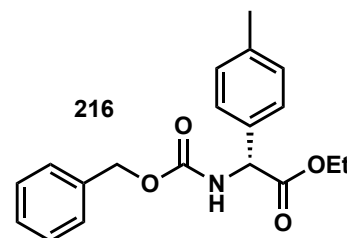
TLC:	R_f (*i*-hexanes/EtOAc 3:1) = 0.65.
¹H-NMR:	(501 MHz, CDCl₃): mixture of two regioisomers with a ratio of 1:0.05 and two rotamers of the main regioisomer with a ratio of 1:0.27. δ 7.39 – 7.28 (m, 5H), 7.25 (d, J = 7.5 Hz, 2H), 7.16 (d, J = 7.7 Hz, 2H), 5.79 (d, J = 7.4 Hz, 1H$_{maj}$), 5.60 (s, 1H$_{min}$), 5.32 (d, J = 7.4 Hz, 1H$_{maj}$), 5.18 (s, 1H$_{min}$), 5.09 (q, J = 12.3 Hz, 2H), 4.30–4.05 (m, 2H), 2.49 (s, 3H$_{min}$), 2.34 (s, 3H$_{maj}$), 1.21 (t, J = 7.1 Hz, 3H).
¹³C-NMR:	(126 MHz, CDCl₃): δ = 171.08, 155.47, 138.50, 136.35, 133.96, 129.74, 128.67, 128.33, 128.31, 127.15, 67.20, 62.01, 57.88, 21.29, 14.14.
ES-HRMS:	calculated for $C_{19}H_{21}N_1NaO_4$ ([M+Na]⁺): 350.13627, found: 350.13632.
HPLC:	(Chiralpak IB-3 column, *n*-heptane/*i*-PrOH 96:4, 1 mL/min, 25 °C, 206 nm): t_R (minor) = 7.9 min, t_R (major) = 8.7 min, e.r. = 83.5:16:5 (67% e.e.).
$[\alpha]_D^{25}=$	–66.7 (c = 0.11, CHCl₃).
r.r.	20:1 (favoring the *para* isomer), determined via ¹H-NMR analysis.

ethyl 2-(((benzyloxy)carbonyl)amino)-2-(2,4,6-trimethoxyphenyl)acetate (217)

Prepared following *General Procedure E* with deviations, from hemiaminal **46** (12.7 mg, 0.05 mmol, 1.0 equiv.) and 1,3,5-trimethoxybenzene (**42**, 42 mg, 0.25 mmol, 5 equiv.) using **IDPi-01-a** (0.9 mg, 0.5 µmol, 1 mol%) in CH_2Cl_2 (0.1 M) over 36 h reaction time at 30 °C. Purification by preparative thin layer chromatography (eluent: *i*-hexanes/EtOAc 2:1) afforded **217** as white solid (12 mg, 0.030 mmol, 60%).
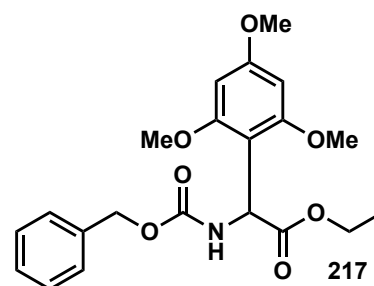
TLC: R_f (*i*-hexanes/EtOAc 2:1) = 0.45.

¹H-NMR: (501 MHz, CDCl₃): mixture of two rotamers with a ratio of 1:0.2. δ 7.41 – 7.28 (m, 5H), 6.11 (s, 2H_{maj}), 6.09 (s, 2H_{min}), 6.03 (d, J = 9.8 Hz, 1H_{maj}), 5.94 (d, J = 9.9 Hz, 1H_{min}), 5.85 (d, J = 9.8 Hz, 1H_{maj}), 5.66 (d, J = 9.4 Hz, 1H_{min}), 5.12 (q, J = 12.3 Hz, 2H), 4.21 – 4.07 (m, 2H), 3.81 (s, 3H), 3.80 (s, 6H), 1.16 (t, J = 7.1 Hz, 3H).

¹³C-NMR: (126 MHz, CDCl₃): δ = 172.07, 161.45, 158.78, 156.31, 136.67, 128.61, 128.33, 128.18, 107.44, 90.96, 67.01, 61.36, 56.04, 55.50, 48.30, 14.32.

ES-HRMS: calculated for $C_{21}H_{25}N_1NaO_7$ ([M+Na]⁺): 426.15232, found: 426.15218.

ethyl 2,2-bis(2,4,6-trimethoxyphenyl)acetate (47)

Obtained following *General Procedure E* with deviations, from hemiaminal **46** (50.7 mg, 0.2 mmol, 1.0 equiv.) and 1,3,5-trimethoxybenzene (**42**, 168 mg, 1.0 mmol, 5 equiv.) using $HNTf_2$ (0.2 M stock solution in CH_2Cl_2, 0.1 mL, 20 µmol, 10 mol%) in CH_2Cl_2 (0.1 M) over 36 h reaction time at 30 °C. Purification by silica gel flash column chromatography (eluent: *i*-hexanes/MTBE 9:1 → 1:1) afforded **47** as white crystalline solid (63 mg, 0.16 mmol, 78%).
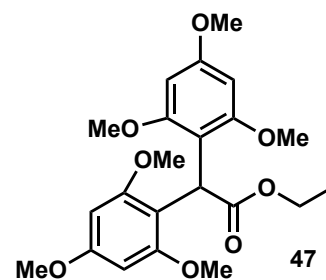
TLC: R_f (*i*-hexanes/EtOAc 2:1) = 0.30.

¹H-NMR: (501 MHz, CDCl₃): δ = 6.09 (s, 4H), 5.63 (s, 1H), 4.16 (q, J = 7.1 Hz, 2H), 3.77 (s, 6H), 3.68 (s, 12H), 1.21 (t, J = 7.1 Hz, 3H).

¹³C-NMR: (126 MHz, CDCl₃): δ = 173.80, 159.73, 159.37, 110.03, 91.39, 60.37, 56.18, 55.30, 37.12, 14.48.

ES-HRMS: calculated for $C_{22}H_{28}NaO_8$ ([M+Na]⁺): 443.16764, found: 443.16776.

methyl (*R*)-2-((((9H-fluoren-9-yl)methoxy)carbonyl)amino)-2-(p-tolyl)acetate (218)

Prepared following *General Procedure D* with deviations, from *N,O*-acetal **53** (36.9 mg, 0.1 mmol, 1.0 equiv.) and toluene (**3**, 1.0 mL) using **IDPi-01-a** (8.9 mg, 5 µmol, 5 mol%) over 24 h reaction time at 30 °C. Purification by silica gel flash column chromatography (eluent: *i*-hexanes/MTBE 4:1) gave **218** as white solid (15.1 mg, 37.6 µmol, 38%).
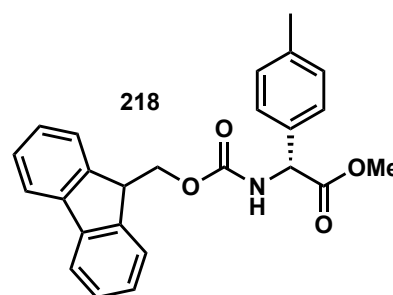
TLC:	R_f (*i*-hexanes/MTBE 2:1) = 0.62.
^{1}H-NMR:	(501 MHz, CDCl$_3$): mixture of two regioisomers with a ratio of 1:0.07 and two rotamers of the main regioisomer with a ratio of 1:0.18. δ 7.76 (d, J = 7.6 Hz, 2H), 7.58 (d, J = 7.5 Hz, 2H), 7.40 (t, J = 7.5 Hz, 2H), 7.35–7.21 (m, 4H), 7.19 (d, J = 8.0 Hz, 2H), 5.81 (d, J = 7.4 Hz, 1H$_{maj}$), 5.74 (d, J = 7.3 Hz, 1H$_{min}$), 5.68 (s, 1H$_{min}$), 5.62 (d, J = 7.5 Hz, 1H$_{min}$), 5.35 (d, J = 7.3 Hz, 1H$_{maj}$), 5.11 (s, 1H$_{min}$), 4.47–4.32 (m, 2H), 4.22 (t, J = 7.2 Hz, 1H$_{maj}$), 4.15 (s, 1H$_{min}$), 3.74 (s, 3H$_{maj}$), 3.70 (s, 3H$_{min}$), 2.49 (s, 1H$_{min}$), 2.35 (s, 3H$_{maj}$).
^{13}C-NMR:	(126 MHz, CDCl$_3$): δ = 171.65, 155.51, 144.00 (C$_{min}$), 143.90 (C$_{maj}$), 141.43, 138.70, 133.73, 129.85, 127.84, 127.24, 127.21, 125.22, 120.12, 67.28, 57.83, 52.96, 47.29, 21.31.
ESI-HRMS:	calculated for C$_{25}$H$_{23}$N$_1$NaO$_4$ ([M+Na]$^+$): 424.15192, found: 424.15216.
HPLC:	(Chiralpak IB-3 column, *n*-heptane/*i*-PrOH 96:4, 1 mL/min, 25 °C, 254 nm): t_R (minor) = 15.6 min, t_R (major) = 33.4 min, e.r. = 90:10 (80% e.e.).
$[\propto]_D^{25}=$	–67.9 (c = 0.11, CHCl$_3$).
r.r.	93.5:6.5 (favoring the *para* isomer), determined via ^{1}H-NMR analysis.

isopropyl (*R*)-2-((((9H-fluoren-9-yl)methoxy)carbonyl)amino)-2-(p-tolyl)acetate (219)

Prepared following *General Procedure D* with deviations, from *N,O*-acetal **55** (39.7 mg, 0.1 mmol, 1.0 equiv.) and toluene (**3**, 1.0 mL) using **IDPi-01-a** (8.9 mg, 5 µmol, 5 mol%) over 24 h reaction time at 30 °C. Purification by silica gel flash column chromatography (eluent: *i*-hexanes/MTBE 4:1) afforded **219** as white solid (16.8 mg, 39.1 µmol, 39%).
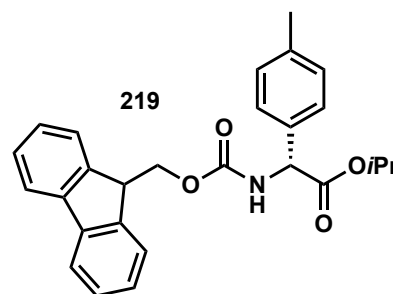
|	
TLC:	R_f (*i*-hexanes/MTBE 2:1) = 0.75.
^{1}H-NMR:	(501 MHz, CDCl$_3$): mixture of two regioisomers with a ratio of 1.0:0.03 and two rotamers of the main regioisomer with a ratio of 1.0:0.23. δ 7.76 (d, J = 7.6 Hz, 2H), 7.59 (d, J = 7.5 Hz, 2H), 7.40 (t, J = 7.6 Hz, 2H), 7.35–7.19 (m, 4H), 7.17 (d, J = 7.7 Hz, 2H), 5.83 (d, J = 7.4 Hz, 1H$_{maj}$), 5.73 (s, 1H$_{min}$), 5.57 (d, J = 7.5 Hz, 1H$_{min}$), 5.30 (d, J = 7.4 Hz, 1H$_{maj}$), 5.12 (d, J = 5.4 Hz, 1H$_{min}$), 5.06 (p, J = 6.2 Hz, 1H), 4.38 (qd, J = 10.7, 7.3 Hz, 2H), 4.22 (t, J = 7.2 Hz, 1H), 4.15 (s, 1H$_{min}$), 2.50 (s, 3H$_{min}$), 2.35 (s, 3H$_{maj}$), 1.28 (d, J = 6.2 Hz, 3H), 1.12 (d, J = 6.2 Hz, 3H).
^{13}C-NMR:	(126 MHz, CDCl$_3$): δ = 170.64, 155.51, 144.04, 143.94, 141.42, 138.38, 134.04, 129.70, 127.82, 127.19, 127.10, 125.25, 120.10, 69.80, 67.23, 57.95, 47.30, 21.86, 21.50, 21.30.
ESI-HRMS:	calculated for C$_{27}$H$_{27}$N$_1$NaO$_4$ ([M+Na]$^+$): 452.18322, found: 452.18347.
HPLC:	(Chiralpak IC-3 column, *n*-heptane/*i*-PrOH 90:10, 1 mL/min, 25 °C, 254 nm): t_R (minor) = 10.9 min, t_R (major) = 19.9 min, e.r. = 89.5:10.5 (79% e.e.).
$[\alpha]_D^{25} =$	–55.2 (c = 0.14, CHCl$_3$).
r.r.	97:3 (favoring the *para* isomer), determined via ^{1}H-NMR analysis.

isopropyl (*R*)-2-((((9H-fluoren-9-yl)methoxy)carbonyl)amino)-2-(p-tolyl)acetate (220)

Prepared following *General Procedure E* with deviations, from hemiaminal **41** (44.7 mg, 0.2 mmol, 1.0 equiv.) and 1,3,5-trimethoxybenzene (**42**, 168 mg, 1 mmol, 5 equiv.) using HNTf$_2$ (0.2 M stock solution in CH$_2$Cl$_2$, 0.1 mL, 20 µmol, 10 mol%) in CH$_2$Cl$_2$ (0.1 M) over 14 h reaction time at 30 °C. Purification by silica gel flash column chromatography (eluent: *i*-hexanes/EtOAc 10:1 → 1:1) afforded **220** as white solid (52 mg, 1.4 mmol, 70%).
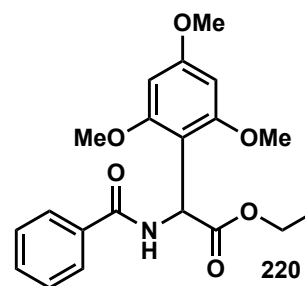
^{1}H-NMR:	(501 MHz, CDCl$_3$): 7.83 – 7.77 (m, 2H), 7.51 – 7.44 (m, 1H), 7.44 – 7.38 (m, 2H), 7.23 (d, J = 9.1 Hz, 1H), 6.51 (d, J = 9.1 Hz, 1H), 6.15 (s, 2H), 4.23 – 4.10 (m, 3H), 3.86 (s, 6H), 3.82 (s, 3H), 1.18 (t, J = 7.1 Hz, 3H).
^{13}C-NMR:	(126 MHz, CDCl$_3$): δ = 171.91, 166.79, 161.47, 159.07, 134.87, 131.46, 128.56, 127.33, 91.23, 61.44, 56.22, 55.53, 46.89, 14.34.
ESI-HRMS:	calculated for C$_{20}$H$_{23}$N$_1$NaO$_6$ ([M+Na]$^+$): 396.14176, found: 396.14210.

Gram-Scale Synthesis of Arylglycine Derivates
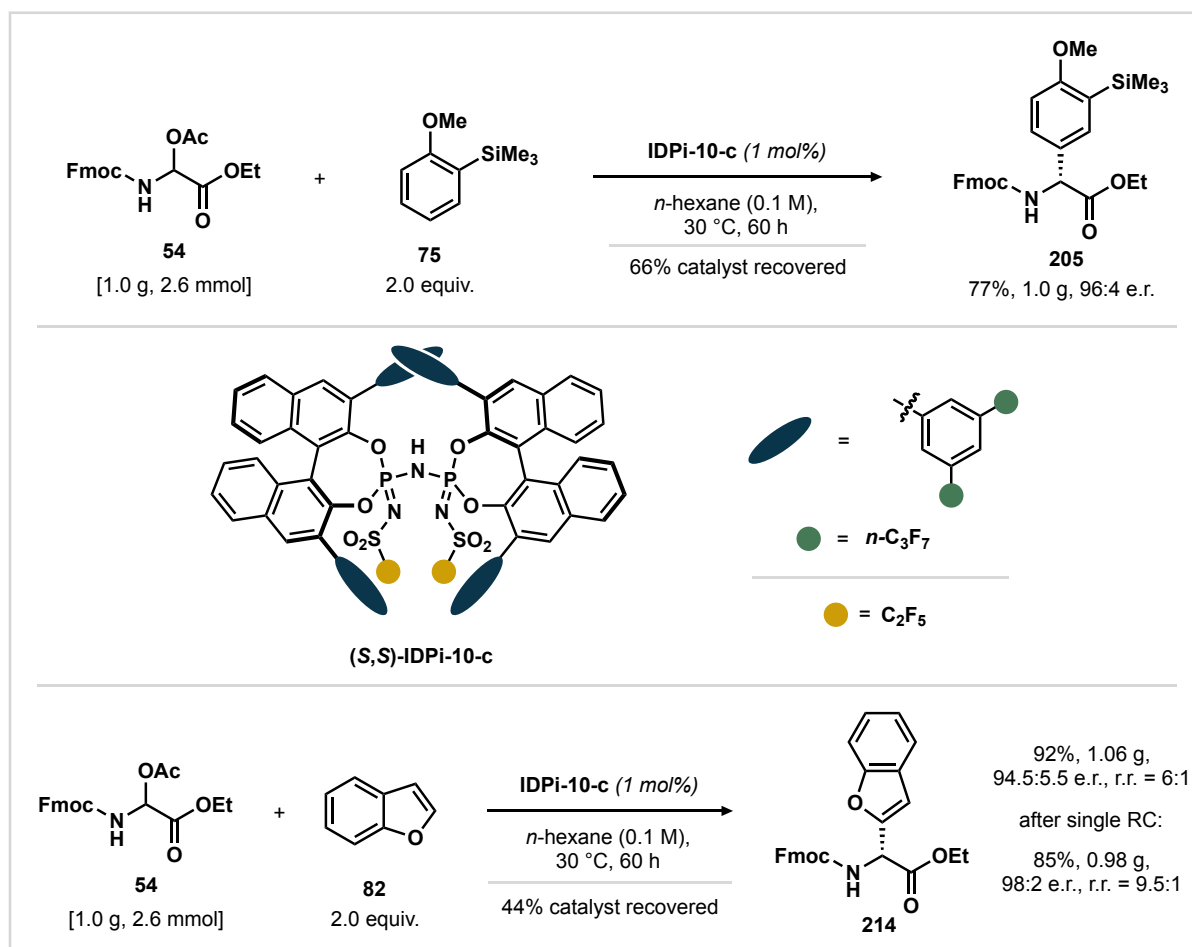
Figure 7.1: Gram-scale synthesis of arylglycine derivates.

Gram-Scale Synthesis of: ethyl (*R*)-2-((((9*H*-fluoren-9-yl)methoxy)carbonyl)amino)-2-(4-methoxy-3-(trimethylsilyl)phenyl)acetate (205)

N,O-acetal **54** (1.0 g, 2.60 mmol, 1.0 equiv.) was given to a flame-dried 100 mL Schlenk tube under an atmosphere of argon followed by **IDPi-10-c** (70 mg, 26.1 µmol, 1 mol%). The tube was cooled to –78 °C and *n*-hexane (27 mL) was added followed by the dropwise addition of (2-methoxyphenl)trimethylsilane (**75**, 0.98 mL, 5.22 mmol, 2.0 equiv.). The heterogeneous mixture was allowed to warm to room temperature and then stirred at 30 °C for 60 h whereupon complete conversion of *N,O*-acetal **54** was observed. The reaction was quenched with triethylamine (30 µL), adsorbed on celite® and purified via flash column chromatography on silica gel (eluent: *i*-hexanes/MTBE 5:1 → 2:1) to yield the desired arylglycine **205** (1.0 g, 1.99 mmol, 77%) as white solid.
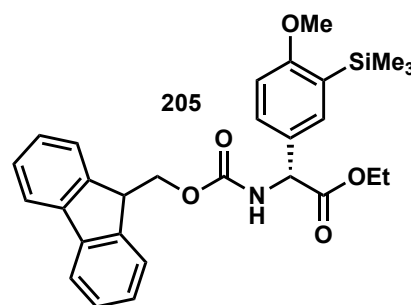
*For the analytical data of **205** isolated herein, see the corresponding entry at section 5.2 of this supporting information.*

To reisolate **IDPi-10-c**, the silica gel column was flushed (eluent: CH_2Cl_2/EtOAc 99:1) after complete elution of arylglycine **205**. The obtained solution was concentrated and the residue was purified via flash column chromatography on silica gel (eluent: *i*-hexanes/CH_2Cl_2 1:1 → CH_2Cl_2/EtOAc 99.5:0.5) to yield **IDPi-10-c** as salt. After acidification over DOWEX 50WX8 (H-form, eluted with CH_2Cl_2), the reisolated catalyst **IDPi-10-c** (46 mg, 17.1 μmol, 66%) was obtained spectroscopically pure as off-white solid.

Gram-Scale Synthesis of ethyl (*R*)-2-((((9H-fluoren-9-yl)methoxy)carbonyl)amino)-2-(benzofuran-2-yl)acetate (214)

N,O-acetal **54** (1.0 g, 2.60 mmol, 1.0 equiv.) was given to a flame-dried 100 mL Schlenk tube under an atmosphere of argon followed by **IDPi-10-c** (70 mg, 26.1 μmol, 1 mol%). The tube was cooled to –78 °C and CyMe (27 mL) was added followed by the dropwise addition of benzofuran (**82**, 0.57 mL, 5.22 mmol, 2.0 equiv.). The heterogeneous mixture was allowed to warm to room temperature and then stirred at 30 °C for 5 d whereupon complete conversion of the *N,O*-acetal **54** was observed. The reaction was quenched with triethylamine (30 μL), adsorbed on celite® and purified via flash column chromatography on silica gel (eluent: *i*-hexanes/MTBE 5:1 to 3:1) to yield the desired arylglycine **214** (1.06 g, 2.40 mmol, 92%) as white solid with an enantiomeric ratio of 94.5:5.5 and a regioisomeric ratio of 86:14. The compound **214** can be recrystallized from *i*-hexanes and CH_2Cl_2 to yield arylglycine **214** (0.98 g, 2.22 mmol, 85%) as white solid with an increased enantiomeric ratio of 98:2 and a regioisomeric ratio of 91:9 after a single recrystallization.
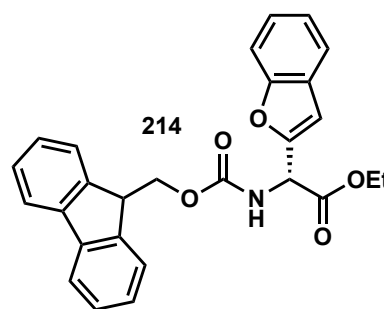
*For the analytical data of **214** isolated herein, see the corresponding entry at section 5.2 of this supporting information. LC-data of the recrystallized compound as to be found below:*

2D-LC: (1. dimension: 100 mm Zorbax RX-Sil, *n*-heptane/*i*-PrOH 99.5:0.5, 308 K, 220 nm): t_R (major regioisomer) = 3.1 min, t_R (minor regioisomer) = 3.3 min, r.r. = 91:9.
(2. dimension: Chiralpak IB-3, *n*-heptane/*i*-PrOH 80:20, 298 K, 220 nm): t_R (minor enantiomer) = 5.9 min, t_R (major enantiomer) = 6.9 min, e.r. = 97.5:2.5 (95% e.e.).

To reisolate **IDPi-10-c**, the silica gel column was flushed (eluent: CH_2Cl_2/EtOAc 99:1) after complete elution of arylglycine **214**. The obtained solution was concentrated and the residue

was purified via flash column chromatography on silica gel (eluent: *i*-hexanes/CH$_2$Cl$_2$ 1:1 $\rightarrow$ CH$_2$Cl$_2$/EtOAc 99.5:0.5) to yield **IDPi-10-c** as salt. After acidification over DOWEX 50WX8 (H-form, eluted with CH$_2$Cl$_2$), the reisolated catalyst **IDPi-10-c** (31 mg, 11.5 µmol, 44%) was obtained spectroscopically pure as off-white solid.

7.1.7 Determination of the Absolute Configuration

The absolute configuration of the produced arylglycine products was determined via comparison with an enantiopure sample as described below: commercially available enantiopure *D*-(−)-phenylglycin-ethylester hydrochloride (**221**, purchased from https://www.sigmaaldrich.com/DE/de, CAS registry number = 17609-48-2) was transformed to the *N*-Fmoc protected amino acid ester **63** (scheme **7.2**). HPLC-analysis and subsequent comparison with arylglycine **63** prepared following General Procedure D using **IDPi-13-f** (see scheme **4.4**) shows formation of the (*R*)-arylglycine **63** as predominant enantiomer.
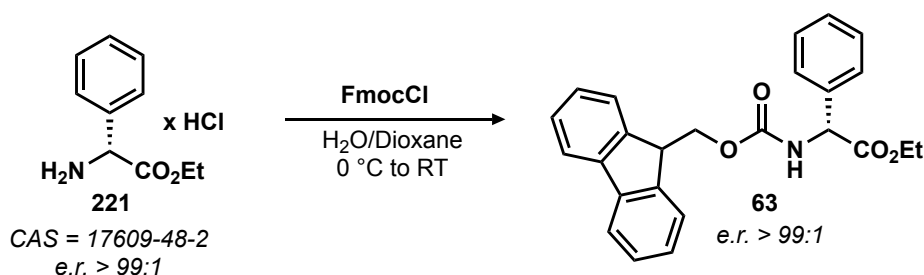
Scheme 7.2: Synthesis of phenylglycine **63** from commercial enantiopure amino acid **221**.

ethyl (R)-2-((((9H-fluoren-9-yl)oxy)carbonyl)amino)-2-phenylacetate (63)

Following a procedure reported by Hulme, ethyl (*R*)-2-amino-2-phenylacetate hydrochloride (**221**, e.r. > 99:1, 500 mg, 2.31 mmol, 1.0 equiv.) was given to a round bottom flask, dissolved in dioxane (7 mL) and a 15% aqueous solution of Na$_2$CO$_3$ (7 mL) was added. The mixture was cooled to 0 °C and stirred for 10 min, then 9-fluorenylmethoxycarbonylchlorid (600 mg, 2.31 mmol, 1.0 equiv.) was added in one portion, the mixture was allowed to warm to room temperature and stirred for 18 h. Water (20 mL) and CH$_2$Cl$_2$ (20 mL) was added, the layers were separated and the organic layer was washed with water (3 x 20 mL) and brine (20 mL) and then dried (Na$_2$SO$_4$). The solution was concentrated under reduced pressure to yield the desired carbamate **63** (915 mg, 2.30 mmol, 98%) as white solid which was used as reference without further purification.
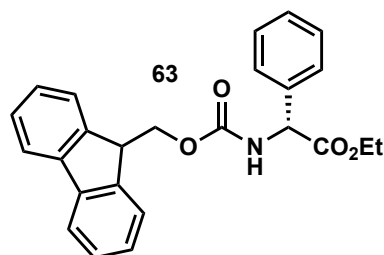
7. Experimental Section

HPLC: (Chiralpak IB-3 column, *n*-heptane/*i*-PrOH 95:5, 298 K, 254 nm): t_R (minor) = 13.3 min, t_R (major) = 19.2 min, e.r. > 99.5:0.5 (>99% e.e.).
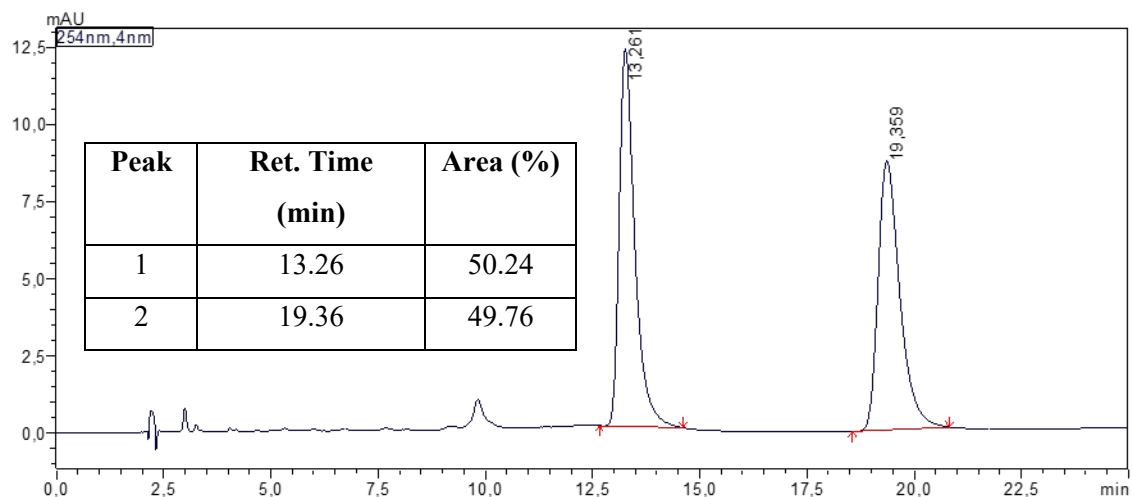
Figure 7.1: HPLC-traces of racemic **63**, obtained using HNTf₂ as achiral catalyst.

Peak	Ret. Time (min)	Area (%)
1	13.26	50.24
2	19.36	49.76
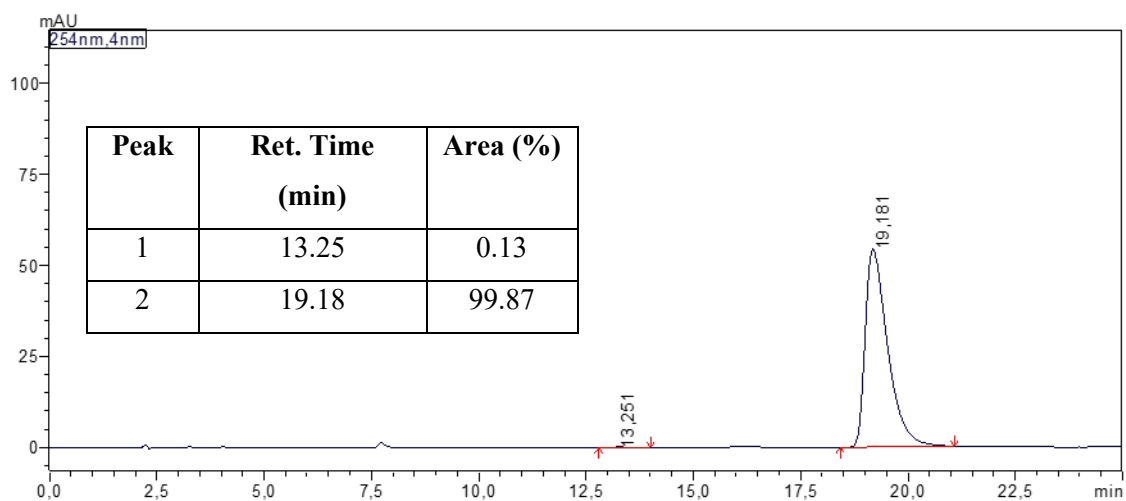
Figure 7.2: HPLC-traces of enantioenriched (*R*)-**63**, obtained from enantiopure **221**.

Peak	Ret. Time (min)	Area (%)
1	13.25	0.13
2	19.18	99.87
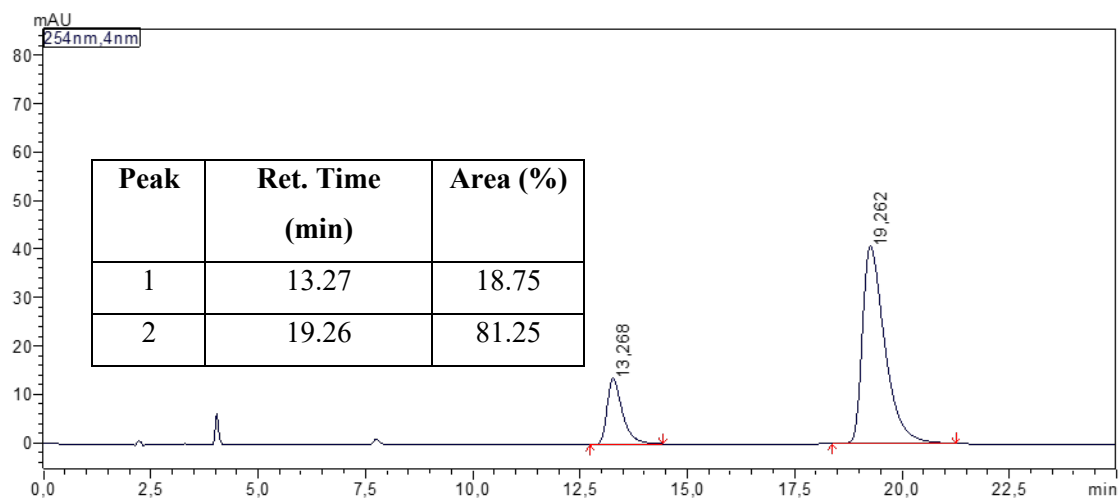
Figure 7.3: HPLC-traces of enantioenriched **63**, obtained using **IDPi-13-f** as chiral catalyst.

Peak	Ret. Time (min)	Area (%)
1	13.27	18.75
2	19.26	81.25

157

7.1.8 Mechanistic Investigations

Reactivity Assessment via Acetate Scrambling Experiments

During initial reaction optimization studies, we noticed that only a small choice of highly acidic (*S,S*)-IDPi catalysts are able to promote C–C bond formation in the Friedel–Crafts reaction between *N,O*-acetals **54** and toluene (**3**). To gain insights in the limiting factors that prevent product formation using less acidic catalysts, we were interested in the development of tools that enable the monitoring of the interaction between the used *N,O*-acetals **54** and (*S,S*)-IDPis. Based on earlier studies, we expected iminium ion formation upon reaction of **54** with the IDPi-catalyst followed by ion pair **X** formation with the corresponding anion of the IDPi be a possible reaction pathway.[205] To investigate the latter, we designed an "acetate scrambling" experiment (exchange of acetate-h₃ and acetate-d₃ on *N,O*-acetal **54** as described in scheme **7.3**) promoted by Brønsted acid catalysts adding deuterated acetic acid as mechanistic probe:
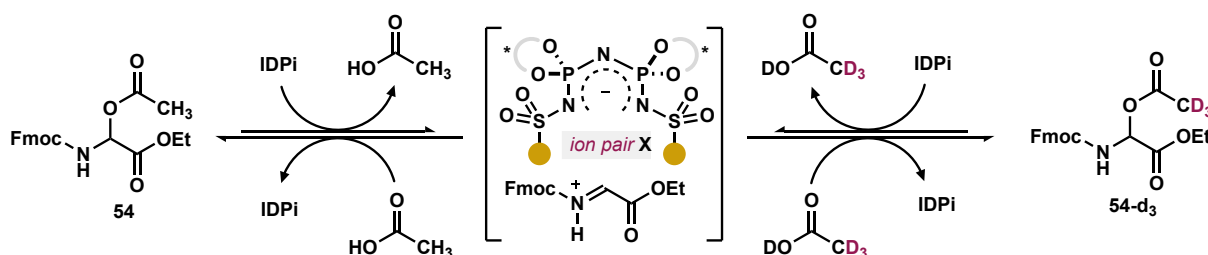
Scheme 7.3: Design and mechanistic concept of the acetate scrambling experiments.
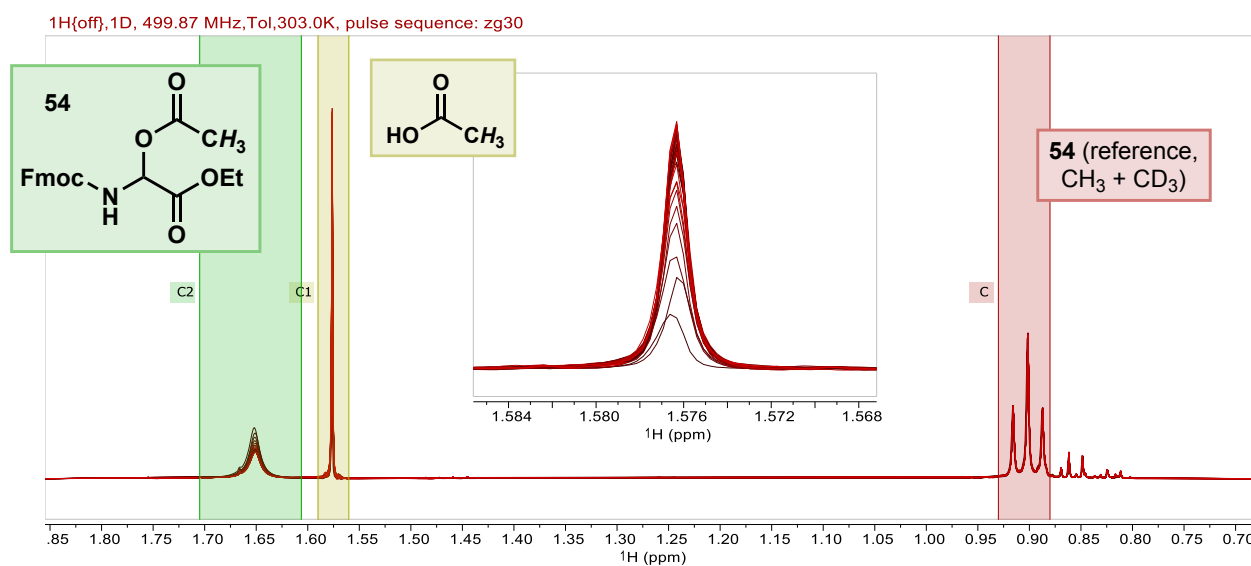
Figure 7.4: Quantification of the acetate scrambling experiment via ¹H-NMR analysis (exemplified spectroscopic data collected for the reaction with **IDPi-01-a**).

The respective catalyst (2.5 µmol, 5 mol%) and *N,O*-acetal **54** (19.2 mg, 50 µmol, 1.0 equiv.) were given to an oven dried NMR tube, the tube was placed under an atmosphere of argon and a solution of acetic acid-d_4 in PhMe-d_8 (0.071 M solution, 0.7 mL, 50 µmol acetic acid-d_4, 1.0 equiv.) was added. The tube was shaken and the homogeneous mixture was directly monitored via ^{1}H-NMR analysis. The equilibration between **54**-h_3 and **54**-d_3 was observed through the formation of free acetic acid-h_3 (signal at ca 1.58 ppm) and the decrease of the signal corresponding to the acetate group of **54**-h_3 (signal at ca 1.65 ppm) using the signal of the methyl group of the ethyl ester terminus as relatively constant reference (signal at ca 0.9 ppm, sum of **54**-h_3 and **54**-d_3).

General Remark for the Evaluation of Kinetic NMR Experiments: Kinetic ^{1}H-NMR experiments were generally acquired with single scans (30° pulses) until an appropriate conversion was reached. The data was then imported with the Reaction Monitoring Plugin into MNOVA 14.3.2 and processed therein (phase correction, baseline correction, integration). Unless noted otherwise, the first NMR spectrum of each kinetic series was used as absolute concentration reference using total CH3COOX integral (AcOH + AcOX) as reference signal (= 100 mol%). This integral was found to be constant for all reactions performed. For the reaction with additional AcOH, the acetate signal of the starting material was used as reference signal (= 100 mol%). As this point no significant conversion was observed.

The observed rates are shown in the diagrams below:
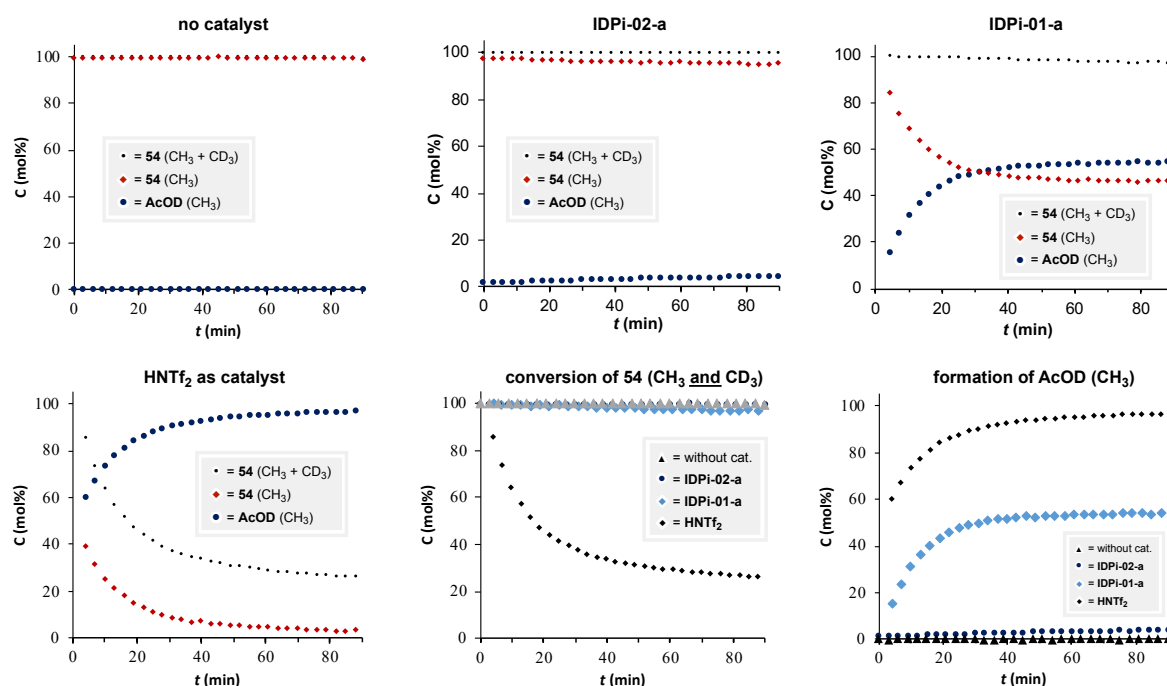
Figure 7.5: Observed rates of equilibration in the acetate scrambling experiments.

Without the presence of an acid catalyst, no acetate scrambling can be observed in the chosen timescale (left diagram upper row). Similarly, using **IDPi-02-a** (<u>inactive</u> in the Friedel–Crafts reaction towards **56**), only extremely slow exchange of acetate-h_3 with acetate-d_3 in **54** can be found (middle diagram upper row). When catalyst **IDPi-01-a** (<u>active</u> in the Friedel–Crafts reaction towards **56**) however is used, complete equilibration between **54**-h_3 and **54**-d_3 is observed within 40 minutes (right diagram upper row). This significant difference in the rate of equilibration observed for **IDPi-01-a** in comparison with **IDPi-02-a** is in agreement with the respective catalyst's activity (or inactivity) in the Friedel–Crafts reaction between **54** and the arenes **3** investigated herein.

Based on these experiments as well as previous investigations using reactive iminium ion intermediates, we propose the formation of ion pair **X** from **54** and **IDPi-01-a** as crucial intermediate for the subsequent Friedel–Crafts reaction.[205] The less acidic catalyst **IDPi-02-a** however is not able to sufficiently activate *N,O*-acetal **54** towards the formation of ion pair **X** (or to sufficiently stabilize ion pair **X** and to therefore prolonging its lifetime so that the subsequent nucleophilic attack of arene substrates **3** is possible).

Intriguingly, using HNTf$_2$ as catalyst, complete equilibration between **54**-h_3 and **54**-d_3 can be observed before the first NMR measurement was performed (left diagram bottom row). Furthermore, consumption of **54** towards arylglycin **56** can be observed in the investigated timescale, leading to additional release of AcOD-h_3 (see middle and right diagram bottom row).

Investigation of Inhibitory Effects of Acetic Acid

As described in section 7.1 of this experimental section, we propose the formation of ion pair **X** from *N,O*-acetal **54** and (*S,S*)-IDPi catalysts in an equilibrium state to be a crucial intermediate towards the subsequent Friedel–Crafts type formation of arylglycine products. Consequentially, the concentration of free acetic acid in the system, released from the leaving group of converted *N,O*-acetal **54**, should increase with the proceeding of the reaction, shifting the equilibrium away from ion pair **X** and therefore slowing down the reaction or even inhibiting it completely at higher levels of conversion (scheme **7.4**).
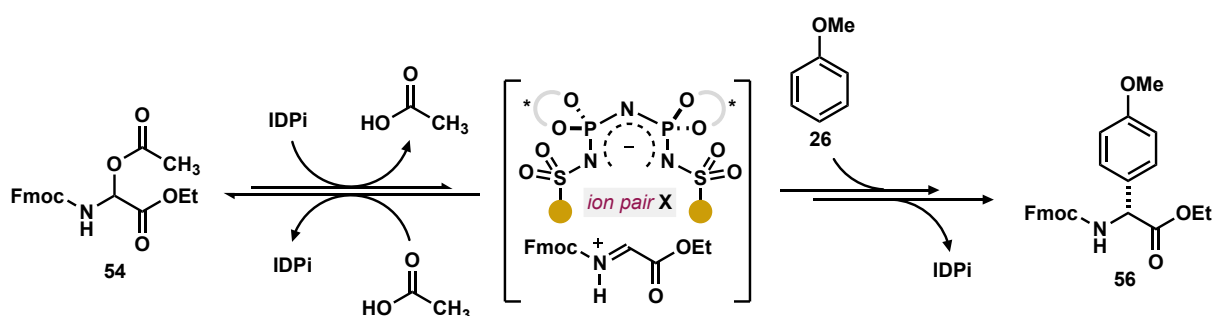
Scheme 7.4: Ion pair **X** formation towards the formation of arylglycine **56**.

To further investigate the inhibitory effects of acetic acid in the Friedel–Crafts reaction reported herein, the rates of reaction of **54** with anisole (**26**) as mechanistic probe towards arylglycine **56** using **IDPi-10-c** were measured with an optional addition of acetic acid:
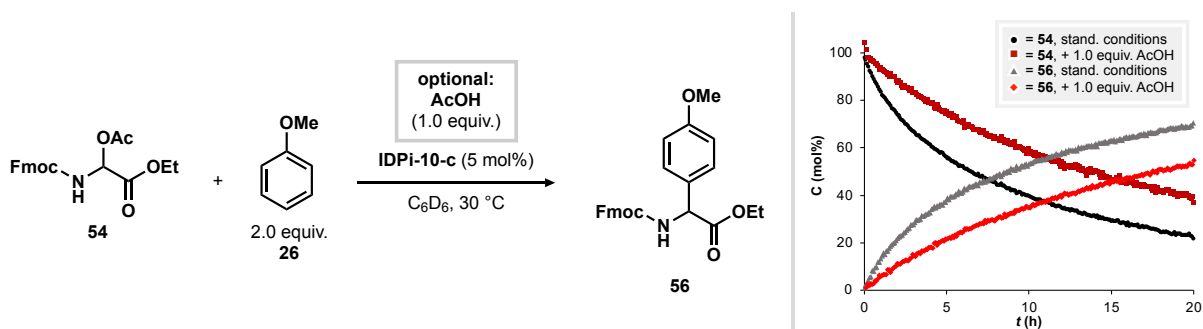
Figure 7.6: Concept and measured rates for the acetic acid inhibition experiment.

IDPi-10-c (6.7 mg, 2.5 µmol, 5 mol%) and *N,O*-acetal **2c** (19.2 mg, 50 µmol, 1.0 equiv.) were given to an oven dried NMR tube, the tube was placed under an atmosphere of argon and a stock solution of anisole (**26**) in C$_6$D$_6$ (0.143 M solution, 0.7 mL, 0.1 mmol of **26**, 2.0 equiv.) or a stock solution of anisole (**26**) <u>and</u> acetic acid (0.143 M solution regarding **26**, 0.0712 M regarding acetic acid, 0.7 mL, 0.1 mmol of **26**, 2.0 equiv. of **26**; 0.05 mmol of acetic acid, 1.0 equiv. of acetic acid) was added. The tube was shaken and the homogeneous mixture was directly monitored via ^{1}H-NMR analysis. The conversion of starting material **54** was monitored

through the decrease of **54**'s acetate signals (signals at 1.56 ppm) and the formation of the Friedel–Crafts product **56** was monitored via the product **56**'s Ar–O–CH_3 signal (figure **7.7**).
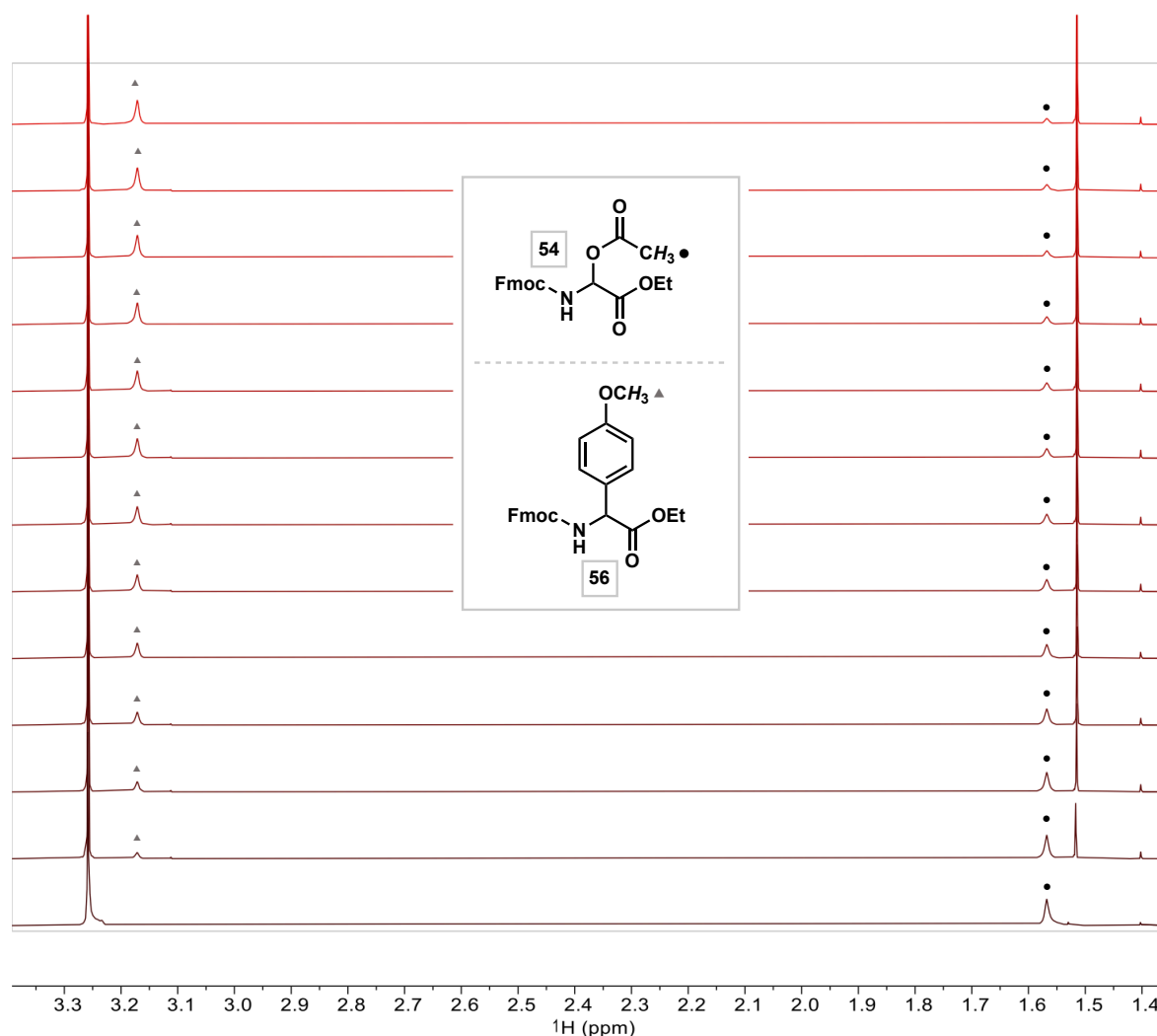
Figure 7.7: Determination of reaction rates via ^{1}H-NMR (exemplified in the reaction without AcOH).

General Remark for the Evaluation of Kinetic NMR Experiments: Kinetic ^{1}H-NMR experiments were generally acquired with single scans (30° pulses) until an appropriate conversion was reached. The data was then imported with the Reaction Monitoring Plugin into MNOVA 14.3.2 and processed therein (phase correction, baseline correction, integration). Unless noted otherwise, the first NMR spectrum of each kinetic series was used as absolute concentration reference using total CH3COOX integral (AcOH + AcOX) as reference signal (= 100 mol%). This integral was found to be constant for all reactions performed. For the reaction

with additional AcOH, the acetate signal of the starting material was used as reference signal (= 100 mol%). As this point no significant conversion was observed.

As displayed above (figure **7.7**), a significantly slower rate of product **56** formation can be observed upon addition of 1.0 equivalent of acetic acid compared to the reference reaction without additional acetic acid. This observation supports the suggested inhibitory properties of acetic acid for the formation of product **56** under the described reaction conditions.

To investigate the effect of additional acetic acid on the enantioselectivities of the products, the following experiments have been carried out:

entry	arene	solvent	AcOH	yield (%)	e.r.
1	PhMe (**3**)	neat	–	55	90:10
2	PhMe (**3**)	neat	1.0 equiv.	35	90:10
3	anisole (**26**)	CyMe	–	67	87:13
4	anisole (**26**)	CyMe	1.0 equiv.	63	88:12
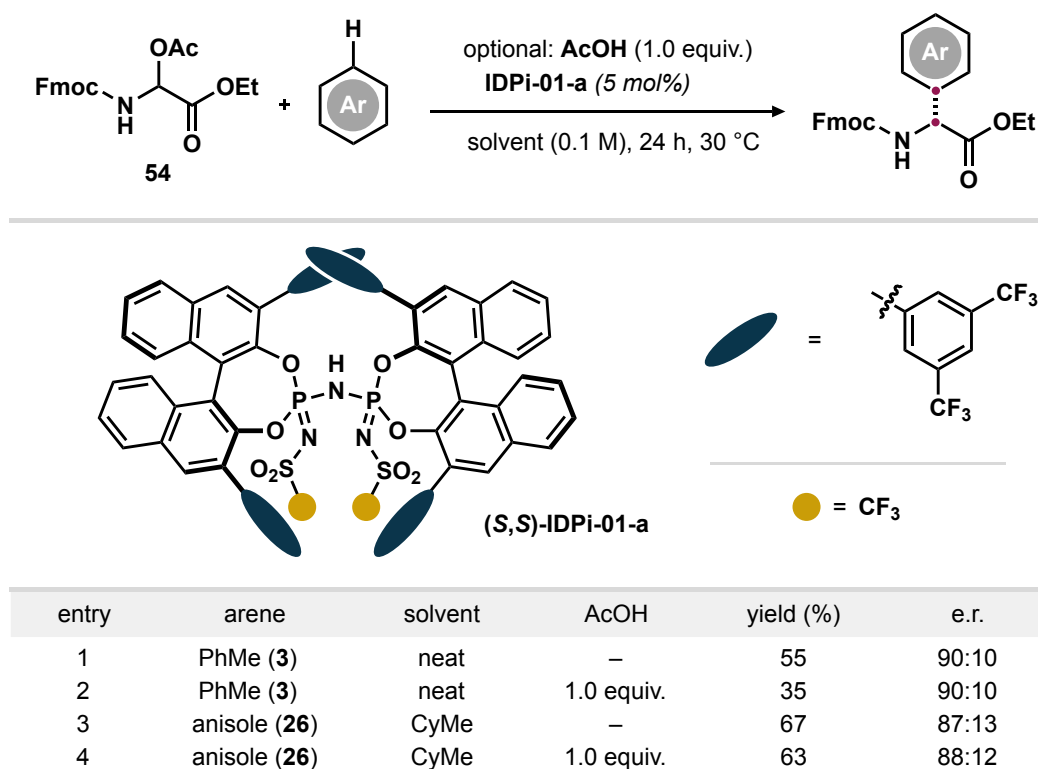
Scheme 7.8: Effect of additional AcOH on the enantiomeric ratios of the products.

An oven dried 1 mL screwcap vial equipped with a magnetic stirring bar was charged with the catalyst (5 mol%) and *N,O*-acetal **54** (9.6 mg, 1.0 equiv., 0.025 mmol). The vial was evacuated under high vacuum and subsequently placed under an atmosphere of argon. Solvent (0.3 mL) was added quickly followed by **26** (*optional for entries 3 and 4*, 5.4 µL, 2.0 equiv., 0.05 mmol), the vial was sealed and the mixture was stirred at 30 °C for 24 h. The reaction was then quenched via addition of triethylamine (0.3 M solution in PhMe, 50 µL), dimethylsulfone (2.0 M solution in MeCN, 12.5 µL, 1.0 equiv.) was added as internal standard and the mixture was diluted with CHCl₃ (0.2 mL). An aliquot of the reaction was diluted with CDCl₃ (0.6 mL) and analyzed via ¹H-NMR to determine the reaction yield. The remaining mixture was purified via preparative

thin layer chromatography (PTLC) for the subsequent HPLC analysis for the determination of the enantiomeric ratio.

For toluene (**3**), addition of AcOH significantly slows down the reaction which leads to visibly lower yields for product **56** (entries 1 and 2). The enantiomeric ratio of the formed product **1a** however was found to be identical for both reactions.

For the reaction of anisole (**26**), the yield on product **69** is very similar for both reactions (entries 3 and 4, with or without additional AcOH), which is most likely due to the increased nucleophilicity of **26**. The enantiomeric ratio was found to be very similar for both reactions with a slightly increased enantiomeric ratio for the reaction with additional AcOH.

As described above, the influence of additional AcOH on the observed enantiomeric ratio is only minimal. On the basis of these experiments we therefore conclude that a potential kinetic resolution of starting material **54** does not play a relevant role in the process investigated herein.

Kinetic Isotope Effect Studies

As a mechanistic probe towards the determination of the rate limiting step of the Friedel–Crafts reaction between *N,O*-acetal **54** and toluene (**3**), direct competition kinetic isotope effect (KIE) studies were performed as described below (scheme **7.9**):
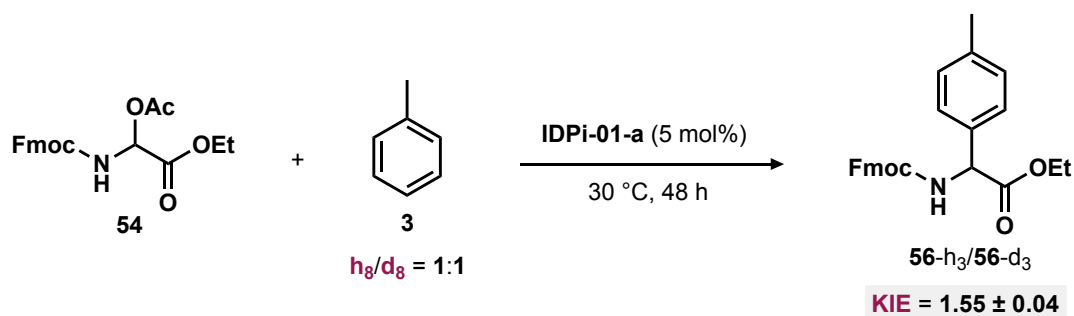
Scheme 7.9: Direct competition KIE studies with a 1:1 mixture of toluene-h_8 and toluene-d_8.

IDPi-01-a (8.9 mg, 5 µmol, 5 mol%) was given to a flame dried Schlenk tube under an atmosphere of argon followed by *N,O*-acetal **54** (38.3 mg, 0.1 mmol, 1.0 equiv.). 1 mL of a 1:1 (*v/v*) mixture of toluene-h_8 and toluene-d_8 (premixed, equals 4.694 mmol toluene-h_8 and 4.706 mmol toluene-d_8, ratio PhMe-h_8/PhMe-d_8 = 0.998:1) was added and the mixture was stirred at 30 °C for 48 h. The reaction was then stopped via the addition of NEt$_3$ (stock solution, 0.3 M in CH$_2$Cl$_2$, 200 µL) and applied directly on a silica gel column equilibrated with *i*-hexanes. The mixture was flushed with *i*-hexanes (100 mL) and then purified via flash column chromatography on silica gel (*i*-hexanes/MTBE 4:1) to yield the mixture of arylglycine **56**-h_7 and **1a**-d_7. The experiment was performed twice, and the average of both experiments was used for the determination of the KIE. The KIE was determined via NMR analysis (ratio of **56**-h_3 to **56**-d_3) of the isolated product **56** as described below:

With regards to the high excess of toluene in the system (**3**-h_8 as well as **3**-d_8), changes in concentration of arene **3** were neglected for the determination of the KIE at hand. The average of three different signal sets was used, taking into account both rotameric species if present:

1.) Ratio of *H* at C6 (**56**-h_7 + **56**-d_7, 5.25 ppm and 5.10 ppm) to C*H*$_3$ at C5 (**56**-h_7 only, 2.31 ppm and 2.35 ppm), determined via ^{1}H-NMR.

2.) Ratio of C6 (C$_\alpha$) in **56**-h_7 (57.5 ppm and 57.9 ppm) to C6 (C$_\alpha$) in **56**-d_7 (57.4 ppm and 57.8 ppm) via 13C-NMR (integration of the two separate peaks).
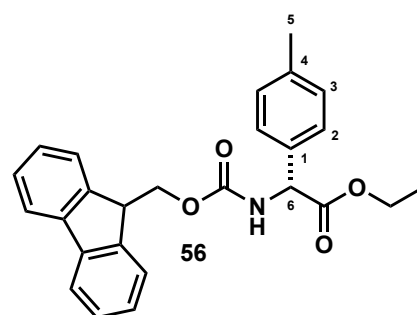
3.) Ratio of C1 in **56**-h$_7$ (C$_{ipso}$, 170.82 ppm) to C1 in **56**-d$_7$ (C$_{ipso}$, 170.85 ppm) via 13C-NMR (integration of the two separate peaks).

The corresponding spectra are shown below (**figures 7.8-7.11**).

	^{1}H		
	Int (C$_a$)	Ar-Me	KIE
major	1	1.79	1.48
minor	0.14	0.26	1.63

	^{13}C		
	Int(H-7)	Int (D7)	KIE
C$_{a, major}$	0.48	0.29	1.66
C$_{a, minor}$	3.73	2.33	1.60
C$_{ipso, major}$	1.64	1.00	1.64

KIE (average)	1.60 ± 0.07
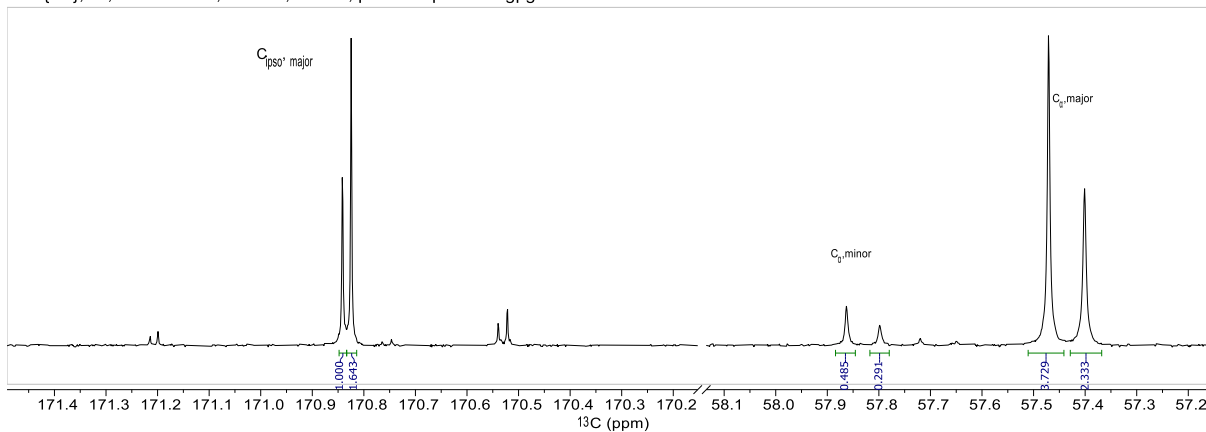
Figure 7.8: Experiment 1 for the determination of the KIE.

		^{1}H	
	Int (C$_a$)	Ar-Me	KIE
major	1	1.77	1.44
minor	0.14	0.25	1.47
		^{13}C	
	Int(H-7)	Int (D7)	KIE
C$_{a, major}$	0.52	0.34	1.53
C$_{a, minor}$	4.16	2.75	1.51
C$_{ipso, major}$	1.52	1.00	1.52
	KIE (average)	1.49	±0.04

13C{1H},1D, 150.94 MHz,CD2Cl2,233.0K, pulse sequence: zgpg30
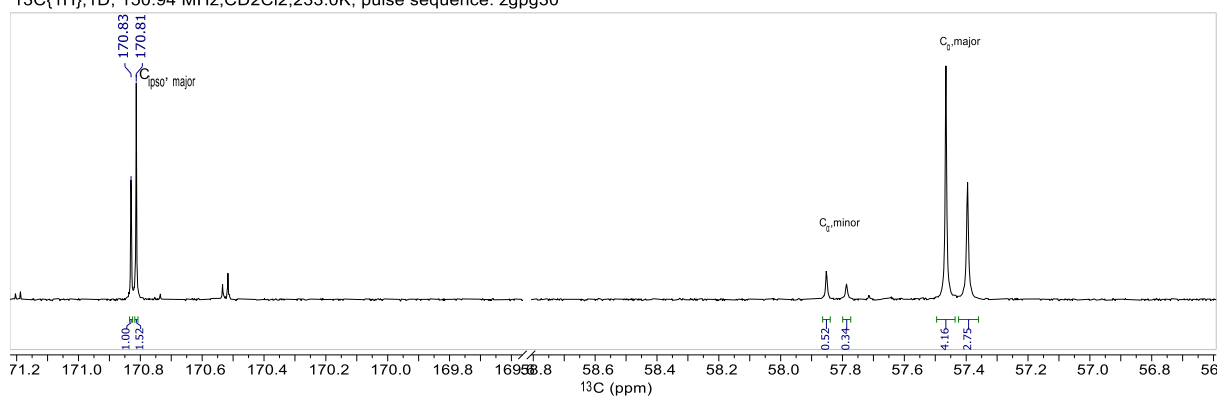
Figure 7.9: Experiment 2 for the determination of the KIE.

1H{off},1D, 600.20 MHz,CD2Cl2,233.0K, pulse sequence: zg30
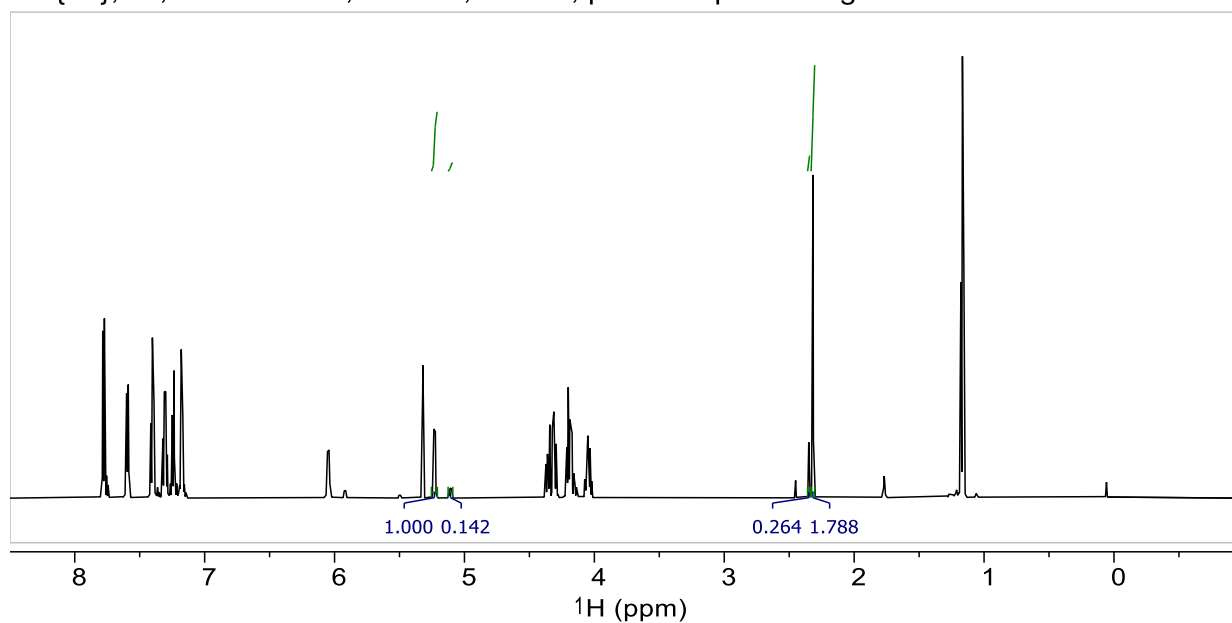
Figure 7.10: Full ^{1}H-NMR spectrum (exemplarily for experiment 1) for the determination of the KIE.

13C{1H},1D, 150.94 MHz,CD2Cl2,233.0K, pulse sequence: zgpg30

13C (ppm)
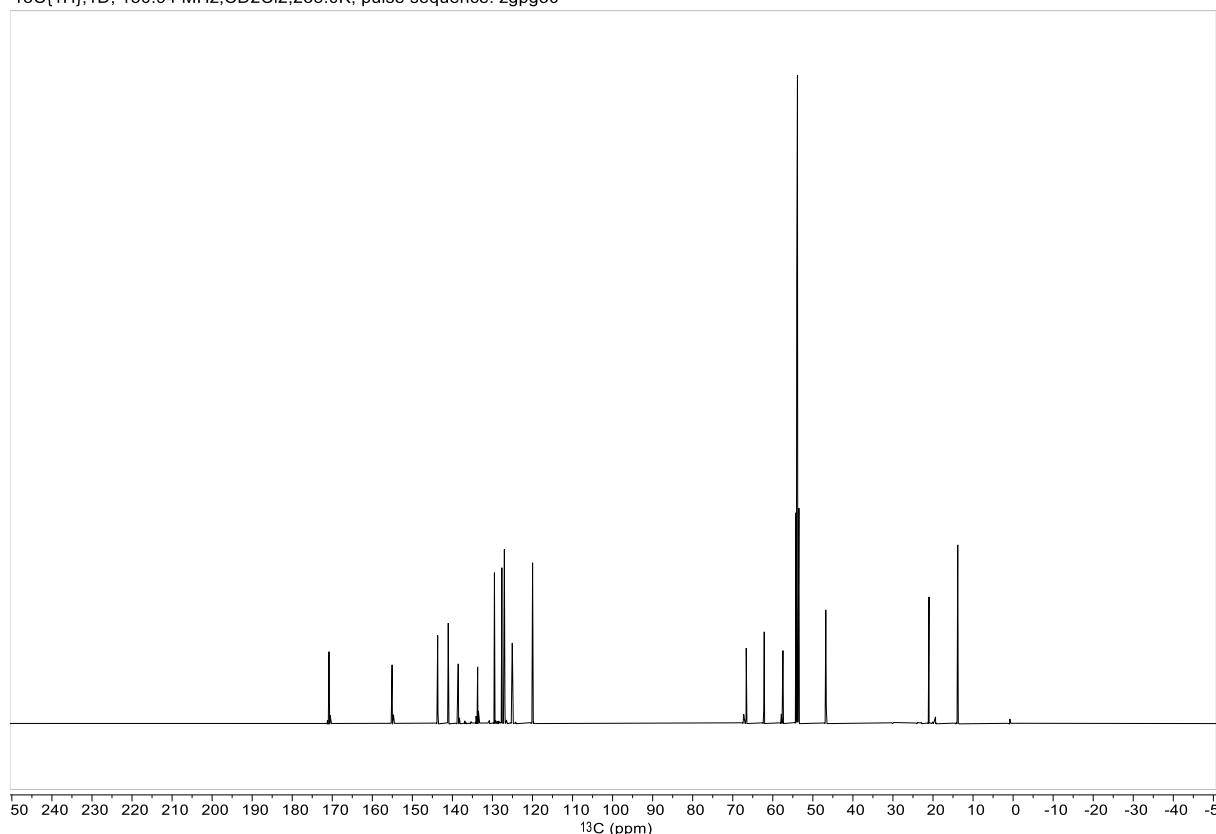
Figure 7.11: Full ^{13}C-NMR spectrum (exemplarily for experiment 1) for the determination of the KIE.

Based on the above measurements (figure **7.8** and **7.9**), the KIE was determined as average of both experiments:

$$\text{KIE} = \frac{(\text{KIE}_1 + \text{KIE}_2)}{2} = 1.545$$

The corresponding standard deviation was determined as follows:

$$\sigma_{KIE} = \sqrt{\frac{\sigma_1{}^2}{2^2} + \frac{\sigma_2{}^2}{2^2}} = \sqrt{\frac{0.07^2}{2^2} + \frac{0.04^2}{2^2}} = 0.040$$

On the basis of the above calculations, a resulting KIE of **1.545 ± 0.040** could be determined.

Catalyst Stability Studies

Initial studies on the Friedel–Crafts reaction of *N,O*-acetal **54** with toluene (**3**) quickly revealed that the highly reactive nature of the electrophile (or rather its corresponding iminium ion) leads to visible hydrolysis of the (*S,S*)-IDPi's phosphoramide core which results in a stepwise degradation of the catalyst to the corresponding iminoimidodiphosphate (*i*IDP) and finally to the corresponding imidodiphosphate (IDP) (figure **7.12**).
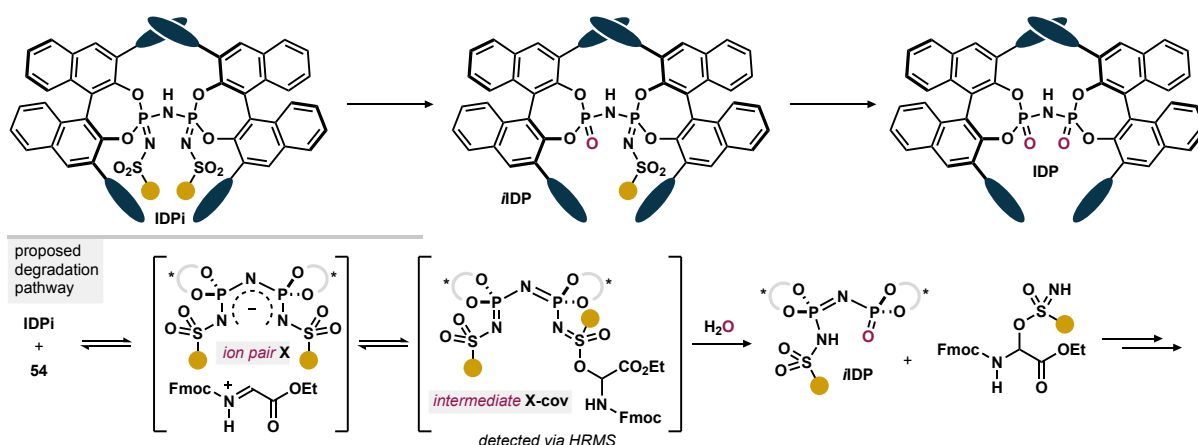
Figure 7.12: Stepwise degradation IDPi-catalysts.

As *i*IDP's as well as IDP's proved to be inactive in the Friedel–Crafts reaction investigated herein (see table **4.4**), hydrolysis of the catalytically active IDPi catalysts represents a problem that hinders successful C–C bond formation. To avoid this problem, we therefore optimized our catalysts to not only yield the desired arylglycine products with increased enantiomeric- and regioisomeric ratios, but also to be more resistant towards hydrolytic degradation which, consequentially, correlates with increased yields.

Finally, optimized catalysts **IDPi-10-c** and **IDPi-13-c**, used for the reaction scope (see scheme **4.4** and **4.7**) were found to be significantly more resilient towards hydrolytic degradation compared to benchmark **IDPi-01-a** as determined via ^{31}P-NMR studies (figure **7.13**) described as follows:

Evaluation of the stability of catalyst **IDPi-13-c** compared to benchmark catalyst **IDPi-01-a**:
The respective catalyst (1.25 µmol, 5 mol%) and *N,O*-acetal **54** (9.6 mg, 25 µmol, 1.0 equiv.) were given to an oven dried screwcap vial. The vial was placed under an atmosphere of argon and PhMe (0.3 mL) was added. The mixture was stirred at 30 °C for 20 h and then quenched via with NEt$_3$ (0.3 M solution in PhMe, 50 µL). The solution was transferred to an NMR tube

and analyzed via ^{31}P-NMR to determine the relative amount of catalyst degradation (see figure **7.13**).

Evaluation of the stability of catalyst **IDPi-13-c** compared to benchmark catalyst **IDP-01-a**:

The respective catalyst (1.25 µmol, 5 mol%) and *N,O*-acetal **54** (9.6 mg, 25 µmol, 1.0 equiv.) were given to an oven dried screwcap vial. The vial was placed under an atmosphere of argon and *n*-pentane (0.3 mL) was added quickly followed by anisole (**26**, 5.4 µL, 50 µmol, 2.0 equiv.). The mixture was stirred at 30 °C for 20 h and then quenched via with NEt$_3$ (0.3 M solution in PhMe, 50 µL). The solution was transferred to an NMR tube and analyzed via ^{31}P-NMR to determine the relative amount of catalyst degradation towards and (figure **7.13**).
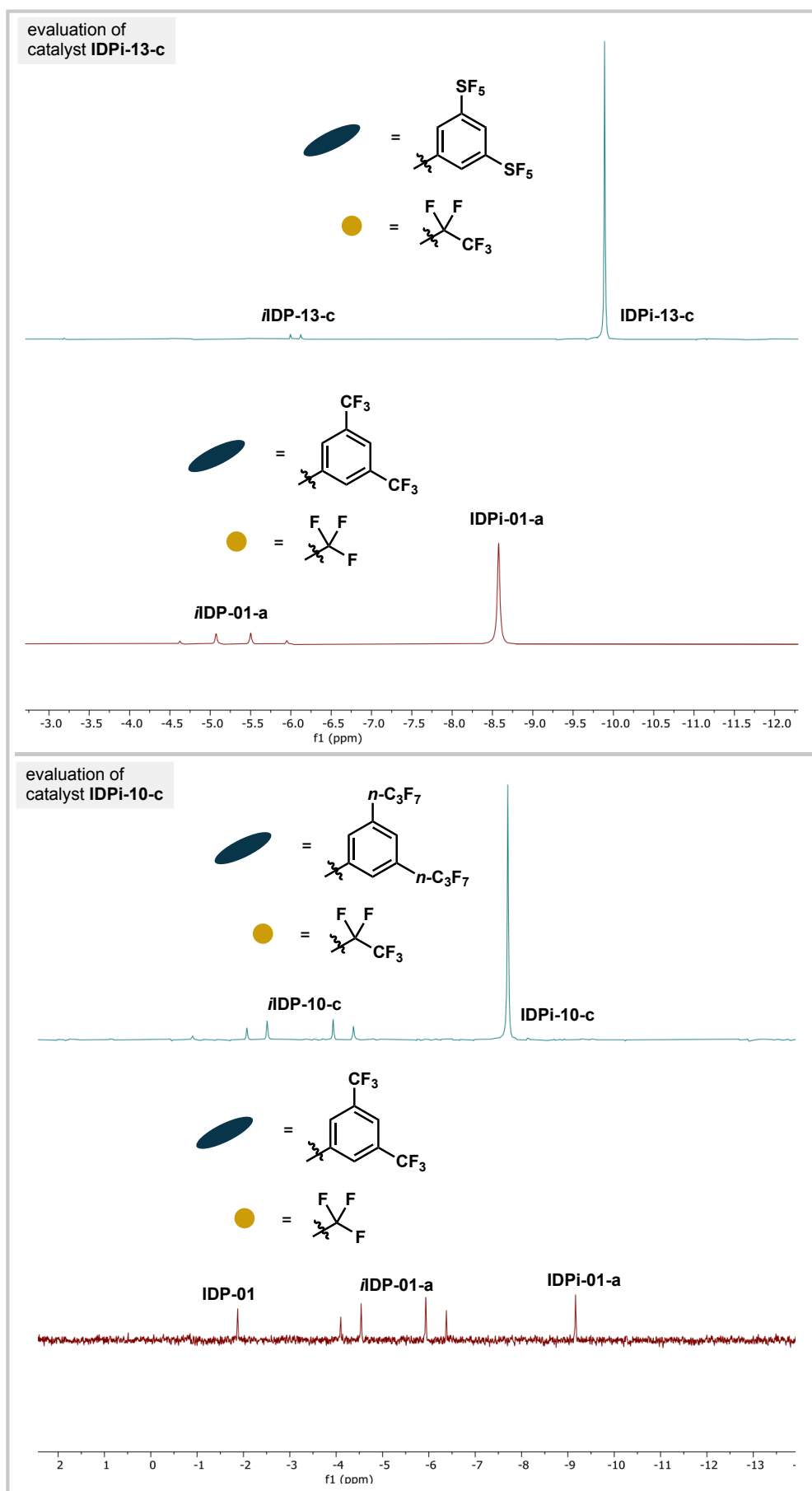
Figure 7.13: ^{31}P-NMR spectra to evaluate the stability of **IDPi-13-c** and **IDPi-10-c**.

Computational Methods

Preliminary structures were generated at the GFN0-xTB[206] level using the xtb program version 6.6.0, followed by exploration of the conformational landscape at the same level of theory using Grimme's Conformer–Rotamer Ensemble Sampling Tool (CREST)[207], version 2.12. All resulting conformers were subsequently optimized at the GFN2-xTB level and, eventually, subjected to DFT geometry optimizations.[208]

All DFT calculations were conducted using ORCA version 5.0.3.[209] GFN2-xTB conformers were subjected to DFT-level geometry optimizations using the PBE exchange-correlation functional[210] and Grimme's DFT-D3 scheme[211] with Becke–Johnson damping[212] along with the def2-SVP basis set[213] (VeryTightSCF convergence criterion) in Cartesian coordinates (COPT keyword). The Resolution of Identity (RI) approximation[214] in the Split-RI-J variant[215] using a corresponding auxiliary basis set[216] was used. True ground-state structures were verified by subsequent vibrational frequency calculation at the same level of theory via absence of imaginary frequencies.

Refined electronic energies were obtained using the M06-2X exchange-correlation functional[217] in conjunction with the def2-TZVP basis set.

Gibbs free energies were calculated using the M06-2X/def2-TZVP energies in combination with thermochemical corrections from the vibrational frequency calculations acquired by using Duarte's otherm.py in a 1 M solution standard state at 303 K.[218,219]

Following this protocol, at total number of 41 ion pair conformers were evaluated at the M06-2X/def2-TZVP | PBE-D3/def2-SVP level of theory. The conformer with the lowest Gibbs free energy was used for discussion.

Calculated Structure of Iminium Ion Pair X
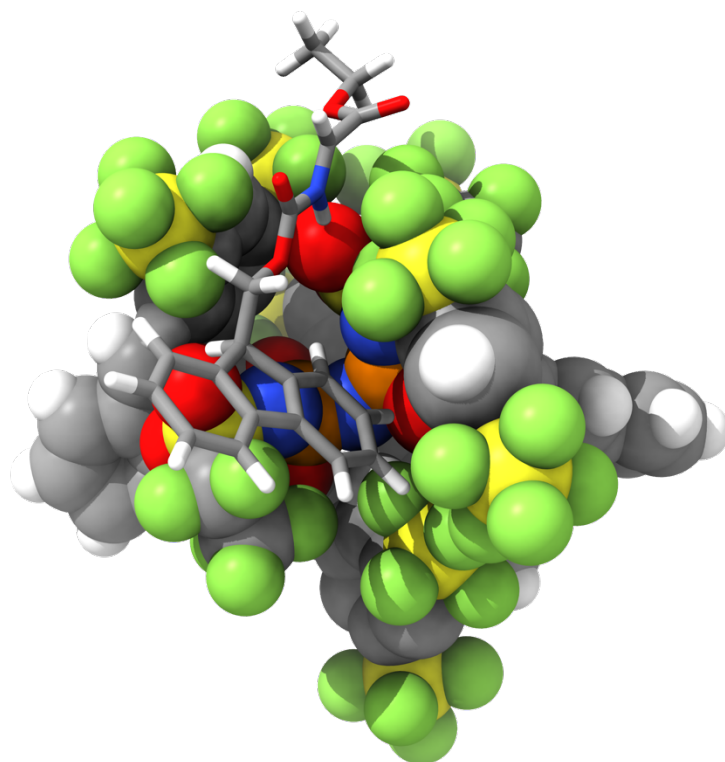
Figure 7.14: Calculated structure of iminium ion pair **X** (white = hydrogen; grey = carbon; red = oxygen; blue = nitrogen; yellow = sulfur; green = fluorine; orange = phosphorus).
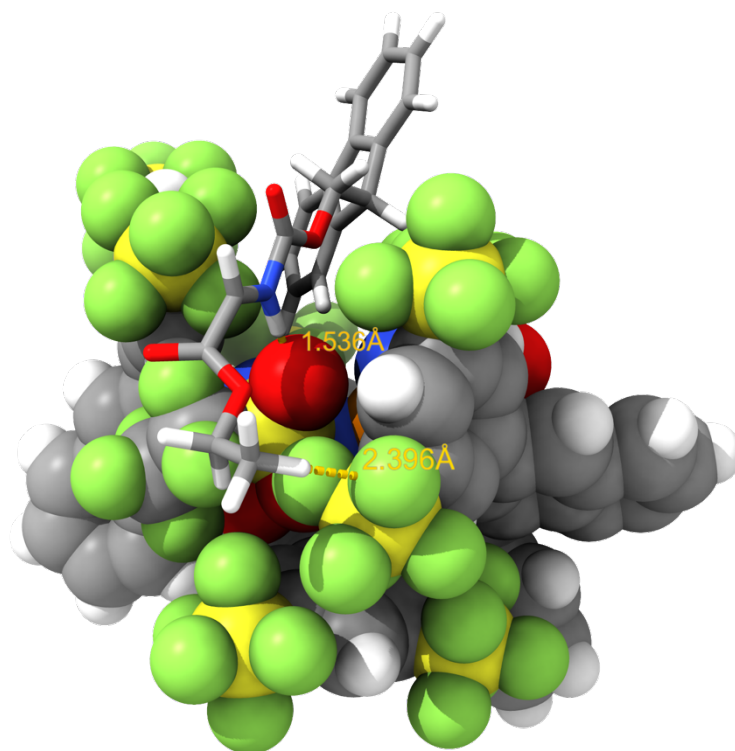
Figure 7.15: Calculated H–Bond interactions within ion pair **X**.
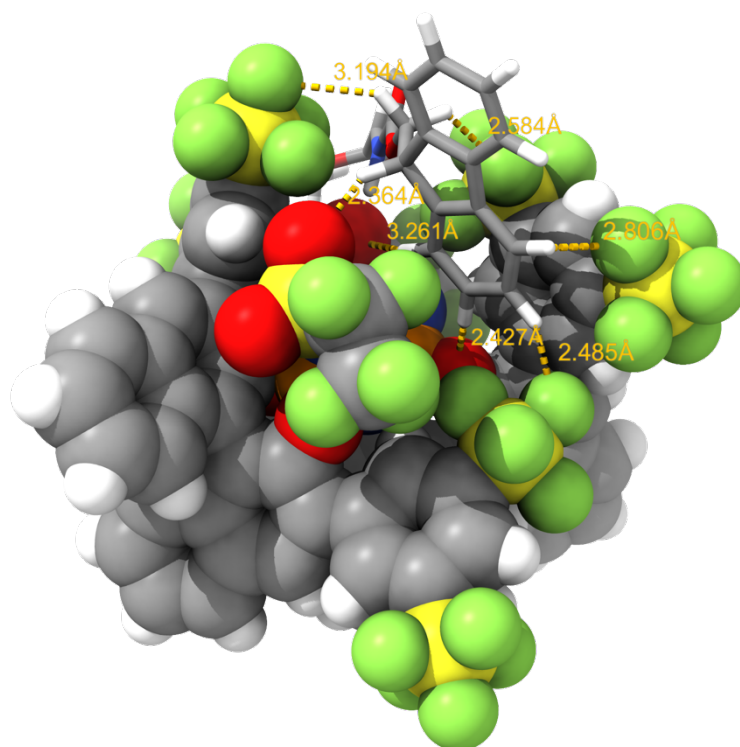
Figure 7.16: Calculated H–Bond interactions within ion pair **X**, interactions with the fluorenyl backbone of electrophile **54**.

Molecular Electrostatic Potential
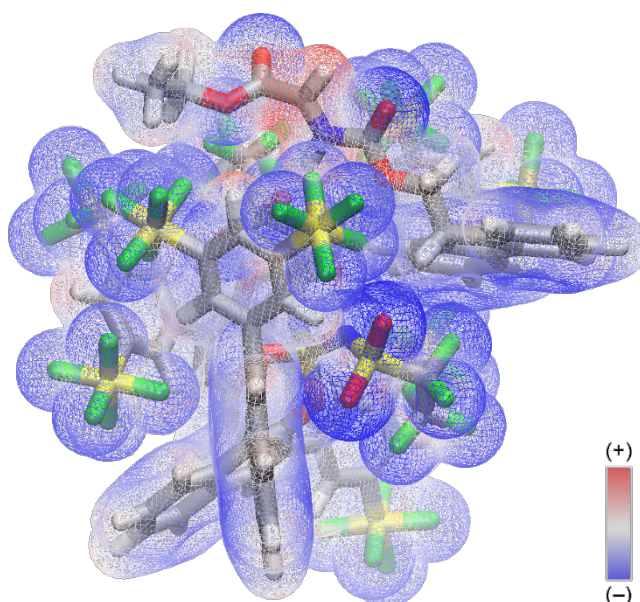
Figure 7.17: Isosurface of the electron density ($\rho = 0.015$) colored by electrostatic potential.

XYZ Structures

Electronic energy (a. u.) | M06-2X/def2-TZVP	–14123.9575606678
Thermochemical Corrections (a. u.) | PBE-D3(BJ)/def2-SVP	1.149237608
Imaginary Frequencies	Zero
Gibbs Free Energy (a. u.)	–14122.808323060

215

```
C    -4.603982   -3.976447    6.420440
C    -3.894899   -4.974413    5.701380
C    -4.725026   -2.701054    5.892636
C    -3.339889   -4.693191    4.461645
C    -4.152680   -2.375437    4.628409
C    -3.463289   -3.396966    3.880877
H    -2.781364   -5.469984    3.922072
H    -5.042245   -4.214132    7.401221
H    -3.775758   -5.978669    6.135106
H    -5.252549   -1.911092    6.449020
C    -2.882926   -3.057067    2.608800
C    -4.241793   -1.060756    4.097379
C    -3.628141   -0.715973    2.900515
C    -2.912537   -1.725897    2.197307
O    -2.188412   -1.356256    1.063825
H    -4.799847   -0.295075    4.657507
C    -2.249093   -4.083142    1.738170
C    -3.008591   -5.216994    1.274686
C    -0.906655   -3.954359    1.360497
C    -2.339987   -6.221676    0.487907
C    -0.951913   -6.090862    0.237299
C    -0.204581   -4.990971    0.659172
O    -0.196048   -2.844007    1.778140
H    -0.451679   -6.891133   -0.324918
C    -4.399802   -5.384739    1.538031
C    -5.089304   -6.485035    1.051844
C    -4.428617   -7.473422    0.275882
C    -3.078350   -7.340028   -0.002867
H    -4.991417   -8.337188   -0.108110
H    -2.549849   -8.097153   -0.603163
H    -4.935992   -4.611419    2.100992
H    -6.167469   -6.576680    1.249816
P    -0.532931   -1.309445    1.242440
N     0.031395   -0.248493    2.285618
N     0.029722   -1.190224   -0.240984
O     2.007961   -0.330537   -1.648393
C     2.586421   -0.527625   -2.891564
C     2.212417   -1.613305   -3.691265
C     1.120195   -2.544260   -3.288518
```

C	-0.143559	-2.023208	-3.011325
O	-0.256409	-0.648971	-2.813610
C	-1.314834	-2.822540	-2.853022
C	-1.151462	-4.204365	-2.860895
H	-2.033994	-4.854733	-2.760233
C	0.133901	-4.803262	-2.984073
C	0.301108	-6.216213	-2.879717
H	-0.597434	-6.841096	-2.762402
C	1.563881	-6.786862	-2.887110
H	1.688027	-7.871454	-2.755114
C	2.710953	-5.962766	-3.036864
H	3.711779	-6.417005	-2.992315
C	2.579304	-4.593838	-3.220582
H	3.471922	-3.965294	-3.332409
C	1.295307	-3.972798	-3.196061
C	2.891207	-1.807803	-4.949981
C	2.489842	-2.793314	-5.900649
H	1.615854	-3.422076	-5.685428
C	3.177939	-2.958422	-7.094160
H	2.843147	-3.722025	-7.812268
C	4.301750	-2.147659	-7.402557
H	4.840471	-2.291187	-8.351056
C	4.704750	-1.165158	-6.512906
H	5.561914	-0.514463	-6.745540
C	4.012520	-0.964167	-5.282307
C	4.397212	0.065507	-4.382631
H	5.260083	0.700152	-4.637151
C	3.691184	0.318639	-3.212301
P	0.400457	-0.153256	-1.370609
N	0.162545	1.440334	-1.228737
S	-0.138781	-0.192808	3.902157
C	1.566553	-0.687205	4.599614
S	-1.273099	2.119097	-1.381384
C	-1.063166	3.170580	-2.960427
O	-1.056074	-1.201681	4.479566
O	-0.280819	1.223429	4.314658
O	-1.466571	3.187925	-0.344158
O	-2.410860	1.208013	-1.608041
C	2.095688	-2.094310	4.202901
C	-0.507224	2.470811	-4.234297
F	1.401968	-0.662962	5.941829
F	2.485061	0.230010	4.248699
F	3.202536	-2.370270	4.919929
F	1.183726	-3.045160	4.446226
F	2.423739	-2.121535	2.898942
F	-0.542168	3.346407	-5.251679
F	-1.245703	1.404509	-4.557753
F	0.770240	2.081911	-4.055375
F	-0.233027	4.195743	-2.654422
F	-2.281725	3.674170	-3.257233
C	-3.750554	0.668739	2.374621

C	-4.463519	0.903342	1.180887
C	-3.258695	1.756681	3.123682
C	-4.696460	2.219241	0.776882
C	-4.226256	3.319928	1.499311
C	-3.519968	3.054366	2.673707
H	-2.664514	1.574155	4.029399
H	-4.866239	0.055856	0.614740
H	-4.415294	4.343787	1.165220
C	1.274947	-5.034226	0.503915
C	2.097809	-3.911435	0.250458
H	1.645976	-2.927058	0.081212
C	3.488855	-4.080690	0.206296
C	4.107539	-5.328534	0.337753
H	5.194013	-5.443194	0.292152
C	3.269750	-6.429454	0.516769
C	1.889503	-6.300147	0.634802
H	1.278379	-7.183503	0.850650
C	-2.662448	-2.203398	-2.781447
C	-3.629757	-2.681809	-1.877457
C	-4.930291	-2.173064	-1.953177
C	-5.317823	-1.209348	-2.884660
H	-6.345312	-0.838534	-2.919404
C	-4.329051	-0.713042	-3.741023
C	-3.015527	-1.184368	-3.695077
H	-2.259574	-0.795308	-4.382721
C	4.153273	1.408180	-2.307922
C	5.472027	1.360046	-1.812301
H	6.097156	0.484697	-2.023855
C	5.960668	2.417657	-1.041298
C	5.189706	3.543826	-0.744574
H	5.587304	4.365650	-0.140358
C	3.887890	3.566411	-1.251713
C	3.344170	2.521266	-2.003695
H	-3.359166	-3.435923	-1.127228
H	2.314957	2.573772	-2.374979
S	-6.189305	-2.768538	-0.770780
S	-4.807701	0.572200	-4.969047
F	-5.682536	-0.521309	-5.818547
F	-3.502815	0.258071	-5.911930
F	-3.967367	1.731780	-4.177675
F	-6.153265	0.993934	-4.134231
F	-5.232666	1.701495	-6.073454
F	-6.732647	-1.245051	-0.467184
F	-7.322753	-2.930385	-1.939364
F	-5.132404	-2.621183	0.490189
F	-5.729575	-4.326009	-1.001333
F	-7.288883	-3.317006	0.305480
S	-2.978778	4.476887	3.689594
S	-5.700265	2.538644	-0.719371
F	-2.538887	5.346594	2.336016
F	-2.481868	5.765238	4.569381

F	-3.385999	3.737287	5.084382
F	-1.456663	3.891775	3.805580
F	-4.459998	5.172073	3.615880
F	-6.984547	1.732979	-0.109570
F	-6.590223	2.863482	-2.054943
F	-5.196087	1.175149	-1.456134
F	-4.468542	3.380352	-1.414664
F	-6.298109	3.946175	-0.088695
H	0.800616	3.321817	4.196383
H	1.108709	2.286032	1.441724
H	0.633794	5.802492	3.865508
H	1.445251	5.474542	6.283672
H	-0.983726	4.608030	-0.013422
O	0.433151	4.937527	1.983896
C	1.685147	3.883234	3.825734
C	1.249096	5.190095	3.177107
C	2.135802	2.239245	1.826325
C	2.435494	5.037994	6.078296
N	-0.819664	5.653998	0.230215
C	2.524863	2.978293	2.945166
C	2.648191	4.241364	4.949796
C	-0.008182	6.026509	1.405106
H	2.786982	0.773799	0.367305
H	3.354415	5.887762	7.857127
C	3.078765	1.385401	1.229191
C	3.507736	5.266596	6.961841
H	2.122728	5.786607	2.848386
C	-1.346723	6.615623	-0.447156
C	3.840996	2.870888	3.466753
C	3.923306	3.670800	4.694877
O	-3.335927	6.019151	-1.584975
C	-2.106829	6.478356	-1.731046
O	0.146424	7.184563	1.708370
C	4.387659	1.283307	1.734550
C	4.772737	4.704567	6.710121
C	4.783748	2.031591	2.853448
C	4.990302	3.902039	5.578334
H	5.101474	0.596342	1.261273
H	5.600598	4.894446	7.410262
O	-1.540816	6.871558	-2.733947
H	5.980714	3.462054	5.385966
H	5.806953	1.942891	3.248114
C	-4.211618	6.010545	-2.770062
C	-5.588154	6.470731	-2.349952
H	-4.218544	4.965916	-3.129876
H	-3.744606	6.655941	-3.539131
H	-6.016556	5.794771	-1.587138
H	-6.255870	6.452424	-3.234278
H	-5.570250	7.505373	-1.954359
H	-1.100047	7.638500	-0.096644
S	4.589158	-2.628717	-0.025970

S	4.008771	-8.100613	0.559433
F	3.465978	-1.587959	0.534032
F	5.577038	-1.325806	-0.239941
F	5.812109	-3.537577	-0.638820
F	5.210308	-2.791378	1.472736
F	4.046573	-2.388391	-1.560301
F	2.834467	-8.698548	-0.429927
F	5.226930	-7.609370	1.536160
F	4.934906	-7.773806	-0.760486
F	4.664012	-9.593206	0.580056
F	3.120257	-8.528820	1.867266
S	2.878777	5.059985	-0.956472
F	4.123101	6.063853	-1.295032
F	2.401347	5.126094	-2.520968
F	1.952790	6.406133	-0.693936
F	1.545053	4.169855	-0.590941
F	3.277620	5.114893	0.636711
S	7.677221	2.339884	-0.406596
F	8.225575	1.732430	-1.828730
F	7.463116	0.816748	0.161492
F	9.210135	2.273842	0.145121
F	7.990102	3.859607	-0.938572
F	7.236248	2.946246	1.051753

7.1.9 Crystallographic Data
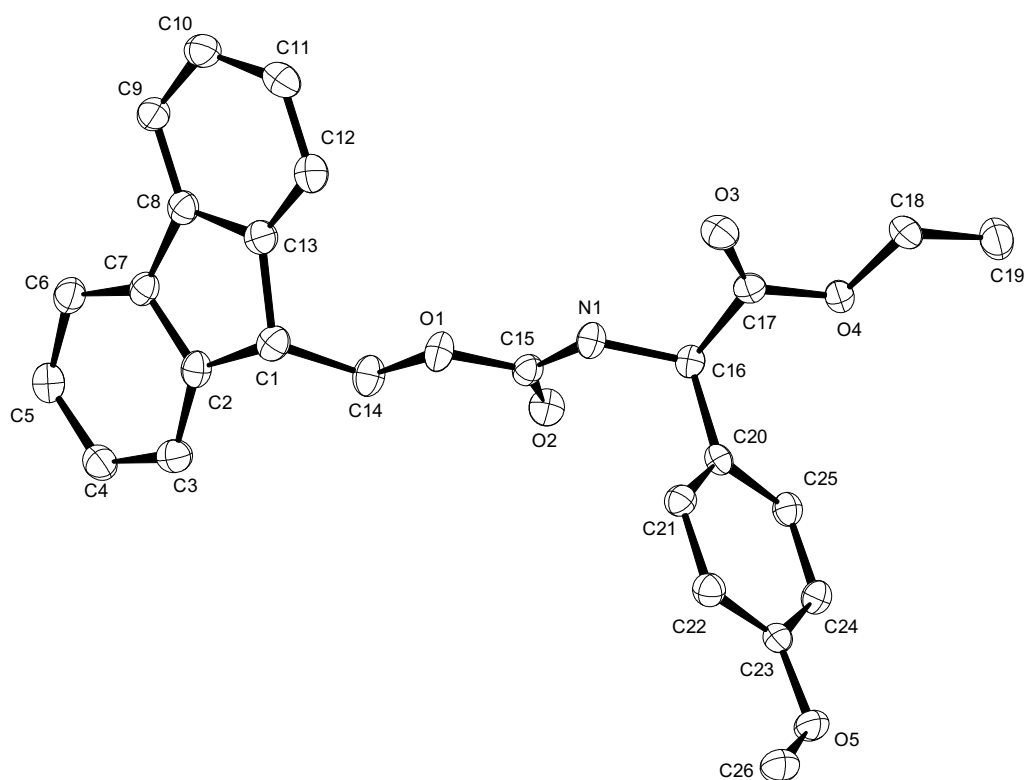
Figure 7.18: X-Ray structure of compound 69 (H atoms omitted).

Table 7.1: Crystal data and structure refinement.

Identification code	14764
Empirical formula	$C_{26} H_{25} N O_5$
Color	colorless
Formula weight	431.47 g · mol^{-1}
Temperature	100(2) K
Wavelength	1.54178 Å
Crystal system	ORTHORHOMBIC
Space group	**P2$_1$2$_1$2$_1$, (no. 19)**
Unit cell dimensions	a = 4.9650(2) Å $\quad$ α= 90°.
	b = 15.3800(5) Å $\quad$ β= 90°.
	c = 28.5256(9) Å $\quad$ γ= 90°.
Volume	2178.26(13) Å^3
Z	4
Density (calculated)	1.316 Mg · m^{-3}
Absorption coefficient	0.743 mm^{-1}
F(000)	912 e
Crystal size	0.107 x 0.096 x 0.031 mm^3
range for data collection	3.098 to 72.230°.
Index ranges	-6 ≤ h ≤ 5, -17 ≤ k ≤ 18, -35 ≤ 1 ≤ 35
Reflections collected	78403
Independent reflections	4200 [R_{int} = 0.0876]

Reflections with I>2σ(I)	3509	
Completeness to = 67.679°	99.3 %	
Absorption correction	Gaussian	
Max. and min. transmission	0.98 and 0.94	
Refinement method	Full-matrix least-squares on F^2	
Data / restraints / parameters	4200 / 0 / 299	
Goodness-of-fit on F^2	1.087	
Final R indices [I>2 σ (I)]	$R_1 = 0.0379$	$wR^2 = 0.0923$
R indices (all data)	$R_1 = 0.0560$	$wR^2 = 0.0992$
Absolute structure parameter	0.23(14)	
Largest diff. peak and hole	0.4 and -0.3 e · Å^{-3}	

O(1)-C(14)	1.454(3)	O(1)-C(15)	1.347(3)
O(2)-C(15)	1.220(3)	O(3)-C(17)	1.207(3)
O(4)-C(17)	1.330(3)	O(4)-C(18)	1.454(3)
O(5)-C(23)	1.371(3)	O(5)-C(26)	1.432(3)
N(1)-C(15)	1.347(3)	N(1)-C(16)	1.452(3)
N(1)-H(1)	0.92(4)	C(1)-C(2)	1.520(4)
C(1)-C(13)	1.521(4)	C(1)-C(14)	1.521(4)
C(2)-C(3)	1.381(4)	C(2)-C(7)	1.402(4)
C(3)-C(4)	1.388(4)	C(4)-C(5)	1.392(4)
C(5)-C(6)	1.391(4)	C(6)-C(7)	1.390(4)
C(7)-C(8)	1.465(4)	C(8)-C(9)	1.391(4)
C(8)-C(13)	1.400(4)	C(9)-C(10)	1.396(4)
C(10)-C(11)	1.391(4)	C(11)-C(12)	1.392(4)
C(12)-C(13)	1.380(4)	C(16)-C(17)	1.528(4)
C(16)-C(20)	1.522(4)	C(16)-H(16)	0.97(3)
C(18)-C(19)	1.504(4)	C(20)-C(21)	1.388(4)
C(20)-C(25)	1.398(4)	C(21)-C(22)	1.394(4)
C(22)-C(23)	1.389(4)	C(23)-C(24)	1.398(4)
C(24)-C(25)	1.376(4)		
C(15)-O(1)-C(14)	113.3(2)	C(17)-O(4)-C(18)	116.3(2)
C(23)-O(5)-C(26)	117.2(2)	C(15)-N(1)-C(16)	118.6(2)
C(15)-N(1)-H(1)	120(2)	C(16)-N(1)-H(1)	119(2)
C(2)-C(1)-C(13)	102.1(2)	C(2)-C(1)-C(14)	110.3(2)
C(14)-C(1)-C(13)	115.5(2)	C(3)-C(2)-C(1)	129.1(2)
C(3)-C(2)-C(7)	120.8(2)	C(7)-C(2)-C(1)	110.1(2)
C(2)-C(3)-C(4)	118.8(3)	C(3)-C(4)-C(5)	120.8(3)
C(6)-C(5)-C(4)	120.6(3)	C(7)-C(6)-C(5)	118.7(2)
C(2)-C(7)-C(8)	108.7(2)	C(6)-C(7)-C(2)	120.3(3)
C(6)-C(7)-C(8)	131.0(2)	C(9)-C(8)-C(7)	130.4(2)
C(9)-C(8)-C(13)	120.8(3)	C(13)-C(8)-C(7)	108.8(2)
C(8)-C(9)-C(10)	118.4(3)	C(11)-C(10)-C(9)	120.8(3)
C(10)-C(11)-C(12)	120.3(3)	C(13)-C(12)-C(11)	119.4(3)
C(8)-C(13)-C(1)	110.1(2)	C(12)-C(13)-C(1)	129.5(2)
C(12)-C(13)-C(8)	120.3(3)	O(1)-C(14)-C(1)	107.9(2)
O(1)-C(15)-N(1)	111.5(2)	O(2)-C(15)-O(1)	123.2(2)
O(2)-C(15)-N(1)	125.3(2)	N(1)-C(16)-C(17)	108.8(2)

N(1)-C(16)-C(20)	113.8(2)	N(1)-C(16)-H(16)	108.8(16)
C(17)-C(16)-H(16)	106.5(16)	C(20)-C(16)-C(17)	109.4(2)
C(20)-C(16)-H(16)	109.2(16)	O(3)-C(17)-O(4)	125.2(2)
O(3)-C(17)-C(16)	124.9(2)	O(4)-C(17)-C(16)	109.9(2)
O(4)-C(18)-C(19)	106.8(2)	C(21)-C(20)-C(16)	121.8(2)
C(21)-C(20)-C(25)	118.5(2)	C(25)-C(20)-C(16)	119.8(2)
C(20)-C(21)-C(22)	121.2(2)	C(23)-C(22)-C(21)	119.5(2)
O(5)-C(23)-C(22)	124.7(2)	O(5)-C(23)-C(24)	115.5(2)
C(22)-C(23)-C(24)	119.8(2)	C(25)-C(24)-C(23)	120.1(2)
C(24)-C(25)-C(20)	121.0(2)		
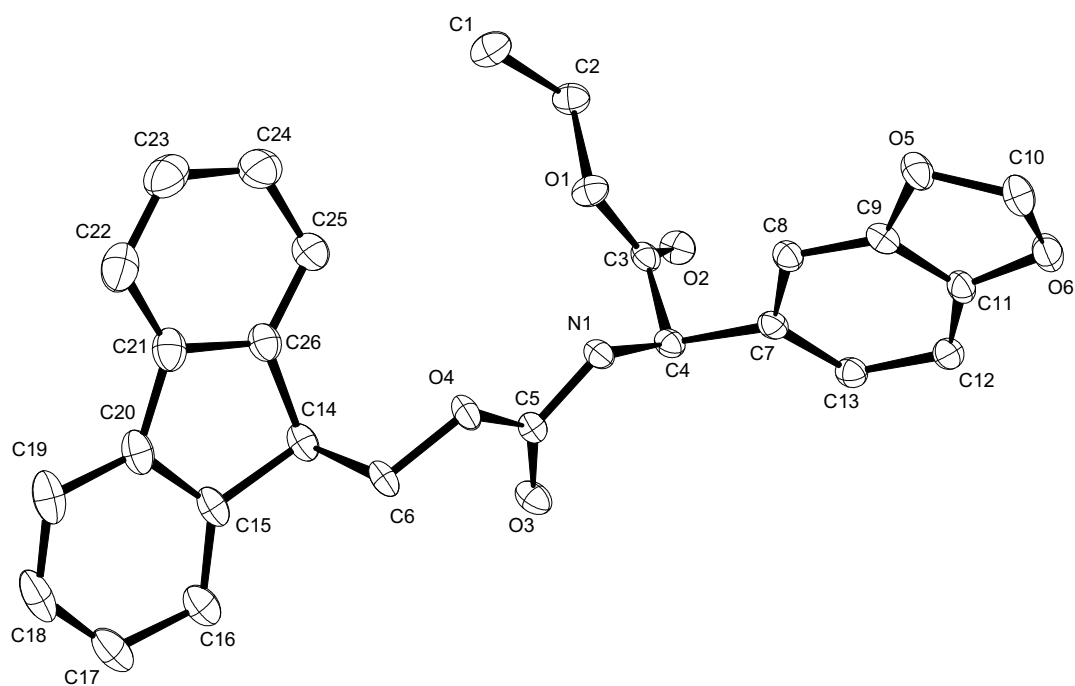
Figure 7.19: X-Ray structure of compound **203** (H atoms omitted).

Table 7.3: Crystal data and structure refinement.

Identification code	15002
Empirical formula	$C_{26}H_{23}NO_6$
Color	colorless
Formula weight	445.45 $g \cdot mol^{-1}$
Temperature	100(2) K
Wavelength	0.71073 Å
Crystal system	MONOCLINIC
Space group	**P2₁, (no. 4)**
Unit cell dimensions	a = 11.8304(5) Å α = 90°.
	b = 5.3051 (2) Å β = 92.125(2)°.
	c = 16.9907(7) Å γ = 90°.
Volume	1065.63(7) $Å^3$
Z	2
Density (calculated)	1.388 $Mg \cdot m^{-3}$
Absorption coefficient	0.099 mm^{-1}
F(000)	468 e
Crystal size	0.220 x 0.114 x 0.050 mm^3
range for data collection	2.062 to 31.055°.
Index ranges	-17 ≤ h ≤ 17, -7 ≤ k ≤ 7, -24 ≤ l ≤ 24
Reflections collected	241683
Independent reflections	6831 [R_{int} = 0.0441]
Reflections with I>2 σ (I)	6614
Completeness to = 25.242°	99.8 %
Absorption correction	Semi-empirical from equivalents

Max. and min. transmission	1.00 and 0.97	
Refinement method	Full-matrix least-squares on F^2	
Data / restraints / parameters	6831 / 1 / 311	
Goodness-of-fit on F^2	1.079	
Final R indices [I>2 σ (I)]	$R_1 = 0.0305$	$wR^2 = 0.0829$
R indices (all data)	$R_1 = 0.0317$	$wR^2 = 0.0842$
Absolute structure parameter	0.14(11)	
Largest diff. peak and hole	0.3 and -0.2 e · Å^{-3}	

Table 7.4: Bond lengths [Å] and angles [°].

O(1)-C(2)	1.4568(13)	O(1)-C(3)	1.3270(13)
O(2)-C(3)	1.2115(14)	O(3)-C(5)	1.2169(14)
O(4)-C(5)	1.3507(14)	O(4)-C(6)	1.4418(13)
O(5)-C(9)	1.3747(14)	O(5)-C(10)	1.4365(15)
O(6)-C(10)	1.4398(18)	O(6)-C(11)	1.3759(14)
N(1)-H(1)	0.842(19)	N(1)-C(4)	1.4497(14)
N(1)-C(5)	1.3570(13)	C(1)-C(2)	1.5062(18)
C(3)-C(4)	1.5334(15)	C(4)-H(4)	0.94(2)
C(4)-C(7)	1.5227(15)	C(6)-C(14)	1.5348(17)
C(7)-C(8)	1.4084(15)	C(7)-C(13)	1.3915(15)
C(8)-C(9)	1.3758(15)	C(9)-C(11)	1.3877(16)
C(11)-C(12)	1.3751(17)	C(12)-C(13)	1.4076(15)
C(14)-H(14)	1.01(3)	C(14)-C(15)	1.5162(16)
C(14)-C(26)	1.5127(18)	C(15)-C(16)	1.3871(18)
C(15)-C(20)	1.4037(18)	C(16)-C(17)	1.3991(18)
C(17)-C(18)	1.395(3)	C(18)-C(19)	1.391(3)
C(19)-C(20)	1.3946(18)	C(20)-C(21)	1.470(2)
C(21)-C(22)	1.391(2)	C(21)-C(26)	1.4045(18)
C(22)-C(23)	1.399(3)	C(23)-C(24)	1.392(3)
C(24)-C(25)	1.396(2)	C(25)-C(26)	1.3939(18)
C(3)-O(1)-C(2)	117.65(9)	C(5)-O(4)-C(6)	115.87(9)
C(9)-O(5)-C(10)	104.62(10)	C(11)-O(6)-C(10)	104.62(9)
C(4)-N(1)-H(1)	116.6(13)	C(5)-N(1)-H(1)	119.5(13)
C(5)-N(1)-C(4)	120.49(9)	O(1)-C(2)-C(1)	106.19(10)
O(1)-C(3)-C(4)	111.23(9)	O(2)-C(3)-O(1)	125.10(10)
O(2)-C(3)-C(4)	123.56(10)	N(1)-C(4)-C(3)	112.12(9)
N(1)-C(4)-H(4)	108.2(12)	N(1)-C(4)-C(7)	112.48(9)
C(3)-C(4)-H(4)	106.6(12)	C(7)-C(4)-C(3)	105.98(8)
C(7)-C(4)-H(4)	111.3(12)	O(3)-C(5)-O(4)	125.18(10)
O(3)-C(5)-N(1)	125.77(11)	O(4)-C(5)-N(1)	109.02(10)
O(4)-C(6)-C(14)	111.07(9)	C(8)-C(7)-C(4)	119.28(9)
C(13)-C(7)-C(4)	119.53(10)	C(13)-C(7)-C(8)	121.07(10)
C(9)-C(8)-C(7)	116.57(10)	O(5)-C(9)-C(8)	127.92(11)
O(5)-C(9)-C(11)	109.71(10)	C(8)-C(9)-C(11)	122.29(11)
O(5)-C(10)-O(6)	107.16(10)	O(6)-C(11)-C(9)	109.67(10)
C(12)-C(11)-O(6)	128.20(11)	C(12)-C(11)-C(9)	122.07(10)

C(11)-C(12)-C(13)	116.54(10)	C(7)-C(13)-C(12)	121.45(11)
C(6)-C(14)-H(14)	109.9(13)	C(15)-C(14)-C(6)	108.37(10)
C(15)-C(14)-H(14)	113.9(13)	C(26)-C(14)-C(6)	112.23(10)
C(26)-C(14)-H(14)	110.1(13)	C(26)-C(14)-C(15)	102.24(10)
C(16)-C(15)-C(14)	128.72(12)	C(16)-C(15)-C(20)	121.13(12)
C(20)-C(15)-C(14)	110.11(11)	C(15)-C(16)-C(17)	118.35(14)
C(18)-C(17)-C(16)	120.49(14)	C(19)-C(18)-C(17)	121.28(13)
C(18)-C(19)-C(20)	118.35(15)	C(15)-C(20)-C(21)	108.54(11)
C(19)-C(20)-C(15)	120.39(13)	C(19)-C(20)-C(21)	131.03(14)
C(22)-C(21)-C(20)	130.81(13)	C(22)-C(21)-C(26)	120.80(14)
C(26)-C(21)-C(20)	108.32(11)	C(21)-C(22)-C(23)	118.50(15)
C(24)-C(23)-C(22)	120.75(15)	C(23)-C(24)-C(25)	120.83(15)
C(26)-C(25)-C(24)	118.65(14)	C(21)-C(26)-C(14)	110.35(11)
C(25)-C(26)-C(14)	129.21(12)	C(25)-C(26)-C(21)	120.44(12)

Note: the absolute structure of compounds **69** and **203** was not determined unambiguously via X-ray analysis (see respective absolute structure parameter). For the determination of the absolute structure of arylglycine products prepared in this work please see section 7.1.5.

7.2 Asymmetric Organocatalytic Scriabine Reaction

7.2.1 Synthesis of Substrates and Reagents

General Procedure F (GP F): Synthesis of Acylals
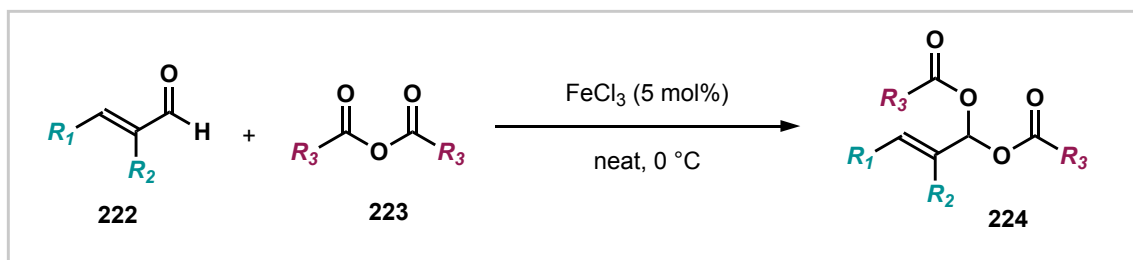
Following a procedure reported by Gandon,[184] to a flame dried Schlenk tube was added the used enal (**222**, 1.0 equiv.) followed by the used anhydride (**223**, 3.0 equiv.). The mixture was cooled to 0 °C in an ice bath and anhydrous FeCl$_3$ (5 mol%) was added in one portion. The mixture was stirred for 30 min at 0 °C and then poured into a separating funnel containing EtOAc (20 mL) and a saturated solution of NaHCO$_3$ (20 mL). The layers were separated and the aqueous layer was extracted with EtOAc (3x20 mL). The combined organic layers were dried over anhydrous Na$_2$SO$_4$ and concentrated under reduced pressure. The crude product was purified via flash column chromatography on silica gel (eluent: *n*-pentane/EtOAc mixtures) to yield the desired acylals **224** as colorless oils. The products were stored under an Ar atmosphere at 4 °C.

(*E*)-but-2-ene-1,1-diyl diacetate (117)

Prepared following *General Procedure F*, from *E*-crotonaldehyde (**140**, 1.0 mL, 12.1 mmol, 1.0 equiv.) and acetic anhydride (**225**, 3.42 mL, 36.3 mmol, 3.0 equiv.) using $FeCl_3$ (98.0 mg, 0.60 mmol, 5 mol%) as catalyst at 0 °C for 30 min. Purification by silica gel flash column chromatography (eluent: *i*-hexanes/EtOAc 20:1) gave **117** as colorless oil (775 mg, 4.50 mmol, 38%).
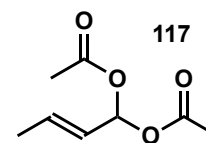
^{1}H-NMR:	(501 MHz, CD_2Cl_2): δ = 7.04 (dt, J = 6.3, 0.8 Hz, 1H), 6.02 (dqd, J = 15.6, 6.6, 0.9 Hz, 1H), 5.55 (ddq, J = 15.5, 6.4, 1.7 Hz, 1H), 2.05 (s, 6H), 1.78 – 1.71 (m, 3H).
^{13}C-NMR:	(126 MHz, CD_2Cl_2): δ = 168.64, 132.83, 124.67, 89.37, 20.64, 17.29.
EI-HRMS:	calculated for $C_8H_{16}O_4N_1$ ([M+NH$_4$]$^+$): 190.10738, found: 190.10737.

The spectroscopic data is in agreement with the reported literature.[184]

(*E*)-pent-2-ene-1,1-diyl diacetate (118)

Prepared following *General Procedure F*, from trans-2-pentenale (**116**, 0.15 mL, 1.5 mmol, 1.0 equiv.) and acetic anhydride (**225**, 0.43 mL, 4.5 mmol, 3.0 equiv.) using $FeCl_3$ (12.2 mg, 75 µmol, 5 mol%) as catalyst at 0 °C for 30 min. Purification by silica gel flash column chromatography (eluent: *i*-hexanes/EtOAc 20:1) gave **118** as colorless oil (213 mg, 1.15 mmol, 77%).
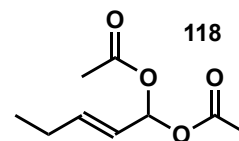
^{1}H-NMR:	(501 MHz, CD_2Cl_2): δ = 7.06 (dd, J = 6.3, 0.9 Hz, 1H), 6.05 (dtd, J = 15.6, 6.2, 0.9 Hz, 1H), 5.52 (ddt, J = 15.6, 6.3, 1.7 Hz, 1H), 2.10 (td, J = 6.8, 1.7 Hz, 2H), 2.05 (s, 6H), 1.01 (t, J = 7.4 Hz, 3H).
^{13}C-NMR:	(126 MHz, CD_2Cl_2): δ = 168.64, 139.26, 122.40, 89.48, 24.94, 20.66, 12.43.
EI-HRMS:	calculated for $C_9H_{18}O_4N_1$ ([M+NH$_4$]$^+$): 204.12303, found: 204.12306.

The spectroscopic data is in agreement with the reported literature.[184]

(*E*)-3-phenylprop-2-ene-1,1-diyl diacetate (119)

Prepared following *General Procedure F*, from cinnamaldehyde (**141**, 198 mg, 1.5 mmol, 1.0 equiv.) and acetic anhydride (**225**, 0.43 mL, 4.5 mmol, 3.0 equiv.) using FeCl$_3$ (12.2 mg, 75 µmol, 5 mol%) as catalyst at 0 °C for 30 min. Purification by silica gel flash column chromatography (eluent: *i*-hexanes/EtOAc 20:1) gave **119** as white crystalline solid (193 mg, 0.825 mmol, 55%).
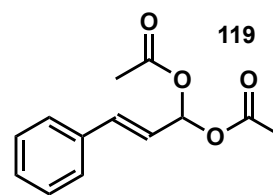
^{1}H-NMR:	(501 MHz, CD$_2$Cl$_2$): δ = 7.44 (dt, J = 8.1, 1.4 Hz, 2H), 7.39 – 7.34 (m, 2H), 7.33 – 7.25 (m, 2H), 6.85 (dd, J = 16.1, 1.7 Hz, 1H), 6.23 (ddd, J = 16.0, 6.2, 1.8 Hz, 1H), 2.10 (d, J = 1.0 Hz, 6H).
^{13}C-NMR:	(126 MHz, CD$_2$Cl$_2$): δ = 168.66, 135.26, 135.08, 128.78, 128.68, 126.93, 121.99, 89.35, 20.67.
ESI-HRMS:	calculated for C$_{13}$H$_{14}$O$_4$Na$_1$ ([M+Na]$^+$): 257.07843, found: 257.07823.

cyclohex-1-en-1-ylmethylene diacetate (120)

Prepared following *General Procedure F*, from cyclohex-1-ene-1-carbaldehyde (**226**, 0.35 mL, 3.10 mmol, 1.0 equiv.) and acetic anhydride (**225**, 1.16 mL, 12.3 mmol, 4.0 equiv.) using FeCl$_3$ (5.0 mg, 31 µmol, 1 mol%) as catalyst at 0 °C for 30 min. Purification by silica gel flash column chromatography (eluent: *i*-hexanes/MTBE 10:1) gave **120** as yellow oil (292 mg, 1.38 mmol, 44%).
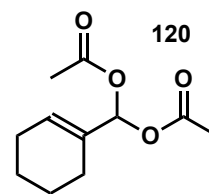
^{1}H-NMR:	(501 MHz, CD$_2$Cl$_2$): δ = 7.02 (s, 1H), 6.02 – 5.96 (m, 1H), 2.08 (s, 6H), 2.07 – 2.02 (m, 4H), 1.69 – 1.56 (m, 4H).
^{13}C-NMR:	(126 MHz, CD$_2$Cl$_2$): δ = 168.98, 132.23, 128.88, 91.83, 24.86, 22.62, 22.11, 21.03.

cyclopent-1-en-1-ylmethylene diacetate (121)

Prepared following *General Procedure F*, from cyclopent-1-ene-1-carbaldehyde (**227**, 0.5 mL, 4.94 mmol, 1.0 equiv.) and acetic anhydride (**225**, 1.40 mL, 14.8 mmol, 3.0 equiv.) using $FeCl_3$ (40.1 mg, 0.25 mmol, 5 mol%) as catalyst at 0 °C for 30 min. Purification by silica gel flash column chromatography (eluent: *i*-hexanes/Et_2O 8:1) gave **121** as yellow oil (695 mg, 4.94 mmol, 71%).
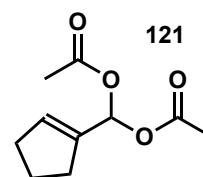
^{1}H-NMR:	(501 MHz, CD_2Cl_2): δ = 7.31 (s, 1H), 5.93 (d, J = 2.1 Hz, 1H), 2.43 – 2.36 (m, 4H), 2.09 (s, 6H), 1.94 (p, J = 7.6 Hz, 2H).
^{13}C-NMR:	(126 MHz, $CDCl_3$): δ = 168.87, 138.13, 131.77, 87.67, 32.41, 30.48, 23.03, 20.90.
EI-HRMS:	calculated for $C_{10}H_{18}O_4N_1$ ($[M+NH_4]^+$): 216.12303, found: 216.12292.

(*E*)-but-2-ene-1,1-diyl bis(2-methylpropanoate) (122)

Prepared following *General Procedure F* with deviations, from *E*-crotonaldehyde (**140**, 0.75 mL, 9.0 mmol, 3.0 equiv.) and isobutyric acid anhydride (**228**, 0.5 mL, 3.0 mmol, 1.0 equiv.) using $FeCl_3$ (5 mg, 30 μmol, 1 mol%) as catalyst at 0 °C for 30 min. Purification by silica gel flash column chromatography (eluent: *i*-hexanes/EtOAc 20:1) gave **122** as colorless oil (493 mg, 2.16 mmol, 72%).
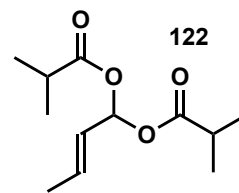
^{1}H-NMR:	(501 MHz, CD_2Cl_2): δ = 7.08 (d, J = 6.3 Hz, 1H), 6.02 (dqd, J = 15.4, 6.6, 0.9 Hz, 1H), 5.57 (ddq, J = 15.5, 6.4, 1.8 Hz, 1H), 2.56 (dq, J = 14.0, 7.1 Hz, 2H), 1.76 (dd, J = 6.6, 1.7 Hz, 3H), 1.17 (dd, J = 7.0, 1.9 Hz, 12H).
^{13}C-NMR:	(126 MHz, $CDCl_3$): δ = 174.95, 132.79, 124.95, 89.66, 34.01, 18.88, 18.70, 17.74.
EI-HRMS:	calculated for $C_{12}H_{24}O_4N_1$ ($[M+NH_4]^+$): 246.16998, found: 246.16996.

(*E*)-but-2-ene-1,1-diyl bis(3-methylbutanoate) (123)

Prepared following *General Procedure F* with deviations, from *E*-crotonaldehyde (**140**, 1.0 mL, 12.1 mmol, 1.0 equiv.) and isovaleric acid anhydride (**157**, 7.2 mL, 36.3 mmol, 3.0 equiv.) using $FeCl_3$ (98 mg, 0.61 mmol, 5 mol%) as catalyst at 0 °C for 30 min. Purification by silica gel flash
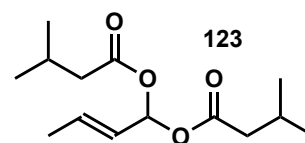
column chromatography (eluent: *i*-hexanes/Et₂O 20:1) gave **123** as colorless oil (1.10 g, 4.30 mmol, 36%).

¹H-NMR:	(501 MHz, CDCl₃): δ = 7.12 (d, J = 6.4 Hz, 1H), 6.03 (dqd, J = 15.6, 6.6, 0.9 Hz, 1H), 5.56 (ddq, J = 15.5, 6.5, 1.7 Hz, 1H), 2.20 (dd, J = 7.1, 4.0 Hz, 4H), 2.11 (dq, J = 13.6, 6.7 Hz, 2H), 1.75 (dd, J = 6.6, 1.7 Hz, 3H), 0.95 (d, J = 6.6 Hz, 12H).
¹³C-NMR:	(126 MHz, CD₂Cl₂): δ = 170.87, 132.95, 124.97, 89.50, 43.29, 25.69, 22.41, 22.37, 17.71.
EI-HRMS:	calculated for C₁₄H₂₈O₄N₁ ([M]⁺): 274.20128, found: 274.20142.

(*E*)-but-2-ene-1,1-diyl bis(2,2-dimethylpropanoate) (124)

Prepared following *General Procedure F* with deviations, from *E*-crotonaldehyde (**140**, 0.41 mL, 5.0 mmol, 1.0 equiv.) and pivalic acid anhydride (**160**, 3.04 mL, 15 mmol, 3.0 equiv.) using FeCl₃ (8.1 mg, 0.05 mmol, 5 mol%) as catalyst at 0 °C for 30 min. Purification by kugelrohr distillation (0.08 mBar, 50 °C → 70 °C) gave **124** as colorless oil (679 mg, 2.65 mmol, 53%).
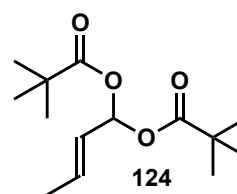
¹H-NMR:	(501 MHz, CDCl₃): δ = 7.05 (d, J = 6.1 Hz, 1H), 6.00 (dqd, J = 15.6, 6.6, 1.0 Hz, 1H), 5.57 (ddq, J = 15.5, 6.1, 1.7 Hz, 1H), 1.75 (dd, J = 6.7, 1.7 Hz, 3H), 1.19 (s, 18H).
¹³C-NMR:	(126 MHz, CDCl₃): δ = 176.37, 132.41, 125.00, 89.69, 38.85, 26.99, 17.78.
EI-HRMS:	calculated for C₁₄H₂₈O₄N₁ ([M+NH₄]⁺): 274.20128, found: 274.20132.

but-2-yne-1,1-diyl diacetate (126)

Prepared following *General Procedure F* with deviations, from but-2-ynal (**229**, 681 mg, 10 mmol, 1.0 equiv.) and acetic anhydride (**225**, 2.80 mL, 30 mmol, 3.0 equiv.) using FeCl₃ (81 mg, 0. 5 mmol, 5 mol%) as catalyst at 0 °C for 30 min. Purification by kugelrohr distillation (10 mBar, 65 °C → 70 °C) gave **126** as colorless oil (679 mg, 2.65 mmol, 53%).
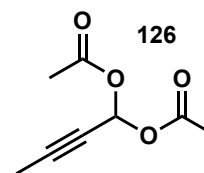
¹H-NMR:	(501 MHz, CDCl₃): δ = 7.20 (q, J = 1.9 Hz, 1H), 2.11 (s, 6H), 1.90 (d, J = 1.9 Hz, 3H).
¹³C-NMR:	(126 MHz, CD₂Cl₂): δ = 168.35, 84.54, 79.99, 72.54, 20.81, 3.77.

(*E*)-3-phenylprop-2-ene-1,1-diyl bis(2,2,2-trichloroacetate) (142)

Prepared following *General Procedure F* with deviations, from cinnamaldehyd (**141**, 792 mg, 6.0 mmol, 1.0 equiv.) and
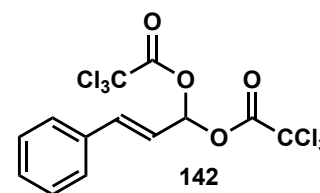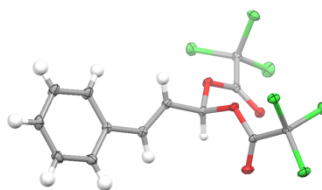
trichloroacetic anhydride (**230**, 3.30 mL, 18 mmol, 3.0 equiv.) using FeCl$_3$ (49 mg, 0.30 mmol, 5 mol%) as catalyst at 0 °C for 30 min. Purification by silica gel flash column chromatography (eluent: *n*-pentanes/Et$_2$O 30:1) gave **142** as colorless crystalline solid (679 mg, 2.65 mmol, 53%). For further purification, the compound **142** can be recrystallized from *n*-pentanes or *i*-hexanes to yield crystals of high purity.

^{1}H-NMR:	(501 MHz, CDCl$_3$): δ = 7.55 – 7.47 (m, 2H), 7.45 – 7.34 (m, 4H), 7.11 (d, J = 16.0 Hz, 1H), 6.40 (dd, J = 16.0, 6.7 Hz, 1H).
^{13}C-NMR:	(126 MHz, CD$_2$Cl$_2$): δ = 159.79, 139.44, 134.19, 130.00, 129.05, 127.62, 117.75, 96.20, 88.98.
EI-HRMS:	Decomposition during measurement toward cinnamaldehyde, mass could not be found.
X-Ray:	See section **7.2.4** for crystallographic data.

7.2.2 Catalyst Synthesis

Synthesis of Benzofurylbromides

2-((tert-butyldimethylsilyl)oxy)-4-(trifluoromethyl)benzaldehyde (230)

Following a procedure reported by List, 2-hydroxy-4-(trifluoromethyl)benzaldehyde (**148**, 553 mg, 2.9 mmol, 1.0 equiv.) was given to a flame dried Schlenk tube equipped with a magnetic stirring bar under an atmosphere of argon followed by anhydrous CH_2Cl_2 (6 mL) and pyridine (0.71 mL, 8.7 mmol, 3.0 equiv.).[144] The flask was cooled to 0 °C and TBSOTf (1.0 mL, 4.4 mmol, 1.5 equiv.) was added dropwise. The mixture was allowed to warm to room temperature and stirred for 16 h. A saturated solution of $NaHCO_3$ (20 mL) was added followed by CH_2Cl_2 (10 mL) and the layers were separated. The aqueous layer was extracted with CH_2Cl_2 (3 x 20 mL) and dried over anhydrous Na_2SO_4 and concentrated under reduced pressure. The crude product was purified via flash column chromatography on silica gel (eluent: *i*-hexanes/MTBE 40:1) to yield the desired product **230** (469 mg, 1.54 mmol, 53%) as colorless oil.
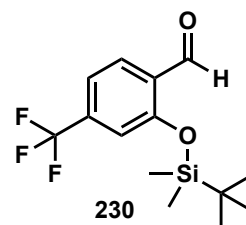
^{1}H-NMR:	(501 MHz, CDCl$_3$): δ = 10.48 (d, J = 0.8 Hz, 1H), 7.91 (dd, J = 8.2, 1.0 Hz, 1H), 7.29 (ddd, J = 8.6, 1.5, 0.7 Hz, 1H), 7.14 – 7.10 (m, 1H), 1.04 (s, 9H), 0.31 (s, 6H).
^{13}C-NMR:	(126 MHz, CDCl$_3$): δ = 189.26, 158.84, 136.9 (q, J = 33.2 Hz), 129.60, 129.41, 124.40, 118.2 (q, J = 3.7 Hz), 117.5 (q, J = 3.9 Hz), 25.73, 18.50, -4.20.
^{19}F-NMR:	(471 MHz, CDCl$_3$): δ = –63.6 (s).

tert-butyl(2-(2,2-dibromovinyl)-5-(trifluoromethyl)phenoxy)dimethylsilane (231)

Following a procedure reported by List, 2-((tert-butyldimethylsilyl)oxy)-4-(trifluoromethyl)benzaldehyde (**230**, 469 mg, 1.54 mmol, 1.0 equiv.) was given to a flame dried Schlenk tube equipped with a magnetic stirring bar under an atmosphere of argon followed by anhydrous CH_2Cl_2 (7.5 mL).[144] The tube was cooled to 0 °C and CBr$_4$ (766 mg, 2.3 mmol, 1.5 equiv.) and PPh$_3$ (1.21 g, 4.63 mmol, 3.0 equiv.). The mixture was allowed to warm to room temperature and stirred for 16 h. The mixture was then poured onto a saturated solution of Na_2SO_3 and the layers were separated. The aqueous layer was extracted with CH_2Cl_2 (3x20 mL)
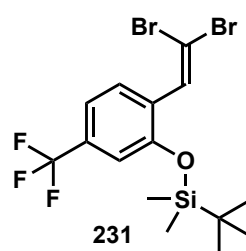
and the combined organic layers were washed with brine and dried over anhydrous Na_2SO_4 and concentrated under reduced pressure. The crude product was purified via flash column chromatography on silica gel (eluent: *i*-hexane/EtOAc 99:1) to yield the desired product **231** (570 mg, 1.24 mmol, 80%) as yellow oil.

¹H-NMR:	(501 MHz, CDCl₃): δ = 7.73 (d, J = 8.1 Hz, 1H), 7.54 (s, 1H), 7.25 – 7.21 (m, 1H), 7.04 – 7.00 (m, 1H), 1.03 (s, 9H), 0.23 (s, 6H).
¹³C-NMR:	(126 MHz, CDCl₃): δ = 153.17, 132.96, 131.70, 131.44, 130.84, 129.85, 117.8 (q, J = 3.6 Hz), 116.3 (q, J = 3.9 Hz), 92.02, 25.60, 18.21, -4.43.
¹⁹F-NMR:	(471 MHz, CDCl₃): δ = –62.9 (s).

2-(2,2-dibromovinyl)-5-(trifluoromethyl)phenol (232)

Following a procedure reported by List, *tert*-butyl (2-(2,2-dibromovinyl)-5-(trifluoromethyl)phenoxy)dimethylsilane (**231**, 570 mg, 1.24 mmol, 1.0 equiv.) was given to a flame dried Schlenk tube equipped with a magnetic stirring bar under an atmosphere of argon followed by anhydrous THF (6.0 mL). The tube was cooled to 0 °C and TBAF (1.0 M solution in THF, 1.6 mL, 1.60 mmol, 1.28 equiv.) was added dropwise. The mixture was allowed to warm to room temperature and stirred for 16 h. Water (20 mL) was added and the layers were separated. The aqueous layer was extracted with MTBE (3x20 mL) and the combined organic layers were washed with brine and dried over anhydrous Na_2SO_4 and concentrated under reduced pressure. The crude product was purified via flash column chromatography on silica gel (eluent: *i*-hexane/EtOAc 20:1) to yield the desired product **232** (340 mg, 0.98 mmol, 79%) as yellow oil.
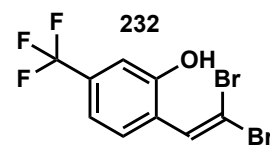
¹H-NMR:	(501 MHz, CD₂Cl₂): δ = 7.67 (d, J = 8.1 Hz, 1H), 7.58 (s, 1H), 7.22 (dd, J = 8.1, 1.7 Hz, 1H), 7.11 (d, J = 1.7 Hz, 1H), 5.78 (s, 1H).
¹³C-NMR:	(126 MHz, CD₂Cl₂): δ = 153.39, 131.95, 130.35, 126.89, 125.22, 123.06, 117.60 (q, J = 3.8 Hz), 113.11 (q, J = 3.9 Hz), 94.11.
¹⁹F-NMR:	(471 MHz, CD₂Cl₂): δ = –63.29 (s).

2-bromo-6-(trifluoromethyl)benzofuran (150)

Following a procedure reported by List, CuI (8.3 mg, 43 μmol, 5 mol%) and K₃PO₄ (368 mg, 1.73 mmol, 2.0 equiv.) were given to a flame dried Schlenk tube equipped with a magnetic stirring bar under an atmosphere
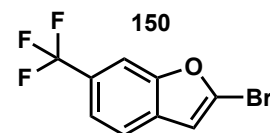
of argon followed by a solution of 2-(2,2-dibromovinyl)-5-(trifluoromethyl)phenol (**232**, 300 mg, 0.87 mmol, 1.0 equiv.) in anhydrous THF (4.0 mL). The tube was sealed and heated to 80 °C for 16 h. The mixture was then cooled to room temperature, diluted with MTBE (15 mL) and filtered through a plug of celite. The filtrate was concentrated under reduced pressure and purified via flash column chromatography on silica gel (eluent: *i*-hexanes) to yield the desired bromide **150** (193 mg, 0.87 mmol, 84%) as colorless oil.

¹H-NMR:	(501 MHz, CD$_2$Cl$_2$): δ = 7.75 (dq, J = 1.6, 0.8 Hz, 1H), 7.66 (dt, J = 8.2, 0.8 Hz, 1H), 7.55 – 7.49 (m, 1H), 6.86 (d, J = 1.0 Hz, 1H).
¹³C-NMR:	(126 MHz, CD$_2$Cl$_2$): δ = 121.10, 120.82 (q, J = 3.7 Hz), 108.98, 108.80 (q, J = 4.3 Hz).
¹⁹F-NMR:	(471 MHz, CD$_2$Cl$_2$): δ = –61.55 (s).

5-bromo-2-(1,3-dioxolan-2-yl)phenol (233)

4-bromo-2-hydroxybenzaldehyde (**152**, 5.0 g, 24.9 mmol, 1.0 equiv.) was given to a 100 mL round bottom flask followed by anhydrous PhMe (50 mL). Ethylene glycol (2.1 mL, 37.4 mmol, 2.0 equiv.) was added followed by *p*-TsOH・H$_2$O (95 mg, 0.5 mmol, 2 mol%) and a Dean-Stark apparatus attached with a reflux condenser was attached to the flask. The mixture was heated to reflux for 2 d, then cooled to room temperature and a saturated solution off NaHCO$_3$ (30 mL) was added. The layers were separated and the aqueous layer was extracted with MTBE (3x20 mL). The combined organic layers were washed with brine and dried over anhydrous Na$_2$SO$_4$ and concentrated under reduced pressure. The crude product was purified via flash column chromatography on silica gel (eluent: *i*-hexane/MTBE 20:1 → 1:1) to yield the desired product **233** (5.60 g, 22.8 mmol, 92%) as yellow oil.
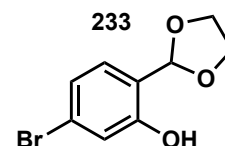
¹H-NMR:	(501 MHz, CDCl$_3$): δ = 7.89 (s, 1H), 7.10 – 7.06 (m, 2H), 7.02 (dd, J = 8.1, 1.9 Hz, 1H), 5.89 (s, 1H), 4.18 – 4.02 (m, 4H).
¹³C-NMR:	(126 MHz, CDCl$_3$): δ = 156.38, 129.52, 124.13, 123.23, 120.60, 120.03, 104.00, 64.96.

2-(1,3-dioxolan-2-yl)-5-(perfluoropropyl)phenol (234)

Following a procedure reported by List, copper (1.0 g, 16.3 mmol, 4.0 equiv.) was added to a flame dried microwave vial followed by anhydrous DMF (6.5 mL) and then 5-bromo-2-(1,3-dioxolan-2-yl)phenol (233, 1.0 g, 4.1 mmol, 1.0 equiv.). The mixture was degassed via bubbling constant stream of argon for 10 min through the solution, then perfluoropropyl-1-iodide (1.0 mL, 6.9 mmol, 1.7 equiv.) was added in one portion, the vial was sealed and then heated to 90 °C for 16 h. The mixture was then cooled to room temperature, diluted with H_2O (10 mL) and MTBE (10 mL) and filtered through a plug of celite. The filtrate was concentrated under reduced pressure and purified via flash column chromatography on silica gel (eluent: *n*-pentane/Et_2O 2:1) to yield the desired compound (234, 1.08 g, 3.20 mmol, 79%) as colorless oil.

^{1}H-NMR:	(501 MHz, CDCl$_3$): δ = 8.03 (s, 1H), 7.38 (d, J = 7.9 Hz, 1H), 7.11 (d, J = 8.9 Hz, 2H), 6.00 (s, 1H), 4.20 – 4.06 (m, 4H).
^{13}C-NMR:	(126 MHz, CDCl$_3$): δ = 155.65, 128.61, 124.89, 118.18 (t, J = 6.6 Hz), 116.10 (t, J = 6.6 Hz), 103.54, 66.01, 65.11.
^{19}F-NMR:	(471 MHz, CDCl$_3$): δ = –80.05 (t, J = 10.0 Hz), –111.85 (q, J = 10.1 Hz), –126.42 (s).
EI-HRMS:	calculated for $C_{12}H_9O_3F_7$ ([M]$^+$): 334.04344, found: 334.04368.

2-hydroxy-4-(perfluoropropyl)benzaldehyde (153)

2-(1,3-dioxolan-2-yl)-5-(perfluoropropyl)phenol (234, 1.0 g, 3.0 mmol, 1.0 equiv.) was given to a 50 mL round bottom flask and dissolved in THF (15 mL). An aqueous solution of HCl (10%, 10 mL) was added at 0 °C and the mixture was then allowed to warm to room temperature. The solution was stirred for 16 h, then H_2O (10 mL) was added and the layers were separated. The aqueous layer was extracted with Et_2O (3x20 mL) and the combined organic layers were washed with a concentrated aqueous solution of $NaHCO_3$ (20 mL), dried over anhydrous Na_2SO_4 and concentrated under reduced pressure. The crude product (153, 850 mg, 2.9 mmol, 98%) was used in the subsequent step without further purification.
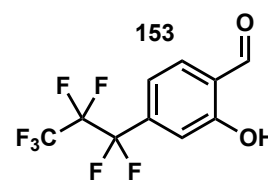
^{1}H-NMR:	(501 MHz, CDCl$_3$): δ = 11.06 (s, 1H), 10.00 (s, 1H), 7.73 (dt, J = 8.5, 0.8 Hz, 1H), 7.24 (d, J = 7.0 Hz, 2H).

¹⁹F-NMR: (471 MHz, CDCl₃): δ = –80.00 (t, J = 9.7 Hz), –112.64 (q, J = 9.9 Hz), –126.24 (s).

2-((*tert*-butyldiphenylsilyl)oxy)-4-(perfluoropropyl)benzaldehyde (235)

To a flame dried 250 mL 2-neck flask was added imidazole (613 mg, 9.0 mmol, 3.0 equiv.) followed by anhydrous CH₂Cl₂ (100 mL) and 2-hydroxy-4-(perfluoropropyl)benzaldehyde (**153**, 870 mg, 3.0 mmol, 1.0 equiv.). The flask was cooled to 0 °C and TBDPSCl (1.2 mL, 4.5 mmol, 1.5 equiv.) was added dropwise. The mixture was allowed to warm to room temperature and stirred for 24 h. H₂O (100 ml) was added and the layers were separated. The aqueous layer was extracted with CH₂Cl₂ (3x50 mL), washed with brine, dried over anhydrous Na₂SO₄ and concentrated under reduced pressure. The crude product was purified via flash column chromatography on silica gel (eluent: *i*-hexanes/MTBE 40:1 → 30:1) to yield the desired compound **235** (950 mg, 1.8 mmol, 60%) as yellow oil.
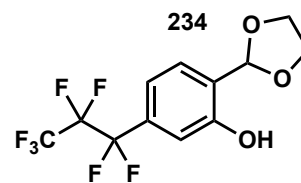
¹H-NMR: (501 MHz, CDCl₃): δ = 10.79 (d, J = 0.8 Hz, 1H), 7.92 (d, J = 8.1 Hz, 1H), 7.74 – 7.65 (m, 4H), 7.50 – 7.44 (m, 2H), 7.43 – 7.38 (m, 4H), 7.14 (d, J = 8.2 Hz, 1H), 6.70 (d, J = 1.6 Hz, 1H), 1.16 (s, 9H).

¹³C-NMR: (126 MHz, CDCl₃): δ = 189.19, 158.48, 135.46, 131.02, 130.79, 129.09, 128.88, 128.36, 119.38 (t, J = 7.0 Hz), 26.69, 19.89.

¹⁹F-NMR: (471 MHz, CDCl₃): δ = –80.23 (t, J = 9.5 Hz), –112.90 (d, J = 9.5 Hz), –126.89 (s).

tert-butyl(2-(2,2-dibromovinyl)-5-(perfluoropropyl)phenoxy)diphenylsilane (154)

A flame dried Schlenk tube was charged with 2-((*tert*-butyldiphenylsilyl)oxy)-4-(perfluoropropyl)benzaldehyde (**235**, 3.21 g, 6.1 mmol, 1.0 equiv.) followed by anhydrous CH₂Cl₂ (30 mL). The tube was cooled to 0 °C and CBr₄ (3.0 g, 9.1 mmol, 1.5 equiv.) and PPh₃ (4.78 g, 18.2 mmol, 3 equiv.) were added. The tube was sealed and allowed to slowly warm to room temperature. The mixture was stirred for 16 h, then a saturated solution of Na₂S₂O₃ (50 mL) was added and the layers were separated. The aqueous layer was extracted with CH₂Cl₂ (3x50 mL) and the combined organic layers were dried over anhydrous Na₂SO₄ and concentrated under reduced pressure. The crude product was purified via flash

column chromatography on silica gel (eluent: *i*-hexane/PhMe 99:1) to yield the desired product **154** (2.84 g, 4.15 mmol, 68%) as colorless oil.

<table>
<tr><td>**¹H-NMR:**</td><td>(501 MHz, CDCl₃): δ = 7.78 (s, 1H), 7.73 (d, J = 8.2 Hz, 1H), 7.69 – 7.62 (m, 4H), 7.48 – 7.41 (m, 2H), 7.40 – 7.33 (m, 4H), 7.08 (dd, J = 8.2, 1.7 Hz, 1H), 6.63 (d, J = 1.7 Hz, 1H), 1.15 (s, 9H).</td></tr>
<tr><td>**¹³C-NMR:**</td><td>(126 MHz, CDCl₃): δ = 153.02, 135.54, 132.97, 131.68, 130.50, 129.54, 128.17, 119.07 (t, J = 6.6 Hz), 117.81 (t, J = 7.3 Hz), 92.47, 26.73, 19.77.</td></tr>
<tr><td>**¹⁹F-NMR:**</td><td>(471 MHz, CDCl₃): δ = –80.23 (t, J = 9.5 Hz), –112.24 (d, J = 9.6 Hz), –126.93 (s).</td></tr>
</table>

2-(2,2-dibromovinyl)-5-(perfluoropropyl)phenol (236)

Following a procedure reported by List, *tert*-butyl(2-(2,2-dibromovinyl)-5-(perfluoropropyl)phenoxy)diphenylsilane (**154**, 2.84 g, 4.15 mmol, 1.0 equiv.) was given to a flame dried Schlenk tube equipped with a magnetic stirring bar under an atmosphere of argon followed by anhydrous THF (21 mL).[144] The tube was cooled to 0 °C and TBAF (1.0 M solution in THF, 6.3 mL, 6.3 mmol, 1.5 equi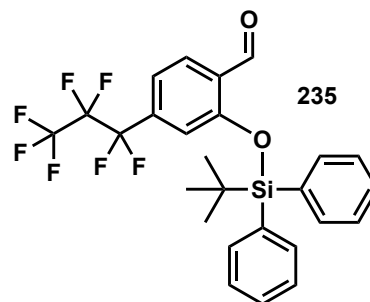v.) was added dropwise. The mixture was allowed to warm to room temperature and stirred for 16 h. Water (50 mL) was added and the layers were separated. The aqueous layer was extracted with MTBE (3x50 mL) and the combined organic layers were washed with brine and dried over anhydrous Na₂SO₄ and concentrated under reduced pressure. The crude product was purified via flash column chromatography on silica gel (eluent: *i*-hexane/CH₂Cl₂ 10:1) to yield the desired product **236** (1.41 g, 3.16 mmol, 76%) as yellow oil.
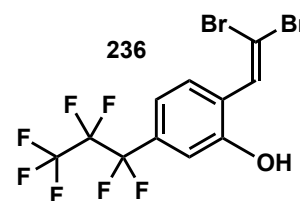
<table>
<tr><td>**¹H-NMR:**</td><td>(501 MHz, CDCl₃): δ = 7.67 (d, J = 8.1 Hz, 1H), 7.56 (s, 1H), 7.18 (dd, J = 8.2, 1.7 Hz, 1H), 7.08 – 7.04 (m, 1H), 5.19 (s, 1H).</td></tr>
<tr><td>**¹⁹F-NMR:**</td><td>(471 MHz, CDCl₃): δ = –80.01 (t, J = 10.0 Hz), –111.85 (d, J = 9.8 Hz), –126.35 (s).</td></tr>
</table>

2-bromo-6-(perfluoropropyl)benzofuran (151)

Following a procedure reported by List, CuI (10 mg, 51 μmol, 5 mol%) and K_3PO_4 (436 mg, 2.05 mmol, 2.0 equiv.) were given to a flame dried Schlenk tube equipped with a magnetic stirring bar under an atmosphere of argon followed by a solution of 2-(2,2-dibromovinyl)-5-(perfluoropropyl)phenol (**236**, 458 mg, 1.02 mmol, 1.0 equiv.) in anhydrous THF (4.5 mL). The tube was sealed and heated to 80 °C for 16 h. The mixture was then cooled to room temperature, diluted with MTBE (20 mL) and filtered through a plug of celite. The filtrate was concentrated under reduced pressure and purified via flash column chromatography on silica gel (eluent: *i*-hexanes) to yield the desired bromide **151** (354 mg, 0.97 mmol, 95%) as colorless oil.
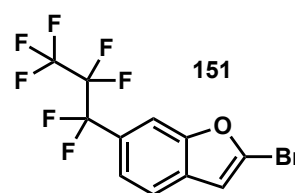
¹H-NMR:	(501 MHz, CD$_2$Cl$_2$): δ = 7.72 (s, 1H), 7.68 (d, J = 8.1 Hz, 1H), 7.48 (dd, J = 8.4, 1.5 Hz, 1H), 6.87 (d, J = 0.9 Hz, 1H).
¹³C-NMR:	(126 MHz, CD$_2$Cl$_2$): δ = 154.94, 132.10, 131.63, 121.70 (t, J = 6.6 Hz), 120.51, 109.85 (t, J = 7.4 Hz), 108.54.
¹⁹F-NMR:	(471 MHz, CD$_2$Cl$_2$): δ = –80.38 (t, J = 10.0 Hz), –110.33 (d, J = 10.3 Hz), –126.48 (s).

2-((tert-butyldiphenylsilyl)oxy)-5-chloro-4-methylbenzaldehyde (237)

To a flame dried 250 mL 2-neck flask was added imidazole (2.40 g, 35.2 mmol, 3.0 equiv.) followed by anhydrous CH$_2$Cl$_2$ (140 mL) and 5-chloro-2-hydroxy-4-methylbenzaldehyde (**238**, 2.0 g, 11.7 mmol, 1.0 equiv.). The flask was cooled to 0 °C and TBDPSCl (4.6 mL, 17.6 mmol, 1.5 equiv.) was added dropwise. The mixture was allowed to warm to room temperature and stirred for 24. H$_2$O (150 ml) was added and the layers were separated. The aqueous layer was extracted with CH$_2$Cl$_2$ (3x60 mL), washed with brine, dried over anhydrous Na$_2$SO$_4$ and concentrated under reduced pressure. The crude product was purified via flash column chromatography on silica gel (eluent: *i*-hexanes/MTBE 30:1) to yield the desired compound **237** (3.35 g, 8.2 mmol, 70%) as yellow oil.
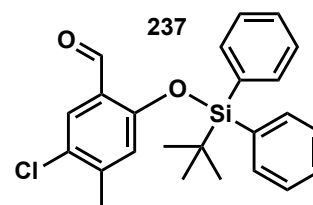
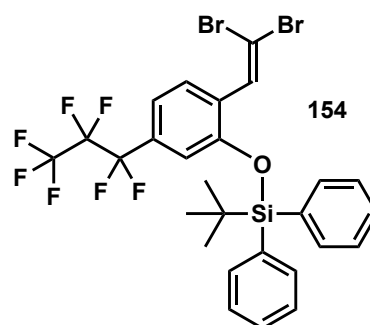|	
¹H-NMR:	(501 MHz, CDCl$_3$): δ = 10.65 (s, 1H), 7.73 (dt, J = 6.9, 1.4 Hz, 4H), 7.52 – 7.45 (m, 2H), 7.42 (dd, J = 8.0, 6.6 Hz, 4H), 6.37 (s, 1H), 2.02 (s, 3H), 1.14 (s, 9H).

tert-butyl(4-chloro-2-(2,2-dibromovinyl)-5-methylphenoxy)diphenylsilane (239)

A flame dried Schlenk tube was charged with 2-((*tert*-butyldiphenylsilyl)oxy)-5-chloro-4-methylbenzaldehyde (**237**, 2.45 g, 6.0 mmol, 1.0 equiv.) followed by anhydrous CH_2Cl_2 (7.5 mL). The tube was cooled to 0 °C and CBr_4 (2.99 g, 9.0 mmol, 1.5 equiv.) and PPh_3 (4.72 g, 18. mmol, 3 equiv.) were added. The tube was sealed and allowed to slowly warm to room temperature. The mixture was stirred for 16 h, then a saturated solution of $Na_2S_2O_3$ (50 mL) was added and the layers were separated. The aqueous layer was extracted with CH_2Cl_2 (3x50 mL) and the combined organic layers were dried over anhydrous Na_2SO_4 and concentrated under reduced pressure. The crude product was purified via flash column chromatography on silica gel (eluent: *i*-hexane/EtOAc 100:1 → 40:1) to yield the desired product **239** (2.88 g, 5.1 mmol, 85%) as pale yellow oil.
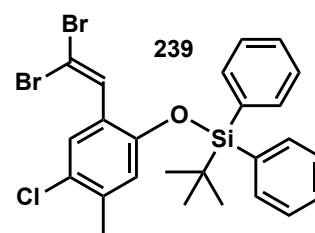
^{1}H-NMR:	(501 MHz, CD_2Cl_2): δ = 7.75 – 7.66 (m, 5H), 7.50 – 7.43 (m, 2H), 7.43 – 7.36 (m, 5H), 6.34 (d, J = 0.8 Hz, 1H), 1.98 (s, 3H), 1.11 (s, 9H).
^{13}C-NMR:	(126 MHz, CD_2Cl_2): δ = 151.79, 137.72, 135.87, 133.19, 132.49, 130.61, 129.17, 128.35, 126.32, 126.12, 121.80, 91.10, 26.71, 20.19, 19.82.

4-chloro-2-(2,2-dibromovinyl)-5-methylphenol (240)

Following a procedure reported by List, *tert*-butyl(4-chloro-2-(2,2-dibromovinyl)-5-methylphenoxy)diphenylsilane (**239**, 2.88 g, 5.10 mmol, 1.0 equiv.) was given to a flame dried Schlenk tube equipped with a magnetic stirring bar under an atmosphere of argon followed by anhydrous THF (25 mL).[144] The tube was cooled to 0 °C and TBAF (1.0 M solution in THF, 7.65 mL, 7.65 mmol, 1.5 equiv.) was added dropwise. The mixture was allowed to warm to room temperature and stirred for 16 h. Water (60 mL) was added and the layers were separated. The aqueous layer was extracted with MTBE (3x50 mL) and the combined organic layers were washed with brine and dried over anhydrous Na_2SO_4 and concentrated under reduced pressure. The crude product was purified via flash column chromatography on silica gel (eluent: *i*-hexane/EtOAc 20:1 → 10:1) to yield the desired product **240** (1.23 g, 3.76 mmol, 74%) as yellow oil.
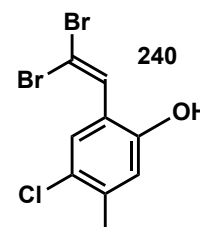
^{1}H-NMR:	(501 MHz, CD_2Cl_2): δ = 7.56 (s, 1H), 7.50 (s, 1H), 6.73 (d, J = 0.9 Hz, 1H), 5.53 (s, 1H), 2.30 (s, 3H).

^{13}C-NMR: (126 MHz, CDCl$_3$): δ = 151.17, 138.12, 135.30, 130.39, 129.06, 128.04, 118.16, 92.62, 20.27.

2-bromo-5-chloro-6-methylbenzofuran (241)

Following a procedure reported by List, CuI (28 mg, 0.15 mmol, 5 mol%) and K$_3$PO$_4$ (1.26 g, 5.87 mmol, 2.0 equiv.) were given to a flame dried Schlenk tube equipped with a magnetic stirring bar under an atmosphere of argon followed by a solution of 4-chloro-2-(2,2-dibromovinyl)-5-methylphenol (**240**, 958 mg, 2.93 mmol, 1.0 equiv.) in anhydrous THF (15 mL). The tube was sealed and heated to 80 °C for 16 h. The mixture was then cooled to room temperature, diluted with MTBE (40 mL) and filtered through a plug of celite. The filtrate was concentrated under reduced pressure and purified via flash column chromatography on silica gel (eluent: *i*-hexanes) to yield the desired bromide **241** (522 mg, 2.12 mmol, 73%) as colorless crystalline solid.
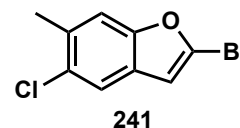
^{1}H-NMR: (501 MHz, CD$_2$Cl$_2$): δ = 7.50 (s, 1H), 7.34 (s, 1H), 6.68 (d, J = 0.9 Hz, 1H), 2.46 – 2.43 (m, 3H).

^{13}C-NMR: (126 MHz, CD$_2$Cl$_2$): δ = 154.92, 132.82, 130.06, 129.11, 128.17, 120.20, 112.92, 108.16, 20.88.

EI-HRMS: calculated for C$_9$H$_6$O$_1$Cl$_1$Br$_1$ ([M]$^+$): 243.92852, found: 243.92889.

4-methylnaphthalen-2-ol (242)

Following a procedure reported by Toste, AlCl$_3$ (4.0 g, 30 mmol, 1.5 equiv.) were given to a flame dried Schlenk tube under an atmosphere of argon followed by CH$_2$Cl$_2$ (20 mL).[220] The tube was cooled to 0 °C and phenylacetic acid chloride (**243**, 2.65 mL, 20 mmol, 1.0 equiv.) was added dropwise. After complete addition, the tube was purged with propyne (gas bubbled through the reaction mixture via balloon). The mixture was stirred at 0 °C for 5 min and then warmed to room temperature. The reaction was stirred at room temperature for 3 h, then H$_2$O (20 mL) was added slowly and the layers were separated. The aqueous layer was extracted with CH$_2$Cl$_2$ (3x20 mL) and the combined organic layers were washed with brine, dried over anhydrous Na$_2$SO$_4$ and concentrated under reduced pressure. The crude product was purified via flash column chromatography on silica gel (eluent: *i*-hexanes/MTBE 10:1 → 6:1) to yield the product **242** (2.97 g, 19.0 mmol, 95%) as red oil.
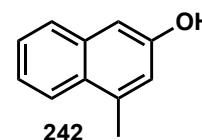
¹H-NMR:	(501 MHz, CDCl₃): δ = 7.91 (dd, J = 8.4, 1.2 Hz, 1H), 7.68 (dd, J = 8.2, 1.3 Hz, 1H), 7.43 (ddd, J = 8.2, 6.8, 1.4 Hz, 1H), 7.36 (ddd, J = 8.2, 6.8, 1.4 Hz, 1H), 7.04 – 6.94 (m, 2H), 4.97 (s, 1H), 2.66 (s, 3H).
¹³C-NMR:	(126 MHz, CDCl₃): δ = 152.89, 136.83, 134.89, 128.25, 127.01, 126.30, 124.10, 123.44, 118.50, 107.66, 19.32.

The spectroscopic data is in agreement with the reported literature.[220]

2-hydroxy-4-methyl-1-naphthaldehyde (244)

Following a procedure reported by Walzer, 4-methylnaphthalen-2-ol (**242**, 2.66 g, 16.7 mmol, 1.0 equiv.) was given to a flame dried Schlenk tube followed by 100 mL CH₂Cl₂.[221] The solution was cooled to 0 °C and SnCl₄ (2.65 mL, 22.6 mmol, 1.35 equiv.) was added dropwise. The mixture was stirred at 0 °C for 1 h and then 1,1-dichlor-dimethylether (2.1 mL, 22.6 mmol, 1.35 equiv.) was added dropwise. The mixture was stirred for 1h at 0 °C and then allowed to warm to room temperature. The mixture was stirred at room temperature for 1 h and then quenched via addition of ice water (50 mL). The layers were separated, the aqueous layer was extracted with CH₂Cl₂ (3x20 mL) and the combined organic layers were washed with brine, dried over anhydrous Na₂SO₄ and concentrated under reduced pressure. The crude product was purified via flash column chromatography on silica gel (eluent: *i*-hexanes/MTBE 30:1 → 15:1) to yield the product **244** (2.25 g, 12.1 mmol, 72%) as light red solid.
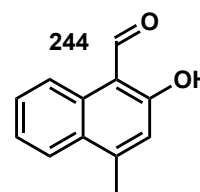
¹H-NMR:	(501 MHz, CDCl₃): δ = 13.23 (s, 1H), 10.75 (s, 1H), 7.97 (dd, J = 8.3, 1.3 Hz, 1H), 7.61 (ddd, J = 8.4, 6.9, 1.3 Hz, 1H), 7.46 (ddd, J = 8.2, 7.0, 1.2 Hz, 1H), 7.01 (s, 1H), 2.69 (d, J = 1.0 Hz, 3H).
¹³C-NMR:	(126 MHz, CDCl₃): δ = 192.88, 164.89, 147.66, 133.13, 128.88, 127.55, 125.50, 124.48, 119.89, 119.22, 110.49, 20.67.

2-((tert-butyldimethylsilyl)oxy)-4-methyl-1-naphthaldehyde (245)

To a flame dried 500 mL 2-neck flask was added imidazole (2.52 g, 37.1 mmol, 3.0 equiv.) followed by anhydrous CH_2Cl_2 (150 mL) and **2-hydroxy-4-methyl-1-naphthaldehyde** (**244**, 2.3 g, 12.4 mmol, 1.0 equiv.). The flask was cooled to 0 °C and TBSCl (2.3 mL, 18.5 mmol, 1.5 equiv.) was added dropwise. The mixture was allowed to warm to room temperature and stirred for 24. H_2O (150 ml) was added and the layers were separated. The aqueous layer was extracted with EtOAc (3x60 mL), washed with brine, dried over anhydrous Na_2SO_4 and concentrated under reduced pressure. The crude product was purified via flash column chromatography on silica gel (eluent: *i*-hexanes/EtOAc 30:1) to yield the desired compound **245** (1.85 g, 6.2 mmol, 66%) as yellow solid.
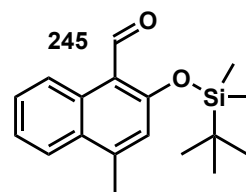
^{1}H-NMR:	(501 MHz, CD_2Cl_2): δ = 10.81 (s, 1H), 9.31 (ddd, J = 8.7, 1.3, 0.7 Hz, 1H), 7.97 (ddd, J = 8.4, 1.5, 0.7 Hz, 1H), 7.60 (ddd, J = 8.5, 6.8, 1.4 Hz, 1H), 7.47 (ddd, J = 8.2, 6.9, 1.3 Hz, 1H), 6.96 (q, J = 1.0 Hz, 1H), 2.71 (d, J = 1.0 Hz, 3H), 1.06 (s, 9H), 0.34 (s, 6H).
^{13}C-NMR:	(126 MHz, CD_2Cl_2): δ = 191.99, 161.80, 145.61, 132.36, 129.47, 128.88, 125.68, 125.13, 124.57, 122.11, 118.11, 25.90, 20.63, 18.77, -3.90.

tert-butyl((1-(2,2-dibromovinyl)-4-methylnaphthalen-2-yl)oxy)dimethylsilane (246)

A flame dried Schlenk tube was charged with 2-((*tert*-butyldimethylsilyl)oxy)-4-methyl-1-naphthaldehyde (**245**, 1.85 g, 6.2 mmol, 1.0 equiv.) followed by anhydrous CH_2Cl_2 (28 mL). The tube was cooled to 0 °C and CBr_4 (3.07 g, 9.3 mmol, 1.5 equiv.) and PPh_3 (4.85 g, 18.5 mmol, 3 equiv.) were added. The tube was sealed and allowed to slowly warm to room temperature. The mixture was stirred for 16 h, then a saturated solution of $Na_2S_2O_3$ (50 mL) was added and the layers were separated. The aqueous layer was extracted with CH_2Cl_2 (3x50 mL) and the combined organic layers were dried over anhydrous Na_2SO_4 and concentrated under reduced pressure. The crude product was purified via flash column chromatography on silica gel (eluent: *i*-hexane/MTBE 30:1) to yield the desired product **246** (2.60 g, 5.70 mmol, 93%) as yellow oil.

¹H-NMR:	(501 MHz, CD$_2$Cl$_2$): δ = 7.98 – 7.91 (m, 1H), 7.79 (dd, J = 8.2, 1.2 Hz, 1H), 7.60 (s, 1H), 7.51 (ddd, J = 8.3, 6.8, 1.3 Hz, 1H), 7.42 (ddd, J = 8.2, 6.8, 1.3 Hz, 1H), 6.96 – 6.92 (m, 1H), 2.66 (t, J = 0.8 Hz, 3H), 1.07 (s, 9H), 0.25 (s, 6H).
¹³C-NMR:	(126 MHz, CD$_2$Cl$_2$): δ = 150.00, 137.01, 134.35, 131.85, 128.60, 126.62, 125.18, 124.61, 123.98, 121.98, 120.11, 94.46, 27.14, 25.88, 19.81, –3.90.

1-(2,2-dibromovinyl)-4-methylnaphthalen-2-ol (247)

Following a procedure reported by List, *tert*-butyl((1-(2,2-dibromovinyl)-4-methylnaphthalen-2-yl)oxy)dimethylsilane (**246**, 2.60 g, 5.70 mmol, 1.0 equiv.) was given to a flame dried Schlenk tube equipped with a magnetic stirring bar under an atmosphere of argon followed by anhydrous THF (25 mL).[144] The tube was cooled to 0 °C and TBAF (1.0 M solution

in THF, 8.6 mL, 8.6 mmol, 1.5 equiv.) was added dropwise. The mixture was allowed to warm to room temperature and stirred for 16 h. Water (100 mL) was added and the layers were separated. The aqueous layer was extracted with MTBE (3x50 mL) and the combined organic layers were washed with brine and dried over anhydrous Na$_2$SO$_4$ and concentrated under reduced pressure. The crude product was purified via flash column chromatography on silica gel (eluent: *i*-hexane/EtOAc 20:1) to yield the desired product **247** (1.34 g, 3.93 mmol, 69%) as yellow solid.
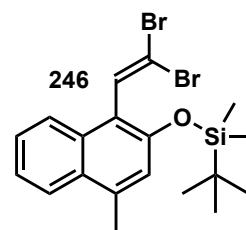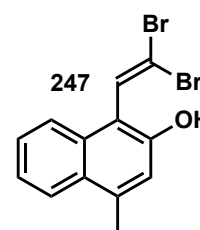
¹H-NMR:	(501 MHz, CDCl$_3$): δ = 7.98 – 7.92 (m, 1H), 7.69 (dt, J = 8.5, 0.9 Hz, 1H), 7.65 (s, 1H), 7.52 (ddd, J = 8.2, 6.8, 1.3 Hz, 1H), 7.05 (d, J = 1.1 Hz, 1H), 5.18 (s, 1H), 2.67 (s, 3H).
¹³C-NMR:	(126 MHz, CDCl$_3$): δ = 149.37, 137.92, 132.45, 131.70, 128.20, 126.90, 124.61, 124.11, 123.80, 118.54, 113.65, 96.73, 19.51.
EI-HRMS:	calculated for C$_{13}$H$_{10}$O$_1$Br$_2$ ([M]$^+$): 339.90931, found: 339.90946.

2-bromo-5-methylnaphtho[2,1-*b*]furan (248)

Following a procedure reported by List, CuI (30 mg, 0.16 mmol, 5 mol%) and K$_3$PO$_4$ (1.33 g, 6.24 mmol, 2.0 equiv.) were given to a flame dried Schlenk tube equipped with a magnetic stirring bar under an atmosphere of argon followed by a solution of 1-(2,2-dibromovinyl)-4-methylnaphthalen-2-
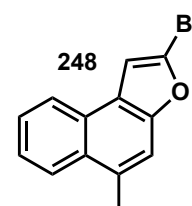
ol (**247**, 1.07 g, 3.20 mmol, 1.0 equiv.) in anhydrous THF (15 mL). The tube was sealed and heated to 80 °C for 16 h. The mixture was then cooled to room temperature, diluted with MTBE (40 mL) and filtered through a plug of celite. The filtrate was concentrated under reduced pressure and purified via flash column chromatography on silica gel (eluent: *i*-hexanes) to yield the desired bromide **248** (725 mg, 2.78 mmol, 89%) as colorless crystalline solid.

^{1}H-NMR:	(501 MHz, CD$_2$Cl$_2$): δ = 8.12 – 8.04 (m, 2H), 7.61 (ddd, J = 8.0, 6.9, 1.4 Hz, 1H), 7.55 (ddd, J = 8.3, 6.9, 1.5 Hz, 1H), 7.47 (s, 1H), 7.18 (d, J = 1.0 Hz, 1H), 2.74 (d, J = 1.1 Hz, 3H).
^{13}C-NMR:	(126 MHz, CD$_2$Cl$_2$): δ = 153.74, 132.61, 130.16, 127.13, 126.78, 125.56, 125.48, 125.24, 124.19, 122.98, 112.50, 107.79, 20.18.
EI-HRMS:	calculated for C$_{13}$H$_9$O$_1$Br$_1$ ([M]$^+$): 259.98314, found: 259.98344.

Synthesis of 3,3'-BINOLs

(S)-3,3'-bis(6-(trifluoromethyl)benzofuran-2-yl)-[1,1'-binaphthalene]-2,2'-diol (249)

A Schlenk tube was charged with (*S*)-2,2'-(2,2'-bis(methoxymethyl)-[1,1'-binaphthalene]-3,3'-diyl)bis(4,4,5,5-tetramethyl-1,3,2-dioxaborolane) (**185**, 142 mg, 0.23 mmol, 1.0 equiv.), 2-bromo-6-(trifluoromethyl)benzofuran (**150**, 180 mg, 0.70 mmol, 3.0 equiv.) and K$_2$CO$_3$ (187 mg, 1.36 mmol, 6.0 equiv.). A 4:1 (*v:v*) mixture of H$_2$O and 1,4-dioxane (1.2 mL, 0.1 M) was added and the mixture was degassed in a constant
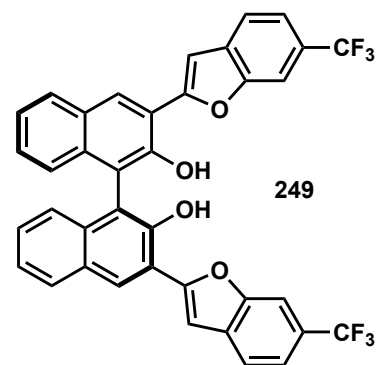
stream of Ar bubbling through the mixture under stirring for 20 min. Pd(PPh$_3$)$_4$ (26 mg, 23 µmol, 10 mol%) was added, the tube was sealed and heated to 110 °C for 16 h. The mixture was then cooled to room temperature, diluted with CH$_2$Cl$_2$ (100 mL) and water (100 mL) was added. The layers were separated, the aqueous layer was extracted with CH$_2$Cl$_2$ (3 x 70 mL) and the combined organic extracts were concentrated under reduced pressure.

The obtained residue was dissolved in THF (2 mL) and HCl (4.0 M solution in 1,4-dioxane, 1.0 mL) and the mixture was stirred for 16 h at room temperature. HCl (aqueous, 10%, 10 mL) was then added and the layers were separated. The aqueous layers was extracted with EtOAc (3 x 70 mL), the combined organic extracts were washed with brine (100 mL) and dried over anhydrous Na$_2$SO$_4$. The solids were filtered off, the filtrate was adsorbed on celite® and the solvent was removed under reduced pressure. The crude mixture was purified via recrystallization: the crude mixture was dissolved in a minimal amount of warm CH$_2$Cl$_2$ and *i*-

206

hexanes was added slowly. The mixture was left at room temperature for 2 h and then cooled to –20 °C for 16 h whereupon colorless crystalline solids formed to yield the desired product **249** (95 mg, 0.15 mmol, 64%).

¹H-NMR: (501 MHz, CD$_2$Cl$_2$): δ = 8.83 (s, 2H), 8.08 (d, J = 8.2 Hz, 2H), 7.91 (s, 2H), 7.72 (d, J = 8.1 Hz, 2H), 7.57 – 7.50 (m, 4H), 7.46 (ddd, J = 8.1, 6.8, 1.2 Hz, 2H), 7.35 (ddd, J = 8.3, 6.7, 1.3 Hz, 2H), 7.18 – 7.13 (m, 2H), 6.06 (s, 2H).

¹³C-NMR: (126 MHz, CD$_2$Cl$_2$): δ = 154.89, 153.75, 150.49, 133.80, 133.20, 129.72, 129.69, 129.49, 128.89, 126.98 (q, J = 32.3 Hz), 126.24, 125.43, 124.38, 124.08, 122.27, 120.35 (q, = 3.7 Hz), 119.23, 112.39, 108.81 (q, J = 4.1 Hz), 107.69.

¹⁹F-NMR: (471 MHz, CDCl$_3$): δ = –61.29 (s).

ESI-HRMS: calculated for C$_{38}$H$_{19}$F$_6$O$_4$ ([M-H]$^-$): 653.11930, found: 653.11946.

(*S*)-3,3'-bis(6-(perfluoropropyl)benzofuran-2-yl)-[1,1'-binaphthalene]-2,2'-diol (250)

A Schlenk tube was charged with (*S*)-2,2'-(2,2'-bis(methoxymethoxy)-[1,1'-binaphthalene]-3,3'-diyl)bis(4,4,5,5-tetramethyl-1,3,2-dioxaborolane) (**185**, 220 mg, 0.35 mmol, 1.0 equiv.), 2-bromo-6-(perfluoropropyl)benzofuran (**151**, 354 mg, 0.97 mmol, 3.0 equiv.) and K$_2$CO$_3$ (268 mg, 1.94 mmol, 6.0 equiv.). A 4:1 (*v:v*) mixture of H$_2$O and 1,4-dioxane (4.4 mL) was added and the mixture was degassed in a constant stream of
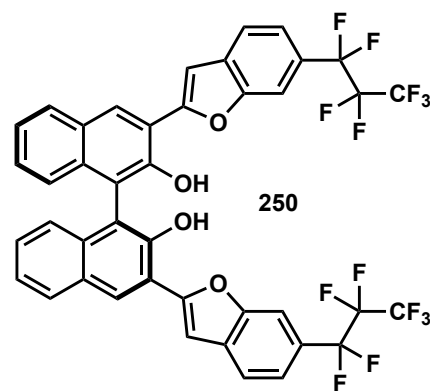
Ar bubbling through the mixture under stirring for 20 min. Pd(PPh$_3$)$_4$ (37 mg, 32 µmol, 10 mol%) was added, the tube was sealed and heated to 110 °C for 16 h. The mixture was then cooled to room temperature, diluted with CH$_2$Cl$_2$ (100 mL) and water (100 mL) was added. The layers were separated, the aqueous layer was extracted with CH$_2$Cl$_2$ (3 x 70 mL) and the combined organic extracts were concentrated under reduced pressure.

The obtained residue was dissolved in THF (2.5 mL) and HCl (4.0 M solution in 1,4-dioxane, 1.6 mL) and the mixture was stirred for 16 h at room temperature. HCl (aqueous, 10%, 20 mL) was then added and the layers were separated. The aqueous layers was extracted with EtOAc (3 x 50 mL), the combined organic extracts were washed with brine (30 mL) and dried over anhydrous Na$_2$SO$_4$. The solids were filtered off, the filtrate was adsorbed on celite® and the solvent was removed under reduced pressure. The crude mixture was purified via flash column

chromatography on silica gel (eluent: *i*-hexanes/EtOAc 30:1) to yield the (*S*)-BINOL **250** (250 mg, 0.29 mmol, 83%) as off-white solid.

¹H-NMR:	(501 MHz, CD$_2$Cl$_2$): δ = 8.86 (s, 2H), 8.10 (d, J = 8.1 Hz, 2H), 7.88 (s, 2H), 7.77 (d, J = 8.2 Hz, 2H), 7.61 (d, J = 0.9 Hz, 2H), 7.48 (ddd, J = 8.1, 6.7, 1.3 Hz, 4H), 7.38 (ddd, J = 8.2, 6.9, 1.3 Hz, 2H), 7.17 (dd, J = 8.4, 1.0 Hz, 2H), 5.94 (s, 2H).
¹³C-NMR:	(126 MHz, CD$_2$Cl$_2$): δ = 154.95, 153.89, 150.48, 133.77, 133.48, 129.73, 129.72, 129.61, 128.99, 125.49, 124.96, 124.36, 122.13, 121.68, 119.15, 112.28, 110.31, 107.69.
¹⁹F-NMR:	(471 MHz, CDCl$_3$): δ = –80.31 (t, J = 9.9 Hz), –110.05 (q, J = 10.0 Hz), –126.40 (s).
ESI-HRMS:	calculated for C$_{42}$H$_{19}$F$_{14}$O$_4$ ([M-H]$^-$): 853.10653, found: 853.10636.

(*S*)-3,3'-bis(5-chloro-6-methylbenzofuran-2-yl)-[1,1'-binaphthalene]-2,2'-diol (251)

A Schlenk tube was charged with (*S*)-2,2'-(2,2'-bis(methoxymethoxy)-[1,1'-binaphthalene]-3,3'-diyl)bis(4,4,5,5-tetramethyl-1,3,2-dioxaborolane) (**185**, 500 mg, 0.80 mmol, 1.0 equiv.), 2-bromo-5-chloro-6-methylbenzofuran (**241**, 460 mg, 1.87 mmol, 2.4 equiv.) and K$_2$CO$_3$ (662 mg, 4.80 mmol, 6.0 equiv.). A 4:1 (*v:v*) mixture of H$_2$O and 1,4-dioxane (11.2 mL) was added and the mixture was degassed in a constant stream of Ar bubbling through the mixture under stirring for 20 min. Pd(PPh$_3$)$_4$ (69 mg, 60 µmol, 7.5 mol%) was added, the tube was

251

sealed and heated to 110 °C for 16 h. The mixture was then cooled to room temperature, diluted with CH$_2$Cl$_2$ (50 mL) and water (50 mL) was added. The layers were separated, the aqueous layer was extracted with CH$_2$Cl$_2$ (3 x 30 mL) and the combined organic extracts were concentrated under reduced pressure.

The obtained residue was dissolved in THF (6.0 mL) and HCl (4.0 M solution in 1,4-dioxane, 3.6 mL) and the mixture was stirred for 16 h at room temperature. HCl (aqueous, 10%, 30 mL) was then added and the layers were separated. The aqueous layers was extracted with EtOAc (3 x 50 mL), the combined organic extracts were washed with brine (30 mL) and dried over anhydrous Na$_2$SO$_4$. The solids were filtered off, the filtrate was adsorbed on celite® and the solvent was removed under reduced pressure. The crude mixture was purified via flash column

chromatography on silica gel (eluent: *i*-hexanes/EtOAc 20:1 → 10:1) to yield the (*S*)-BINOL **251** (324 mg, 0.53 mmol, 66%) as off-white solid.

^{1}H-NMR:	(501 MHz, acetone-d$_6$): δ = 8.71 (s, 2H), 8.64 (s, 2H), 8.10 (d, *J* = 8.1 Hz, 2H), 7.70 (s, 2H), 7.64 (s, 2H), 7.59 (d, *J* = 1.1 Hz, 2H), 7.41 (ddd, *J* = 8.1, 6.7, 1.2 Hz, 2H), 7.07 (dd, *J* = 8.3, 1.2 Hz, 2H), 2.52 (s, 6H).
^{13}C-NMR:	(126 MHz, acetone-d$_6$): δ = 154.32, 153.86, 152.38, 135.06, 133.11, 130.09, 129.81, 129.71, 129.54, 128.37, 128.34, 124.99, 124.90, 121.86, 120.77, 114.47, 113.51, 107.76, 20.81.
ESI-HRMS:	calculated for $C_{38}H_{23}Cl_2O_4$ ([M−H]$^-$): 613.09789, found: 613.09806.

(*S*)-3,3'-bis(5-methylnaphtho[2,1-b]furan-2-yl)-[1,1'-binaphthalene]-2,2'-diol (252)

Prepared following <u>GP X</u>. A Schlenk tube was charged with (*S*)-2,2'-(2,2'-bis(methoxymethyl)-[1,1'-binaphthalene]-3,3'-diyl)bis(4,4,5,5-tetramethyl-1,3,2-dioxaborolane) (**185**, 500 mg, 0.80 mmol, 1.0 equiv.), 2-bromo-5-methylnaphtho[2,1-*b*]furan (**248**, 512 mg, 2.0 mmol, 2.5 equiv.) and K$_2$CO$_3$ (662 mg, 4.80 mmol, 6.0 equiv.). A 4:1 (*v:v*) mixture of H$_2$O and 1,4-dioxane (11.2 mL) was added and the mixture was degassed in a constant stream of Ar bubbling through the mixture under stirring for 20 min. Pd(PPh$_3$)$_4$ (69 mg, 60 μmol, 7.5 mol%) was added, the tube was sealed and heated to 110 °C for 16 h. The mixture

252

was then cooled to room temperature, diluted with CH$_2$Cl$_2$ (50 mL) and water (50 mL) was added. The layers were separated, the aqueous layer was extracted with CH$_2$Cl$_2$ (3 x 30 mL) and the combined organic extracts were concentrated under reduced pressure.

The obtained residue was dissolved in THF (6.0 mL) and HCl (4.0 M solution in 1,4-dioxane, 3.6 mL) and the mixture was stirred for 16 h at room temperature. HCl (aqueous, 10%, 30 mL) was then added and the layers were separated. The aqueous layers was extracted with EtOAc (3 x 50 mL), the combined organic extracts were washed with brine (30 mL) and dried over anhydrous Na$_2$SO$_4$. The solids were filtered off, the filtrate was adsorbed on celite® and the solvent was removed under reduced pressure. The crude mixture was purified via flash column chromatography on silica gel (eluent: *i*-hexanes/CH$_2$Cl$_2$ 10:1 → 2:1) to yield the (*S*)-BINOL **252** (400 mg, 0.62 mmol, 78%) as off-white solid.

¹H-NMR:	(501 MHz, acetone-d_6): δ = 8.77 (s, 2H), 8.66 (s, 2H), 8.26 (dd, J = 8.1, 1.5 Hz, 2H), 8.17 (d, J = 1.0 Hz, 2H), 8.16 – 8.13 (m, 2H), 8.11 (d, J = 8.1 Hz, 2H), 7.77 (s, 2H), 7.61 (ddd, J = 8.2, 6.8, 1.3 Hz, 2H), 7.56 (ddd, J = 8.2, 6.8, 1.4 Hz, 2H), 7.41 (ddd, J = 8.1, 6.7, 1.2 Hz, 2H), 7.30 (ddd, J = 8.2, 6.7, 1.3 Hz, 2H), 7.12 (d, J = 8.4 Hz, 2H), 2.84 (d, J = 1.0 Hz, 6H).
¹³C-NMR:	(126 MHz, acetone-d_6): δ = 152.47, 152.40, 152.24, 134.80, 133.35, 130.75, 130.04, 129.58, 128.93, 127.99, 127.66, 127.19, 126.02, 125.48, 125.11, 124.83, 124.28, 121.47, 114.59, 113.41, 107.49, 20.22.
ESI-HRMS:	calculated for $C_{46}H_{29}O_4$ ([M-H]⁻): 645.20713, found: 645.20738.

Synthesis of Benzofuryl-IDPis

(*S*,*S*)-(6-(trifluoromethyl)benzofuranyl)-C_6F_5 IDPi (IDPi-25-b)

Prepared according to <u>GP C</u>: (*S*)-3,3'-bis(6-(trifluoromethyl)benzofuran-2-yl)-[1,1'-binaphthalene]-2,2'-diol (**249**, 78 mg, 0.12 mmol, 2.1 equiv.) was given to a flame dried Schlenk tube under an atmosphere of argon and dissolved in anhydrous PhMe (1.7 mL). ((perfluorophenyl)sulfonyl)phosphorimidoyl trichloride (**155,** 46 mg, 0.12 mmol, 2.1 equiv.) was added followed by triethylamine (0.13 mL, 0.92 mmol, 16 equiv.) and the

mixture was stirred at room temperature for 30 min. Hexamethyldisilazane (12 µL, 57 µmol, 1.0 equiv.) was added, the mixture was stirred for another 20 min at room temperature and subsequently heated to 130 °C for 4 days. The tube was then cooled to room temperature, diluted with CH_2Cl_2 (5 mL) and quenched via the addition of HCl (10%, 5 mL). The layers were separated, and the aqueous layer was extracted with CH_2Cl_2 (3 x 10 mL), the combined organic extracts were dried over anhydrous Na_2SO_4 and concentrated under reduced pressure. The crude residue was purified via flash column chromatography on silica gel (eluent: EtOAc/*i*-hexanes 3:1 → EtOAc/acetone 98:2) and the isolated salt was acidified via filtration over a short plug of DOWEX 50WX8 (H-form, eluted with CH_2Cl_2) to yield (*S*,*S*)-**IDPi-25-b** (75 mg, 40 µmol, 70%) as off-white solid.
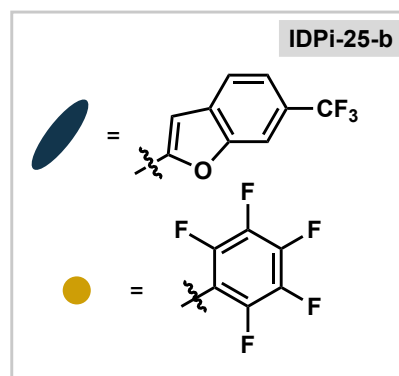
TLC:	R$_F$ (CH_2Cl_2/EtOAc 9:1) = 0.34.

¹H-NMR:	(501 MHz, CD$_2$Cl$_2$): δ = 8.63 (s, 2H), 8.12 (dd, J = 8.4, 3.4 Hz, 4H), 7.93 (s, 2H), 7.86 (dd, J = 11.5, 7.7 Hz, 4H), 7.72 – 7.51 (m, 8H), 7.42 – 7.35 (m, 2H), 7.28 (s, 2H), 7.19 (dd, J = 11.6, 8.1 Hz, 8H), 6.95 (s, 2H), 6.81 (d, J = 8.0 Hz, 2H).
¹³C-NMR:	(126 MHz, CD$_2$Cl$_2$): δ = 153.64, 153.28, 152.68, 152.18, 142.27, 141.84, 132.70, 132.43, 132.14, 132.02, 132.00, 131.68, 130.07, 129.57, 129.53, 129.05, 128.75, 128.58, 127.82, 127.65, 127.46, 127.26, 126.93, 126.59, 126.34, 126.14, 125.70, 123.99, 123.54, 123.19, 122.86, 122.40, 122.08, 121.60, 120.86, 120.61, 119.66, 108.82, 108.79, 108.34, 108.27, 107.91.
¹⁹F-NMR:	(471 MHz, CD$_2$Cl$_2$): δ =–61.44 (s), –61.63 (s), –136.68 (d, J = 21.6 Hz), –145.61 (s), –159.59 (s).
³¹P-NMR:	(202 MHz, CD$_2$Cl$_2$) δ = –14.06.
ESI-HRMS:	calculated for C$_{88}$H$_{36}$F$_{22}$N$_3$O$_{12}$P$_2$S$_2$ ([M-H]⁻): 1870.08698, found: 1870.08923.

(*S,S*)-(6-(perfluoropropyl)benzofuranyl)-C$_6$F$_5$ IDPi (IDPi-26-b)

Prepared according to GP C: (*S*)-3,3'-bis(6-(perfluoropropyl)benzofuran-2-yl)-[1,1'-binaphthalene]-2,2'-diol (**250**, 215 mg, 0.25 mmol, 2.1 equiv.) was given to a flame dried Schlenk tube under an atmosphere of argon and dissolved in anhydrous PhMe (1.7 mL). ((perfluorophenyl)sulfonyl)phosphorimidoyl trichloride (**155,** 96 mg, 0.25 mmol, 2.1 equiv.) was added followed

by triethylamine (0.27 mL, 1.9 mmol, 16 equiv.) and the mixture was stirred at room temperature for 30 min. Hexamethyldisilazane (25 µL, 0.12 mmol, 1.0 equiv.) was added, the mixture was stirred for another 20 min at room temperature and subsequently heated to 130 °C for 4 days. The tube was then cooled to room temperature, diluted with CH$_2$Cl$_2$ (5 mL) and quenched via the addition of HCl (10%, 10 mL). The layers were separated, and the aqueous layer was extracted with CH$_2$Cl$_2$ (3 x 10 mL), the combined organic extracts were dried over anhydrous Na$_2$SO$_4$ and concentrated under reduced pressure. The crude residue was purified via flash column chromatography on silica gel (eluent: EtOAc/*i*-hexanes 3:1 → EtOAc 100% → EtOAc/acetone 97:3) and the isolated salt was acidified via filtration over a short plug of
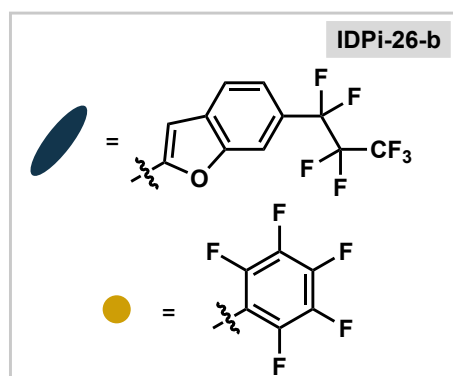
DOWEX 50WX8 (H-form, eluted with CH$_2$Cl$_2$) to yield (**S,S**)-**IDPi-26-b** (78 mg, 34 µmol, 29%) as off-white solid.

^{1}H-NMR:	(501 MHz, CD$_2$Cl$_2$): δ = 8.63 (s, 2H), 8.18 (d, J = 8.2 Hz, 2H), 8.13 (d, J = 8.4 Hz, 2H), 7.98 – 7.90 (m, 6H), 7.72 – 7.64 (m, 4H), 7.62 (s, 2H), 7.60 – 7.54 (m, 2H), 7.45 – 7.39 (m, 4H), 7.26 (dt, J = 8.6, 4.5 Hz, 8H), 7.03 (s, 2H), 6.80 (dd, J = 8.2, 1.5 Hz, 2H).
^{13}C-NMR:	(126 MHz, CD$_2$Cl$_2$): δ = 153.33, 152.90, 152.30, 151.74, 141.75, 132.55, 132.36, 131.81, 131.58, 131.24, 129.62, 129.05, 128.69, 128.20 (d, J = 11.7 Hz), 127.35 (d, J = 6.4 Hz), 126.90, 126.42, 122.81, 122.19, 121.83, 121.62, 121.07, 120.55, 120.19, 117.03, 109.90, 109.39, 107.88, 107.52.
^{19}F-NMR:	(471 MHz, CD$_2$Cl$_2$): δ = –80.35 (t, J = 9.9 Hz), –80.50 (t, J = 10.0 Hz), –110.16 (q, J = 9.9 Hz), –110.50 (p, J = 10.9 Hz), –126.34 - –126.64 (m), –136.35 - –136.91 (m), –145.63 (s), –159.60 (s).
^{31}P-NMR:	(202 MHz, CD$_2$Cl$_2$) δ = –14.30.
ESI-HRMS:	calculated for C$_{96}$H$_{36}$F$_{38}$N$_3$O$_{12}$P$_2$S$_2$ ([M-H]$^-$): 2270.06143, found: 2270.06258.

(*S,S*)-(5-chloro-2,6-dimethylbenzofuranyl)-C$_6$F$_5$ IDPi (IDPi-28-b)

Prepared according to GP C: (*S*)-3,3'-bis(5-chloro-6-methylbenzofuran-2-yl)-[1,1'-binaphthalene]-2,2'-diol (**251**, 217 mg, 0.35 mmol, 2.1 equiv.) was given to a flame dried Schlenk tube under an atmosphere of argon and dissolved in anhydrous PhMe (2.5 mL). ((perfluorophenyl)sulfonyl)phosphorimidoyl trichloride (**155, 134** mg, 0.35 mmol, 2.1 equiv.) was added followed by triethylamine (0.37 mL, 2.7 mmol, 16 equiv.) and the mixture was stirred at room temperature for 30 min. Hexamethyldisilazane (35 µL, 0.17 mmol, 1.0 equiv.) was added, the mixture was stirred for another 20 min at room temperature and subsequently heated to 130 °C for 4 days. The tube was then cooled to room temperature, diluted with CH$_2$Cl$_2$ (10 mL) and quenched via the addition of HCl (10%, 10 mL). The layers were separated, and the aqueous layer was extracted with CH$_2$Cl$_2$ (3 x 10 mL), the combined organic extracts were dried over anhydrous Na$_2$SO$_4$ and concentrated under reduced pressure. The crude residue was purified via flash column chromatography on silica gel (eluent: PhMe/EtOAc 50:1 → 20:2) and the isolated salt was acidified via filtration over a short plug
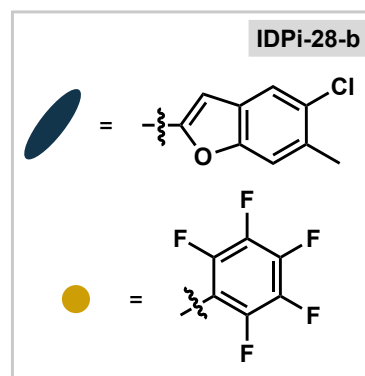
of DOWEX 50WX8 (H-form, eluted with CH_2Cl_2) to yield **(*S,S*)-IDPi-28-b** (145 mg, 81 μmol, 48%) as off-white solid.

¹H-NMR:	(501 MHz, CD_2Cl_2): δ = 8.59 (s, 2H), 8.10 (d, J = 8.3 Hz, 2H), 8.01 (d, J = 8.2 Hz, 2H), 7.81 (s, 2H), 7.66 (s, 2H), 7.61 (t, J = 7.6 Hz, 2H), 7.52 (s, 2H), 7.35 (t, J = 7.6 Hz, 2H), 7.24 (t, J = 7.5 Hz, 2H), 7.00 (s, 2H), 6.60 (s, 2H), 2.55 (s, 6H).
¹³C-NMR:	(126 MHz, CD_2Cl_2): δ = 153.47, 153.25, 150.86, 145.24, 143.17, 142.49, 138.38, 136.63, 133.87, 132.64, 132.02, 131.92, 131.84, 131.72, 129.94, 129.79, 129.38, 129.33, 129.10, 128.90, 128.57, 128.50, 128.01, 127.75, 127.48, 127.20, 127.06, 125.65, 123.12, 122.48, 122.12, 121.79, 121.28, 112.97, 112.43, 107.94, 107.38, 21.13.
¹⁹F-NMR:	(471 MHz, CD_2Cl_2): δ = –136.73 (s), –146.10 (s), –159.70 (s).
³¹P-NMR:	(202 MHz, CD_2Cl_2) δ = –16.19.
ESI-HRMS:	calculated for $C_{88}H_{44}F_{10}Cl_4N_3O_{12}P_2S_2$ ([M-H]⁻): 1790.04417, found: 1790.04475.

(*S,S*)-(2,5-dimethylnaphtho[2,1-*b*]furanyl)-C₆F₅ IDPi (IDPi-29-b)

Prepared according to <u>GP C</u>: (*S*)-3,3'-bis(5-methylnaphtho[2,1-b]furan-2-yl)-[1,1'-binaphthalene]-2,2'-diol (**252**, 293 mg, 0.45 mmol, 2.1 equiv.) was given to a flame dried Schlenk tube under an atmosphere of argon and dissolved in anhydrous PhMe (2.5 mL). ((perfluorophenyl)sulfonyl)phosphorimidoyl trichloride (**155,** 173 mg, 0.45 mmol, 2.1 equiv.) was added followed by triethylamine (0.48 mL, 3.5 mmol, 16 equiv.) and the mixture was stirred at room temperature for 30 min.
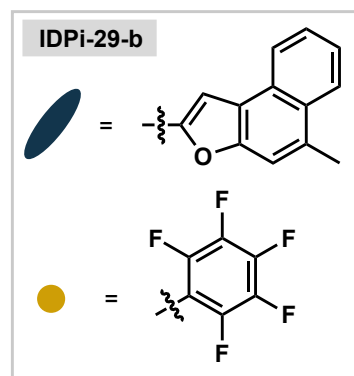
Hexamethyldisilazane (45 μL, 0.21 mmol, 1.0 equiv.) was added, the mixture was stirred for another 20 min at room temperature and subsequently heated to 130 °C for 4 days. The tube was then cooled to room temperature, diluted with CH_2Cl_2 (10 mL) and quenched via the addition of HCl (10%, 10 mL). The layers were separated, and the aqueous layer was extracted with CH_2Cl_2 (3 x 10 mL), the combined organic extracts were dried over anhydrous Na_2SO_4 and concentrated under reduced pressure. The crude residue was purified via flash column chromatography on silica gel (eluent: PhMe/EtOAc 40:1 → 20:1) and the isolated salt was acidified via filtration over a short plug of DOWEX 50WX8 (H-form, eluted with CH_2Cl_2) to yield **(*S,S*)-IDPi-29-b** (160 mg, 86 μmol, 40%) as off-white solid.

¹H-NMR:	(501 MHz, CDCl₃): δ = 8.49 (s, 2H), 8.13 (d, J = 8.4 Hz, 2H), 8.08 (d, J = 8.1 Hz, 2H), 8.03 – 7.98 (m, 4H), 7.90 (q, J = 4.8 Hz, 2H), 7.77 – 7.67 (m, 8H), 7.64 (t, J= 7.5 Hz, 2H), 7.49 (dt, J = 24.9, 7.3 Hz, 4H), 7.42 (s, 2H), 7.37 (dd, J = 19.0, 7.7 Hz, 2H), 7.24 (d, J = 8.4 Hz, 2H), 7.08 (s, 2H), 6.71 (d, J = 19.3 Hz, 4H), 6.40 (t, J = 7.7 Hz, 2H), 6.20 (t, J = 7.4 Hz, 2H), 4.96 (s, 2H), 2.85 (s, 6H), 2.24 (s, 6H).
¹⁹F-NMR:	(471 MHz, CD₂Cl₂): δ = –134.42 (s), –146.84 (s), –160.36 (s).
³¹P-NMR:	(202 MHz, CD₂Cl₂) δ = –18.04.
ESI-HRMS:	calculated for $C_{104}H_{56}F_{10}N_3O_{12}P_2S_2$ ([M-H]⁻): 1854.26266, found: 1854.26347.

7.2.3 Asymmetric Catalytic Scriabine Reaction

General Procedure G (GP G): Scriabine Reaction of Acylals - Screening
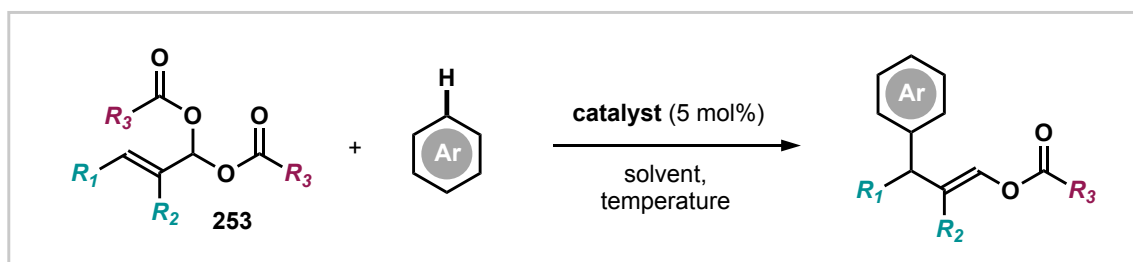
A flame-dried 5 mL finger Schlenk tube under an atmosphere of argon equipped with a magnetic stirring bar was charged with the used organocatalyst (5 mol%) and the used solvent was added (1.0 mL) followed by the arene substrate (0.2 mmol, 2.0 equiv.) and then the acylal reagent (0.1 mmol, 1.0 equiv.). The tube was sealed and stirred at the respective temperature for the indicated reaction time. The mixture was then quenched with triethylamine (0.3 M solution in PhMe, 200 µL) and applied directly on a silica gel column equilibrated with *i*-hexanes. The mixture was flushed with *i*-hexanes (100 mL) and then purified via flash column chromatography on silica gel (*i*-hexanes/MTBE eluents) to yield the desired enol esters usually as colorless oils. *Deviations from the general protocol are indicated at the respective entry.*

On lower scales, the reactions were performed in oven-dried 1 mL screwcap vials under an atmosphere of argon. The reactions were quenched analogously and purified via preparative thin layer chromatography (*i*-hexanes/MTBE eluents) to yield the desired enol esters usually as colorless oils.

Racemic samples as reference for chromatographic analysis were obtained via usage of $HNTf_2$ as acid catalyst.

General Procedure G (GP G): *in situ* Scriabine Reaction - Screening
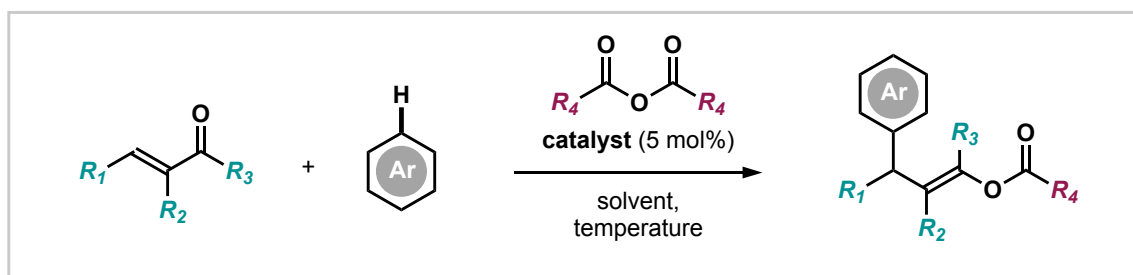
A flame-dried 5 mL finger Schlenk tube under an atmosphere of argon equipped with a magnetic stirring bar was charged with the used organocatalyst (5 mol%) and the used solvent was added (1.0 mL) followed by the arene substrate (0.2 mmol, 2.0 equiv.) and then the

enal/enone (0.1 mmol, 1.0 equiv.). The anhydride activating agent (0.5 mmol, 5 equiv.) was added and the tube was sealed and stirred at the respective temperature for the indicated reaction time. The mixture was then quenched with triethylamine (0.3 M solution in PhMe, 200 µL) and applied directly on a silica gel column equilibrated with *i*-hexanes. The mixture was flushed with *i*-hexanes (100 mL) and then purified via flash column chromatography on silica gel (*i*-hexanes/MTBE eluents) to yield the desired enol esters usually as colorless oils. *Deviations from the general protocol are indicated at the respective entry.*

On lower scales, the reactions were performed in oven-dried 1 mL screwcap vials under an atmosphere of argon. The reactions were quenched analogously and purified via preparative thin layer chromatography (*i*-hexanes/MTBE eluents) to yield the desired enol esters usually as colorless oils.

Racemic samples as reference for chromatographic analysis were obtained via usage of $HNTf_2$ as acid catalyst.

(*E*)-3-(p-tolyl)prop-1-en-1-yl acetate (254)

Prepared following *General Procedure G* with deviations, from prop-2-ene-1,1-diyl diacetate (**256**, 7.9 mg, 50 µmol, 1.0 equiv.) in PhMe (**3**, 0.5 mL, 30 mmol, 3.0 equiv.) using $HNTf_2$ (0.2 M stock solution in CH_2Cl_2, 4 drops, ca 5 mol%) as catalyst at 30 °C for 1 h. Purification of the reaction mixture via preparative thin layer chromatography (eluent: *i*-hexane/EtOAc 10:1) gave **254** as colorless oil (4.0 mg, 21 µmol, 42%).
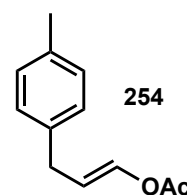
¹H-NMR:	(501 MHz, CD_2Cl_2): δ = 7.17 – 7.04 (m, 5H), 6.79 (dt, J = 24.2, 5.5 Hz, 1H), 2.73 – 2.62 (m, 2H), 2.31 – 2.29 (m, 3H), 2.04 (s, 3H), 2.00 (s, 5H).

(*E*)-3-(4-methoxyphenyl)but-1-en-1-yl acetate (127)

Prepared following *General Procedure G*, from (*E*)-but-2-ene-1,1-diyl diacetate (**117**, 7.9 mg, 50 µmol, 1.0 equiv.) and anisole (**26**, 11 µL, 0.1 mmol, 2.0 equiv.) in PhMe (0.5 mL, 0.1 M) using **IDPi-01-a** (4.5 mg, 2.5 µmol, 5 mol%) as catalyst at 30 °C for 16 h. Purification of the reaction mixture via preparative thin layer chromatography (eluent: *i*-hexane/MTBE 10:1) gave **127** as colorless oil (3.0 mg, 13.6 µmol, 27%).
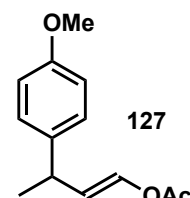
TLC:	R_f (*i*-hexanes/EtOAc 9:1) = 0.45.

¹H-NMR:	(501 MHz, CDCl$_3$): δ = 7.14 (d, J = 8.7 Hz, 2H), 7.10 (dd, J = 12.5, 1.3 Hz, 1H), 6.87 – 6.80 (m, 2H), 5.58 (dd, J = 12.5, 7.7 Hz, 1H), 3.77 (s, 3H), 3.45 (p, J = 6.8 Hz, 1H), 2.08 (s, 3H), 1.35 (d, J = 7.0 Hz, 3H).
ESI-HRMS:	calculated for C$_{13}$H$_{16}$O$_3$ ([M]$^+$): 220.10940, found: 220.10939.
HPLC:	(Chiralpak IA-3, MeOH/H$_2$O 80:20, 298 K, 220 nm): t$_R$ (major) = 37.2 min, t$_R$ (minor) = 44.1 min, e.r. = 65:35 (30% e.e.).
E/Z:	5:1, as determined via HPLC- and ¹H-NMR analysis.

The analytical data is in agreement with previously reported data.[184]

(*E*)-3-(4-methoxyphenyl)-2-methylbut-1-en-1-yl acetate (128)

Prepared following *General Procedure G*, from ((*E*)-2-methylbut-2-ene-1,1-diyl diacetate (**125**, 4.7 mg, 25 µmol, 1.0 equiv.) and anisole (**26**, 5.4 µL, 0.05 mmol, 2.0 equiv.) in *n*-pentane (0.25 mL, 0.1 M) using **IDPi-01-a** (1.6 mg, 0.6 µmol, 2.5 mol%) as catalyst at 30 °C for 16 h. Purification of the reaction mixture via preparative thin layer chromatography (eluent: *i*-hexane/MTBE 10:1) gave **128** as colorless oil (5.6 mg, 24 µmol, 95%).
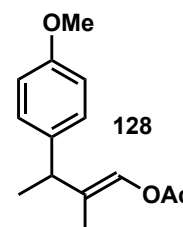
¹H-NMR:	(501 MHz, CDCl$_3$): δ = 7.15 – 7.09 (m, 2H), 6.83 (d, J = 8.7 Hz, 2H), 3.79 (s, 3H), 3.38 (q, J = 7.1 Hz, 1H), 2.15 (s, 3H), 1.51 (d, J = 1.5 Hz, 3H), 1.37 (d, J = 7.1 Hz, 3H).
EI-HRMS:	calculated for C$_{14}$H$_{18}$O$_3$ ([M]$^+$): 234.12504, found: 234.12506.
HPLC:	(Chiralpak IA-3, MeCN/H$_2$O 50:50, 298 K, 220 nm): t$_R$ (min) = 8.0 min, t$_R$ (major) = 9.6 min, e.r. = 84.5:15.5 (69% e.e.).
E/Z:	6:1, as determined via ¹H-NMR analysis.

(*E*)-3-(benzofuran-2-yl)but-1-en-1-yl acetate (132)

Prepared following *General Procedure G*, from ((*E*)-2-methylbut-2-ene-1,1-diyl diacetate (**117**, 4.7 mg, 25 µmol, 1.0 equiv.) and benzofurane (**82**, 5.5 µL, 0.05 mmol, 2.0 equiv.) in *n*-pentane (0.25 mL, 0.1 M) using **IDPi-01-a** (1.6 mg, 0.6 µmol, 2.5 mol%) as catalyst at 30 °C for 16 h. Purification of the reaction mixture via preparative thin layer chromatography (eluent: *i*-hexane/MTBE 10:1) gave **132** as colorless oil (5.6 mg, 24 µmol, 95%).
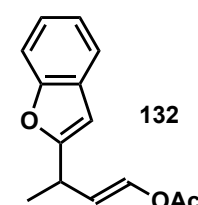
¹H-NMR: (501 MHz, CDCl₃): δ = 7.51 – 7.47 (m, 1H), 7.44 – 7.40 (m, 1H), 7.29 (dd, J = 12.5, 1.1 Hz, 1H), 7.20 (dtd, J = 20.5, 7.4, 1.3 Hz, 2H), 6.42 (t, J = 1.0 Hz, 1H), 5.63 (dd, J = 12.5, 8.3 Hz, 1H), (p, J = 8.0 Hz, 1H), 2.13 (s, 3H), 1.48 (d, J = 7.0 Hz, 3H).

¹³C-NMR: (126 MHz, CDCl3): δ = 167.72, 136.43, 128.61, 123.50, 122.53, 120.51, 116.20, 110.92, 101.28, 32.55, 20.70, 19.14.

ESI-HRMS: calculated for C₁₄H₁₄O₃Na ([M+Na]⁺): 253.08351, found: 253.08334.

HPLC: (Chiralpak IA-3, MeCN/H₂O 55:45, 298 K, 220 nm): t_R (min) = 6.7 min, t_R (major) = 8.0 min, e.r. = 91.5:8.5 (83% e.e.).

E/Z: 6:1, as determined via ¹H-NMR analysis.

(E)-(2-(benzofuran-2-yl)cyclohexylidene)methyl acetate (133)

Prepared following *General Procedure G*, from cyclohex-1-en-1-ylmethylene diacetate (**120**, 5.3 mg, 25 µmol, 1.0 equiv.) and benzofurane (**82**, 5.5 µL, 0.05 mmol, 2.0 equiv.) in *n*-pentane (0.25 mL, 0.1 M) using **IDPi-01-a** (1.6 mg, 0.6 µmol, 2.5 mol%) as catalyst at 0 °C for 16 h. Purification of the reaction mixture via preparative thin layer chromatography (eluent: *i*-hexane/EtOAc 20:1) gave **133** as colorless oil (2.9 mg, 11 µmol, 43%). Elimination toward dienol acetate **134** was observed as significant side reaction.
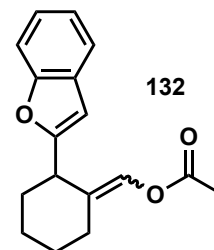
¹H-NMR: (501 MHz, CDCl₃): δ = 7.51 – 7.48 (m, 1H), 7.45 – 7.41 (m, 1H), 7.24 – 7.15 (m, 2H), 6.87 (q, J = 1.2 Hz, 1H), 6.47 (t, J = 1.1 Hz, 1H), 3.61 (t, J = 5.6 Hz, 1H), 2.43 – 2.34 (m, 2H), 2.25 – 2.16 (m, 1H), 2.13 (s, 3H), 1.91 (ddt, J = 12.9, 8.3, 4.0 Hz, 1H), 1.72 (td, J = 9.1, 3.6 Hz, 1H), 1.66 – 1.54 (m, 3H).

EI-HRMS: calculated for C₁₇H₁₈O₃ ([M]⁺): 270.12504, found: 270.12519.

E/Z: >20:1, as determined via ¹H-NMR analysis.

(E)-3-(benzofuran-2-yl)but-1-en-1-yl isobutyrate (136)

Prepared following *General Procedure G*, from (E)-but-2-ene-1,1-diyl bis(2-methylpropanoate) (**122**, 5.7 mg, 25 µmol, 1.0 equiv.) and benzofurane (**82**, 5.5 µL, 0.05 mmol, 2.0 equiv.) in *n*-pentane (0.25 mL, 0.1 M) using **IDPi-01-a** (1.6 mg, 0.6 µmol, 2.5 mol%) as catalyst at 0 °C for 16 h. Purification of the reaction mixture via preparative thin layer
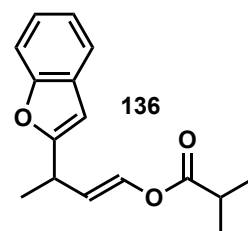
chromatography (eluent: *i*-hexane/MTBE 20:1) gave **136** as colorless oil (4.0 mg, 15 μmol, 61%).

¹H-NMR:	(501 MHz, CDCl₃): δ = 7.51 – 7.47 (m, 1H), 7.42 (dd, J = 8.1, 1.0 Hz, 1H), 7.30 (dd, J = 12.5, 1.1 Hz, 1H), 7.25 – 7.15 (m, 2H), 6.42 (d, J = 1.0 Hz, 1H), 5.64 (dd, J = 12.5, 8.3 Hz, 1H), 3.72 – 3.65 (m, 1H), 2.62 (hept, J = 7.0 Hz, 1H), 1.49 (d, J = 7.0 Hz, 3H), 1.21 (dd, J = 7.0, 1.2 Hz, 6H).
¹³C-NMR:	(126 MHz, CDCl3): δ = 174.48, 161.84, 155.16, 137.04, 129.11, 123.87, 122.93, 120.91, 116.38, 111.13, 101.56, 34.19, 33.01, 19.41, 18.89.
EI-HRMS:	calculated for $C_{16}H_{18}O_3$ ([M]⁺): 258.12504, found: 258.12528.
2D-HPLC:	1st dimension: (Eclipse Plus C18, MeCN/H₂O 60:40, 298 K, 220 nm): t_R = 2.2 min.
	2nd dimension: (Chiralpak IA-3, MeOH/H₂O - Gradient = 60% - 10' - 85% MeOH, 298 K, 220 nm): t_R (minor) = 14.2 min, t_R (major) = 16.2 min, e.r. = 93.5:6.5 (87% e.e.).
E/Z:	>20:1, as determined via ¹H-NMR analysis.

(*E*)-3-(benzofuran-2-yl)but-1-en-1-yl pivalate (147)

Prepared following *General Procedure G*, from (*E*)-but-2-ene-1,1-diyl bis(2,2-dimethylpropanoate) (**124**, 5.7 mg, 25 μmol, 1.0 equiv.) and benzofurane (**82**, 5.5 μL, 0.05 mmol, 2.0 equiv.) in *n*-pentane (0.25 mL, 0.1 M) using **IDPi-01-a** (1.6 mg, 0.6 μmol, 2.5 mol%) as catalyst at 0 °C for 16 h. Purification of the reaction mixture via preparative thin layer chromatography (eluent: *i*-hexane/MTBE 20:1) gave **147** as colorless oil (6.5 mg, 24 μmol, 95%).
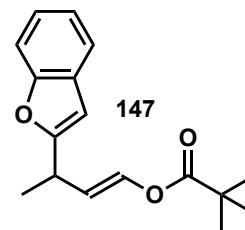
TLC:	R_f (*i*-hexanes/EtOAc 20:1) = 0.55.
¹H-NMR:	(501 MHz, CD₂Cl₂): δ = 7.52 – 7.50 (m, 1H), 7.44 – 7.41 (m, 1H), 7.31 – 7.30 (m, 1H), 7.27 – 7.17 (m, 2H), 6.46 (t, J = 1.0 Hz, 1H), 5.65. (dd, J = 12.5 Hz, 8.3 Hz, 1H), 3.76 – 3.64 (m, 1H), 1.49 (d, J = 7 Hz, 3H), 1.24 (s, 9H).
¹³C-NMR:	(126 MHz, CDCl3): δ = 175.89, 174.44, 161.87, 137.23, 129.12, 123.88, 122.94, 120.92, 116.37, 111.13, 101.55, 38.98, 33.02, 27.10, 19.42.
EI-HRMS:	calculated for $C_{17}H_{20}O_3$ ([M]⁺): 272.14069, found: 272.14118.

HPLC: (Chiralpak OJ-3R, MeCN/H$_2$O 55:45, 298 K, 220 nm): t_R (major) = 19.3 min, t_R (minor) = 22.7 min, e.r. = 93:7 (86% e.e.).

E/Z: >20:1, as determined via ^{1}H-NMR analysis.

7.2.4 Crystallographic Data
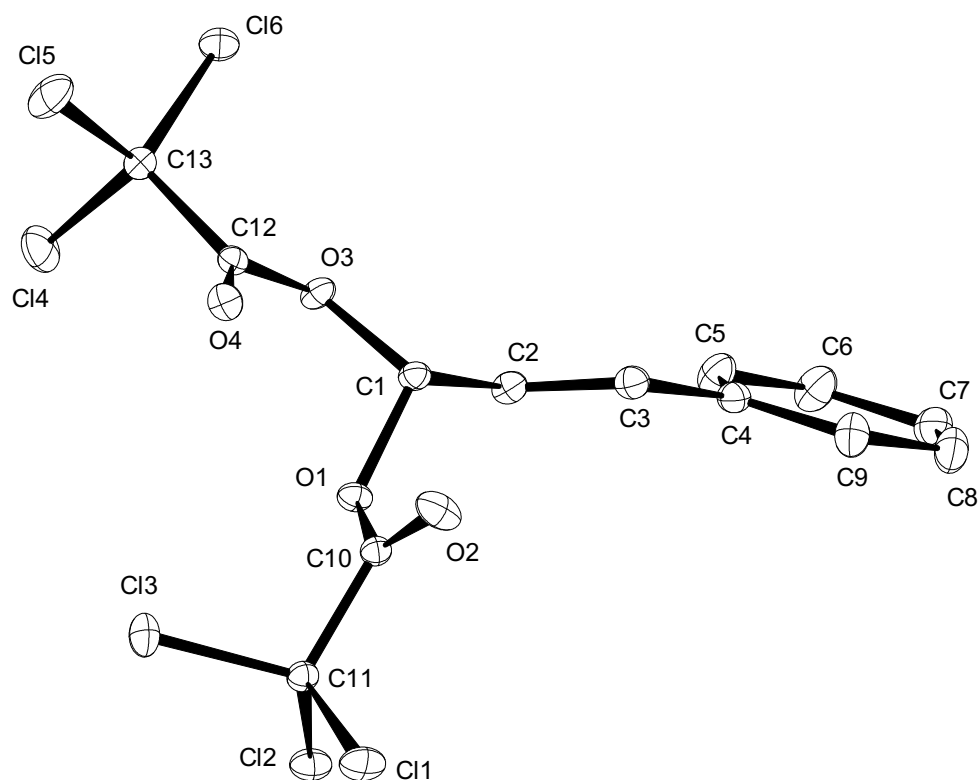
Figure 7.20: X-Ray structure of compound **142** (H-atoms omitted).

Table 7.5: Crystal data and structure refinement.

Identification code	15127
Empirical formula	$C_{13}H_8Cl_6O_4$
Color	colorless
Formula weight	440.89 g · mol^{-1}
Temperature	100(2) K
Wavelength	0.71073 Å
Crystal system	TRICLINIC
Space group	**P$\overline{1}$, (no. 2)**
Unit cell dimensions	a = 8.4578(5) Å α= 109.413(2)°.
	b = 9.8610(6) Å β= 99.269(2)°.
	c = 11.8448(7) Å γ = 107.130(2)°.
Volume	852.84(9) Å^3
Z	2
Density (calculated)	1.717 Mg · m^{-3}
Absorption coefficient	1.021 mm^{-1}
F(000)	440 e
Crystal size	0.36 x 0.229 x 0.106 mm^3
θ range for data collection	1.903 to 33.579°.

Index ranges	$-13 \leq h \leq 12$, $-15 \leq k \leq 15$, $-18 \leq l \leq 18$
Reflections collected	31934
Independent reflections	6682 [$R_{int} = 0.0207$]
Reflections with $I > 2\sigma(I)$	6366
Completeness to $\theta = 25.242°$	100.0 %
Absorption correction	Gaussian
Max. and min. transmission	0.91 and 0.78
Refinement method	Full-matrix least-squares on F^2
Data / restraints / parameters	6682 / 0 / 240
Goodness-of-fit on F^2	1.043
Final R indices [$I > 2\sigma(I)$]	$R_1 = 0.0191$ $wR^2 = 0.0516$
R indices (all data)	$R_1 = 0.0202$ $wR^2 = 0.0522$
Largest diff. peak and hole	0.52 and -0.34 e $\cdot$ Å^{-3}

Table **7.6**: Bond lengths [Å] and angles [°].

Cl(1)-C(11)	1.7504(7)	Cl(2)-C(11)	1.7653(7)
Cl(3)-C(11)	1.7711(7)	Cl(4)-C(13)	1.7709(7)
Cl(5)-C(13)	1.7577(8)	Cl(6)-C(13)	1.7581(7)
O(1)-C(1)	1.4541(8)	O(1)-C(10)	1.3358(8)
O(2)-C(10)	1.1936(9)	O(3)-C(1)	1.4296(9)
O(3)-C(12)	1.3396(8)	O(4)-C(12)	1.1954(9)
C(1)-H(1)	0.956(11)	C(1)-C(2)	1.4814(10)
C(2)-H(2)	0.955(13)	C(2)-C(3)	1.3329(10)
C(3)-H(3)	0.949(13)	C(3)-C(4)	1.4670(10)
C(4)-C(5)	1.3998(11)	C(4)-C(9)	1.3954(11)
C(5)-H(5)	0.976(13)	C(5)-C(6)	1.3866(11)
C(6)-H(6)	0.940(14)	C(6)-C(7)	1.3909(12)
C(7)-H(7)	0.944(15)	C(7)-C(8)	1.3871(12)
C(8)-H(8)	0.961(14)	C(8)-C(9)	1.3919(11)
C(9)-H(9)	0.958(14)	C(10)-C(11)	1.5476(10)
C(12)-C(13)	1.5449(10)		
C(10)-O(1)-C(1)	115.69(5)	C(12)-O(3)-C(1)	115.31(5)
O(1)-C(1)-H(1)	109.0(7)	O(1)-C(1)-C(2)	109.26(5)
O(3)-C(1)-O(1)	105.98(5)	O(3)-C(1)-H(1)	111.2(7)
O(3)-C(1)-C(2)	108.09(6)	C(2)-C(1)-H(1)	113.1(7)
C(1)-C(2)-H(2)	116.3(8)	C(3)-C(2)-C(1)	120.98(7)
C(3)-C(2)-H(2)	122.6(8)	C(2)-C(3)-H(3)	118.9(8)
C(2)-C(3)-C(4)	125.50(7)	C(4)-C(3)-H(3)	115.6(8)
C(5)-C(4)-C(3)	122.26(7)	C(9)-C(4)-C(3)	118.83(7)
C(9)-C(4)-C(5)	118.90(7)	C(4)-C(5)-H(5)	121.1(8)
C(6)-C(5)-C(4)	120.40(7)	C(6)-C(5)-H(5)	118.5(8)
C(5)-C(6)-H(6)	119.9(9)	C(5)-C(6)-C(7)	120.19(8)
C(7)-C(6)-H(6)	119.8(9)	C(6)-C(7)-H(7)	119.4(9)
C(8)-C(7)-C(6)	119.97(7)	C(8)-C(7)-H(7)	120.6(9)
C(7)-C(8)-H(8)	120.4(9)	C(7)-C(8)-C(9)	119.90(8)
C(9)-C(8)-H(8)	119.7(9)	C(4)-C(9)-H(9)	118.7(9)
C(8)-C(9)-C(4)	120.62(8)	C(8)-C(9)-H(9)	120.7(9)
O(1)-C(10)-C(11)	110.51(6)	O(2)-C(10)-O(1)	127.08(6)
O(2)-C(10)-C(11)	122.37(6)	Cl(1)-C(11)-Cl(2)	110.45(4)
Cl(1)-C(11)-Cl(3)	109.53(4)	Cl(2)-C(11)-Cl(3)	109.54(4)
C(10)-C(11)-Cl(1)	109.32(5)	C(10)-C(11)-Cl(2)	111.74(5)
C(10)-C(11)-Cl(3)	106.16(5)	O(3)-C(12)-C(13)	110.08(6)

O(4)-C(12)-O(3)	125.99(7)	O(4)-C(12)-C(13)	123.87(6)
Cl(5)-C(13)-Cl(4)	109.74(4)	Cl(5)-C(13)-Cl(6)	109.77(4)
Cl(6)-C(13)-Cl(4)	110.24(4)	C(12)-C(13)-Cl(4)	105.96(5)

8. References

(1)   Verband der Chemischen Industrie, VCI, accessed 20th of June 2024, https://www.vci.de/fonds/startseite.jsp.

(2)   Taseska, T.; Yu, W.; Wilsey, M. K.; Cox, C. P.; Meng, Z.; Ngarnim, S. S.; Müller, A. M. Analysis of the Scale of Global Human Needs and Opportunities for Sustainable Catalytic Technologies. *Top. Catal.* **2023**, *66*, 338–374.

(3)   Roduner, E. Understanding Catalysis. *Chem. Soc. Rev.* **2014**, *43*, 8226–8239.

(4)   Noyori, R. Asymmetric Catalysis: Science and Opportunities. *Angew. Chem. Int. Ed.* **2002**, *41*, 2008.

(5)   Faradey, M. On New Compounds of Carbon and Hydrogen, and on Certain Other Products Obtained during the Decomposition of Oil by Heat. *Philos. Trans. R. Soc. London* **1825**, *115*, 440–466.

(6)   Dewar, J. 5. On the Oxidation of Phenyl Alcohol, and a Mechanical Arrangement Adapted to Illustrate Structure in the Nonsaturated Hydrocarbons. *Proc. R. Soc. Edinburgh* **1869**, *6*, 82–86.

(7)   Van Tamelen, E. E.; Pappas, S. P.; Kirk, K. L. Valence Bond Isomers of Aromatic Systems. Bicyclo[2.2.0]Hexa-2,5-Dienes (Dewar Benzenes). *J. Am. Chem. Soc.* **1971**, *93*, 6092–6101.

(8)   Robinson, A. Chemistry's Visual Origins. *Nature* **2010**, *465*, 36–36.

(9)   Heidelberg, E. E. Studien Über Die s. g. Aromatischen Säuren. *Justus Liebigs Ann. Chem.* **1866**, *137*, 327–359.

(10)   Armit, J. W.; Robinson, R. CCXI.—Polynuclear Heterocyclic Aromatic Types. Part II. Some Anhydronium Bases. *J. Chem. Soc., Trans.* **1925**, *127*, 1604–1618.

(11)   Balaban, A. T.; Schleyer, P. v. R.; Rzepa, H. S. Crocker, Not Armit and Robinson, Begat the Six Aromatic Electrons. *Chem. Rev.* **2005**, *105*, 3436–3447.

(12)   Crocker, E. C. Application of the Octet Theory to Single-Ring Aromatic Compounds. *J. Am. Chem. Soc.* **1922**, *44*, 1618–1630.

(13)   Hückel, E. Quantentheoretische Beiträge Zum Benzolproblem. *Z. Phys.* **1931**, *70*, 204–286.

(14)   Hückel, E. Quanstentheoretische Beiträge Zum Benzolproblem. *Z. Phys.* **1931**, *72*, 310–337.

(15)   Solà, M. Connecting and Combining Rules of Aromaticity. Towards a Unified Theory

of Aromaticity. *WIREs Comput. Mol. Sci.* **2019**, *9*.

(16)   Hirsch, A.; Chen, Z.; Jiao, H. Spherical Aromaticity In I$_h$ Symmetrical Fullerenes: The 2(N+1)^2 Rule. *Angew. Chem. Int. Ed.* **2000**, *39*, 3915–3917.

(17)   Pham, H. T.; Duong, L. Van; Nguyen, M. T. Electronic Structure and Chemical Bonding in the Double Ring Tubular Boron Clusters. *J. Phys. Chem. C* **2014**, *118*, 24181–24187.

(18)   Duong, L. Van; Pham, H. T.; Tam, N. M.; Nguyen, M. T. A Particle on a Hollow Cylinder: The Triple Ring Tubular Cluster B 27 +. *Phys. Chem. Chem. Phys.* **2014**, *16*, 19470–19478.

(19)   Ghasemabadi, P. G.; Yao, T.; Bodwell, G. J. Cyclophanes Containing Large Polycyclic Aromatic Hydrocarbons. *Chem. Soc. Rev.* **2015**, *44*, 6494–6518.

(20)   Majewski, M. A.; Stępień, M. Bowls, Hoops, and Saddles: Synthetic Approaches to Curved Aromatic Molecules. *Angew. Chem. Int. Ed.* **2019**, *58*, 86–116.

(21)   Gulder, T.; Baran, P. S. Strained Cyclophane Natural Products: Macrocyclization at Its Limits. *Nat. Prod. Rep.* **2012**, *29*, 899.

(22)   Aromaticity. In *The IUPAC Compendium of Chemical Terminology*; International Union of Pure and Applied Chemistry (IUPAC): Research Triangle Park, NC, 2014.

(23)   Merino, G.; Solà, M.; Fernández, I.; Foroutan-Nejad, C.; Lazzeretti, P.; Frenking, G.; Anderson, H. L.; Sundholm, D.; Cossío, F. P.; Petrukhina, M. A.; Wu, J.; Wu, J. I.; Restrepo, A. Aromaticity: Quo Vadis. *Chem. Sci.* **2023**.

(24)   Imhof, P., van der Waal, J. C., *Catalytic Process Development for Renewable Materials*. Wiley-VCH, Weinheim, **2013**.

(25)   Zheng, S.; Wei, Z.; Wozniak, B.; Kallmeier, F.; Baráth, E.; Jiao, H.; Tin, S.; de Vries, J. G. Synthesis of Valuable Benzenoid Aromatics from Bioderived Feedstock. *Nat. Sustain.* **2023**, *6*, 1436–1445.

(26)   Bender, M. Global Aromatics Supply—Today and Tomorrow. In *DGMK Conference: New Technologies and Alternative Feedstocks in Petrochemistry and Refining*; **2013**.

(27)   Heravi, M. M.; Zadsirjan, V.; Saedi, P.; Momeni, T. Applications of Friedel-Crafts Reactions in Total Synthesis of Natural Products. *RSC Adv.* **2018**, *8*, 40061–40163.

(28)   Averill, B. A.; Moulijn, J. A.; Santen, R. A. van; P.W.N.M.; Leeuwen, V. *Catalysis: An Integrated Approach*, Elsevier Science, Amsterdam, **1999**.

(29)   Schmidt, F. *The Importance of Catalysis in the Chemical and Non-Chemical Industries* In *Basic Principles in Applied Catalysis*. Baerns, M., Springer Berlin, Heidelberg, **2004**.

(30)   Humphreys, J.; Lan, R.; Tao, S. Development and Recent Progress on Ammonia Synthesis Catalysts for Haber–Bosch Process. *Adv. Energy Sustain. Res.* **2021**, *2*.

(31)   Catalyst. In *The IUPAC Compendium of Chemical Terminology*; International Union of Pure and Applied Chemistry (IUPAC): Research Triangle Park, NC, **2019**.

(32)   Thomas, J. M.; Williams, R. J. P. Catalysis: Principles, Progress, Prospects. *Philos. Trans. R. Soc. A Math. Phys. Eng. Sci.* **2005**, *363*, 765–791.

(33)   Nagib, D. A. Asymmetric Catalysis in Radical Chemistry. *Chem. Rev.* **2022**, *122*, 15989–15992.

(34)   Bornscheuer, U. *Biocatalysis*. In *Catalysis*; Beller, M., Renken, A., van Santen, R. A., Eds.; Wiley-VCH, Weinheim, **2015**; pp 174–175.

(35)   Walsh, P.; Kozlowski, M. *Fundamentals of Asymmetric Catalysis*; University Science Books: Sausalito, CA, **2009**.

(36)   List, B. Introduction: Organocatalysis. *Chem. Rev.* **2007**, *107*, 5413–5415.

(37)   Berkessel, A.; Gröger, H. *Asymmetric Organocatalysis*, Viley-VCH, Weinheim, **2007**.

(38)   von Liebig, J. Ueber Die Bildung Des Oxamids Aus Cyan. *Justus Liebigs Ann. Chem.* **1860**, *113*, 246–247.

(39)   Knoevenagel, E. Ueber Eine Darstellungsweise Des Benzylidenacetessigesters. *Berichte der Dtsch. Chem. Gesellschaft* **1896**, *29*, 172–174.

(40)   Langenbeck, W. Über Organische Katalysatoren. III. Die Bildung von Oxamid Aus Dicyan Bei Gegenwart von Aldehyden. *Justus Liebigs Ann. Chem.* **1929**, *469*, 16–25.

(41)   Bredig, G.; Fiske, W. S. Durch Katalysatoren Bewirkte Asymmetrische Synthese. *Biochem. Z.* **1912**, 7.

(42)   Pracejus, H. Organische Katalysatoren, LXI. Asymmetrische Synthesen Mit Ketenen, I. Alkaloid-katalysierte Asymmetrische Synthesen von A-Phenyl-propionsäureestern. *Justus Liebigs Ann. Chem.* **1960**, *634*, 9–22.

(43)   Eder, U.; Sauer, G.; Wiechert, R. New Type of Asymmetric Cyclization to Optically Active Steroid CD Partial Structures. *Angew. Chem. Int. Ed.* **1971**, *10*, 496–497.

(44)   Hajos, Z. G.; Parrish, D. R. Asymmetric Synthesis of Bicyclic Intermediates of Natural Product Chemistry. *J. Org. Chem.* **1974**, *39*, 1615–1621.

(45)   List, B.; Lerner, R. A.; Barbas, C. F. Proline-Catalyzed Direct Asymmetric Aldol Reactions. *J. Am. Chem. Soc.* **2000**, *122*, 2395–2396.

(46)   Ahrendt, K. A.; Borths, C. J.; MacMillan, D. W. C. New Strategies for Organic Catalysis: The First Highly Enantioselective Organocatalytic Diels−Alder Reaction. *J. Am. Chem. Soc.* **2000**, *122*, 4243–4244.

(47)   List, B.; Shabat, D.; Zhong, G.; Turner, J. M.; Li, A.; Bui, T.; Anderson, J.; Lerner, R. A.; Barbas, C. F. A Catalytic Enantioselective Route to Hydroxy-Substituted Quaternary

8. References

Carbon Centers: Resolution of Tertiary Aldols with a Catalytic Antibody. *J. Am. Chem. Soc.* **1999**, *121*, 7283–7291.

(48) List, B. *Comprehensive Enantioselective Catalysis: Preface*. In *Comprehensive Enantioselective Catalysis*; Dalko, P. I., Ed.; Wiley-VCH, Weinheim, **2013**; p XXVII.

(49) Fages, F. *Low Molecular Weight Gelators*. In *Topics in Current Chemistry: Preface*; Springer Berlin, Heidelberg, **2005**.

(50) Akiyama, T. Stronger Brønsted Acids. *Chem. Rev.* **2007**, *107*, 5744–5758.

(51) Min, C.; Seidel, D. Asymmetric Brønsted Acid Catalysis with Chiral Carboxylic Acids. *Chem. Soc. Rev.* **2017**, *46*, 5889–5902.

(52) Akiyama, T.; Itoh, J.; Yokota, K.; Fuchibe, K. Enantioselective Mannich-Type Reaction Catalyzed by a Chiral Brønsted Acid. *Angew. Chem. Int. Ed.* **2004**, *43*, 1566–1568.

(53) Uraguchi, D.; Terada, M. Chiral Brønsted Acid-Catalyzed Direct Mannich Reactions via Electrophilic Activation. *J. Am. Chem. Soc.* **2004**, *126*, 5356–5357.

(54) Yang, J.; Wang, R.; Wang, Y.; Yao, W.; Liu, Q.; Ye, M. Ligand-Accelerated Direct C−H Arylation of BINOL: A Rapid One-Step Synthesis of Racemic 3,3′-Diaryl BINOLs. *Angew. Chem. Int. Ed.* **2016**, *55*, 14116–14120.

(55) Noyori, R.; Tomino, I.; Tanimoto, Y. Virtually Complete Enantioface Differentiation in Carbonyl Group Reduction by a Complex Aluminum Hydride Reagent. *J. Am. Chem. Soc.* **1979**, *101*, 3129–3131.

(56) Parmar, D.; Sugiono, E.; Raja, S.; Rueping, M. Complete Field Guide to Asymmetric BINOL-Phosphate Derived Brønsted Acid and Metal Catalysis: History and Classification by Mode of Activation; Brønsted Acidity, Hydrogen Bonding, Ion Pairing, and Metal Phosphates. *Chem. Rev.* **2014**, *114*, 9047–9153.

(57) Schreyer, L.; Properzi, R.; List, B. IDPi Catalysis. *Angew. Chem. Int. Ed.* **2019**, *58*, 12761–12777.

(58) Peng, B.; Ma, J.; Guo, J.; Gong, Y.; Wang, R.; Zhang, Y.; Zeng, J.; Chen, W.-W.; Ding, K.; Zhao, B. A Powerful Chiral Super Brønsted C–H Acid for Asymmetric Catalysis. *J. Am. Chem. Soc.* **2022**, *144*, 2853–2860.

(59) Kaupmees, K.; Tolstoluzhsky, N.; Raja, S.; Rueping, M.; Leito, I. On the Acidity and Reactivity of Highly Effective Chiral Brønsted Acid Catalysts: Establishment of an Acidity Scale. *Angew. Chem. Int. Ed.* **2013**, *52*, 11569–11572.

(60) James, T.; van Gemmeren, M.; List, B. Development and Applications of Disulfonimides in Enantioselective Organocatalysis. *Chem. Rev.* **2015**, *115*, 9388–9409.

(61) Li, A.; Acevedo-Rocha, C. G.; D'Amore, L.; Chen, J.; Peng, Y.; Garcia-Borràs, M.; Gao,

C.; Zhu, J.; Rickerby, H.; Osuna, S.; Zhou, J.; Reetz, M. T. Regio- and Stereoselective Steroid Hydroxylation at C7 by Cytochrome P450 Monooxygenase Mutants. *Angew. Chem. Int. Ed.* **2020**, *132*, 12599–12605.

(62) Kille, S.; Zilly, F. E.; Acevedo, J. P.; Reetz, M. T. Regio- and Stereoselectivity of P450-Catalysed Hydroxylation of Steroids Controlled by Laboratory Evolution. *Nat. Chem.* **2011**, *3*, 738–743.

(63) Mitschke, B.; Turberg, M.; List, B. Confinement as a Unifying Element in Selective Catalysis. *Chem* **2020**, *6*, 2515–2532.

(64) Čorić, I.; List, B. Asymmetric Spiroacetalization Catalysed by Confined Brønsted Acids. *Nature* **2012**, *483*, 315–319.

(65) Yagupolskii, L. M.; Petrik, V. N.; Kondratenko, N. V.; Soovӓli, L.; Kaljurand, I.; Leito, I.; Koppel, I. A. The Immense Acidifying Effect of the Supersubstituent $=NSO_2CF_3$ on the Acidity of Amides and Amidines of Benzoic Acids in Acetonitrile. *J. Chem. Soc., Perkin Trans. 2* **2002**, *11*, 1950–1955.

(66) Kaib, P. S. J.; Schreyer, L.; Lee, S.; Properzi, R.; List, B. Extremely Active Organocatalysts Enable a Highly Enantioselective Addition of Allyltrimethylsilane to Aldehydes. *Angew. Chemie Int. Ed.* **2016**, *55*, 13200–13203.

(67) Díaz-Oviedo, C. D.; Maji, R.; List, B. The Catalytic Asymmetric Intermolecular Prins Reaction. *J. Am. Chem. Soc.* **2021**, *143*, 20598–20604.

(68) Liu, L.; Kim, H.; Xie, Y.; Farès, C.; Kaib, P. S. J.; Goddard, R.; List, B. Catalytic Asymmetric [4+2]-Cycloaddition of Dienes with Aldehydes. *J. Am. Chem. Soc.* **2017**, *139*, 13656–13659.

(69) Zhang, P.; Tsuji, N.; Ouyang, J.; List, B. Strong and Confined Acids Catalyze Asymmetric Intramolecular Hydroarylations of Unactivated Olefins with Indoles. *J. Am. Chem. Soc.* **2021**, *143*, 675–680.

(70) Mahlau, M.; List, B. Asymmetric Counteranion-Directed Catalysis: Concept, Definition, and Applications. *Angew. Chem. Int. Ed.* **2013**, *52*, 518–533.

(71) Yang, J. W.; Hechavarria Fonseca, M. T.; Vignola, N.; List, B. Metal-Free, Organocatalytic Asymmetric Transfer Hydrogenation of α,B-Unsaturated Aldehydes. *Angew. Chem. Int. Ed.* **2005**, *44*, 108–110.

(72) Ouellet, S. G.; Tuttle, J. B.; MacMillan, D. W. C. Enantioselective Organocatalytic Hydride Reduction. *J. Am. Chem. Soc.* **2005**, *127*, 32–33.

(73) Chupakhin, O. N.; Charushin, V. N. Nucleophilic C-H Functionalization of Arenes: A New Logic of Organic Synthesis Expanding the Scope of Nucleophilic Substitution of

Hydrogen in Aromatics. *Pure Appl. Chem.* **2017**, *89*, 1195–1208.

(74) Fittig, R.; König, J. Ueber Das Aethyl- Und Diaethylbenzol. *Justus Liebigs Ann. Chem.* **1867**, *144*, 277–294.

(75) Terrier, F. *Modern Nucleophilic Aromatic Substitution*. Wiley-VCH, Weinheim, **2013**.

(76) Rohrbach, S.; Smith, A. J.; Pang, J. H.; Poole, D. L.; Tuttle, T.; Chiba, S.; Murphy, J. A. Concerted Nucleophilic Aromatic Substitution Reactions. *Angew. Chem. Int. Ed.* **2019**, *58*, 16368–16388.

(77) Glaser, C. Beiträge Zur Kenntniss Des Acetenylbenzols. *Berichte der Dtsch. Chem. Gesellschaft* **1869**, *2*, 422–424.

(78) Ullmann, F.; Bielecki, J. Ueber Synthesen in Der Biphenylreihe. *Berichte der Dtsch. Chem. Gesellschaft* **1901**, *34*, 2174–2185.

(79) Wurtz, A. Ueber Eine Neue Klasse Organischer Radicale. *Justus Liebigs Ann. Chem.* **1855**, *96*, 364–375.

(80) Fittig, R. Ueber Das Monobrombenzol. *Justus Liebigs Ann. Chem.* **1862**, *121*, 361–365.

(81) Meerwein, H.; Büchner, E.; van Emster, K. Über Die Einwirkung Aromatischer Diazoverbindungen Auf α,B-ungesättigte Carbonylverbindungen. *J. für Prakt. Chemie* **1939**, *152*, 237–266.

(82) Kharasch, M. S.; Fields, E. K. Factors Determining the Course and Mechanisms of Grignard Reactions. IV. The Effect of Metallic Halides on the Reaction of Aryl Grignard Reagents and Organic Halides 1. *J. Am. Chem. Soc.* **1941**, *63*, 2316–2320.

(83) Kharasch, M. S.; Fuchs, C. F. Factors Influencing the Course and Mechanisms of Grignard Reactions. XI. The Effect of Metallic Halides on the Reaction of Grignard Reagents with Vinyl Halides and Substituted Vinyl Halides. *J. Am. Chem. Soc.* **1943**, *65*, 504–507.

(84) Cadiot, P.; Chodkiewicz, W. Chemistry of Acetylenes; Viehe, H. G., Ed.; Dekker: New York, **1969**; p 597.

(85) Smidt, J.; Hafner, W.; Jira, R.; Sedlmeier, J.; Sieber, R.; Rüttinger, R.; Kojer, H. Katalytische Umsetzungen von Olefinen an Platinmetall-Verbindungen Das Consortium-Verfahren Zur Herstellung von Acetaldehyd. *Angew. Chem.* **1959**, *71*, 176–182.

(86) Heck, R. F. Acylation, Methylation, and Carboxyalkylation of Olefins by Group VIII Metal Derivatives. *J. Am. Chem. Soc.* **1968**, *90*, 5518–5526.

(87) Heck, R. F. The Arylation of Allylic Alcohols with Organopalladium Compounds. A New Synthesis of 3-Aryl Aldehydes and Ketones. *J. Am. Chem. Soc.* **1968**, *90*, 5526–

5531.

(88) Heck, R. F. Allylation of Aromatic Compounds with Organopalladium Salts. *J. Am. Chem. Soc.* **1968**, *90*, 5531–5534.

(89) Heck, R. F. The Palladium-Catalyzed Arylation of Enol Esters, Ethers, and Halides. A New Synthesis of 2-Aryl Aldehydes and Ketones. *J. Am. Chem. Soc.* **1968**, *90*, 5535–5538.

(90) Heck, R. F. Aromatic Haloethylation with Palladium and Copper Halides. *J. Am. Chem. Soc.* **1968**, *90*, 5538–5542.

(91) Heck, R. F. The Addition of Alkyl- and Arylpalladium Chlorides to Conjugated Dienes. *J. Am. Chem. Soc.* **1968**, *90*, 5542–5546.

(92) Heck, R. F. A Synthesis of Diaryl Ketones from Arylmercuric Salts. *J. Am. Chem. Soc.* **1968**, *90*, 5546–5548.

(93) Sonogashira, K.; Tohda, Y.; Hagihara, N. A Convenient Synthesis of Acetylenes: Catalytic Substitutions of Acetylenic Hydrogen with Bromoalkenes, Iodoarenes and Bromopyridines. *Tetrahedron Lett.* **1975**, *16*, 4467–4470.

(94) Negishi, E.; King, A. O.; Okukado, N. Selective Carbon-Carbon Bond Formation via Transition Metal Catalysis. A Highly Selective Synthesis of Unsymmetrical Biaryls and Diarylmethanes by the Nickel- or Palladium-Catalyzed Reaction of Aryl- and Benzylzinc Derivatives with Aryl Halides. *J. Org. Chem.* **1977**, *42*, 1821–1823.

(95) Milstein, D.; Stille, J. K. A General, Selective, and Facile Method for Ketone Synthesis from Acid Chlorides and Organotin Compounds Catalyzed by Palladium. *J. Am. Chem. Soc.* **1978**, *100*, 3636–3638.

(96) Miyaura, N.; Suzuki, A. Stereoselective Synthesis of Arylated (E)-Alkenes by the Reaction of Alk-1-Enylboranes with Aryl Halides in the Presence of Palladium Catalyst. *J. Chem. Soc. Chem. Commun.* **1979**, No. 19, 866.

(97) Hatanaka, Y.; Hiyama, T. Cross-Coupling of Organosilanes with Organic Halides Mediated by a Palladium Catalyst and Tris(Diethylamino)Sulfonium Difluorotrimethylsilicate. *J. Org. Chem.* **1988**, *53*, 918–920.

(98) Ackermann, L. Metal-Catalyzed Direct Alkylations of (Hetero)Arenes via C-H Bond Cleavages with Unactivated Alkyl Halides. *Chem. Commun.* **2010**, *46*, 4866–4877.

(99) Godula, K.; Sames, D. C-H Bond Functionalization in Complex Organic Synthesis. *Science* **2006**, *312*, 67–72.

(100) Guillemard, L.; Kaplaneris, N.; Ackermann, L.; Johansson, M. J. Late-Stage C–H Functionalization Offers New Opportunities in Drug Discovery. *Nat. Rev. Chem.* **2021**,

5, 522–545.

(101) Phipps, R. J.; Gaunt, M. J. A Meta-Selective Copper-Catalyzed C–H Bond Arylation. *Science* **2009**, *323*, 1593–1597.

(102) Tran, L. D.; Daugulis, O. Iron-Catalyzed Heterocycle and Arene Deprotonative Alkylation. *Org. Lett.* **2010**, *12*, 4277–4279.

(103) Yang, K.; Song, M.; Liu, H.; Ge, H. Palladium-Catalyzed Direct Asymmetric C–H Bond Functionalization Enabled by the Directing Group Strategy. *Chem. Sci.* **2020**, *11*, 12616–12632.

(104) Giri, R.; Shi, B. F.; Engle, K. M.; Maugel, N.; Yu, J. Q. Transition Metal-Catalyzed C–H Activation Reactions: Diastereoselectivity and Enantioselectivity. *Chem. Soc. Rev.* **2009**, *38*, 3242–3272.

(105) Ros, A.; Fernández, R.; Lassaletta, J. M. Functional Group Directed C–H Borylation. *Chem. Soc. Rev.* **2014**, *43*, 3229–3243.

(106) Liu, Y.-J.; Xu, H.; Kong, W.-J.; Shang, M.; Dai, H.-X.; Yu, J.-Q. Overcoming the Limitations of Directed C–H Functionalizations of Heterocycles. *Nature* **2014**, *515*, 389–393.

(107) Weissermel, K.; Arpe, H.-J. *Industrielle Organische Chemie - Bedeutende Vor- Und Zwischenprodukte*, Viley-VCH, Weinheim, **2007**.

(108) Friedel, C.; Crafts, J. M. Sur Une Nouvelle Méthode Générale de Synthèse d'hydrocarbures, d'acétones, Etc. *Compt. Rend.* **1877**, *84*, 1392–1395.

(109) Bandini, M., Umani-Ronchi, A., *General Aspects and Historical Background* In *Catalytic Asymmetric Friedel–Crafts Alkylations*; Bandini, M., Umani-Ronchi, A., Wiley-VCH, Weinheim, **2009**.

(110) Olah, G. A.; Dear, R. E. A. *Historical Friedel–Crafts and Related Reactions*; John Wiley and Sons, New York, **1963**.

(111) D. Macquarrie, *Industrial Friedel–Crafts Chemistry.* In *Catalytic Asymmetric Friedel–Crafts Alkylations*; Bandini, M., Umani-Ronchi, A., Wiley-VCH, Weinheim, **2009**.

(112) Kürti, L.; Czakó, B. *Strategic Applications of Named Reactions in Organic Synthesis*, Elsevier Academic Press, Burlington, **2005**.

(113) Olah, G. A. *Catalysts and Solvents*. In *Friedel–Crafts and Related Reactions*; Olah, G. A., Ed.; John Wiley & Sons, New York, **1963**; pp 205–206.

(114) Wheland, G. W. A Quantum Mechanical Investigation of the Orientation of Substituents in Aromatic Molecules. *J. Am. Chem. Soc.* **1942**, *64*, 900–908.

(115) Boga, C.; Del Vecchio, E.; Forlani, L.; Mazzanti, A.; Todesco, P. E. Evidence for

Carbon–Carbon Meisenheimer–Wheland Complexes between Superelectrophilic and Supernucleophilic Carbon Reagents. *Angew. Chem. Int. Ed.* **2005**, *44*, 3285–3289.

(116) Wilkes, J. S. A Short History of Ionic Liquids—from Molten Salts to Neoteric Solvents. *Green Chem.* **2002**, *4*, 73–80.

(117) Koptyug, V. A. Arenonium Ions (Structure and Reactivity). *Bull. Acad. Sci. USSR Div. Chem. Sci.* **1974**, *23*, 1031–1045.

(118) Olah, G. A.; Meyer, M. W. *Intermediate Complexes*. In *Friedel–Crafts and Related Reactions*; Olah, G. A., Ed.; John Wiley & Sons, New York, **1963**; pp 627–628.

(119) Olah, G. A.; Kuhn, S. J.; Flood, S. H. Aromatic Substitution. VIII. Mechanism of the Nitronium Tetrafluoroborate Nitration of Alkylbenzenes in Tetramethylene Sulfone Solution. Remarks on Certain Aspects of Electrophilic Aromatic Substitution. *J. Am. Chem. Soc.* **1961**, *83*, 4571–4580.

(120) Olah, G. A. Aromatic Substitution. XXVIII. Mechanism of Electrophilic Aromatic Substitutions. *Acc. Chem. Res.* **1971**, *4*, 240–248.

(121) He, T.; Klare, H. F. T.; Oestreich, M. Arenium-Ion-Catalysed Halodealkylation of Fully Alkylated Silanes. *Nature* **2023**, *623*, 538–543.

(122) Evano, G.; Theunissen, C. Beyond Friedel and Crafts: Directed Alkylation of C−H Bonds in Arenes. *Angew. Chem. Int. Ed.* **2019**, *58*, 7202–7236.

(123) Brückner, R. *Reaktionsmechanismen*, Spektrum akademischer Verlag, München, **2004**.

(124) Olah, G. A.; Farooq, O.; Farnia, S. M. F.; Olah, J. A. Friedel-Crafts Chemistry. 11. Boron, Aluminum, and Gallium Tris(Trifluoromethanesulfonate) (Triflate): Effective New Friedel-Crafts Catalysts. *J. Am. Chem. Soc.* **1988**, *110*, 2560–2565.

(125) Brown, H. C.; Nelson, K. L. An Interpretation of Meta Orientation in the Alkylation of Toluene. The Relative Reactivity and Isomer Distribution in the Chloromethylation and Mercuration of Benzene and Toluene. *J. Am. Chem. Soc.* **1953**, *75*, 6292–6299.

(126) Olah, G. A.; Overchuk, N. A. Aromatic Substitution. XXV. Selectivity in the Friedel-Crafts Benzylation, Isopropylation, and TButylation of Benzene and Toluene. *J. Am. Chem. Soc.* **1965**, *87*, 5786–5788.

(127) Mortier, J. *Arene Chemistry*, John Wiley & Sons, New York, **2015**.

(128) Francis, A. W. Liquid-Phase Alkylation of Aromatic Hydrocarbons. *Chem. Rev.* **1948**, *43*, 257–269.

(129) Evano, G.; Theunissen, C. Beyond Friedel and Crafts: Innate Alkylation of C−H Bonds in Arenes. *Angew. Chem. Int. Ed.* **2019**, *58*, 7558–7598.

(130) Paras, N. A.; MacMillan, D. W. C. New Strategies in Organic Catalysis: The First

Enantioselective Organocatalytic Friedel−Crafts Alkylation. *J. Am. Chem. Soc.* **2001**, *123*, 4370–4371.

(131) Bigi, F.; Casiraghi, G.; Casnati, G.; Sartori, G.; Gasparri Fava, G.; Ferrari Belicchi, M. Asymmetric Electrophilic Substitution on Phenols. Enantioselective Ortho-Hydroxyalkylation Mediated by Chiral Alkoxyaluminum Chlorides. *J. Org. Chem.* **1985**, *50*, 5018–5022.

(132) Erker, G.; van der Zeijden, A. A. H. Enantioselective Catalysis with a New Zirconium Trichloride Lewis Acid Containing a "Dibornacyclopentadienyl" Ligand. *Angew. Chem. Int. Ed. Engl.* **1990**, *29*, 512–514.

(133) Poulsen, T. B.; Jørgensen, K. A. Catalytic Asymmetric Friedel−Crafts Alkylation Reactions—Copper Showed the Way. *Chem. Rev.* **2008**, *108*, 2903–2915.

(134) You, S.-L.; Cai, Q.; Zeng, M. Chiral Brønsted Acid Catalyzed Friedel–Crafts Alkylation Reactions. *Chem. Soc. Rev.* **2009**, *38*, 2190–2201.

(135) Terrasson, V.; Marcia de Figueiredo, R.; Campagne, J. M. Organocatalyzed Asymmetric Friedel-Crafts Reactions. *Eur. J. Org. Chem.* **2010**, *2010*, 2635–2655.

(136) Montesinos-Magraner, M.; Vila, C.; Blay, G.; Pedro, J. Catalytic Enantioselective Friedel–Crafts Reactions of Naphthols and Electron-Rich Phenols. *Synthesis* **2016**, *48*, 2151–2164.

(137) Egorov, I. N.; Santra, S.; Kopchuk, D. S.; Kovalev, I. S.; Zyryanov, G. V.; Majee, A.; Ranu, B. C.; Rusinov, V. L.; Chupakhin, O. N. Direct Asymmetric Arylation of Imines. *Adv. Synth. Catal.* **2020**, *362*, 4293–4324.

(138) Gaviña, D.; Escolano, M.; Torres, J.; Alzuet-Piña, G.; Sánchez-Roselló, M.; del Pozo, C. Organocatalytic Enantioselective Friedel-Crafts Alkylation Reactions of Pyrroles. *Adv. Synth. Catal.* **2021**, *363*, 3439–3470.

(139) Lakhdar, S.; Westermaier, M.; Terrier, F.; Goumont, R.; Boubaker, T.; Ofial, A. R.; Mayr, H. Nucleophilic Reactivities of Indoles. *J. Org. Chem.* **2006**, *71*, 9088–9095.

(140) Kempf, B.; Hampel, N.; Ofial, A. R.; Mayr, H. Structure–Nucleophilicity Relationships for Enamines. *Chem. Eur. J.* **2003**, *9*, 2209–2218.

(141) Mayr, H.; Kempf, B.; Ofial, A. R. π-Nucleophilicity in Carbon−Carbon Bond-Forming Reactions. *Acc. Chem. Res.* **2003**, *36*, 66–77.

(142) Ammer, J.; Nolte, C.; Mayr, H. Free Energy Relationships for Reactions of Substituted Benzhydrylium Ions: From Enthalpy over Entropy to Diffusion Control. *J. Am. Chem. Soc.* **2012**, *134*, 13902–13911.

(143) Wu, P.; Nielsen, T. E. Scaffold Diversity from N-Acyliminium Ions. *Chem. Rev.* **2017**,

117, 7811–7856.

(144) Scharf, M. J.; List, B. A Catalytic Asymmetric Pictet–Spengler Platform as a Biomimetic Diversification Strategy toward Naturally Occurring Alkaloids. *J. Am. Chem. Soc.* **2022**, *144*, 15451–15456.

(145) Süssmuth, R. D.; Mainz, A. Nonribosomal Peptide Synthesis—Principles and Prospects. *Angew. Chem. Int. Ed.* **2017**, *56*, 3770–3821.

(146) Tailhades, J. Arylglycine: A Focus on Amino Acid Preparation and Peptide Synthesis. *Int. J. Pept. Res. Ther.* **2022**, *28*, 1–12.

(147) Kaptein, S. J. F.; Goethals, O.; Kiemel, D.; Marchand, A.; Kesteleyn, B.; Bonfanti, J. F.; Bardiot, D.; Stoops, B.; Jonckers, T. H. M.; Dallmeier, K.; Geluykens, P.; Thys, K.; Crabbe, M.; Chatel-Chaix, L.; Münster, M.; Querat, G.; Touret, F.; de Lamballerie, X.; Raboisson, P.; Simmen, K.; Chaltin, P.; Bartenschlager, R.; Van Loock, M.; Neyts, J. A Pan-Serotype Dengue Virus Inhibitor Targeting the NS3–NS4B Interaction. *Nature* **2021**, *598*, 504–509.

(148) Williams, R. M.; Hendrix, J. A. Asymmetric Synthesis of Arylglycines. *Chem. Rev.* **1992**, *92*, 889–917.

(149) Boger, D. L.; Miyazaki, S.; Kim, S. H.; Wu, J. H.; Castle, S. L.; Loiseleur, O.; Jin, Q. Total Synthesis of the Vancomycin Aglycon. *J. Am. Chem. Soc.* **1999**, *121*, 10004–10011.

(150) Boger, D. L.; Kim, S. H.; Miyazaki, S.; Strittmatter, H.; Weng, J.-H.; Mori, Y.; Rogel, O.; Castle, S. L.; McAtee, J. J. Total Synthesis of the Teicoplanin Aglycon. *J. Am. Chem. Soc.* **2000**, *122*, 7416–7417.

(151) Boger, D. L.; Borzilleri, R. M.; Nukui, S.; Beresis, R. T. Synthesis of the Vancomycin CD and DE Ring Systems. *J. Org. Chem.* **1997**, *62*, 4721–4736.

(152) Zuend, S. J.; Coughlin, M. P.; Lalonde, M. P.; Jacobsen, E. N. Scaleable Catalytic Asymmetric Strecker Syntheses of Unnatural α-Amino Acids. *Nature* **2009**, *461*, 968–970.

(153) Beisel, T.; Diehl, A. M.; Manolikakes, G. Palladium-Catalyzed Enantioselective Three-Component Synthesis of α-Arylglycines. *Org. Lett.* **2016**, *18*, 4116–4119.

(154) Enders, D.; Seppelt, M.; Beck, T. Enantioselective Organocatalytic Synthesis of Arylglycines via Friedel-Crafts Alkylation of Arenes with a Glyoxylate Imine. *Adv. Synth. Catal.* **2010**, *352*, 1413–1418.

(155) Ben-Ishai, D.; Sataty, I.; Bernstein, Z. A New Synthesis of N-Acyl Aromatic α-Amino Acids—Amidoalkylation of Aromatic and Heterocyclic Compounds with Glyoxylic

Acid Derivatives. *Tetrahedron* **1976**, *32*, 1571–1573.

(156) Ben-Ishai, D.; Satati, I.; Berler, Z. A New Synthesis of N-Acyl Aromatic α-Amino Acids; Amidoalkylation of Aromatic Compounds with Glyoxylic Acid Derivatives. *J. Chem. Soc., Chem. Commun.* **1975**, No. 9, 349–350.

(157) Obradors, C.; Mitschke, B.; Aukland, M. H.; Leutzsch, M.; Grossmann, O.; Brunen, S.; Schwengers, S. A.; List, B. Direct and Catalytic C -Glycosylation of Arenes: Expeditious Synthesis of the Remdesivir Nucleoside. *Angew. Chem. Int. Ed.* **2022**, *61*, e202114619.

(158) Isidro-Llobet, A.; Álvarez, M.; Albericio, F. Amino Acid-Protecting Groups. *Chem. Rev.* **2009**, *109*, 2455–2504.

(159) You, Y.; Zhang, L.; Cui, L.; Mi, X.; Luo, S. Catalytic Asymmetric Mannich Reaction with N-Carbamoyl Imine Surrogates of Formaldehyde and Glyoxylate. *Angew. Chem. Int. Ed.* **2017**, *56*, 13814–13818.

(160) Savoie, P. R.; Welch, J. T. Preparation and Utility of Organic Pentafluorosulfanyl-Containing Compounds. *Chem. Rev.* **2015**, *115*, 1130–1190.

(161) Lvov, A. G.; Bredihhin, A. Azulene as an Ingredient for Visible-Light- and Stimuli-Responsive Photoswitches. *Org. Biomol. Chem.* **2021**, *19*, 4460–4468.

(162) Watkins, E. J.; Almhjell, P. J.; Arnold, F. H. Direct Enzymatic Synthesis of a Deep-Blue Fluorescent Noncanonical Amino Acid from Azulene and Serine. *ChemBioChem* **2020**, *21*, 80–83.

(163) Moore, M. J.; Qu, S.; Tan, C.; Cai, Y.; Mogi, Y.; Jamin Keith, D.; Boger, D. L. Next-Generation Total Synthesis of Vancomycin. *J. Am. Chem. Soc.* **2020**, *142*, 16039–16050.

(164) Majer, J.; Kwiatkowski, P.; Jurczak, J. Highly Enantioselective Friedel−Crafts Reaction of Thiophenes with Glyoxylates: Formal Synthesis of Duloxetine. *Org. Lett.* **2009**, *11*, 4636–4639.

(165) Zeng, M.; You, S.-L. Asymmetric Friedel-Crafts Alkylation of Indoles: The Control of Enantio- and Regioselectivity. *Synlett* **2010**, *2010*, 1289–1301.

(166) Boger, D. L.; Kim, S. H.; Mori, Y.; Weng, J.-H.; Rogel, O.; Castle, S. L.; McAtee, J. J. First and Second Generation Total Synthesis of the Teicoplanin Aglycon. *J. Am. Chem. Soc.* **2001**, *123*, 1862–1871.

(167) Liu, J.; Luo, C.; Smith, P. A.; Chin, J. K.; Page, M. G. P.; Paetzel, M.; Romesberg, F. E. Synthesis and Characterization of the Arylomycin Lipoglycopeptide Antibiotics and the Crystallographic Analysis of Their Complex with Signal Peptidase. *J. Am. Chem. Soc.* **2011**, *133*, 17869–17877.

(168) Moore, M. J.; Qu, S.; Tan, C.; Cai, Y.; Mogi, Y.; Jamin Keith, D.; Boger, D. L. Next-

Generation Total Synthesis of Vancomycin. *J. Am. Chem. Soc.* **2020**, *142*, 16039–16050.

(169) Huang, Q.; Xia, B.; Li, M.; Guan, H.; Antonietti, M.; Chen, S. Single-Zinc Vacancy Unlocks High-Rate H2O2 Electrosynthesis from Mixed Dioxygen beyond Le Chatelier Principle. *Nat. Commun.* **2024**, *15*, 4157.

(170) Gómez-Gallego, M.; Sierra, M. A. Kinetic Isotope Effects in the Study of Organometallic Reaction Mechanisms. *Chem. Rev.* **2011**, *111*, 4857–4963.

(171) Olah, G. A.; Kuhn, S. J.; Flood, S. H.; Hardie, B. A. Aromatic Substitution. XXII. 1a Acetylation of Benzene, Alkylbenzenes, and Halobenzenes with Methyloxocarbonium (Acetylium) Hexafluoro- and Hexachloroantimonate. *J. Am. Chem. Soc.* **1964**, *86*, 2203–2209.

(172) Effenberger, F.; Maier, A. H. Changing the O Rtho/ P Ara Ratio in Aromatic Acylation Reactions by Changing Reaction Conditions: A Mechanistic Explanation from Kinetic Measurements. *J. Am. Chem. Soc.* **2001**, *123*, 3429–3433.

(173) Olah, G. A.; Kuhn, S. J.; Flood, S. H. Aromatic Substitution. VIII. Mechanism of the Nitronium Tetrafluoroborate Nitration of Alkylbenzenes in Tetramethylene Sulfone Solution. Remarks on Certain Aspects of Electrophilic Aromatic Substitution. *J. Am. Chem. Soc.* **1961**, *83*, 4571–4580.

(174) Nakane, R.; Kurihara, O.; Takematsu, A. Friedel-Crafts Isopropylation in Nonpolar Solvents. *J. Org. Chem.* **1971**, *36*, 2753–2756.

(175) Singleton, D. A.; Thomas, A. A. High-Precision Simultaneous Determination of Multiple Small Kinetic Isotope Effects at Natural Abundance. *J. Am. Chem. Soc.* **1995**, *117*, 9357–9358.

(176) Wambua, V.; Hirschi, J. S.; Vetticatt, M. J. Rapid Evaluation of the Mechanism of Buchwald-Hartwig Amination and Aldol Reactions Using Intramolecular [13]C Kinetic Isotope Effects. *ACS Catal.* **2021**, *11*, 60–67.

(177) Diaz-Oviedo, D. The Catalytic Asymmetric Intermolecular Prins Reaction, Doctoral Thesis, Universität zu Köln, **2022**.

(178) Brunen, S.; Mitschke, B.; Leutzsch, M.; List, B. Asymmetric Catalytic Friedel–Crafts Reactions of Unactivated Arenes. *J. Am. Chem. Soc.* **2023**, *145*, 15708–15713.

(179) Ramachanderan, R.; Schaefer, B. Lily-of-the-Valley Fragrances. *ChemTexts* **2019**, *5*, 11.

(180) Jordi, S.; Kraft, P. Crossing the Boundaries between Marine and Muguet: Discovery of Unusual Lily-of-the-Valley Odorants Devoid of Aldehyde Functions. *Helv. Chim. Acta* **2018**, *101*.

(181) Scriabine, I. Verfahren Zur Herstellung von Phenylsubstituierten Alkanalen.

DE1145161B·1963-03-14, 1963.

(182) Scriabine, I. Alkylaromatic Aldehydes and Their Preparation. US3023247A, 1960.

(183) Scriabine, I. *Bull. Soc. Chim. Fr.* **1961**, 1194.

(184) Pareek, M.; Bour, C.; Gandon, V. Gallium-Catalyzed Scriabine Reaction. *Org. Lett.* **2018**, *20*, 6957–6960.

(185) Snowden, R. L.; Birkbeck, A. A.; Womack, G. B. Catalytic Scriabine Reaction, 2005.

(186) Takashi, Y.; Yoshihiro Yoshida, Y.; Eiji Sajiki, C.; Satoru Fujitsu, Y. Method of Retaining the Quality of 2-Methyl-3-(3,4-Methylendioxyphenl)propanal and Process for Producing the Same. US 2013/0046101 A1, 2013.

(187) Trost, B. M.; Lee, C. B. Geminal Dicarboxylates as Carbonyl Surrogates for Asymmetric Synthesis. Part I. Asymmetric Addition of Malonate Nucleophiles. *J. Am. Chem. Soc.* **2001**, *123*, 3671–3686.

(188) Reiter, M.; Torssell, S.; Lee, S.; MacMillan, D. W. C. The Organocatalytic Three-Step Total Synthesis of (+)-Frondosin B. *Chem. Sci.* **2010**, *1*, 37.

(189) Page, C. G.; Cao, J.; Oblinsky, D. G.; MacMillan, S. N.; Dahagam, S.; Lloyd, R. M.; Charnock, S. J.; Scholes, G. D.; Hyster, T. K. Regioselective Radical Alkylation of Arenes Using Evolved Photoenzymes. *J. Am. Chem. Soc.* **2023**, *145*, 11866–11874.

(190) Vil', V. A.; Merkulova, V. M.; Ilovaisky, A. I.; Paveliev, S. A.; Nikishin, G. I.; Terent'ev, A. O. Electrochemical Synthesis of Fluorinated Ketones from Enol Acetates and Sodium Perfluoroalkyl Sulfinates. *Org. Lett.* **2021**, *23*, 5107–5112.

(191) White, N. A.; Rovis, T. Enantioselective N-Heterocyclic Carbene-Catalyzed β-Hydroxylation of Enals Using Nitroarenes: An Atom Transfer Reaction That Proceeds via Single Electron Transfer. *J. Am. Chem. Soc.* **2014**, *136*, 14674–14677.

(192) Yang, X.; Wang, H.; Jin, Z.; Chi, Y. R. Development of Green and Low-Cost Chiral Oxidants for Asymmetric Catalytic Hydroxylation of Enals. *Green Synth. Catal.* **2021**, *2*, 295–298.

(193) Bendelsmith, A. J.; Kim, S. C.; Wasa, M.; Roche, S. P.; Jacobsen, E. N. Enantioselective Synthesis of α-Allyl Amino Esters via Hydrogen-Bond-Donor Catalysis. *J. Am. Chem. Soc.* **2019**, *141*, 11414–11419.

(194) You, Y.; Zhang, L.; Cui, L.; Mi, X.; Luo, S. Catalytic Asymmetric Mannich Reaction with N-Carbamoyl Imine Surrogates of Formaldehyde and Glyoxylate. *Angew. Chem. Int. Ed.* **2017**, *56*, 13814–13818.

(195) Maciá, E.; Foubelo, F.; Yus, M. Indium-Mediated Diastereoselective Allylation of N-Tert-Butanesulfinyl Imines Derived from α-Ketoesters. *Tetrahedron* **2016**, *72*, 6001–

6010.

(196) Fan, B.; Trant, J. F.; Wong, A. D.; Gillies, E. R. Polyglyoxylates: A Versatile Class of Triggerable Self-Immolative Polymers from Readily Accessible Monomers. *J. Am. Chem. Soc.* **2014**, *136*, 10116–10123.

(197) Zhang, X.; Wang, M.; Ding, R.; Xu, Y.-H.; Loh, T.-P. Highly Enantioselective and Anti -Diastereoselective Catalytic Intermolecular Glyoxylate–Ene Reactions: Effect of the Geometrical Isomers of Alkenes. *Org. Lett.* **2015**, *17*, 2736–2739.

(198) Blaquiere, N.; Shore, D. G.; Rousseaux, S.; Fagnou, K. Decarboxylative Ketone Aldol Reactions: Development and Mechanistic Evaluation under Metal-Free Conditions. *J. Org. Chem.* **2009**, *74*, 6190–6198.

(199) Chau, J.; Zhang, J.; Ciufolini, M. A. A Peterson Avenue to 5-Alkenyloxazoles. *Tetrahedron Lett.* **2009**, *50*, 6163–6165.

(200) Bloux, H.; Dahiya, A.; Hébert, A.; Fabis, F.; Schoenebeck, F.; Cailly, T. Base-Mediated Radio-Iodination of Arenes by Using Organosilane and Organogermane as Radiolabelling Precursors. *Chem. Eur. J.* **2023**, *29*.

(201) Guo, S.; Ma, L.; Zhao, J.; Küçüköz, B.; Karatay, A.; Hayvali, M.; Yaglioglu, H. G.; Elmali, A. BODIPY Triads Triplet Photosensitizers Enhanced with Intramolecular Resonance Energy Transfer (RET): Broadband Visible Light Absorption and Application in Photooxidation. *Chem. Sci.* **2014**, *5*, 489–500.

(202) Ninomiya, M.; Ando, Y.; Kudo, F.; Ohmori, K.; Suzuki, K. Total Synthesis of Actinorhodin. *Angew. Chem. Int. Ed.* **2019**, *58*, 4264–4270.

(203) Gatzenmeier, T.; Turberg, M.; Yepes, D.; Xie, Y.; Neese, F.; Bistoni, G.; List, B. Scalable and Highly Diastereo- and Enantioselective Catalytic Diels–Alder Reaction of α,β-Unsaturated Methyl Esters. *J. Am. Chem. Soc.* **2018**, *140*, 12671–12676.

(204) Schwengers, S. A.; De, C. K.; Grossmann, O.; Grimm, J. A. A.; Sadlowski, N. R.; Gerosa, G. G.; List, B. Unified Approach to Imidodiphosphate-Type Brønsted Acids with Tunable Confinement and Acidity. *J. Am. Chem. Soc.* **2021**, *143*, 14835–14844.

(205) Grossmann, O.; Maji, R.; Aukland, M. H.; Lee, S.; List, B. Catalytic Asymmetric Additions of Enol Silanes to In Situ Generated Cyclic, Aliphatic *N*-Acyliminium Ions. *Angew. Chem. Int. Ed.* **2022**, *61*, 1–6.

(206) Pracht, P.; Caldeweyher, E.; Ehlert, S.; Grimme, S. A Robust, Non-Self-Consistent Tight-Binding Quantum Chemistry Method for Large Molecules. *Chemrxiv* **2019**.

(207) Pracht, P.; Bohle, F.; Grimme, S. Automated Exploration of the Low-Energy Chemical Space with Fast Quantum Chemical Methods. *Phys. Chem. Chem. Phys.* **2020**, *22*, 7169–

7192.

(208) Bannwarth, C.; Ehlert, S.; Grimme, S. GFN2-XTB—An Accurate and Broadly Parametrized Self-Consistent Tight-Binding Quantum Chemical Method with Multipole Electrostatics and Density-Dependent Dispersion Contributions. *J. Chem. Theory Comput.* **2019**, *15*, 1652–1671.

(209) Neese, F. Software Update: The Orca Program System—Version 5.0. *WIREs Comput. Mol. Sci.* **2022**, *12*.

(210) Perdew, J. P.; Burke, K.; Ernzerhof, M. Generalized Gradient Approximation Made Simple. *Phys. Rev. Lett.* **1996**, *77*, 3865–3868.

(211) Grimme, S.; Antony, J.; Ehrlich, S.; Krieg, H. A Consistent and Accurate Ab Initio Parametrization of Density Functional Dispersion Correction (DFT-D) for the 94 Elements H-Pu. *J. Chem. Phys.* **2010**, *132*, 154104.

(212) Grimme, S.; Ehrlich, S.; Goerigk, L. Effect of the Damping Function in Dispersion Corrected Density Functional Theory. *J. Comput. Chem.* **2011**, *32*, 1456–1465.

(213) Weigend, F.; Ahlrichs, R. Balanced Basis Sets of Split Valence, Triple Zeta Valence and Quadruple Zeta Valence Quality for H to Rn: Design and Assessment of Accuracy. *Phys. Chem. Chem. Phys.* **2005**, *7*, 3297.

(214) Eichkorn, K.; Treutler, O.; Öhm, H.; Häser, M.; Ahlrichs, R. Auxiliary Basis Sets to Approximate Coulomb Potentials. *Chem. Phys. Lett.* **1995**, *240*, 283–290.

(215) Neese, F. An Improvement of the Resolution of the Identity Approximation for the Formation of the Coulomb Matrix. *J. Comput. Chem.* **2003**, *24*, 1740–1747.

(216) Weigend, F. Accurate Coulomb-Fitting Basis Sets for H to Rn. *Phys. Chem. Chem. Phys.* **2006**, *8*, 1057–1065.

(217) Zhao, Y.; Truhlar, D. G. The M06 Suite of Density Functionals for Main Group Thermochemistry, Thermochemical Kinetics, Noncovalent Interactions, Excited States, and Transition Elements: Two New Functionals and Systematic Testing of Four M06 Functionals and 12 Other Functionals. *Theor. Chem. Acc.* **2008**, *119*, 525–525.

(218) "otherm.py," can be found under https://github.com/duartegroup/otherm.

(219) Grimme, S. Supramolecular Binding Thermodynamics by Dispersion-Corrected Density Functional Theory. *Chem. Eur. J.* **2012**, *18*, 9955–9964.

(220) Miró, J.; Gensch, T.; Ellwart, M.; Han, S.-J.; Lin, H.-H.; Sigman, M. S.; Toste, F. D. Enantioselective Allenoate-Claisen Rearrangement Using Chiral Phosphate Catalysts. *J. Am. Chem. Soc.* **2020**, *142*, 6390–6399.

(221) Ma, B.; Guckian, K. M.; Liu, X.; Yang, C.; Li, B.; Scannevin, R.; Mingueneau, M.;

8. References

Drouillard, A.; Walzer, T. Novel Potent Selective Orally Active S1P5 Receptor Antagonists. *ACS Med. Chem. Lett.* **2021**, *12*, 351–355.

9. Appendix

9.1 List of Catalyst Structures
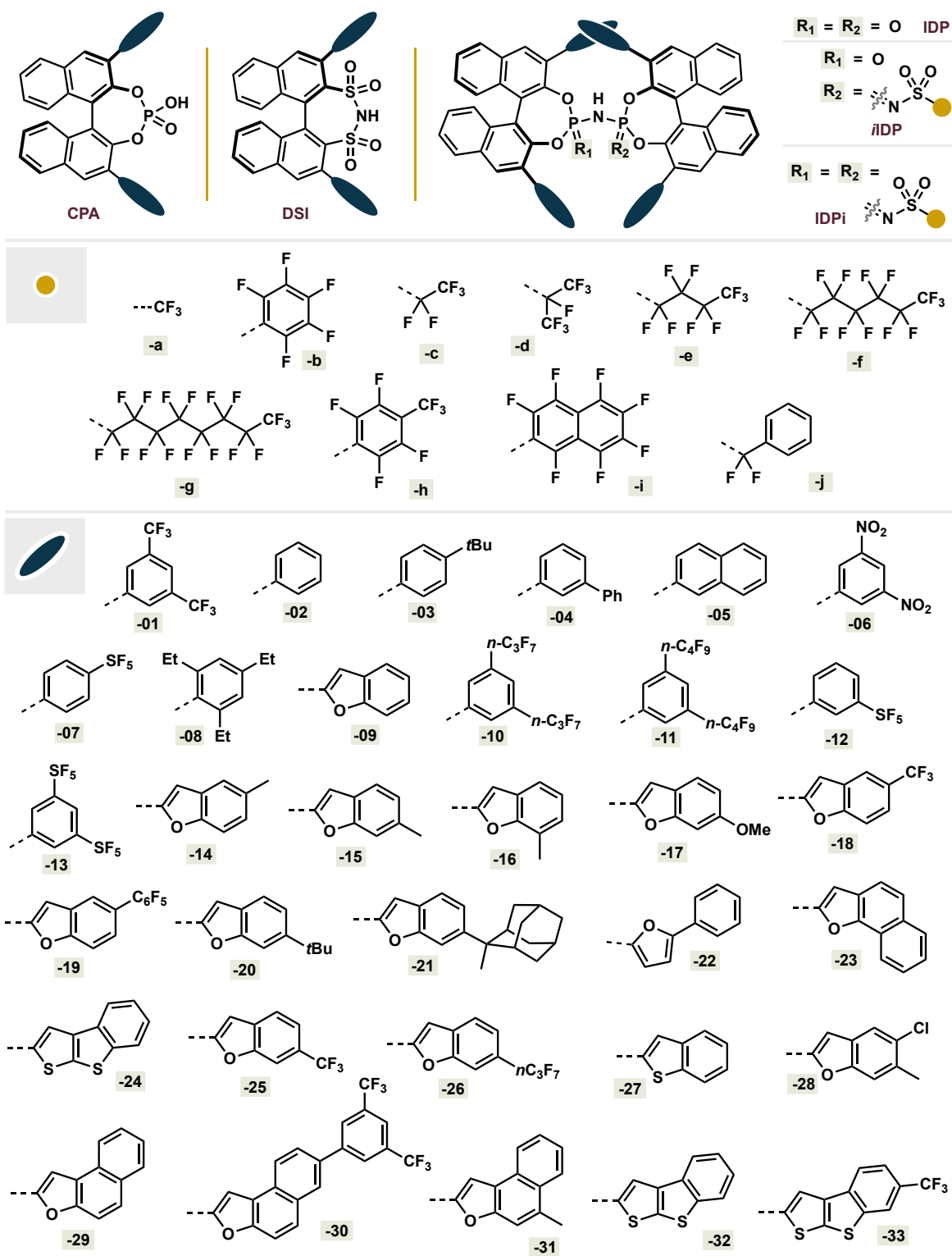
9.2 Erklärung

Hiermit versichere ich an Eides statt, dass ich die vorliegende Dissertation selbstständig und ohne die Benutzung anderer als der angegebenen Hilfsmittel und Literatur angefertigt habe. Alle Stellen, die wörtlich oder sinngemäß aus veröffentlichten und nicht veröffentlichten Werken dem Wortlaut oder dem Sinn nach entnommen wurden, sind als solche kenntlich gemacht. Ich versichere an Eides statt, dass diese Dissertation noch keiner anderen Fakultät oder Universität zur Prüfung vorgelegen hat; dass sie - abgesehen von unten angegebenen Teilpublikationen und eingebundenen Artikeln und Manuskripten - noch nicht veröffentlicht worden ist sowie, dass ich eine Veröffentlichung der Dissertation vor Abschluss der Promotion nicht ohne Genehmigung des Promotionsausschusses vornehmen werde. Die Bestimmungen dieser Ordnung sind mir bekannt. Darüber hinaus erkläre ich hiermit, dass ich die Ordnung zur Sicherung guter wissenschaftlicher Praxis und zum Umgang mit wissenschaftlichem Fehlverhalten der Universität zu Köln gelesen und sie bei der Durchführung der Dissertation zugrundeliegenden Arbeiten und der schriftlich verfassten Dissertation beachtet habe und verpflichte mich hiermit, die dort genannten Vorgaben bei allen wissenschaftlichen Tätigkeiten zu beachten und umzusetzen. Ich versichere, dass die eingereichte elektronische Fassung der eingereichten Druckfassung vollständig entspricht.

—Mülheim an der Ruhr, Juni 2024

_____ (Sebastian Brunen)

Bisher sind folgende Teilpublikationen veröffentlicht worden:

(1) "Direct and Catalytic C-Glycosylation of Arenes: Expeditious Synthesis of the Remdesivir Nucleoside": C. Obradors, B. Mitschke, M. Aukland, M. Leutzsch, O. Grossmann, S. Brunen, S. Schwengers, B. List, *Angew. Chem. Int. Ed.* **2022**, *61*, e202114619.

(2) "Direct Regioselective Dehydrogenation of α-Substituted Cyclic Ketones": S. Schwengers, G. Gerosa, T. Amatov, N. Yasukawa, S. Brunen, M. Leutzsch, B. Mitschke, G. Shevchenko, B. List, *Angew. Chem. Int. Ed.* **2023**, *62*, e202307081.

(3) "Asymmetric Catalytic Friedel–Crafts Reaction of Unactivated Arenes": S. Brunen, B. Mitschke, M. Leutzsch, B. List, *J. Am. Chem. Soc.* **2023**, *145*, 29, 15708-15713.